African Journal of Pharmacy and Pharmacology

Volume 7 Number 22 15 June, 2013

ISSN 1996- 0816

Academic Journals

ABOUT AJPP

The **African Journal of Pharmacy and Pharmacology (AJPP)** is published weekly (one volume per year) by Academic Journals.

African Journal of Pharmacy and Pharmacology (AJPP) is an open access journal that provides rapid publication (weekly) of articles in all areas of Pharmaceutical Science such as Pharmaceutical Microbiology, Pharmaceutical Raw Material Science, Formulations, Molecular modeling, Health sector Reforms, Drug Delivery, Pharmacokinetics and Pharmacodynamics, Pharmacognosy, Social and Administrative Pharmacy, Pharmaceutics and Pharmaceutical Microbiology, Herbal Medicines research, Pharmaceutical Raw Materials development/utilization, Novel drug delivery systems, Polymer/Cosmetic Science, Food/Drug Interaction, Herbal drugs evaluation, Physical Pharmaceutics, Medication management, Cosmetic Science, pharmaceuticals, pharmacology, pharmaceutical research etc. The Journal welcomes the submission of manuscripts that meet the general criteria of significance and scientific excellence. Papers will be published shortly after acceptance. All articles published in AJPP are peer-reviewed.

Submission of Manuscript

Submit manuscripts as e-mail attachment to the Editorial Office at: ajpp@academicjournals.org. A manuscript number will be mailed to the corresponding author shortly after submission.

The African Journal of Pharmacy and Pharmacology will only accept manuscripts submitted as e-mail attachments.

Please read the **Instructions for Authors** before submitting your manuscript. The manuscript files should be given the last name of the first author.

Editors

Editorial Board

Instructions for Author

Electronic submission of manuscripts is strongly encouraged, provided that the text, tables, and figures are included in a single Microsoft Word file (preferably in Arial font).

The **cover letter** should include the corresponding author's full address and telephone/fax numbers and should be in an e-mail message sent to the Editor, with the file, whose name should begin with the first author's surname, as an attachment.

Article Types
Three types of manuscripts may be submitted:

Regular articles: These should describe new and carefully confirmed findings, and experimental procedures should be given in sufficient detail for others to verify the work. The length of a full paper should be the minimum required to describe and interpret the work clearly.
Short Communications: A Short Communication is suitable for recording the results of complete small investigations or giving details of new models or hypotheses, innovative methods, techniques or apparatus. The style of main sections need not conform to that of full-length papers. Short communications are 2 to 4 printed pages (about 6 to 12 manuscript pages) in length.

Reviews: Submissions of reviews and perspectives covering topics of current interest are welcome and encouraged. Reviews should be concise and no longer than 4-6 printed pages (about 12 to 18 manuscript pages). Reviews are also peer-reviewed.

Review Process

All manuscripts are reviewed by an editor and members of the Editorial Board or qualified outside reviewers. Authors cannot nominate reviewers. Only reviewers randomly selected from our database with specialization in the subject area will be contacted to evaluate the manuscripts. The process will be blind review.
Decisions will be made as rapidly as possible, and the journal strives to return reviewers' comments to authors as fast as possible. The editorial board will re-review manuscripts that are accepted pending revision. It is the goal of the AJPP to publish manuscripts within weeks after submission.

Regular articles

All portions of the manuscript must be typed double-spaced and all pages numbered starting from the title page.

The Title should be a brief phrase describing the contents of the paper. The Title Page should include the authors' full names and affiliations, the name of the corresponding author along with phone, fax and E-mail information. Present addresses of authors should appear as a footnote.

The Abstract should be informative and completely self-explanatory, briefly present the topic, state the scope of the experiments, indicate significant data, and point out major findings and conclusions. The Abstract should be 100 to 200 words in length.. Complete sentences, active verbs, and the third person should be used, and the abstract should be written in the past tense. Standard nomenclature should be used and abbreviations should be avoided. No literature should be cited.
Following the abstract, about 3 to 10 key words that will provide indexing references should be listed.

A list of non-standard **Abbreviations** should be added. In general, non-standard abbreviations should be used only when the full term is very long and used often. Each abbreviation should be spelled out and introduced in parentheses the first time it is used in the text. Only recommended SI units should be used. Authors should use the solidus presentation (mg/ml). Standard abbreviations (such as ATP and DNA) need not be defined.

The Introduction should provide a clear statement of the problem, the relevant literature on the subject, and the proposed approach or solution. It should be understandable to colleagues from a broad range of scientific disciplines.

Materials and methods should be complete enough to allow experiments to be reproduced. However, only truly new procedures should be described in detail; previously published procedures should be cited, and important modifications of published procedures should be mentioned briefly. Capitalize trade names and include the manufacturer's name and address. Subheadings should be used. Methods in general use need not be described in detail.

Results should be presented with clarity and precision. The results should be written in the past tense when describing findings in the authors' experiments. Previously published findings should be written in the present tense. Results should be explained, but largely without referring to the literature. Discussion, speculation and detailed interpretation of data should not be included in the Results but should be put into the Discussion section.

The Discussion should interpret the findings in view of the results obtained in this and in past studies on this topic. State the conclusions in a few sentences at the end of the paper. The Results and Discussion sections can include subheadings, and when appropriate, both sections can be combined.

The Acknowledgments of people, grants, funds, etc should be brief.

Tables should be kept to a minimum and be designed to be as simple as possible. Tables are to be typed double-spaced throughout, including headings and footnotes. Each table should be on a separate page, numbered consecutively in Arabic numerals and supplied with a heading and a legend. Tables should be self-explanatory without reference to the text. The details of the methods used in the experiments should preferably be described in the legend instead of in the text. The same data should not be presented in both table and graph form or repeated in the text.

Figure legends should be typed in numerical order on a separate sheet. Graphics should be prepared using applications capable of generating high resolution GIF, TIFF, JPEG or Powerpoint before pasting in the Microsoft Word manuscript file. Tables should be prepared in Microsoft Word. Use Arabic numerals to designate figures and upper case letters for their parts (Figure 1). Begin each legend with a title and include sufficient description so that the figure is understandable without reading the text of the manuscript. Information given in legends should not be repeated in the text.

References: In the text, a reference identified by means of an author‘s name should be followed by the date of the reference in parentheses. When there are more than two authors, only the first author‘s name should be mentioned, followed by ’et al‘. In the event that an author cited has had two or more works published during the same year, the reference, both in the text and in the reference list, should be identified by a lower case letter like ’a‘ and ’b‘ after the date to distinguish the works.

Examples:

Cole (2000), Steddy et al. (2003), (Kelebeni, 1983), (Bane and Jake, 1992), (Chege, 1998; Cohen, 1987a,b; Tristan, 1993,1995), (Kumasi et al., 2001)

References should be listed at the end of the paper in alphabetical order. Articles in preparation or articles submitted for **publication**, unpublished observations, personal communications, etc. should not be included in the reference list but should only be mentioned in the article text (e.g., A. Kingori, University of Nairobi, Kenya, personal communication). Journal names are abbreviated according to Chemical Abstracts. Authors are fully responsible for the accuracy of the references.

Examples:

Ansell J, Hirsh J, Poller L (2004). The pharmacology and management of the vitamin K antagonists: the Seventh ACCP Conference on Antithrombotic and Thrombolytic. Therapy. 126:204-233

Ansell JE, Buttaro ML, Thomas VO (1997). Consensus guidelines for coordinated outpatient oral anticoagulation therapy management. Ann Pharmacother 31 : 604-615

Charnley AK (1992). Mechanisms of fungal pathogenesis in insects with particular reference to locusts. In: Lomer CJ, Prior C (eds) Pharmaceutical Controls of Locusts and Grasshoppers: Proceedings of an international workshop held at Cotonou, Benin. Oxford: CAB International, pp 181-190.

Jake OO (2002).Pharmaceutical Interactions between Striga hermonthica (Del.) Benth. and fluorescent rhizosphere bacteria Of Zea mays, L. and Sorghum bicolor L. Moench for Striga suicidal germination In Vigna unguiculata . PhD dissertation, Tehran University, Iran.

Furmaga EM (1993). Pharmacist management of a hyperlipidemia clinic. Am. J. Hosp. Pharm. 50 : 91-95

Short Communications

Short Communications are limited to a maximum of two figures and one table. They should present a complete study that is more limited in scope than is found in full-length papers. The items of manuscript preparation listed above apply to Short Communications with the following differences: (1) Abstracts are limited to 100 words; (2) instead of a separate Materials and Methods section, experimental procedures may be incorporated into Figure Legends and Table footnotes; (3) Results and Discussion should be combined into a single section.

Proofs and Reprints: Electronic proofs will be sent (e-mail attachment) to the corresponding author as a PDF file. Page proofs are considered to be the final version of the manuscript. With the exception of typographical or minor clerical errors, no changes will be made in the manuscript at the proof stage.

Fees and Charges: Authors are required to pay a $600 handling fee. Publication of an article in the African Journal of Pharmacy and Pharmacology is not contingent upon the author's ability to pay the charges. Neither is acceptance to pay the handling fee a guarantee that the paper will be accepted for publication. Authors may still request (in advance) that the editorial office waive some of the handling fee under special circumstances.

Submission of a manuscript implies: that the work described has not been published before (except in the form of an abstract or as part of a published lecture, or thesis) that it is not under consideration for publication elsewhere; that if and when the manuscript is accepted for publication, the authors agree to automatic transfer of the copyright to the publisher.

African Journal of Pharmacy and Pharmacology

Table of Contents: Volume 7 Number 22 15 June, 2013

ARTICLES

Review

Differentiation of stem and progenitor cells from bone marrow in activated dendritic cells and lymphocytes with anti-malignant properties 1426
Iskra Ventseslavova Sainova, Ilina Valkova, Velichka Pavlova, Elena Nikolova

Research Articles

Analysis of the polysaccharides from *Urtica angustifolia* and their anti-fatigue activity 1438
Haiyue Zhang, Xiaojuan Yan, Zhenling Zhao, Li Ji

Effect of cooking methods on tetracycline residues in pig meat 1448
VanHue Nguyen, MuQing Li, Muhammad Ammar Khan, ChunBao Li, GuangHong Zhou

Impact of high hydrostatic pressure on gel formation of low methoxylpectin 1455
M. N. Eshtiaghi, J. Kuldiloke

Pharmaceutical evaluation of glibenclamide products available in the Jordanian market 1464
Dina El-Sabawi, Sa'ed Abbasi, Suzan Alja'fari, Imad I. Hamdan

African Journal of Pharmacy and Pharmacology

Table of Contents: Volume 7 Number 22 15 June, 2013

ARTICLES

Research Articles

Acetylcholinesterase inhibitors used or tested in Alzheimer's disease therapy; their passive diffusion through blood brain barrier: In vitro study 1471
Jana Zdarova Karasova, Jan Korabecny, Filip Zemek, Vendula Sepsova, Kamil Kuca

Design and optimization of self-nanoemulsifying drug delivery systems of simvastatin aiming dissolution enhancement 1482
Hanaa Mahmoud, Saleh Al-Suwayeh, Shaimaa Elkadi

Investigation of factors effected dissolution variations of hydroxypropyl methylcellulose capsule 1501
Chuanfeng Tong, Zhiquan Wang, Ya Zhong, Min Zhen

In vitro antioxidant, analgesic and cytotoxic activities of *Sepia officinalis* ink and Coelatura aegyptiaca extracts 1512
Sohair R. Fahmy, Amel M. Soliman

Synthesis and neuropharmacological evaluation of some new isoxazoline derivatives as antidepressant and anti-anxiety agents 1523
Jagdish Kumar, Gita Chawla, Himanshu Gupta, Mymoona Akhtar, Om prakash Tanwar, Malay Bhowmik

academicJournals

Vol. 7(22), pp. 1426-1437, 15 June, 2013
DOI 10.5897/AJPPX12.004
ISSN 1996-0816 © 2013 Academic Journals
http://www.academicjournals.org/AJPP

African Journal of Pharmacy and Pharmacology

Review

Differentiation of stem and progenitor cells from bone marrow in activated dendritic cells and lymphocytes with anti-malignant properties

Iskra Ventseslavova Sainova*, Ilina Valkova, Velichka Pavlova and Elena Nikolova

Institute of Experimental Morphology, Pathology and Anthropology with Museum-Bulgarian Academy of Sciences, 1113 Sofia, Bulgaria.

Accepted 24 April, 2013

Dendritic cells (DCs) have been characterized as powerful antigen-presenting cells (APCs), which possess the abilities for immune modulation and are used in composition of anti-malignant vaccines and gene-engineered products. By appropriate cultivation, modifications of DCs have shown abilities for an enhanced expression of specific effector molecules. Studies on their biology are focused on their role as main immune response modulators. These properties characterize them as promising candidates for construction of novel safe vaccines and gene-engineered products. In this direction, attention is directed to development of methods and techniques for transduction of *in vitro*- and/or *ex vivo*-cultivated DCs with previously designed recombinant viral vectors with inserted genes, coding respective malignant antigens. Studies on the biology of lymphocytes are mainly focused on their role in cellular and humoral immune response. Their cultivation and differentiation in the presence of appropriate antigens, on one hand, and by appropriate modifications, on the other hand, have shown the abilities for an enhanced expression of specific effective molecules. These properties have characterized them as promising candidates for construction of novel safe vaccines and gene-engineering products.

Key words: Stem/progenitor cells, dendritic cells, lymphocytes, cell differentiation, recombinant viral vectors/gene constructs, malignant disorders, immunity.

INTRODUCTION

Dendritic cells (DCs) have been found to play a pivotal role in initiating the immune response, including powerful antigen-presenting cells (APCs) (Arthur et al., 1997; Avigan, 2004; Bonini et al., 2001; Bubenik, 2001; Caux et al., 1992; Clark et al., 1992; Gong et al., 1997; Hassan et al., 2000; Inaba et al., 1992; Kaplan et al., 1999; Kim et al., 1994; Reid et al., 1992; Ribas et al., 1997; Siena et al., 1995; Yongqing et al., 2002). In the light of their unique properties, these cells have been proposed as powerful immunomodulation agents, including in the composition of novel vaccines and gene-engineering products for treatment of malignant disorders.

Primitive hematopoietic stem cells (HSCs) have been found to be hierarchically ordered on the basis of quiescence, the most primitive of these, characterized by their Rh/Ho (dull) phenotype and their capacity for long-term hematopoietic reconstitution, are not dormant, but they have been established to cycle slowly in normal steady-state bone marrow (Ballas et al., 2002; Bradford et al., 1997; Bradley et al., 2002; Cheng et al, 1998; Gunechea et al., 2000; Koido et al., 2007; Lai and Kondo, 2007; Le Blannk and Ringden, 2005). Unrelated human MSCs have not been found to elicit T-cell activation *in vitro* and to suppress T-cell activation by tuberculin and unrelated

*Corresponding author. E-mail: iskrasainova@gmail.com

allogeneic lymphocytes in a dose-dependent manner. It has been reported that the Lin-IL-7R+Thy-1-Sca-1loc-Kit(lo) population from adult mouse bone marrow possess a rapid lymphoid-restricted (T-, B-lymphocytes, as well as natural killer (NK) cells) reconstitution capacity *in vivo*, but completely lacked myeloid differentiation potential both *in vivo* and/or *in vitro* (Bovia et al., 2003; Kobari et al., 2001). A single Lin-IL-7R+Thy-1-Sca-1loc-Kit(lo) cell has been established to be able to generate at least both T- and B-cells (Amirayan et al., 1995; Bovia et al., 2003; Bregenholt et al., 1996; Dallas et al., 2007; Gray-Parkin et al., 2002; Green et al., 1992; Ikuta et al., 1990; Jackson and Bell, 1990; Kondo et al., 1997). These data have provided direct evidence for the existence of common lymphoid progenitors in sites of early hematopoiesis. Interferons (IFNs) and protein-kinases (PKRs) have demonstrated abilities to sensitize cells to apoptosis predominantly through the FADD/caspase-8 pathway.

Complex mechanisms, which include molecular, genetic and cellular components, such as *Wnt*-, BMP- and *Notch/Delta*-signaling pathways, have been found to underlie differentiation and functions of stem cells (Caux et al., 1992; Ribas et al., 1997; Terskikh et al., 2006; Vogelstein and Kinzler, 2004). By use of real time poly-merase chain reaction (RT-PCR), an ability for initiation of erythroid (β-globin) and/or myeloid (myeloperoxidase) gene expression programs by the same cell prior to exclusive commitment to the erythroid, myeloid lineages for it has been shown (Bonini et al., 2001; Caux et al., 1992; Curti et al., 2001; Davis et al., 1996; Inaba et al., 1992; Reid et al., 1992; Siena et al., 1995).

These data have supported a model of hematopoietic lineage specification, in which unilineage commitment has been prefaced by a “promiscuous” phase of multilineage locus activation (Bonini et al., 2001; Curti et al., 2001; Engelmayer et al., 2001; Reid et al., 1992; Siena et al., 1995). Protein BCL-6 has also been detec-table in inter- and intra-follicular CD4+ T-cells, but not in other follicular components, including B-cells, plasma cells, monocytes/macrophages and DCs. Genes poten-tially important in myeloid differentiation, such as coding granulocyte colony-stimulating factor (G-CSF) and the enzyme myeloperoxidase, have been found to be located close to the breakpoint in the *t(15;17)*, but have not been conclusively shown to be rearranged in this chromosomal translocation (Bonini et al., 2001; Engelmayer et al., 2001; Reid et al., 1992; Siena et al., 1995).

It has also been proposed that the commitment of common myeloid progenitors to either the megakaryocyte /erythrocyte or the granulocyte/ macrophage lineages are mutually exclusive events (Bonini et al., 2001; Caux et al., 1992; Curti et al., 2001; Hassan et al., 2000; Reid et al., 1992; Siena et al., 1995). It has been concluded that active cell cycling of bone marrow cells, induced by cytokine stimulation, is probably very often associated with an engraftment defect in the normal host, and derangement of these pathways within stem cells, as well as the apparent lineage and differentiation status, have been found to play an important role in the development of malignancies.

In agreement with representing a lymphoid primed progenitor, Lin-Sca-1+c-kit+CD34+Flt3+ cells have been established to display up-regulated IL-7 receptor gene expression (Amirayan et al., 1995; Bregenholt et al., 1996; Dallas et al., 2007; Gray-Parkin et al., 2002; Green et al., 1992; Ikuta et al., 1990; Jackson and Bell, 1990; Kondo et al., 1997). Based on these observations, a revised road map for adult blood lineage development has been proposed. Protein Klotho has been indicated to be able to regulate B-lymphopoiesis via its influence on the hematopoietic microenvironment. SUMO-2 and SUMO-3 have been found as localized to chromosome earlier and accumulated gradually during telophase. These findings have demonstrated that mammalian SUMO-1 shows patterns of utilization that are clearly discrete from the patterns of SUMO-2 and SUMO-3 throughout the cell cycle, arguing that it is functionally distinct and specifically regulated *in vivo*, and on the other hand, that myeloid progenitor number and developmental potential do not decline with age indicates that B-lymphopoiesis is particularly sensitive to defects that accumulate during senescence (Amirayan et al., 1995; Bregenholt et al., 1996; Dallas et al., 2007; Gray-Parkin et al., 2002; Green et al., 1992; Ikuta et al., 1990; Jackson and Bell, 1990; Kondo et al., 1997; Kobari et al., 2000; Lazarus et al., 2005). Diseases and disorders, connected with retardations in these processes, have been defined as clone HSCs malignancies, characterized by independency and/or hypersensitivity of HSCs and/or of haematopoietic precursors to numerous cytokines. In many patients with such diseases, a mutation in such gene has been established, and its presence in erythropoietin-independent erythroid colonies have demonstrated a link with growth factor hypersensitivity, which has been characterized as a key biologic feature of these disorders (Sell, 2004).

Mesenchymal stem cells (MSCs) have been indentified in bone marrow as well as in other tissues of the joint, including adipose, synovium, periosteum, perichondrium, and cartilage, as well as to modulate immune responses, exhibit healing capacities, improve angiogenesis and prevent fibrosis (Djouad et al., 2009; Maitra et al., 2004; Terskikh et al., 2006). These properties have charac-terized these cells as usable for therapeutic applications in many different diseases and disorders. MSCs have also proved abilities to support tissue repair, angiogenesis and concomitant immunomodulation and to provide tissue-specific functional biodiversity, additionally mediated by direct cell-cell communications via adhesion molecule and by exchange of cytokines, exosomes and micro-RNAs (Hass and Otte, 2012; Maitra et al., 2004; Terskikh et al., 2006 Maitra et al., 2004; Terskikh et al., 2006). These features allow MSCs be used for treatment

of various morbid and degenerative processes (Kang et al., 2012; Ra et al., 2011).

BIOLOGICAL PROPERTIES OF DENDRITIC CELLS AND THEIR ROLE IN GENERATION OF ADEQUATE IMMUNE RESPONSE

In the past years, the development of novel therapeutic strategies with DCs has become extensively investigated (Arthur et al., 1997; Bonini et al., 2001; Bubenik 2001; Caux et al., 1992; Clark et al., 1992; Gong et al., 1997; Hassan et al., 2000; Inaba et al., 1992; Kaplan et al., 1999; Kim et al., 1994; Reid et al., 1992; Ribas et al., 1997; Siena et al., 1995; Wang et al., 1995). According to many literature data, granulocyte-macrophage colony-stimulating factor (GM-CSF) mobilizes CD34+ bone marrow progenitor cells both *in vitro* and *in vivo* with an increased frequency and generation of DCs with anti-malignant properties (Banchereau et al., 2000; Caux et al., 1992; Curti et al., 2001; Inaba et al., 1992; Lehtonen et al., 2007; Reid et al., 1992; Siena et al., 1995). In DCs, but not in macrophages, basal expression of SOCS-1 has been detected (Figure 1) (Lehtonen et al., 2007).

Specific protein inhibitors from the SOCS family have been proven as modulators of the activated DCs by IL-4 and GM-CSF cytokine signaling via the JAK/STAT pathway. Similarly, the addition of GM-CSF plus tumor necrosis factor-α (TNF-α), has been found to induce development of DCs from purified CD34+ cells of bone marrow, cord blood and peripheral blood (Caux et al., 1992; Reid et al., 1992; Siena et al., 1995). The critical role of TNF-α for the differentiation of DCs has been supported by the demonstration that this cytokine induces the expression of molecule CD40 on CD34+ cells (Curti et al., 2001; Reid et al., 1992; Siena et al., 1995). Besides that, CD34+/CD40+ cells have been found to express only myeloid markers, significantly increase alloantigen presenting function, compared with total CD34+ cells, and have also given rise to high numbers of DCs. Modulation of DCs differentiation from these bipotent CD34+/CD40+ cells during the later stages of their cultivation, has also been shown by cytokine interleukin-4 (IL-4). On the other hand, appropriate modifications of DCs to express tumor-antigens by *in vitro* and/or *ex vivo*-transfer of genes, coding respective antibodies, has been suggested. Taken together, these data have revealed abilities for development of different therapeutic strategies of DCs for immunotherapy of malignant diseases.

DEVELOPMENT OF NOVEL THERAPEUTIC STRATEGIES WITH DENDRITIC CELLS

The antigen-presenting functions of DCs, could theo-retically be exploited as a new therapeutic tool in cancer therapy in order to amplify immune responses against tumor-specific antigens (Arthur et al., 1997; Avigan, 2004; Bennett et al., 2001; Bonini et al., 2001; Bubenik, 2001; Caux et al., 1992; Clark et al., 1992; Gong et al., 1997; Hassan et al., 2000; Inaba et al., 1992; Kaplan et al., 1999; Kim et al., 1994; Reid et al., 1992; Ribas et al., 1997; Siena et al., 1995). Promising results from clinical trials in patients with malignant lymphoma, melanoma and prostate cancer, have suggested that immuno-therapeutic strategies that take advantage of the antigen presenting properties of DCs, might ultimately prove both efficacious and widely applicable against human malignancies (Fong and Engelman, 2000). Besides that, genetically-modified cells have been widely tested in pre-clinical studies, including anti-malignant agents (Arthur et al., 1997; Avigan, 2004; Bennett et al., 2001; Bonini et al., 2001; Borysievicz et al., 1996; Engelmayer et al., 2001; Eo et al., 2001; Frasca et al., 2006; Gong et al., 1997; Kaplan et al., 1999; Panicali and Paoletti, 1982; Reid et al., 1992; Ribas et al., 1997; Siena et al., 1995; Wang et al., 1995; Wildner and Morris, 2000; Yongqing et al., 2002).

DEVELOPMENT OF NOVEL THERAPEUTIC STRATEGIES WITH HYBRID CELLS, PREPARED BY FUSION OF DENDRITIC AND MALIGNANT CELLS

As alternative method for delivery into DCs, their fusion with tumor cells has been utilized, as well as the hybrid cell-based vaccines have shown high therapeutic activity, even in patients with malignant diseases (Avigan, 2004; Gong et al., 2000; Hiraoka et al., 2004; Walden, 2000; Yongqing et al., 2002). Induced by vaccination with dendritic/tumor fusion cells, antitumor immunity has reacted differently to injected malignant cells and autochthonous malignancies (Xia et al., 2003). It has also been shown that immunization with such fusion cells induces rejection of established metastases (Gong et al., 1997). The observed greatly reduced number of established pulmonary metastases both with and without *in vivo*-administration of IL-2 adoptive transfer of T-cells derived from B16/DC vaccine-primed lymph nodes into B16 tumor-bearing mice has suggested a role for the cells, developed by fusion of malignant cells with DCs hybrid products, as effective cellular vaccines for eliciting T-cell-mediated anti-malignant immunity (Wang et al., 1998). Hybrid cells, developed by fusion between DCs and tumor cells, have been found to express both major histocompatibility complex (MHC) class I- and class II-restricted tumor-associated epitopes and might, therefore, be useful for the induction of tumor-reactive CD8+ and CD4+ T-lymphocytes both *in vitro* and in human vaccination trials (Parkhurst et al., 2003). It has also been demonstrated that immunization with such vaccines, developed by fusion of DCs with mouse 4TOO plasmacytoma cells FC/4TOO hybrid fusion cells plus IL 12 potentiates anti-malignant immunity and the treatment of murine multiple myeloma (Gong et al., 2000; 2002).

Findings about fusions of ovarian cancer cells to autologous or allogeneic DC induced cytolytic T-cell activity and lysis of autologous malignant cells by a MHC class I-restricted mechanism, have suggested that fusions of such malignant cells and DCs activate T-cell responses against autologous malignancies, and the fusions are probably functional, when they are generated with either autologous or allogeneic DCs. It has also been demonstrated that sequential stimulation with hybrid cells, derived by fusion of DCs with breast carcinoma fusion cells and anti-CD3/CD28, results in a marked expansion of activated tumor-specific T-lymphocytes, which has suggested these fusion cells are probably effective antigen-presenting cells (APCs), which stimulate inhibitory T-cells that limit vaccine efficacy (Vasiri et al., 2008). On the other hand, the results, according to which the *ex vivo*-exposure of DCs to TGF-β has not appeared to lessen the efficacy of DCs vaccines, suggest that tumor-derived TGF-β probably reduces the efficacy of DC/malignant cell hybrid fusion vaccine via an *in vivo*-mechanism, and the neutralization produced by the fusion cells TGF-β might enhance the effectiveness of DCs-based immunotherapy (Kao et al., 2003). The immunogenicity of a DCs/malignant cells fusion hybrid cells-based vaccines has been increased by heat-treated tumor cells (Koido et al., 2007).

DEVELOPMENT OF NOVEL THERAPEUTIC STRATEGIES WITH CELLS BY INSERTION OF ADDITIONAL CYTOKINE GENES AND ANTIGENS BY TRANSFECTION WITH RECOMBINANT GENE CONSTRUCTS

It has been demonstrated that initial materials for gene-engineering manipulations could be used by both DNA- and RNA-viruses, as well as bacterial plasmids and yeast's genomes (Arthur et al., 1997; Avigan, 2004; Bennett et al., 2001; Bonini et al., 2001; Borysievicz et al., 1996; Bubenik, 2001; Chen et al., 1997; Chun et al., 1999; Domi and Moss, 1995; Engelmayer et al., 2001; Eo et al., 2001; Frasca et al., 2006; Gambotto et al., 1999; Gong et al., 1997; Guenechea et al., 2000; Hass et al., 2000; Kaplan et al., 1999; Kauffman et al., 2001; Martinet et al., 1997; Palese and Roizman, 1996; Panicali and Paoletti, 1982; Reid et al., 1992; Ribas et al., 1997; Siena et al., 1995; Wang et al., 1995; Wildner and Morris, 2000; Yongqing et al., 2002). This indicates eventual existence of a possibility for insertion of genes, coding cell receptors, cytokines, enzymes, complement components, apoptosis activators and/or inhibitors, surface antigens, as well as markers for malignancy. Many studies have suggested that hybrid viral vector systems could improve the suicide gene therapy of tumors. These results would have significant implications for the improvement of clinical gene therapy in HIV/AIDS and malignantdiseases.Inasimilarway,theobservedelimination of the protective effect in depletion of CD8+ T-lymphocytes, but not of CD4+ T-cells *in vivo* from animals, vaccinated with vaccines, developed on the basis of *adenoviral* genome recombinant gene construct *Ad2CMV-gp100* mice, containing gene for glycoprotein (*gp*) from *cytomegalovirus* (*CMV*) genome, has suggested that these virus recombinants, encoding tumor antigens, could probably be useful as vaccines to induce specific T-cell immunity for therapy of malignant diseases.

DEVELOPMENT OF NOVEL THERAPEUTIC STRATEGIES WITH DENDRITIC CELLS, CONTAINING ADDITIONAL CYTOKINE GENES AND ANTIGENS BY TRANSFECTION WITH RECOMBINANT GENE CONSTRUCTS

In investigation on the role of intra-tumor treatmet on the survival of tumor-bearing experimental animals with herpes-simplex virus (HSV), expression of IL-4 has been found to prolong their survival, whereas expression of IL-10 to reduce it (Bennett et al., 2001; Hassan et al., 2000; Liu et al., 2005; Panicali and Paoletti, 1982; Wildner and Morris, 2000). These finding have suggested further investigation on the improvement in the combination of oncolytic viral therapy and immunomodulatory strategies. They have also supported the full use of recombinant *adenovirus*-transduced DCs for *in vivo*-immunization against tumor-associated antigens. In laboratory conditions, human DCs, transduced with recombinant virus gene construct *AdV/IL-10*, have been shown to inhibit mixed leukocyte culture, reduced cell surface expression of co-stimulatory molecules CD80/CD86, as well as exhibited inability for production of the potent allo-stimulatory cytokine IL-12 (Coates et al., 2001). In investigation on the *in vivo*-properties of the so modified DCs, skin transplantation of humanized immunodeficient non-obese diabetic/severe combined immunodeficient (NOD/SCID) mice, engrafted with human skin, reconstituted via intra-peritoneal injection with allogeneic mononuclear cells (MNCs) mixed with 1×10^6 autologous to the skin donor DCs, transduced with either recombinant virus gene construct *AdV/IL-10* or of recombinant viral vector *AdV/MX-17*, a reduced skin graft rejection, characterized by reduced infiltration with mononuclear cells and less dermo-epidermal junction destruction in comparison with the animals with inoculation of DCs, modified with the control virus alone, has been observed. Transduced by appropriate *adenoviral* gene constructs, immature DCs have shown the abilities to differentiate in different directions in respective appropriate conditions of cultivation (Addison et al., 1995; Chen et al., 1997; Dietz and Vuk-Pavlović, 1998; Gambotto et al., 1999; Lu et al., 1998). For example, in the presence of monocyte-conditioned medium, they have indicated ability to express the surface markers

of mature DCs, such as CD25, CD83, high levels of molecules CD86 and HLA-DR, or to secrete of IL-12. Their ability to induce T-cell growth has also been enhanced. Similarly, in transfer of bacterial gene *lacZ*, coding the enzyme beta-galactosidase by *recombinant retrovirus* gene constructs in human DCs, increased expression levels of MHC class I and II molecules, as well as of CD1a, CD80, CD86, CD13, CD33, CD40 and CD54 has been demonstrated (Aicher et al., 1997). So modified DCs have also shown high stimulatory activity in both allogeneic and autologous mixed lymphocyte reaction (MLR). These data have also supported the efficiency of the recombinant viral vectors in studies on the biology of DCs, including the expression of specific antigens for active immune therapy (Aicher et al., 1997; Dietz and Vuk-Pavlović, 1998; Lu et al., 1998).

COMBINED THERAPEUTIC STRATEGIES WITH DENDRITIC CELLS

For further increase of the potency of the vaccine, a combined variation of both technologies has been applied, in which interleukin-18-transfected DCs have been used to prepare dendritic cells-tumor cells conjugates (Wen et al., 2001). Immunization with such conjugates has significantly increased the production of Th1 cytokine-producing cells, the number of antigen-specific CD8+ T-cells, as well as the anti-malignant immunity.

However, the fact that an increased Th1 cytokine production and stronger anti-malignant effect have not been observed in mice, depleted of IFN-γ, has also supported the maintenance of DCs/malignant cells conjugates as potent anti-malignant vaccines, and interleukin-18 could be additionally administered by gene transfection of cells for enhancement of this immunity, which is probably mediated mainly by IFN-γ. Immunization with gene-modified hybrid products, derived by fusion of DCs with malignant cells, received by their fusion with *IL-12* gene-transferred cancer cells, has shown an ability to elicit a previously enhanced anti-malignant effect in experimental therapeutic models *in vivo* (Suzuki et al., 2005). It has also been indicated that a hybrid vaccine, based on *GM-CSF* gene-modified DCs, might be an attractive strategy for anti-malignant immunotherapy with potentially increased therapeutic efficacy (Cao et al., 1999). Immunization of mice with engineered *DCRMAT/J558-IL-4* hybrids *in vitro* has elicited stronger J558 tumor-specific CTLs responses and has also induced more efficient protective immunity against J558 tumor challenge, and respectively, *in vivo* in comparison of hybrid vaccines *DCRMAT/J558* (Liu, 2003). Similar results have been observed in immunization of C57BL/6 mice with gene-engineered *DC/J558-IL-4* hybrids (Xia et al., 2005). It has also been demonstrated that gene-engineered fusion hybrid vaccines, could be an attractive strategy for cancer immunotherapy. These results have indicated that gene-engineered fusion hybrid vaccines, combined with gene-modified tumor and DCs vaccines, as well as their combination with Th1 gene-modified tumor with DCs, might be attractive strategies for cancer immunotherapy (Liu, 2003; Xia et al., 2004).

DEVELOPMENT OF NOVEL THERAPEUTIC STRATEGIES BY LYMPHOCYTE ELIMINATION AND DIFFERENTIATION THERAPY

By understanding molecular basis, gene expression mechanisms and signaling pathways, which are involved in development and differentiation of HSCs, development of differentiation therapy and elimination therapy strategies have been developed (Cheung et al., 2003). A mutation in one or more genes, which are included in any of the mentioned cascade mechanisms, could be characterized as a probable key biologic feature of these disorders. The most common example is transplantation of allogenic HSCs with graft versus leukemia effect (Figures 1 and 2) (Amirayan et al., 1995; Bregenholt et al., 1996; Cheung et al., 2003; Dallas et al., 2007; Glymcher and Murphy, 2000; Gray-Parkin et al., 2002; Green et al., 1992; Ikuta et al., 1990; Jackson and Bell, 1990; Kondo et al., 1997).

DEVELOPMENT OF NOVEL THERAPEUTIC STRATEGIES BY LYMPHOCYTE DIFFERENTIATION ON THE INFLUENCE OF RECOMBINANT VACCINES, CARRYING SPECIFIC ANTIGENS

Vaccination strategies with recombinant *poliovirus* vectors have induced protective immunity against challenge with lethal doses of ovalbumin-expressing malignant melanoma cell line (Mandl et al., 1998). Similarly, novel mechanisms, by which *vaccinia virus* has been found to interfere with the onset of host immune responses by blocking the interferon-gamma (IFN-γ-) signal cascade mechanism through the dephosphorylating activity of the viral phosphatase VH1, have been revealed. Tumor infiltrating lymphocytes isolated from metastatic melanoma patients have been characterized as predominantly cytotoxic T-lymphocytes (CTLs) with an ability to recognize and kill autologous tumor cells after their *in vitro*-cultivation (Borysiewicz et al., 1996; Hodge et al., 1997; Overwijk et al., 1999; Tsang et al., 1995). In mice, inoculated with *IL-15*-expressing *vaccinia virus* in addition to an increase in NK cells in the spleen, enhanced expression of interleukin-12 (IL-12) and IFN-γ, as well as induction of cytokines, has been established. In this way, a possibility for cytokine influence on the response mediated by human HSV therapy, has been suggested, which could probably be due to the host immune response (Andreansky et al., 1998; Liu et al., 2005). Thus, cytokine expression might be an important adjunct to tumor therapy utilizing genetically engineered

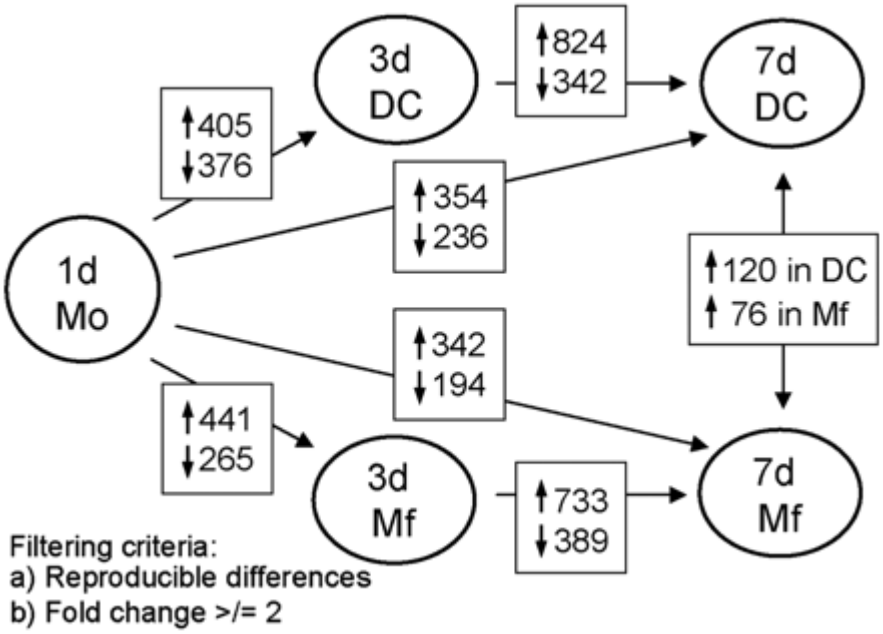

Figure 1. Experimental set-up and numbers of regulated genes during macrophage and DC differentiation (Lehtonen et al., 2007).

HSV. However, in this experimental model system, the degree of attenuation in viral virulence, attained with co-expression of IL-15, has been much less than that, achieved with co-expression of IL-2, which has suggested that the response, mediated by peripheral NK cells, is probably stronger to IL-2 than to IL-15. Immunohistochemical analyses of mouse brains after viral inoculation have shown marked accumulation of inflammatory cells, composed primarily of monocytes/macrophages/microglia, with various proportions of CD8+ and CD4+ T-cells (Figures 2 and 3) (Glymcher and Murphy, 2000), as well as few B-lymphocytes (Andreansky et al., 1998). These results have also implied that virus-encoded inhibitors of apoptosis, such as the caspase-8 inhibitor CrmA, could block the IFN-mediated apoptosis, and therefore, they are probably able to constitute an alternative family of inhibitors of IFNs in the cell.

In *CEA*-transgenic mouse model of anti-tumor effects in terms of survival, CD8+ and CD4+ responses, specific for carcino-embryonic antigen (CEA), have been observed (Figures 2 and 3) (Glymcher and Murphy, 2000; Tsang et al., 1995). The utilization of a diversified immunization scheme, using a recombinant *vaccinia virus*, followed by recombinant *avian pox virus*, has been shown to be far superior to the use of either one alone in eliciting CEA-specific T-cell responses (Hodge et al., 1997). These studies have demonstrated that the use of cytokines and diversified prime and boost regimens could be combined with the use of recombinant viral vectors, expressing multiple co-stimulatory molecules to further amplify T-cell responses. IL-2 has also been found to induce their proliferation and to augment their cytotoxic activity such that they eliminated autologous malignant cells.

The addition of GM-CSF to *rF-CEA* or *rF-CEA/TRICOM* vaccinations via the simultaneous administration of recombinant viral vector *rF-GM-CSF* has enhanced CEA-specific T-cell response (Sadegah et al., 2000). Because protein Bcl-3 has been characterized as a member of inhibitors from the subfamily the Nuclear Factor-kappaB (NFκB), a regulation mechanism on the apoptosis and survival of activated T-cells, supported by the balance in the concentration of various members of this family, has been suggested (Glymcher and Murphy, 2000; Mitchell et al., 2001). It has also been proposed that the deliberate induction of self-reactivity by use of a recombinant viral vector, could lead to tumor destruction, but CD4+ T-lymphocytes (Figure 3) are probably an integral part of this process, and hence, targeting tissue differentiation antigens vaccine strategies might be valuable in malignancies, arising from non-essential cells, tissues and organs, such as melanocytes, prostate, testis, breast and ovary (Aruga et al., 1997; Glymcher and Murphy, 2000; Grosenbach et al., 2001; Itoh et al., 1995; 1986; Kent et al., 1998; Rosenberg, 1996; Rosenberg et al., 1994; Siders et al., 1998; Wang et al., 1995; Zhai et al., 1996). Treatment of patients with metastatic melanoma with tumor-infiltrating lymphocytes (TILs) and IL-2 has resulted in objective immune responses in them.

Studies on the specific T-cell responses via stimulation of peripheral blood lymphocytes with specific peptide epitopes from the CEA have demonstrated clear differences in establishment of T-cell lines post-immunization. These lines have been CD8+ and/or CD4+/CD8+, to lyse cells, transformed by *Epstein-Barr virus* (*EBV*) B-

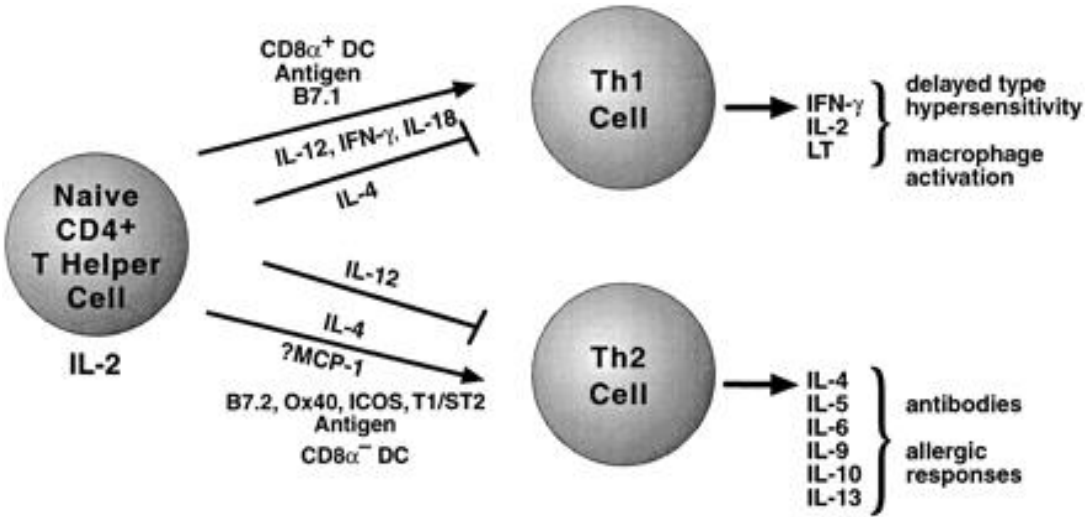

Figure 2. Signals, influencing differentiation of T-helper lymphocytes (Glymcher and Murphy, 2000).

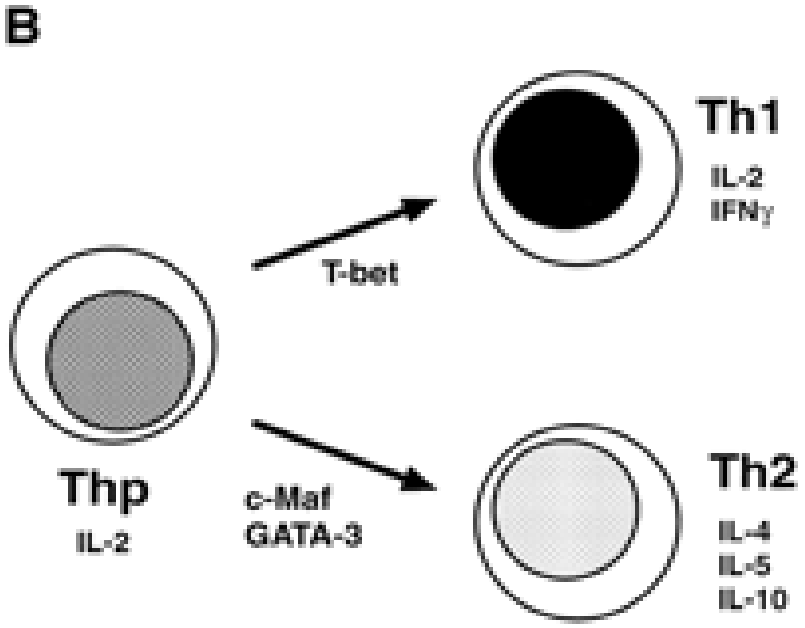

Figure 3. Transcription factors, influencing differentiation of T-helper lymphocytes (A); Tissue-specific factors that regulate $CD4^+$ T-helper cell differentiation (B) (Glymcher and Murphy, 2000).

lymphocytes and transduced with gene *CEA*, and to lyse CEA-positive carcinoma cells in a human leukocyte antigens (HLA) restricted manner (Hodge et al., 1997; Sadegah et al., 2000; Tsang et al., 1995). It has also been suggested as a model ofmetastatic growth inhibition, mediated by non-lymphocyte effective cells, including monocytes/ macrophages, neutrophils and anti-angiogenic chemokines/cytokines (Itoh et al., 1986). As a result, these effective molecules could be expressed by *HSV* in productively infected cells both *in vitro* and *in vivo*. *HSV*, expressing genes *IL-4* and/or *IL-10*, has shown an ability to infect and destroy glioma cells *in vitro* (Andreansky et al., 1998). Similarly, intra-cerebral inoculation of *HSV*, expressing either IL-4 or IL-10 into syngeneic mouse glioma GL-261 cells, implanted in the brains of immune-competent C57BL/6 mice, have been found to produce dramatically opposite physiologic responses. It has also been shown that *IL-4-HSV* significantly prolonged survival of tumor bearers, whereas tumor-bearing mice, receiving the *IL-10-HSV*, have had a median survival, identical to that of saline treated controls (Andreansky et al., 1998; Hassan et al., 2000; Liu et al.,

2005). These studies could have direct bearing on the design of vaccine clinical trials for infectious agents and/or malignancy-associated antigens, in which T-lymphocyte co-stimulatory molecules would be employed to enhance antigen-specific T-cell responses.

In examination of the clinical and environmental safety and immunogenicity in the first clinical trial of a live recombinant *vaccinia virus*, expressing proteins E6 and E7 of types 16 and 18 of *human papilloma virus* (*HPV*), in each patient has been found an anti-*vaccinia virus* antibody response and three of the eight patients have developed an *HPV*-specific antibody response (Adams et al., 2001). In one of three available patients, *HPV*-specific CTLs have also been detected. As highly effective method, with no significant toxicity in mice, gene therapy strategies for treatment of malignant disorders by using of recombinant *adenoviral* vectors, containing gene *IL-12*, have been characterized (Cordier et al., 1995; Tozola et al., 1997). In vaccination with synthetic RAS peptide, representing mutation *k-ras* in their malignant diseases, a transient *ras*-specific T-lymphocyte response has been induced (Kung et al., 2000). These results have indicated that specific T-cell responses against uniquely harbored mutations in malignant cells could be induced in cancer patients by vaccination. In this way, recombinant *adenoviral* gene constructs, encoding malignant antigens, have been proven as useful vaccines, inducing specific T-lymphocyte immunity for therapy of malignant disorders (Cordier et al., 1995; Tozola et al., 1997).

DEVELOPMENT OF NOVEL THERAPEUTIC STRATEGIES WITH LYMPHOCYTES AND THEIR PRECURSORS BY INSERTION OF ADDITIONAL CYTOKINE GENES AND ANTIGENS WITH RECOMBINANT GENE CONSTRUCTS

Human T-lymphocytes have shown abilities to be efficiently transduced under clinically applicable conditions, by *adenoviral* gene constructs after 7 days of culture, in the presence of IL-2 and/or IL-7 (Di Nicola et al., 1999; Rosenberg et al., 1998; Zhang et al., 1996). A significant improvement in transduction efficiencies of mouse and human T-lymphocytes by a prolonged pre-incubation with IL-2 and by the addition of the recombinant *adenoviral* vector *Lipofectamine* has also been indicated (Di Nicola et al., 1999). In transfer of chimeric immune receptor genes, ligated into vector *pMSCVneo*, in human lymphocytes, a mediated antigen-specific non-MHC-restricted cytokine release and malignancy cytotoxicity, as well as inhibition of human xenograft engraftment in experimental mice with severe immunodeficiency, combined with non-obese diabetes (NOD/SCID), has been observed (Douglas et al., 2001). Similarly, a clinically applicable protocol that meets good clinical practice criteria regarding the gene system for transduction and expansion of primary human T-lymphocytes, in which recombinant gene construct, encoding a single chain FvG250 antibody chimeric receptor (ch-Rec), specific for a RCC-associated antigen (TAA), has been designed in preparation of a clinical phase I/II study in patients with renal cell carcinoma (RCC) (Douglas et al., 1999; Lamers et al., 2002; Wu et al., 1999; Zhou et al., 2003). According to the results from other studies, evidence of increase of the anti-malignant effect *in vivo* of lymphocytes, transduced by recombinant *herpesviral* gene construct *HSVtk-DLI*, has been provided (Burt et al., 2003). The observed enhanced cytotoxicity of TILs, transduced with recombinant *retroviral* vector with insertion of gene for TNF, has been ascribed to autocrine effects of this cytokine, which has probably included augmentation of adhesion molecules (CD2 and CD11a) and IL-2 receptor expression, as well as elevation of production of IFNs, lymphotoxin, GM-CSF, as well as their paracrine effects on target cells to facilitate them to be differentiated and genetically-modify lymphocytes (Rosenberg et al., 1990). Treatment with TILs, transduced with *retroviral*-mediated gene transduction to introduce gene, connected with neomycin resistance, plus addition of cytokine IL-2, has also been proven to mediate the regression of metastatic melanoma (Guenechea et al., 2000; Hass et al., 2000). These data have confirmed the feasibility and safety of strategies, based on recombinant *retroviral* vectors gene transfer for human gene therapy and have implications for the designing of TILs with improved anti-malignant potency, as well as for the possible use of lymphocytes for the gene therapy of other diseases (Zhang et al., 2004; Zhang et al., 2002).

Conclusion

DCs and lymphocytes have been characterized as hopeful vehicles for appropriate modulation of the immune response in the presence of appropriate growth factors, cytokines and specific antigens. In this way, they have shown abilities for differentiation in respective directions in the presence of appropriate recombinant viral gene constructs, coding respective antigens, on one hand, and as cell vaccines by gene-engineering manipulations with recombinant vectors, carrying genes for respective malignant antigens or cytokines, on the other. These properties characterize them as promising candidates for construction of novel and safe therapeutic products on their basis, by use of new technologies.

REFERENCES

Adams N, Borysiewicz L, Fiander A, Man S, Jasani B, Navabi H, Lipetz C, Evans AS, Mason M (2001). Clinical studies of *human papilloma* vaccines in pre-invasive and invasive cancer. Vaccine 19(17-19):2549–2556.

Addison C, Braciak T, Ralston R, Muller WJ, Gauldie J, Graham FL (1995). Intratumoral injection of an *adenovirus* expressing interleukin-2 induces regression and immunity in a murine breast cancer model. Proc. Natl. Acad. Sci. USA 92:8522–8526.

Aicher A, Westermann J, Cayeux S, Willimsky G, Daemen K, Blankenstein T, Uckert W, Dörken B, Pezzutto A (1997). Successful *retroviral* mediated transduction of a reporter gene in human dendritic cells: feasibility of therapy with gene-modified antigen presenting cells. Exp. Hematol. 25(1):39-44.

Amirayan AN, Furrie E, Deleuil F, Mellor A, Leserman L, Machy P (1995). Influence of MHC class I molecules on T-cell proliferation induced by CD3 or Thy-1 stimulation. Immunology 86:71-78.

Andreansky SS, He B, van Cott J, McGhee J, Markert JM, Gillespie GY, Roizman BR, Whitley J (1998). Treatment of intracranial gliomas in immunocompetent mice using *herpes simplex viruses* that express murine interleukins. Gene Ther. 5:2177–2185.

Arthur J, Butterfield L, Roth MD, Bui LA, Kiertscher SM, Lau R, Dubinett S, Glaspy J, McBride WH, Economou JS (1997). A comparison of gene transfer methods in human dendritic cells. Cancer Gene Ther. 4:1023–1028.

Aruga A, Aruga E, Cameron MJ, Chang AE (1997). Different cytokine profiles released by CD4+ and CD8+ tumor-draining lymph node cells involved in mediating tumor regression. J. Leukoc. Biol. 61:507–516.

Avigan D (2004). Dendritic cell-tumor fusion vaccines for renal cell carcinoma. Clin. Cancer Res. 10:6347S-6352S.

Ballas CB, Zielske SP, Gerson SL (2002). Adult bone marrow stem cells for cell and gene therapies: implications for greater use. J. Cell. Biochem. Suppl. 38:20–28.

Banchereau J, Briere F, Caux C, Davoust J, Lebesque S, Liu YJ, Pulendran B, Palucka K (2000). Immunobiology of dendritic cells. Ann. Rev. Immunol. 18:767-811.

Bennett JJ, Malhotra S, Wong RJ, Delman K, Zager J, St-Louis M, Johnson P, Fong Y (2001). Interleukin 12 secretion enhances antitumor efficacy of oncolytic *herpes simplex viral* therapy for colorectal cancer. Ann. Surg. 233(6):819-826.

Bonini C, Lee SP, Riddell SR, Greenberg PD (2001). Targeting antigen in mature dendritic cells for simultaneous stimulation of CD4+ and CD8+ T-cells. J. Immunol. 166(8):5250–5257.

Borysiewicz LK, Flander A, Numako M, Man S, Wilkinson GW, Westmoreland D, Evans AS, Adams M, Stacey SN, Boursnell ME, Rutherford E, Hickling JK, Inglis SC (1996). A recombinant *vaccinia virus* encoding *human papillomavirus* types 16 and 18, E6 and E7 proteins as immunotherapy for cervical cancer. Lancet 347:1523–1527.

Bovia F, Salmon P, Matthes T, Kvell K, Nguyen TH, Verner-Favre C, Barnet M, Nagy M, Leuba F, Arrighi JF, Piguet V, Trono D, Zibler RH (2003). Efficient transduction of primary human B-lymphocytes and nondividing myeloma B-cells with *HIV-1*-derived *lentiviral* vectors. Blood 101(5):1727-1733.

Bradford GB, Williams B, Rossi R, Bertoncello I (1997). Quiescence, cycling, and turnover in the primitive hematopoietic stem cell compartment. Exp. Hematol. 25:445-453.

Bradley JA, Bolton EM, Pedersen RA (2002). Stem cell medicine encounters the immune system. Nat. Rev. Immunol. 2:859-871.

Bregenholt S, Ropke M, Skov S, Claesson MH (1996). Ligation of MHC class I molecules on peripheral blood T-lymphocytes induces new phenotypes and functions. J. Immunol. 157:993-999.

Bubenik J (2001). Genetically engineered dendritic cell-based cancer vaccines. Int. J. Oncol. 18(3):475–478.

Burt RK, Drobisky WR, Seregina T, Traynor A, Oyama Y, Keever-Taylor C, StefjaJ, Kuzel TM, Brush M, Rodriques J, Burns W, Tennant L, Link C (2003). *Herpes simplex* thymidine kinase gene-transduced donor lymphocyte infusions. Exp. Hematol. 31:903–910.

Cao X, Zhang W, Wang J, Zhang M, Huang X, Hamada H, Chen W (1999). Therapy of established tumour with a hybrid cellular vaccine generated by using granulocyte-macrophage colony-stimulating factor genetically modified dendritic cells. Immunology 97(4):616-625.

Caux C, Dezutter-Dambuyant S, Schmitt D, Banchereau J (1992). GM-CSF and TNF-α cooperate in the generation of dendritic Langherans cells. Nature 360:258–261.

Chen L, Chen D, Block E, O'Donnell M, Kufe DW, Clinton SK (1997). Eradication of murine bladder carcinoma by intratumor injection of a bicistronic *adenoviral* vector carrying cDNAs for the IL-12 heterodimer and its inhibition by the IL-12 p40 subunit homodimer. J. Immunol. 159:351–359.

Cheng L, Du C, Lavau C, Chen S, Tong J, Chen BP, Scollay R, Hawley RG, Hill B (1998). Sustained gene expression in *retrovirally* transduced, engrafting human hematopoietic stem cells and their lympho-myeloid progeny. Blood 92(1):83-92.

Cheung N-KV, Guo H-F, Modak S, Cheung IY (2003). Anti-idiotypic antibody facilitates scFv chimeric immune receptor gene transduction and clonal expansion of human lymphocytes for tumor therapy. Hybrid. Hybridomics 22:209–218.

Chun S, Daheshia M, Lee S, Rouse BT (1999). Immune modulation by IL-10 gene transfer via viral vector and plasmid DNA: implication for gene therapy. Cell. Immunol. 194:194–204.

Clark EA, Grabstein KH, Shu GL (1992). Cultured human follicular dendritic cells. Growth characteristics and interactions with B-lymphocytes. J. Immunol. 148(11):3327-3335.

Coates PTH, Krishnan R, Kireta S, Johnston J, Russ GR (2001). Human myeloid dendritic cells transduced with an *adenoviral* interleukin-10 gene construct inhibit human skin graft rejection in humanized NOD-scid chimeric mice. Gene Ther. 8(16):1224–1233.

Cordier L, Duffour M, Sabourin J, Lee MG, Cabannes J, Ragot T, Perricaudet M, Haddada H (1995). Complete recovery of mice from a pre-established tumor by direct intratumoral delivery of an *adenovirus* vector harboring the murine IL-12 gene. Gene Ther. 2:16–21.

Curti A, Fogli M, Ratta M, Biasco G, Tura S, Lemoli RM (2001). Dendritic cell differentiation from hematopoietic CD34+ progenitor cells. J. Biol. Regul. Homeostat. Agents 15:49–52.

Dallas MH, Varnum-Finney B, Martin PJ, Bernstein ID (2007). Enhanced T-cell reconstitution by hematopoietic progenitors expanded *ex vivo*-using the Notch ligand Delta1. Blood 109:3579-3587.

Davis NL, Brown KW, Johnson RE (1996). A viral vaccine vector that expresses foreign genes in lymph nodes and protects against mucosal challenge. J. Virol. 70:3781–3787.

Dietz AB, Vuk-Pavlović S (1998). High efficiency *adenovirus*-mediated gene transfer to human dendritic cells. Blood 91(2):392-398.

Djouad F, Bouffi C, Ghannam S, Noël D, Jorgensen C (2009). Mesenchymal stem cells: innovative therapeutic tools for rheumatic diseases. Nat. Rev. Rheumatol. 5:392-399.

Douglas J, Kelly P, Evans JT, Garcia JV (1999). Efficient transduction of human lymphocytes and CD34+ cells via *human immunodeficiency virus*-based gene transfer vectors. Hum. Gene Ther. 10(6):935-945.

Douglas JL, Lin WY, Panis ML, Veres G (2001). Efficient human immunodeficiency virus-based vector transduction of unstimulated human mobilized peripheral blood CD34+ cells in the SCID-hu Thy/Liv model of human T-cell lymphopoiesis. Hum. Gene Ther. 12(4):401-413.

Di Nicola M, Milanesi M, Magni M, Bregni M, Carlo-Stella C, Longoni P, Tomanin R, Ravagnani F, Scarpa M, Jordan C, Gianni AM (1999). Recombinant *adenoviral* vector *lipofectAMINE* complex for gene transduction into human T-lymphocytes. Hum. Gene Ther. 10:1875–1884.

Domi A, Moss B (1995). Engineering of a *vaccinia virus* bacterial artificial chromosome in *Escherichia coli* by *bacteriophage λ*−based recombination. Nat. Meth. 2:95–97.

Douglas J, Kelly P, Evans JT, Garcia JV (1999). Efficient transduction of human lymphocytes and CD34+ cells via *human immunodeficiency virus*-based gene transfer vectors. Hum. Gene Ther. 10:935-945.

Douglas JL, Lin WY, Panis ML, Veres G (2001). Efficient *human immunodeficiency virus*-based vector transduction of unstimulated human mobilized peripheral blood CD34+ cells in the SCID-hu Thy/Liv model of human T-cell lymphopoiesis. Hum. Gene Ther. 12:401-413.

Engelmayer J, Larsson M, Lee A, Lee M, Cox W, Steinman R, Bhardwaj N (2001). Mature dendritic cells infected with *canarypox virus* elicit strong anti-human immunodeficiency virus CD8+ and CD4+ T-cell responses from chronically infected individuals. J. Virol. 75(5):2142–2153.

Eo S, Gierynska M, Kamar A, Rouse B (2001). Prime-boost immunization with DNA vaccine: mucosal route of administration changes the rules. J. Immunol. 166(91):5473–5479.

Fong L, Engelman EG (2000). Dendritic cells in cancer immunotherapy. Ann. Rev. Immunol. 18:245-273.

Frasca L, Fedele G, Deaglio S, Capuano C, Palazzo R, Vaisitti T, Malavasi F, Ausiello CM (2006). CD38 orchestrates migration,

survival, and Th1 immune response of human mature dendritic cells. Blood 107(6):2392-2399.
Gambotto A, Tuting T, McVey D, Kovesdi I, Tahara H, Lotze MT, Robbins PD (1999). Induction of antitumor immunity by direct intratumoral injection of a recombinant *adenovirus* vector expressing interleukine-12. Cancer Gene Ther. 6:45–53.
Glymche LH, Murphy KM (2000). Lineage commitment in the immune system: the T-helper lymphocyte grows up. Genes Dev. 14:1693-1711.
Gong J, Chen D, Kashiwaba M, Kufe D (1997). Induction of antitumor activity by immunization with fusions of dendritic and carcinoma cells. Natl. Med. 3(5):558–561.
Gong J, Chen L, Chen D, Kashiwaba M, Manome Y, Tanaka T, Kufe D (1997). Induction of antigen-specific antitumor immunity with *adenovirus*-transduced dendritic cells. Gene Ther. 4:1023–1028.
Gong J, Nikrui N, Chen D, Koido S, Wu Z, Tanaka Y, Cannistra S, Avigan D, Kufe D (2000). Fusions of human ovarian carcinoma cells with autologous or allogeneic dendritic cells induce antitumor immunity. J. Immunol. 165:1705-1711.
Gong J, Koido S, Chen D, Tanaka Y, Huang L, Avigan D, Anderson K, Ohno T, Kufe D (2002). Immunization against murine multiple myeloma with fusions of dendritic and plasmacytoma cells is potentiated by interleukin-12. Blood 99(7): pp. 2512–2517.
Gray-Parkin K, Stephan RP, Apilado RG, Lill-Elghanian DA, Lee KP, Saha B, Witte PL (2002). Expression of CD28 by bone marrow stromal cells and its involvement in B-lymphopoiesis. J. Immunol. 169:2292-2302.
Green DR, Bissonnette RP, Glynn JM, Shi Y (1992). Activation-induced apoptosis in lymphoid systems. Semin. Immunol. 4:379-388.
Grosenbach DW, Barrientos JC, Scholm J, Hodge JW (2001). Synergy of vaccine strategies to amplify antigen-specific immune responses and antitumor effects. Cancer Res. 61:4497–4505.
Guenechea G, Gan OI, Inamitsu T, Dorrell C, Pereira DS, Kelly M, Naldini L, Dick JE (2000). Transduction of human CD34+ CD38- bone marrow and cord blood-derived SCID-repopulating cells with third-generation *lentiviral* vectors. Mol. Ther. 1(6):566-573.
Hass R, Otte A (2012). Mesenchimal stem cells as all-round supporters in a normal and neoplastic microenvironment. Cell Commun. Signal 10:26.
Hassan W, Sanford MA, Woo SL, Chen SH, Hall SJ (2000). Prospects for *herpes-simplex-virus* thymidine-kinase and cytokine gene transduction as immunomodulatory gene therapy for prostate cancer. World J. Urol. 18(2):130–135.
Hiraoka K, Yamamoto S, Otsuru S, Nakai S, Tamai K, Morishita R, Ogihara T, Kaneda Y (2004). Enhanced tumor-specific long-term immunity of *hemagglutinating virus* of Japan-mediated dendritic cell-tumor fused cell vaccination by coadministration with CpG oligodeoxynucleotides. J. Immunol. 173:4297-4307.
Hodge JW, McLaughlin JP, Kantor JA, Schlom J (1997). Diversified prime and boost protocols using recombinant *vaccinia virus* and recombinant non-replicating *avian pox virus* to enhance T-cell immunity and antitumor responses. Vaccine 15(6-7):759–768.
Ikuta K, Kina T, MacNeil I, Uchida N, Peault B, Chien YH, Weissman IL (1990). A developmental switch in thymic lymphocyte maturation potential occurs at the level of hematopoietic stem cells. Cell 62:863-874.
Inaba K, Inaba M, Romani N, Aya H, Deguchi M, Ikehara S, Muramatsu S, Steinman RM (1992). Generation of large numbers of dendritic cells from mouse bone marrow cultures supplemented with granulocyte/macrophage colonystimulating factor. J. Exp. Med. 176:1693-1702.
Itoh Y, Koshita Y, Takahashi M, Watanabe N, Kohgo Y, Niitsu Y (1995). Characterization of tumor-necrosis-factor-gene-transduced tumor-infiltrating lymphocytes from ascitic fluid of cancer patients: analysis of cytolytic activity, growth rate, adhesion molecule expression and cytokine production. Cancer Immunol. Immunother. 40:95–102.
Itoh K, Tilden A, Balch C (1986). Interleukin-2 activation of cytotoxoic T-lymphocytes infiltration into human metastatic melanoma. Cancer Res. 46:3011–3017.
Jackson DG, Bell JI (1990). Isolation of a cDNA encoding the human CD38 (T10) molecule, a cell surface glycoprotein with an unusual discontinuous pattern of expression during lymphocyte differentiation. J. Immunol. 144:2811-2815.
Kang SK, Shin S, Ko MS, Jo JY, Ra JC (2012). Journey of mesenchymal stem cells for homing: strategies to enchance efficacy and safety of stem cell therapy. Stem Cell Int. 2012:342968.
Kao JY, Gong Y, Chen CM, Zheng QD, Chen JJ (2003). Tumor-derived TGF-β reduces the efficacy of dendritic cell/tumor fusion vaccine. J. Immunol. 170:3806-3811.
Kaplan J, Yu Q, Piraino S, Pennington SE, Shankara S, Woodworth LA, Roberts BL (1999). Induction of antitumor immunity with dendritic cells transduced with *adenovirus* vector-encoding endogenous tumor-associated antigens. J. Immunol. 163:699–707.
Kauffman E, Bublot M, Gettig R, Limbash K, Pincus S, Taylor J (2001). Live viral vectors. In: New vaccine technologies, Ronald WE (ed.), BioChem Pharma, Inc. Northborough, Massachusetts, USA. P 303.
Kent SJ, Zhao A, Best SJ, Chandler JD, Boyle DB, Ramshaw IA (1998). Enchanced T-cell immunogenicity and protective efficacy of a *Human Immunodeficiency Virus Type I* vaccine regimen consisting of consecutive priming with DNA and boosting with *recombinant fowlpox virus*. J. Virol. 72:10180–10188.
Kim HS, Zhang X, Choi YS (1994). Activation and proliferation of follicular dendritic cell-like cells by activated T-lymphocytes. J. Immunol. 153(7):2951-2961.
Kobari L, Pflumio F, Giarratana M, Li X, Titeux M, Izac B, Leteurtre F, Coulombel L, Douay L (2000). *In vitro*- and *in vivo*-evidence for the long-term multilineage (myeloid, B-, NK, and T-) reconstitution capacity of *ex vivo*-expanded human CD34(+) cord blood cells. Exp. Hematol. 28:1470-1480.
Kobari L, Giarratana MC, Pflumio F, Izac B, Coulombel L, Douay L (2001). CD133+ cell selection is an alternative to CD34+ cell selection for *ex vivo*-expansion of hematopoietic stem cells. J. Hematother. Stem Cell Res. 10:273-281.
Koido S, Hara E, Homma S, Mitsunaga M, Takahara A, Nagasaki E, Kawahara H, Watanabe M, Toyama Y, Yanagisawa S, Kobayashi S, Yanaga K, Fujise K, Gong J, Tajiri H (2007). Synergistic induction of antigen-specific CTL by fusions of TLR-stimulated dendritic cells and heat-stressed tumor cells. J. Immunol. 179:4874-4883.
Kondo M, Weissman IL, Akashi K (1997). Identification of clonogenic common lymphoid progenitors in mouse bone marrow. Cell 91:661-672.
Kung SK, An DS, Chen IS (2000). A *murine leukemia virus* (*MuLV*) long terminal repeat derived from *rhesus macaques* in the context of a *lentivirus* vector and *MuLV gag* sequence results in high-level gene expression in human T-lymphocytes. J. Virol. 74:3668-3681.
Lai AY, Kondo M (2007). Identification of a bone marrow precursor of the earliest thymocytes in adult mouse. Proc. Natl. Acad. Sci. U. S. A. 104: 6311–6316.
Lamers CHJ, Willemsen RA, Luider BA, Debets R, Bolhuis RLH (2002). Protocol for gene transduction and expansion of human T-lymphocytes for clinical immunogene therapy of cancer. Cancer Gene. Ther. 9:613–623.
Lazarus HM, Koc ON, Devine SM, Curtin P, Maziarz RT, Holland HK, Shpall EJ, McCarthy P, Atkinson K, Cooper BW, Gerson SL, Laughlin MJ, Loberiza FR, Moseley AB, Bacigalupo A (2005). Cotransplantation of HLA-identical sibling culture-expanded mesenchymal stem cells and hematopoietic stem cells in hematologic malignancy patients. Biol. Blood Marrow Transplant. 11:389–398.
Lehtonen A, Ahlfors H, Veckman V, Miettinen M, Lahesmaa R, Julkunen I (2007). Gene expression profilling during differentiation of human monocytes to macrophages or dendritic cells. J. Leukoc. Biol. 82(3):710-720.
Liu Y (2003). Engineered fusion hybrid vaccine of *IL-4* gene-modified myeloma and relative mature dendritic cells enhances antitumor immunity. Leukoc. Res. 26(8):757.
Liu R, Varghese S, Rabkin SD (2005). Oncolytic *herpes simplex virus* vector therapy of breast cancer in *C3(1)/SV40* T-antigen transgenic mice. Cancer Res. 65(4):1532–1540.
Lu L, Lee W-C, Gambotto A, Zhong C, Robbins PD, Qian S, Fung JJ, Thomson AW (1998). Transduction of dendritic cells with *adenoviral* vectors encoding CTLA4-Ig markedly reduces their allostimulatory ability. Transplantation 65:106–109.
Maitra B, Szekely E, Gjini K, Laughlin MJ, Dennis J, Haynesworth SE, Koc ON (2004). Human mesenchymal stem cells support unrelated

donor hematopoietic stem cells and suppress T-cell activation. Bone Marrow Transplant. 33:597–604.
Mandl S, Sigal LJ, Rock KL, Andino R (1998). *Poliovirus* vaccine vectors elicit antigen-specific cytotoxic T-cells and protect mice against lethal challenge with malignant melanoma cells expressing a model antigen. Proc. Natl. Acad. Sci. U. S. A. 95:8216–8221.
Martinet W, Saelens X, Deroo T, Neirynck S, Contreras R, Min Jou W, Fiers W (1997). Protection of mice against a lethal influenza challenge by immunization with yeast-derived recombinant influenza neuraminidase. Eur. J. Biochem. 247:332–338.
Mitchell TC, Haldeman D, Kedl RM, Teague TK, Schaefer BC, White J, Zhu Y, Keppler J, Marrack P (2001). Immunological adjuvants promote activated T-cell survival via induction of *Bcl-3*. Nat. Immunol. 2:397–402.
Overwijk WW, Lee DS, Surman DR, Irvine KR, Touloukian CE, Chan CC, Carroll MW, Moss B, Rosenberg SA, Restifo NP (1999). Vaccination with a recombinant *vaccinia virus* encoding a"self" antigen induces autoimmune vitiligo and tumor cell destruction in mice: requirement for CD4+ T-lymphocytes. Proc. Natl. Acad. Sci. U. S. A. 96:2982–2987.
Palese P, Roizman B (1996). Genetic engineering of viruses and of virus vectors: a preface. Proc. Natl. Acad. Sci. U. S. A. 93: p. 11287.
Panicali D, Paoletti E (1982). Construction of poxviruses as cloning vectors: insertion of the thymidine kinase gene from *herpes simplex virus* into the DNA of infectious *vaccinia virus*. Proc. Natl. Acad. Sci. U. S. A. 79:4927–4931.
Parkhurst MR, De Pan C, Riley JP, Rosenberg SA, Shu S (2003). Hybrids of dendritic cells and tumor cells generated by electrofusion simultaneously present immunodominant epitopes from multiple human tumor-associated antigens in the context of MHC class I and class II molecules. J. Immunol. 170:5317-5325.
Ra JC, Kang SK, Shin S, Park HG, Joo SA, Kim JG, Kang B-C, Lee SY, Nakama K, Piao M, Sohl B, Kurtz A (2011): Stem cell treatment for patients with autoimmune disease by systematic infusion of culture-expanded autologous adipose tissue derived mesenchymal stem cells. J. Transl. Med. 9:181.
Reid CDL, Stackpole A, Meager A, Tikepae J (1992). Interaction of tumor necrosis factor with granulocyte-macrophage colony-stimulating factor and other cytokines in the regulation of dendritic cell growth *in vitro* from bipotent CD34+ progenitors in human bone marrow. J. Immunol. 149:2681-2688.
Ribas A, Butterfield L, McBride W, Jilani SM, Bui LA, Vollmer CM, Lau R, Dissette VB, Hu B, Chen AY, Glaspy JA, Economou JS (1997). Genetic immunization for the melanoma antigen MART-1/melan-A using *recombinant adenovirus*-transduced murine dendritic cells. Cancer Res. 57:2865–2869.
Rosenberg S (1996). The immunotherapy of solid cancers based on cloning the genes encoding tumor-rejection antigens. Ann. Rev. Med. 47:481–491.
Rosenberg SA, Yannelli JR, Yang JC, Topalian SL, Schwartzentruber DJ, Weber JS, Parkinson DR, Seipp CA, Einhorn JH, White DE (1994). Treatment of patients with metastatic melanoma with altologous tumor-infiltrating lymphocytes and interleukin-2. J. Natl. Cancer Inst. 86:1159–1166.
Rosenberg S, Zhai Y, Yang J, Schwartzentruber DJ, Hwu P, Marincola FM, Topalian SL, Restifo NP, Seipp CA, Einhorn JH, White DE (1998). Immunizing patients with metastatic melanoma using recombinant *adenoviruses* encoding MART-1 and gp1000 melanoma antigens. J. Natl. Cancer Inst. 90:1894–1900.
Rosenberg SA, Aebersold P, Cornetta K, Kasid A, Morgan RA, Moen R, Karson EM, Lotze MT, Yang JC, Topalian SL, Merino MJ, Culver K, Miller D, Blaese M, Anderson WF (1990). Gene transfer into humans - immunotherapy of patients with advanced melanoma, using tumor-infiltrating lymphocytes modified by *retroviral* gene transduction. N Engl. J. Med. 323:570–578.
Sadegah M, Weiss W, Sacci JB (2000). Improving protective immunity induced by DNA-based immunization: priming with antigen and GM-CSF encoding plasmid DNA and boosting with antigen expressing recombinant *poxvirus*. J. Immunol. 164:5905–5912.
Sell S (2004). Stem cell origin of cancer and differentiation therapy. Crit. Rev. Oncol. Hematol. 51:1–28.
Siders W, Wright P, Hixon J, Alvord WG, Back TC, Wiltrout RH, Fenton RG (1998). T-cell and NK cell independent inhibition of hepatic metastases by systemic administration of IL-12-expressing recombinant *adenovirus*. J. Immunol. 160:5465–5474.
Siena S, Di Nicola M, Bregni M, Mortarini R, Anichini A, Lombardi L, Ravagnani F, Parmiani G, Gianni AM (1995). Massive *ex vivo*-generation of functional dendritic cells from mobilized CD34+ blood progenitors for anticancer therapy. Exp. Hematol. 23:1463-1471.
Suzuki T, Fukuhara T, Tanaka M, Nakamura A, Akiyama K, Sakakibara T, Koinuma D, Kikuchi T, Tazawa R, Maemondo M, Hagiwara K, Saijo Y, Nukiwa T (2005). Vaccination of dendritic cells loaded with interleukin-12-secreting cancer cells augments *in vivo*-antitumor immunity: characteristics of syngeneic and allogeneic antigen-presenting cell cancer hybrid cells. Clin. Cancer Res. 11:58-66.
Terskikh AV, Bryant PJ, Schwartz PH (2006). Mammalian stem cells. Pediatric Res. 59:13R-20R.
Tozola E, Hunt K, Swisher S (1997). *In vivo*-cancer gene therapy with a recombinant *interleukin-2 adenovirus* vector. Cancer Gene Ther. 4:17–25.
Tsang KY, Zaremba S, Nieroda CA, Zhu MZ, Hamilton JM, Schlom J (1995). Generation of human cytotoxicic T-cells specific for human carcinoembryonic antigen epitopes from patients immunized with recombinant *vaccinia-CEA* vaccine. J. Natl. Cancer Inst. 87:982–990.
Vasiri B, Wu Z, Crawford K, Rosenblatt J, Zarwan C, Bissonnette A, Kufe D, Avigan D (2008). Fusions of dendritic cells with breast carcinoma stimulate the expansion of regulatory T-cells while concomitant exposure to IL-12, CpG oligodeoxynucleotides, and anti-CD3/CD28 promotes the expansion of activated tumor reactive cells. J. Immunol. 181:808-821.
Vogelstein B, Kinzler KW (2004). Cancer genes and pathways they control. Nat. Med. 10:789–799.
Walden P (2000). Hybrid cell vaccination for cancer immunotherapy. Adv. Exp. Med. Biol. 465:347-354.
Wang J, Saffold S, Cao X, Krauss J, Chen W (1998). Eliciting T-cell immunity against poorly immunogenic tumors by immunization with dendritic cell-tumor fusion vaccines. J. Immunol. 161:5516-5524.
Wang M, Bronte V, Chen PW, Gritz L, Panicali D, Rosenberg SA, Restifo NP (1995). Active immunotherapy of cancer with a non-replicating recombinant *fowlpox virus* encoding a model tumor-associated antigen. J. Immunol. 154:4685–4692.
Wu AG, Liu X, Mazumder A, Bellanti JA, Meehan KR (1999). Improvement of gene transduction efficiency in T-lymphocytes using *retroviral* vectors. Hum. Gene Ther. 10:977–982.
Wen Ju D, Tao Q, Lou G, Bai M, He L, Yang Y, Cao X (2001). Interleukin-18-transfection enhances antitumor immunity induced by dendritic cell-tumor cell conjugates. Cancer Res. 61:3735-3740.
Wildner O, Morris JC (2000). The role of the E1B 55 kDa gene product in oncolytic *adenoviral* vectors expressing *herpes simplex virus-tk*: assessment of antitumor efficacy and toxicity. Cancer Res. 60(15):4167-4174.
Xia D, Li F, Xiang J (2004). Engineered fusion hybrid vaccine of *IL-18* gene-modified tumor cells and dendritic cells induces enhanced antitumor immunity. Cancer Biother. Radiopharm. 19(3):322-330.
Xia D, Chan T, Xiang J (2005). Dendritic cell/myeloma hybrid vaccine. Meth. Mol. Med. 113: 225–234.
Xia J, Tanaka Y, Koido S, Liu C, Mukherjee P, Gendler SJ, Gong J (2003). Prevention of spontaneous breast carcinoma by prophylactic vaccination with dendritic/tumor fusion cells. J. Immunol. 170:1980-1986.
Yongqing Z, Chan WT, Saxena A, Xiang J (2002). Engineered fusion hybrid vaccine of IL-4 gene-modified myeloma and relative mature dendritic cells enhances antitumor immunity. Leuk. Res. 26(18):757–763.
Zhai Y, Yang J, Kawakami Y, Spiess P, Wadsworth SC, Cardoza LM, Couture LA, Smith AE, Rosenberg SA (1996). Antigen-specific tumor vaccines: development and characterization of recombinant *adenoviruses* encoding *MART1* or *gp100* for cancer therapy. J. Immunol. 156:700–710.
Zhang J, Hu C, Geng Y, Blatt L, Taylor M (1996). Gene therapy with *adeno-associated virus* carrying an interferon gene results in tumor growth suppression and regression. Cancer Gene Ther. 3:31–38.
Zhang XY, La Russa VF, Reiser J (2004). Transduction of bone marrow-derived mesenchymal stem cells by using *lentivirus* vectors

pseudotyped with modified RD114 envelope glycoproteins. J. Virol. 78:1219-1229.
Zhang XY, La Russa VF, Bao L, Kolls J, Schwarzenberger P, Reiser J (2002). *Lentiviral* vectors for sustained transgene expression in human bone marrow-derived stromal cells. Mol. Ther. 5:555-565.
Zhou X, Cui Y, Huang X, Yu Z, Thomas AM, Ye Z, Pardoll DM, Jaffee EM, Cheng L (2003). *Lentivirus*-mediated gene transfer and expression in established human tumor antigen-specific cytotoxic T-cells and primary unstimulated T-cells. Hum. Gene Ther. 14:1089-1105.

academicJournals

Vol. 7(22), pp. 1438-1447, 15 June, 2013
DOI 10.5897/AJPP12.170
ISSN 1996-0816 © 2013 Academic Journals
http://www.academicjournals.org/AJPP

African Journal of Pharmacy and Pharmacology

Full Length Research Paper

Analysis of the polysaccharides from *Urtica angustifolia* and their anti-fatigue activity

Haiyue Zhang[1]*, Xiaojuan Yan[1], Zhenling Zhao[1] and Li Ji[2]

[1]College of Chemical and Life Science, Changchun University of Technology, Changchun 130012, PR China.
[2]Jilin Province Key Laboratory on Chemistry and Biology of Natural Drugs in Changbai Mountain, School of Life Science, Northeast Normal University, Changchun 130024, PR China.

Accepted 15 April, 2013

The crude polysaccharides (UA) were obtained from *Urtica angustifolia* by hot water extraction, 80% ethanol precipitation and deproteination by using sevage reagent in a yield of 1.6%. The polysaccharides were fractionated into six fractions. Their sugar compositions and structures were analyzed by high performance liquid chromatography (HPLC) and nuclear magnetic resonance spectrometer (NMR). The HPLC analysis results showed that UA contain two neutral polysaccharide fractions and four acidic fractions. The neutral fractions are mainly composed of glucose (Glc), and the acidic fractions are mainly composed of galacturonic acid (GalA). The NMR results showed that the neutral fractions are starch-like polysaccharides and the acidic fractions are rhamnogalacturonan (RG)-I domian containing pectin. The anti-fatigue activity of the polysaccharides was evaluated in mice and the results showed *U. angustifolia* polysaccharides increased the swimming time, and the average swimming time of the low doses (LD), middle doses (MD) and high doses (HD) group were increased by 85.4, 114.6 and 151.2%, respectively. The blood urea nitrogen content of the LD, MD and HD group was reduced by12.8, 13.6 and 19.8% compared with that of control group, respectively. The hepatic glycogen of every treated group was higher than that of control group, increasing rates were 87.0, 469.6, and 747.8%, respectively.

Key words: *Urtica angustifolia*, polysaccharide, anti-fatigue, structure analysis.

INTRODUCTION

Urtica is a perennial wild herb. It is rich in natural resources and has very strong vitality. *Urtica* is a kind of traditional medicine edible wild plant in China. Nettle (the same meaning with *Urtica*) is stated to possess hypoglycemic properties (Newall et al., 1996). Moreover, it has been shown that a preparation containing various plants extraction with nettle had antidiabetic activity (Petlevski et al., 2001). *Urtica angustifolia* belongs to the family of Urticeae, and is widely distributed in China. Moreover, nettle is known in folk medicine as hypotensive and antidiabetic (Ziyyat et al., 1997). Nettle plant roots and rhizomes can also treat high blood pressure, hand and foot numbness, diabetes, leprosy, weak labor wounds, indigestion, and constipation. It can also be used to treat polio sequelae and hernia pain etc. (Quan 1997).

At present, Europe, the United States and other developed countries have researched on the nettle, especially the *Urtica dioica*. In particular, the development of medicine in Germany has made remarkable achievements.

*Corresponding author. E-mail: zhhaiyue@163.com. Tel: (+86)-13596055178. Fax: (+86)-431-85712163.

They have had specific studies on different parts of the chemical composition of U. dioica and obtained that the active ingredients are sterols, flavonoids, organic acids, phenols, phenylpropanoids, plant proteins and polysaccharides (Kraus and Spiteller, 1990; Kavtaradze et al., 2001; Neugebauer et al., 1995; Zhang et al., 2011).

U. angustifolia is widely distributed in northwest regions of china. Its claimed benefits include anti-inflammatory, analgesic effect, anti-intoxication, spasmolysis and improving immune function, and also restrain hyperplasia of prostate (Bnouham et al., 2003; Schulze-Tanzil et al., 2002; Konrad et al., 2000). But the anti-fatigue effects of *U. angustifolia* and the dose-dependent relation have not been reported (Dong et al., 2007; Guo et al., 2006). The present study was designed to investigate the anti-fatigue effects of *U. angustifolia* and its effective dose.

MATERIALS AND METHODS

Plants

The roots of *U. Angustifolia* were cultivated and collected in October at Liuhe, Jilin, China. The diethylaminoethyl (DEAE)-cellulose and sepharose CL-6B were purchased from Sigma. All other chemicals were of analytical grade.

Animals

Swiss mice weighing 18 to 22 g were used. The animals were kept in a room at a controlled temperature of 22 ± 2°C with a 12 to 12 h light-dark cycle. The animals were treated according to the ethical guidelines of the Animal Center, College of Animal Science and Technology, Jilin University.

Experimental

Total carbohydrate content was determined by the phenol-sulfuric acid method (Dubois et al., 1956). The standards used in the assay were prepared with the ratio of the monosaccharide that constituted the polysaccharide to be tested, according to the sugar composition. Uronic acid contents were determined by the m-hydroxydiphenyl method (Blumenkrantz and Asboe-Hansen, 1973) using galacturonic acid as a standard. Gel permeation and anion-exchange chromatographies were monitored by assaying the total sugar and uronic acid contents. Protein content was determined by the Bradford assay using bovine serum albumin as the standard.

Extraction

The roots of *U. angustifolia* were dried at 50°C for three days before grinding. The ground material (900 g) were extracted with 8.0 L distilled water at 100°C for 2 h and filtered through four sheets of gauze (100 mesh). The solid material was extracted twice again under the same conditions. The filtrates were combined, centrifuged to remove water-insoluble materials, concentrated to 200 ml and precipitated by the addition of 4 volumes of 95% ethanol. After centrifuging and re-dissolving the precipitate by distilled water, the solution with Sevag reagent (1:4 n-butanol:chloroform, v/v, 40 ml) to remove proteins (Sevag et al., 1938). After precipitation by ethanol again and drying in vacuum, the deproteined polysaccharide fraction UA (14.4 g) was obtained. The procedure for the extraction and fractionation of *U. angustifolia* polysaccharides is shown in Figure 1.

Chromatography on DEAE-cellulose

Analytical chromatography on DEAE-cellulose

The UA (10 mg) was dissolved in distilled water (1 ml) and loaded on a DEAE-cellulose (Cl^-) column (1.5 × 14 cm) pre-equilibrated with distilled water. The column was eluted first with 40 ml distilled water at 1.0 ml/min and then with a linear gradient from 0.0 to 1.0 M NaCl within 400 ml. The eluate was collected at 4 ml per tube and assayed for total sugar and uronic acid contents.

Semi-preparative chromatography on DEAE-cellulose

The UA (9 g) was applied to a DEAE-cellulose column (8.8 cm × 25 cm) and eluted stepwise with distilled water and 0.5 M NaCl. The eluate was monitored by the phenol-sulfuric acid method. The fraction which was eluted by 0.5 M NaCl was dialyzed against distilled water and lyophilized after concentrating to obtain the fraction unbound fraction (UAN) (3.4 g) and bound fraction (UAA) (4.0 g). UAA (4.0 g) was re-dissolved in distilled water, loaded onto a column (3.8 cm × 27) of DEAE-cellulose and eluted stepwise with distilled water, 0.1, 0.3 and 0.5 M NaCl. The four fractions were dialyzed against distilled water and lyophilized after concentrating to obtain the fractions UAA-1 (1.0 g), UAA-2 (0.3 g), UAA-3 (1.7 g) and UAA-4 (0.9 g).

Gel permeation chromatography on sepharose CL-6B

Analytical chromatography on sepharose CL-6B

Each sample (5 to 10 mg) was dissolved in 0.15 M NaCl (1 ml), loaded onto a sepharose CL-6B column (1.5 × 90 cm) and eluted with 0.15 M NaCl at a flow rate of 0.15 ml/min. The eluate was collected at 3 ml per tube and assayed for total sugar and uronic acid contents.

Semi-preparative chromatography on sepharose CL-6B

UAA-3 (1 g) was applied to a preparative sepharose CL-6B column (3.0 × 90 cm) and eluted with 0.15 M NaCl at 0.5 ml/min. The eluate (10 ml per tube) was collected and assayed for total sugar and uronic acid contents. The appropriate fractions were combined, concentrated, dialyzed against distilled water and lyophilized to give UAA-3-1 (110 mg) and UAA-3-2 (540 mg).

High performance gel permeation chromatography

High performance gel permeation chromatography was carried out at 40°C using a TSK-gel G-3000PW_{XL} column (7.8 × 300 mm, TOSOH, Japan) connected to a Shimadzu HPLC system. The column was pre-calibrated with standard dextrans. Sample was eluted with 0.2 M NaCl at a flow rate of 0.6 ml/min and monitored using a refractive index RID-10A detector (Shimadzu, Tokyo, Japan). Sample concentration was 5 mg/ml and injection amount was 20 µl.

Sugar composition analysis

Polysaccharide samples (2 mg) were hydrolyzed first with anhydrous methanol containing 1 M HCl at 80°C for 16 h and then with 2 M trifluoroacetic acid (TFA) at 120°C for 1 h. The resulting

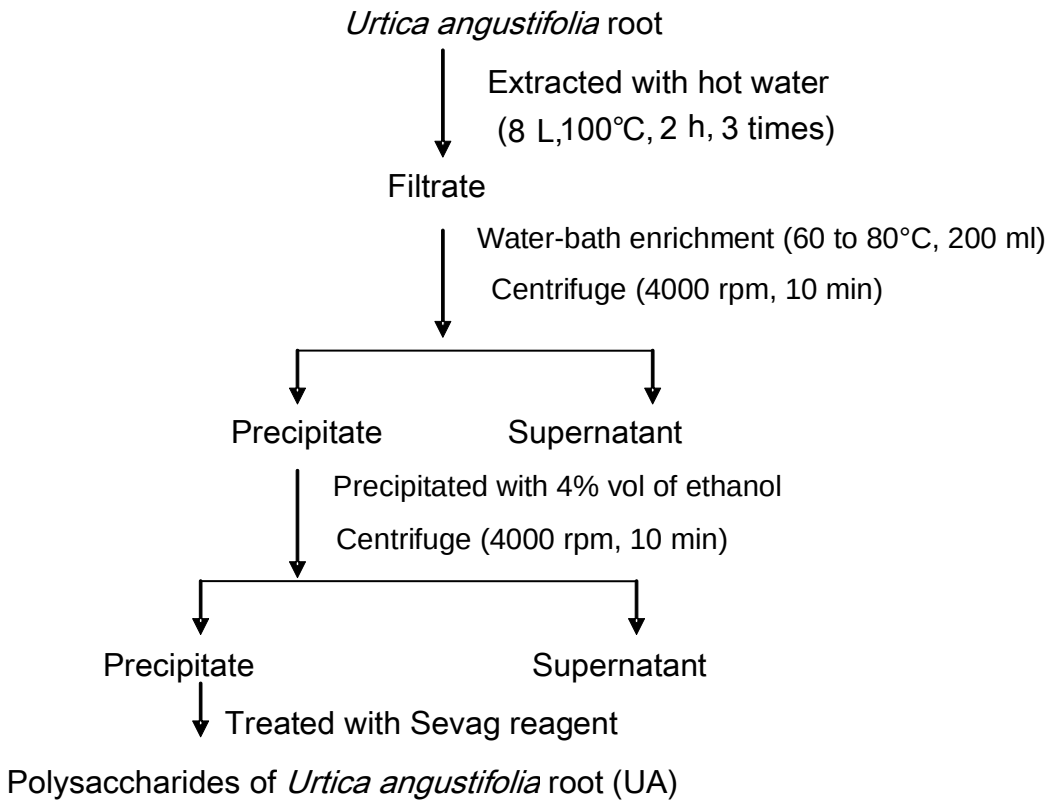

Figure 1. Fractionation scheme of polysaccharides from *Urtica angustifolia* root.

hydrolysates were derivatized with 1-phenyl-3-methyl-5-pyrazolone (PMP) according to the method in the literature (Yang et al., 2005) and analyzed on a DIKMA Inertsil ODS-3 column (4.6 × 150 mm) connected to a Shimadzu HPLC system (LC-10ATvp pump and SPD-10AVD UV-VIS detector). The PMP derivative (20 µl) was injected, eluted with 82.0% phosphate buffer saline solution (PBS) (0.1 M, pH 7.0) and 18.0% acetonitrile (v/v) at a flow rate of 1.0 ml/min and monitored by ultra violet (UV) absorbance at 245 nm.

Nuclear magnetic resonance (NMR) spectra

The carbon nuclear magnetic resonance (^{13}C NMR) spectra were obtained on a Bruker AV600 spectrometer at 150 MHz. The samples (20 mg) were dissolved in D_2O (1 ml, 99.8%) with overnight stirring at room temperature. The spectra were recorded at 25°C after 57,000 scans (Shuqun and Robert, 1997).

Swimming endurance experiment

The mice were randomly divided into 4 groups, 10 mice per group. The collected crude polysaccharide was dissolved in water, respectively. Concentrations were 4, 8, and 12 g/ml. Mice were intra-gastric administrated for ten days, and the doses were 100, 200 and 300 mg/kg/d, respectively. Mice in the control group were given the quivalent volume of water. Ten days later, mice were swam with wire of 5% body weight tied their tails in the pool (length: 50 cm, width: 50 cm, depth: 40 cm) filled with 30 cm depth of water at 25°C ± 1.0°C. The anti-fatigue activity of *U. angustifolia* polysaccharide was evaluated by the weight loaded swimming model in mice. Mice were regarded as exhaustion when they stayed in the water for 8 s, and their swimming time was immediately recorded. The time of each group of mice was averaged and the data of the different groups was analyzed with F-test.

Effect of *U. angustifolia* polysaccharides on the blood urea nitrogen of mice

Mice were randomly divided into 4 groups, 10 mice per group. The crude polysaccharide collected in the present study was dissolved in a small amount of water, respectively. Mice were intra-gastric administrated for 10 days, and the doses were 100, 200 and 300 mg/kg/d, respectively. Mice in the control group were given the equivalent volume of water. Ten days later, mice were swam for 90 min,30 min later after final administration of *U. angustifolia* polysaccharides, mice were forced to swim without wire tied to their tails in the pool (length: 50 cm, width: 50 cm, depth: 40 cm) filled with 30 cm depth of water at 30°C. Blood eye samples were collected after mice have been resting for 60 min. After the blood was put in refrigerator for 3 h, concentrated (2000 rpm), serum urea nitrogen was determinated by automatic biochemical analyzer (Ding et al., 2008).

Increase ratio = (a - b) / b
Reduce ratio = (a - c) / c

Where a is the blood lactate concentration of mice after swimming immediately, b is the blood lactate concentration of mice before swimming and c is the blood lactate concentration of mice after resting for 20 min.

Effect of *U. angustifolia* polysaccharides on the hepatic glycogen of mice

To determine the hepatic glycogen of the mice 30 min later after final administration of *U. angustifolia* polysaccharides, each mouse was killed to get the liver, dried by the dry filter paper, checked at 100 mg weight, to it was added 8 ml Trichloroacetic acid (TCA), centrifuged at 3,000 rpm for 15 min, 4 ml 95% ethyl alcohol (Et-OH) added to the supernatant and finally erected at room temperature overnight. After total precipitation, it will was concentrated for 15 min at 3,000 rpm. The precipitation was erected for 10 min and 2 ml distilled water added to dissolve hepatic glycogen.

Statistical analysis

All the results were expressed as the means ± standard deviation (SD) in the tables, and differences between groups were determined by analysis of variance and Student's t-test. Probability value p less than 0.05 was considered significant.

RESULTS AND DISCUSSION

Isolation of *U. angustifolia* polysaccharides

The water-soluble polysaccharides were extracted from the roots of *U. Angustifolia* with boiling water and deproteined by using the Sevag method. A crude polysaccharide fraction (UA) was obtained with a yield of 1.6 % (w/w). UA contained 44.6% total sugar, 12.7% uronic acid and less than 1% protein. Sugar composition analysis by HPLC indicated that UA consisted of glucose (Glc) (64.3%), galactose (Gal) (8.2%), galacturonic acid (GalA) (15.9%), glucuronic acid (GlcA) (1.3%), mannose (Man) (1.1%), rhamnose (Rha) (2.6%) and arabinose (Ara) (5.9%).

Fractionation by DEAE-cellulose chromatography

Preliminary separation on DEAE-cellulose column

Before fractionation on a semi-preparative scale, we analyzed UA using an analytical DEAE-cellulose column. The profile showed an unbound portion eluted with water and a bound portion eluted with a linear gradient of NaCl. It failed to separate all fractions in a single run of DEAE-cellulose chromatography with a 0.0 to 0.5 M NaCl linear gradient elution, because the abundant unbound neutral polysaccharides interfered with the fine separation of the acidic polysaccharides. Thus, we separated UA first into two fractions on a semi-preparative scale: an unbound fraction (UAN) by water elution with a recovery of 37.4% and a bound fraction (UAA) by 0.5 M NaCl elution, with a recovery of 44.6%. As expected, the unbound portion UAN did not contain uronic acid and was not able to be separated further by anion-exchange chromatography. The bound portion UAA contained uronic acid and could be fractionated continually by a second step of DEAE-cellulose chromatography (Figure 2).

The second run of the separation on DEAE-cellulose column

In the second run of DEAE-cellulose chromatography, the bound portion (UAA) was separated as follows. First, analytical DEAE-cellulose chromatography of UAA was carried out. The elution profile indicated that UAA still contained neutral polysaccharides and a large proportion of acidic polysaccharides. We decided to separate UAA on a preparative DEAE-cellulose column by elution with a stepwise gradient of NaCl. With these elution steps, UAA was separated into four fractions (Figure 2d): UAA-1 (25.9%), UAA-2 (6.4%), UAA-3 (42.0%) and UAA-4 (21.5%) corresponding to 0.0, 0.1, 0.3 and 0.5 M NaCl, respectively. Total sugar and uronic acid assays indicated that UAA-1 was a neutral polysaccharide fraction and UAA-2, UAA-3 and UAA-4 were acidic polysaccharide fractions (Figure 3).

Fractionation by sepharose CL-6B chromatography

All collected fractions from the DEAE-cellulose column were analyzed on a sepharose CL-6B column. As shown in Figure 2, UA gave a wide distribution almost from the void volume to the total volume. By the first separation on DEAE-cellulose, the degree of homogeneity of UAN and UAA was not significantly improved compared to the original UA fraction. After the second separation step, UAA-1 and UAA-2 had a similar distribution to that of the precursor (UAA), showing a polydispersed profile from chromatography on sepharose CL-6B. Thus, UAA-4 had a wide distribution on the column, while UAA-3 could be further fractionated on sepharose CL-6B. UAA-3 presented two major molecular populations, one rich in neutral sugars was eluted first and the other rich in uronic acid was eluted later (Figure 3). Therefore, UAA-3 was further fractionated on sepharose CL-6B to give two fractions UAA-3-1 (12.7%) and UAA-3-2(54.1%).

Homogeneity and molecular weight

The homogeneity of each fraction purified by the combinatorial procedure was analyzed by sepharose CL-6B chromatography and high performance gel permeation chromatography (HPGPC) on a TSK column. On the sepharose CL-6B column, UAA-3-1 and UAA-3-2 each showed a single and symmetrical narrow peak, and the distribution of total sugars was consistent with that of uronic acid (data not shown). The elution profiles from the TSK column showed a single and symmetrical narrow peak for each fraction. These results indicated that UAA-3-1 and UAA-3-2 were homogeneous fractions related to

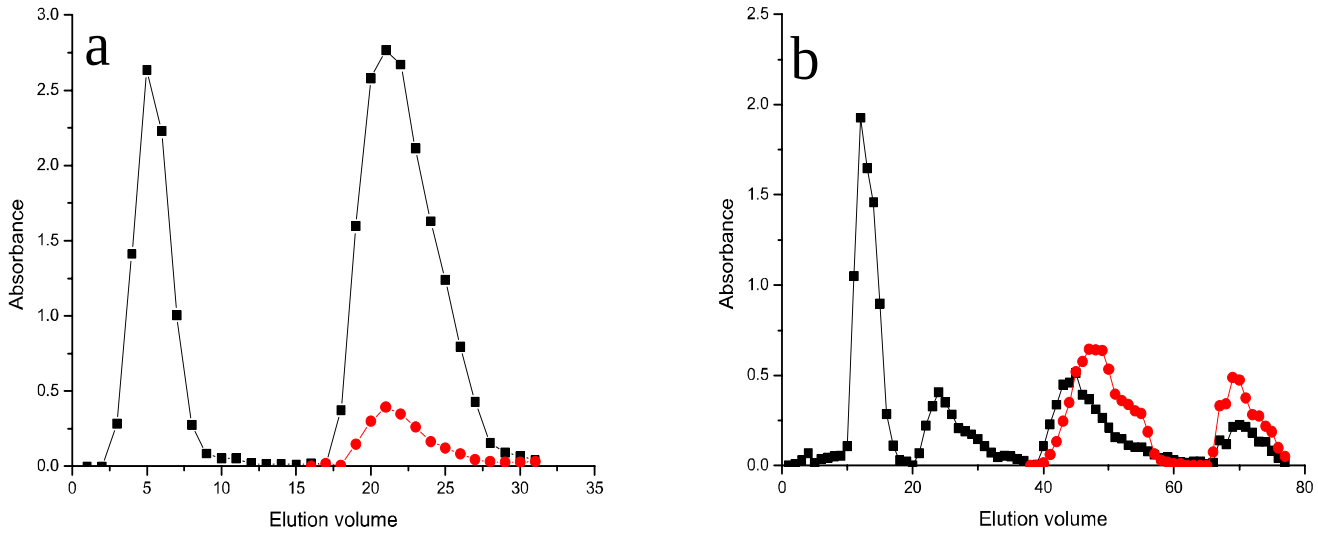

Figure 2. Elution profiles of UA and UAA on DEAE-cellulose column, eluted by a stepwise gradient of NaCl (a and b), respectively (total sugar, -■-; uronic acid, -●-)

molecular weight. The molecular weights were approximately deduced from the calibration curve of dextran standards by HPGPC to be 11 × 10^4 Da (UAA-3-1) and 1 × 10^4 Da (UAA-3-2).

Sugar composition of final fractions

The recoveries and sugar compositions of the collected fractions are listed in Table 1. It shows that there are three neutral fractions UAN, UAA-1 and UAA-2. UAN was mainly composed of glc (92.4%) and contained man, ara and gal as minor components. UAA-1 was only composed of glc (100%). UAA-2 was mainly composed of glc (78.0%) and contained man, ara and gal as minor components. The other four fractions were all acid fractions which showed that UAA-3 was mainly composed of galA, gal and ara, and contained man, glc, glcA and rha as minor components. The ratio of galA, gal to ara was 2.7: 1.2: 1.0. UAA-4 was mainly composed of galA, gal and ara, and contained man, glc, glcA and rha as as minor components. The ratio of galA, gal to ara was 4.3: 1.2: 1.0. UAA-3-1 was mainly composed of gal and ara, and contained man, glc, glcA, galA and rha as minor components. The ratio of gal to ara was 1.3: 1.0. UAA-3-2 was mainly composed of galA (72.1%) and contained man, glc, glcA, galA, ara and rha as minor components.

Features of collected fractions

To get more information about macromolecular features, the obtained fractions were tested with iodine to check for the presence of starch-like glucans. Moreover, NMR, periodate and Smith digestion were also used to characterize the structural features of these homogeneous fractions.

Macromolecular features of UAN and UAA-1

UAN and UAA-1 were two neutral fractions and generated a blue color when tested with iodine, which indicated the presence of starch-like glucans.

Macromolecular features of UAA-3-1 and UAA-3-2

UAA-3-1 contained gal and ara as the main sugars detected and glc, man, rha, galA and glcA as minor components, suggesting that these fractions might be composed of arabinans, galactans and/or arabinogalactans. The ratios of rha/galA determined for UAA-3-1 was 0.75, which is among the RG-I range from 0.05 to 1.0 defined by Schols and Voragen (1996). This suggested that it might contain RG-I domains. RG-I has been reported to be composed of α-(1,4)-linked D-galacturonic acid and α-(1,2)-linked L-rhamnose, which are alternatively combined with each other in the backbone; and some of the rhamnose residues contained side chains, such as arabinan, galactan and arabinogalactan at 4-O-rhamnose (McNeil et al.,1980). The arabinans, galactans and/or arabinogalactans might be associated with RG-I domains in non-covalent form or as side chains of RG-I.

The ^{13}C NMR spectra of UAA-3-1 resembled those of arabinogalactans-α reported in the literature (Gane, 1995; Wang et al., 2005). In the anomeric region, the signals at 108.2 and 106.8 ppm were assigned to α-Ara*f*, and the

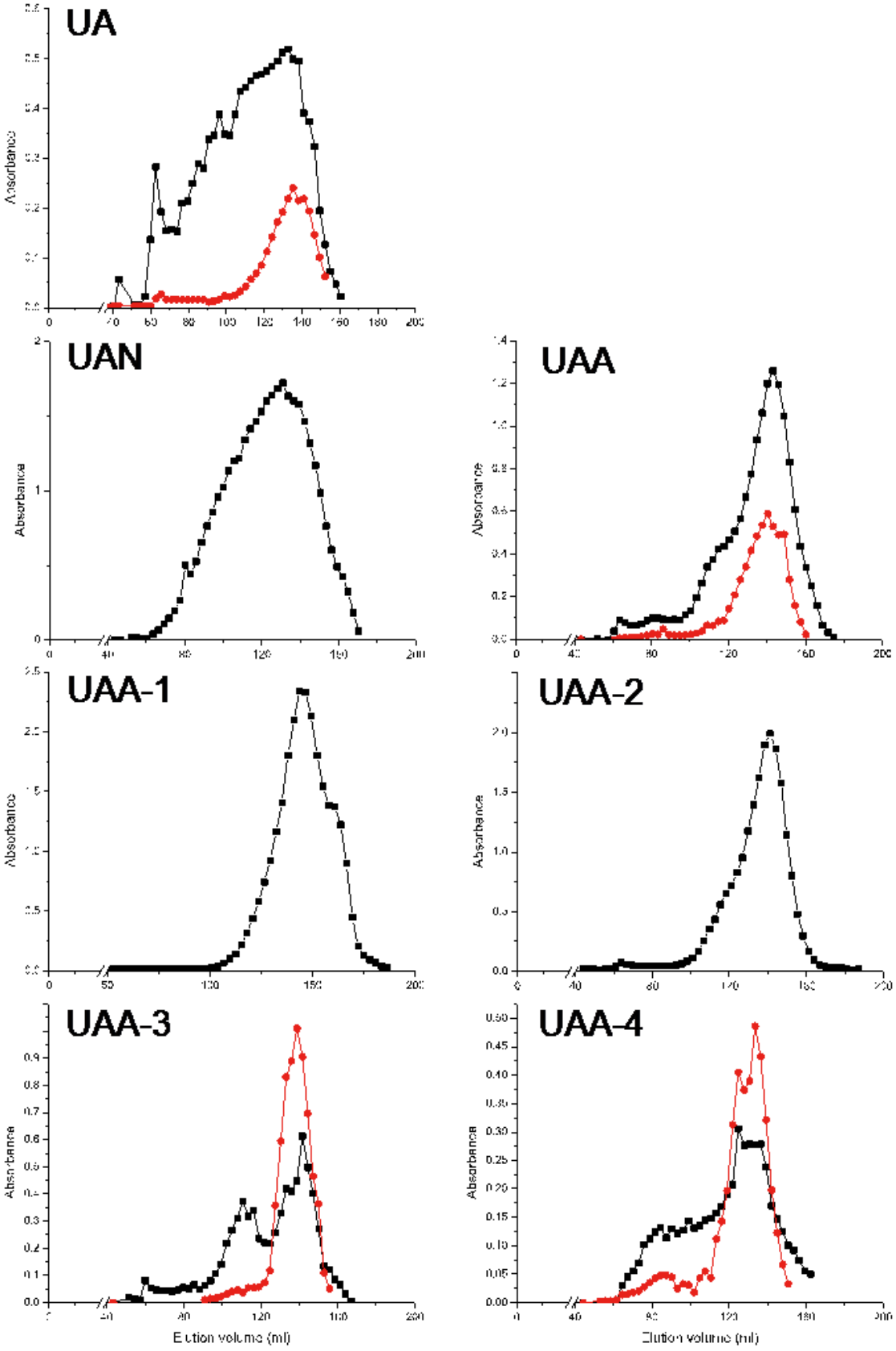

Figure 3. Sugar and uronic acid distribution of the different fractions on sepharose CL-6B (total sugar, -■-; uronic acid, -●-).

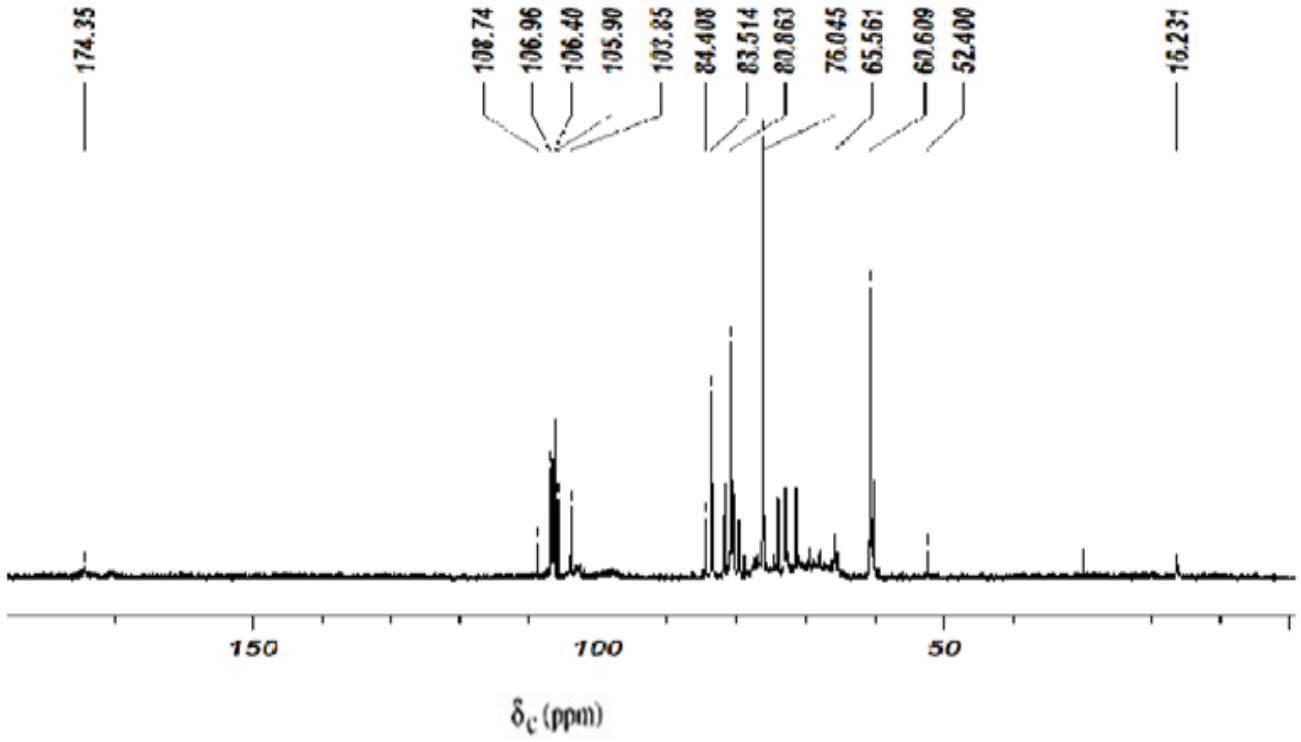

Figure 4. ^{13}C NMR spectra of UAA-3-1.

signals at 106.3 to 103.3 ppm were β-Gal*p*. Although the content of ara is less than that of gal in UAA-3-1, the signals for carbons of α-Ara*f* were obviously stronger than those of β-Gal*p*, which suggested that ara residues were in flexible side chains. Three anomeric carbon signals from ara residues of UAA-3-1 indicated that ara in this fraction might be present in two linkage forms, which usually exist in pectic arabinogalactan, including α-(1-5)-Ara*f* and non-reducing terminal α-Ara*f* (Polle et al., 2002). As seen in Figure 4, the multiple signals for C-1 of β-Gal*p* indicated that gal had more linkage forms. These results implied that UAA-3-1 had very complex structures similarly to other pectins. Ara and gal residues constituted hair regions containing type II arabinogalactan (Pérez et al., 2003), in which gal residues were in the backbone and ara residues were side chains or linked at non-reducing ends. Trace resonances at 19.2 and 172.6 ppm were assigned to C-6 in rha residues and C-6 in uronic acids, which was consistent with the detected sugar compositions (Figure 4).

UAA-3-2 contained high amounts of galA. The NMR spectra (Figure 5) of UAA-3-2 showed predominant resonances from carbons in free galactopyranosyl uronic acid residues in accordance with those previously observed in HG-rich pectins (Catoire et al., 1998). The signals for C-1 to C-6 of unesterified galA residues appeared at 97.8 (C-1), 67.0 (C-2), 67.7 (C-3), 76.8 (C-4), 70.2 (C-5) and 174.3 (C-6) ppm. The result showed that UAA-3-2 is HG-rich pectin, a linear α-(1, 4)-linked D-galacturonic acid. A small amount of neutral sugars that existed in these fractions might constitute RG-I domains linked to homogalacturonan (HG) domains in covalent or non-covalent forms. Pectin structure generally encompasses HG, RG-I and RG-II domains (Vidal et al., 2003; Yapo et al., 2007). Here, HG-rich pectins and RG-I-rich pectins were found in *U. Angustifolia* polysaccharides. However, RG-II domains were not detected by determining their diagnostic sugars (unpublished result). Perhaps the amount of RG-II domains was too low to be detected by the method used (Figure 5).

Swimming endurance experiment

The average time of loaded-weight swimming of mice of the treated groups were all remarkably longer than that of the control group. The average time of loaded-weight swimming of mice of the treated groups were all remarkably longer than that of the control group. The average swimming time of the LD, MD and HD group was increased by 85.4, 114.6 and 151.2%, respectively. These results indicated that *U. angustifolia* polysaccharides had significant effect on the anti-fatigue of the mice in the experiment (Table 2).

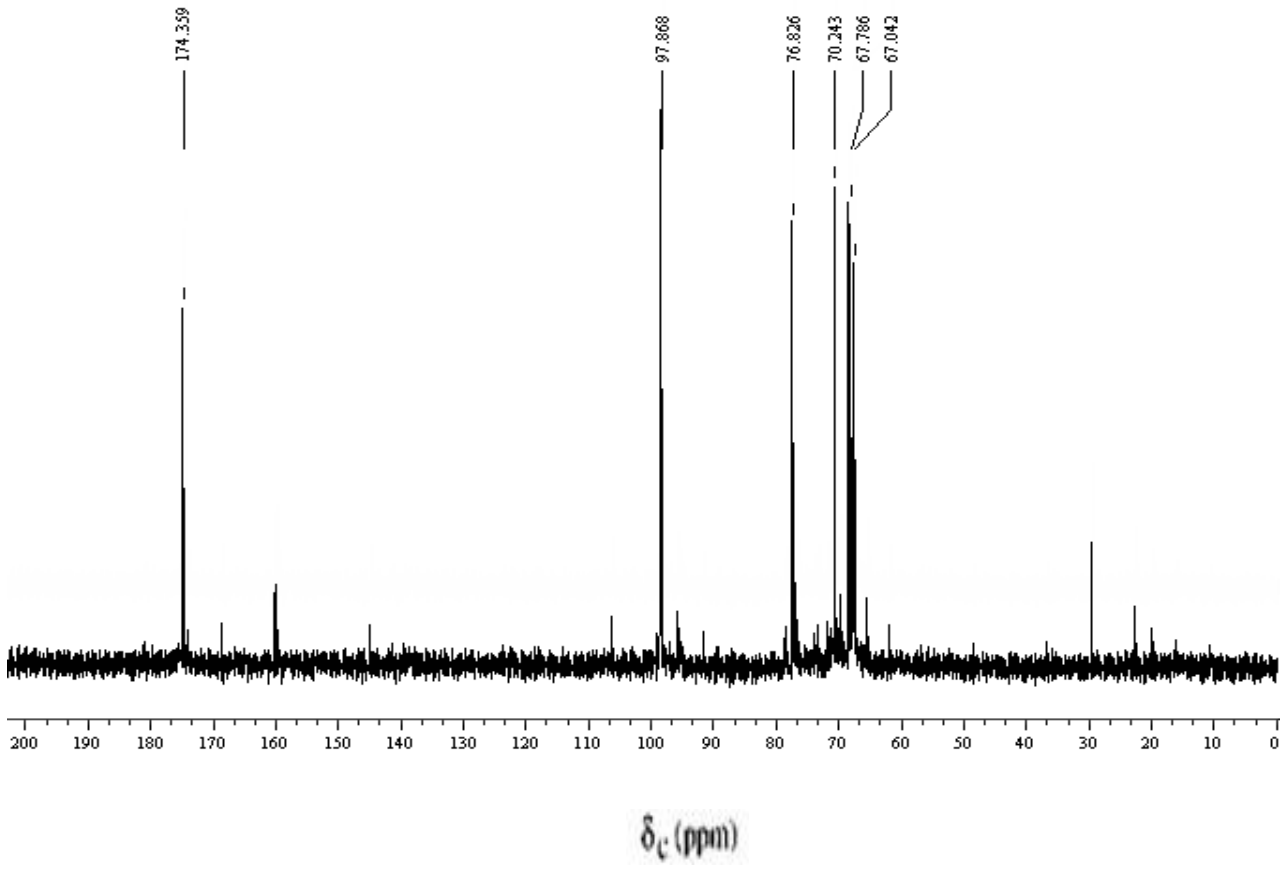

Figure 5. ^{13}C NMR spectra of UAA-3-2.

Blood urea nitrogen analyses

Blood urea nitrogen was the sensitive indicator to evaluate the body load bearing capacity. The blood urea nitrogen content of the LD, MD and HD group was reduced by 12.8, 13.6 and 19.8% compared with that of control group, respectively (Table 3). The results show that the blood urea nitrogen content of mice increased with the rising of the labor and exercise stress. However, the capacity to adapt to the load of mice deteriorated. The phenomenon is more significant when the blood urea nitrogen content is larger.

Hepatic glycogen analyses

Glycogen is an important energy source in the body movement which directly impact on the athletic ability, so improving glycogen reserves to improve speed, and endurance of great significance. The hepatic glycogen of every treated group was higher than that of control (CD) group, increasing rates were 87.0, 469.6, and 747.8%, respectively (Table 4). The results show that nettle root polysaccharide has a positive role to maintain glycogen content levels which can delay the appearance of fatigue.

Conclusion

The crude polysaccharides (UA) were obtained from *U. angustifolia* by using sevage reagent in a yield of 1.6%. The polysaccharides were fractionated into six fractions, using HPLC and NMR to analyze their sugar compositions and structures. The HPLC analysis results showed that UA contained two neutral polysaccharide fractions and four acidic fractions. The neutral fractions are mainly composed of glucose (Glc), and the acidic fractions are mainly composed of galacturonic acid (GalA). The NMR results showed that the neutral fractions are starch-like polysaccharides and the acidic fractions are rhamnogalacturonan (RG)-I domian containing pectin.

Fatigue is a complex process of physiological and biochemical changes, generally referring to recession network of physical and mental state leading to a decline in working ability and efficiency. The fatigue results are multi-faceted; lactic acid accumulation, glycogen lack and material consumption of energy are the major cause of fatigue. Nettle polysaccharide can replenish the energy. The length of swimming time may reflect the extent of exercise-induced fatigue, a strong indicator to evaluate the ability of anti-fatigue exercise. In this study, the length

Table 1. Yield and monosaccharide composition of collected fractions.

Fraction	Yield (g%)[a]	Monosaccharide composition (%)							Structure feature
		Gal	Glc	Ara	Rha	Man	GalA	GlcA	
UA	1.6	8.2	64.3	5.9	2.6	1.1	15.9	1.3	-
UAN	37.4	4.1	92.4	1.5	-	2.1	-	-	Starch-like glucans and arabinogalactans
UAA	44.6	14.7	30.6	10.8	4.6	1.8	35.3	2.2	-
UAA-1	25.9	-	100.0	-	-	-	-	-	Starch-like glucans
UAA-2	6.4	11.9	78.0	7.9	-	2.2	-	-	Starch-like glucans and arabinogalactans
UAA-3	42.0	20.5	4.8	17.0	5.8	1.4	45.8	3.6	-
UAA-4	21.5	14.2	9.6	12.0	8.9	0.8	51.9	9.6	-
UAA-3-1	12.7	41.9	4.8	31.5	7.0	2.3	9.3	4.8	AG-I containing RG-I domains
UAA-3-2	54.1	9.0	4.5	7.1	3.5	1.6	72.1	4.5	α-(1-4)-GalA backbone (HG)

[a]Yield in relation to fraction applied into column.

Table 2. Effect of the *U. angustifolia* polysaccharides on the body weight, swimming time of mice.

Group	Swimming time (s)	Percent of increase to control
Control doses (CD)	41±28	-
Low doses (LD)	76±40	85.4
Middle doses (MD)	88±47	114.6
High doses (HD)	103±80*	151.2

*p < 0.01(compared with CD).

Table 3. Effect of the *U. angustifolia* polysaccharides on the blood urea nitrogen of mice.

Group	Dose (mg/kg)	Blood uria nitrogen (BUN) (mmoL/L)	Percent of decrease to control
Control doses (CD)	-	10.59±0.61	-
Low doses (LD)	100	9.39±1.04*	12.8
Middle doses (MD)	200	9.32±1.65*	13.6
High doses (LD)	300	8.84±0.76**	19.8

*p < 0.05, **p < 0.01(compared with CD).

Table 4. Effect of *U.angustifoli* polysaccharides on the hepatic glycogen of mice.

Group	Dose (mg/kg)	Nitrogen content (mg/g)	Percent of increase to control
Control doses (CD)	-	0.23±0.075	-
Low doses (LD)	100	0.43±0.035	87
Middle doses (MD)	200	1.31±0.81**	496.6
High doses (HD)	300	1.95±0.478**	747.8

**p < 0.01(compared with CD).

of swimming time of nettle polysaccharide dose group was longer than the duration of swimming, playing anti-fatigue role.

Studies have shown that blood urea nitrogen levels of the body increases as the exercise load increase. Determining the changes of blood urea nitrogen in the movement is a simple and feasible method of knowing protein catabolism. From this experiment, blood urea nitrogen levels decreased as the dose increased, in which high-dose levels of blood urea nitrogen were significantly lower than the control group. This product can reduce the catabolism of protein and nitrogen-containing compounds, and enhance the body's ability to adapt to the exercise. The crude polysaccharides (UA)

obtained from *U. angustifolia* has a strong anti-fatigue effect. This indicated that the extractions can be efficient as a potent functional food.

REFERENCES

Bnouham M, Merhfour F, Ziyyat A, Mekhfi H, Aziz M, Legssyer A (2003). Antihyperglycemic activity of the aqueous extract of *Urtica dioica*. Fitoterapia 74:677-681

Blumenkrantz N, Asboe-Hansen G (1973). New method for quantitative determination of uronic acids. Anal. Biochem. 54:484-489.

Catoire L, Goldberg R., Pierron M., Morvan C., Herve´ Du Penhoat C (1998). An efficient procedure for studying pectin structure which combines limited depolymerization and C-^{13} NMR. Eur. Biophys. J. 27:127–136.

Dong YJ, ZhangHY, Guo XL, Li DF (2007). A new kind of health food resources- development and utilization of *Urtica angustifolia*. Sci. Technol. Food Ind. 12:213-215

Dubois M, Gilles KA, Hamilton JK, Rebers PA (1956). Colorimetric method for determination of sugars and related substances. Anal. Chem. 28:350-356.

Ding XH, Gao Y, Chao H, Xia D (2008). Study on Anti-fatigue Effect of Polysaccharide from Moso Bamboo Leaves. Food Sci. 29(4):389-391.

Guo X L, Zhang H Y, Li D F (2006). A new food resources of development value - nettle. Food Technol. 3:58-60

Gane AM, Craik D, Munro SLA, Howlett GJ, Clarke AE, Bacic A (1995). Structural analysis of the carbohydrate moiety of arabinogalactan-proteins from stigmas and styles of *Nicotiana alata*. Carbohydr. Res. 277:67-85

Konrad L, Müller HH, Lenz C (2000). Antiproliferative effects on human prostate cancer cells by a stinging nettle root (*Urtica dioica*) extract. Planta Med. 66(1):44-47

Kraus R, Spiteller G (1990). Lignanglucoside aus Wurzeln von *Urtica dioica*. Liebigs Ann Chem. 12:1205-1213.

Kavtaradze NS, Alaniya MD, Aneli JN (2001). Chemical compounds of *Urtica dioica* growing in Georgia. Chem. Nat. Compd. 37(3):287.

McNeil M, Darvill AG, Albersheim P. (1980). Structure of plant cell walls. X. Rhamnogalacturonan I, a structurally complex pectic polysaccharide in the walls of suspension-cultured sycamore cells. Plant Physiol. 66:1128-1134.

Newall CA, Anderson LA, Phillipson JD (1996). Herbal medicines: a guide for health-care professionals. London: The pharmaceutical press. P 201.

Neugebauer W, Winterhalter P, Schreier P (1995). 3-Hydroxy-α-ionyl-β-D- glucopyranosides from stinging nettle (*Urtica dioica*) leaves. Nat. Prod. Lett. 6(3):177-180.

Polle AY, Ovodova RG, Shashkov AS, Ovodov YS (2002). Some structural features of pectic polysaccharide from tansy, *Tanacetum vulgare* L. Carbohydr. Polym. 49:337-344.

Pérez S, Rodríguez-Carvajal MA, Doco T (2003). A complex plant cell wall polysaccharide: rhamnogalacturonanII. A structure in quest of a function. Biochimie 85:109-121.

Petlevski R, Hadžija M, Slijepčević M, Juretić D (2001). Effect of antidiabetis herbal preparation on serum glucose and fructosamine in NOD mice. J. Ethnopharmacol. 75:2-3

Quan CL, Guo CL (2007). Research on hypoglycemic constituents of natural medicines. J. Liaoning Med. Univ. 28(6):86-88.

Schulze-Tanzil G, Souza PH, Behnke B (2002). Effects of the antirheumatic remedy Hox alpha-a new stinging nettle leaf extract on matrix metalloproteinases in human chondrocytes *in vitro*. Histol, Histopathol. 17(2):477-485

Sedmark JJ, Grossberg SE (1979). A rapid,sensitive,and versatile assay for protein using Coomassie brilliant blue G250. Anal. Biochem. 79:544-552.

Shuqun S, Robert C (1997). Structure of the capsular polysaccharide of Clostridium Perfringens Hobbs 10 determined by NMR spectroscopy. Carbohydr. Res. 305:65-72.

Schols HA, Voragen AGJ (1996). Complex pectins: Structure elucidation using enzymes. In: Visser J, Voragen AGJ (eds.), Pectins and Pectinases. Amsterdam: Elsevier Sci. BV. pp. 3-19.

Vidal S, Williams P, Doco T, Moutounet M, Pellerin P(2003). The polysaccharides of red wine: Total fractionation and characterization. Carbohydr. Polym. 54:439-447.

Wang XS, Liu L, Fang JN. (2005). Immunological activities and structure of pectin from *Centella asiatica*. Carbohydr. Polym 60:95-101.

Yapo BM Lerouge P, Thibault JF, Ralet MC (2007). Pectins from citrus peel cell walls contain homogalacturonans homogenous with respect to molar mass, rhamnogalacturonan I and rhamnogalacturonan II. Carbohydr. Polym. 69:426-435.

Ziyyat A, Legssyer A, Mekhfi H, Dassouli A, Serhrouchni M, Benjelloun W (1997). Phytotherapy of hypertension and diabetes in oriental Morocco. J. Ethnopharmacol. 58(1):45-54.

Zhang HY, Yan XJ, Jiang Y, Han YS, Zhou YF (2011). The extraction, identification and quantification of hypoglycemic active ingredients from stinging nettle (*Urtica angustifolia*). Afr. J. Biotechnol. 10(46):9428-9437.

academicJournals

Vol. 7(22), pp. 1448-1454, 15 June, 2013
DOI 10.5897/AJPP12.454
ISSN 1996-0816 © 2013 Academic Journals
http://www.academicjournals.org/AJPP

African Journal of Pharmacy and Pharmacology

Full Length Research Paper

Effect of cooking methods on tetracycline residues in pig meat

VanHue Nguyen, MuQing Li, Muhammad Ammar Khan, ChunBao Li and GuangHong Zhou*

Key Laboratory of Meat Processing and Quality Control, Ministry of Education, National Center of Meat Quality and Safety Control, MOST, College of Food Science and Technology, Nanjing Agricultural University, Nanjing, 210095, PR China.

Accepted 28 June, 2012

Tetracyclines (TCs) are widely used for disease control in the livestock and poultry industry due to their broad spectrum of activity and affordability. However, some residues have been found to remain in the animals during slaughter and subsequent consumption. The potential of different cooking methods as strategies to reduce TC residues in pork were therefore investigated. Samples of pig muscles containing oxytetracycline (OTC), TC, chlortetracycline (CTC) and doxycycline (DC) residues were subjected to boiling, deep-frying or microwaving and the residues were extracted in a mixture of McIlvaine buffer-ethylenediaminetetraacetic acid (EDTA)/methanol (75:25, v/v), and then analyzed by high performance liquid chromatography (HPLC)-diode array detection on a XBridge™ C_{18} reverse phase chromatographic column. Results show that TC residues in muscles were reduced by 45.35 to 67.05% after boiling for 9 min, 38.17 to 65.74% after deep-frying for 9 min and 38.17 to 48.47% after microwaving for 1 min. It can therefore be concluded that from a safety and toxicological point of view, reduction of TC residues in pig muscle is an additional advantage of cooking as a food processing method and it is recommended that more studies in other kinds of meats be done.

Key words: Tetracyclines, pig muscle, cooking effects, antibiotics residues.

INTRODUCTION

Tetracycline antibiotics (TCs) have a broad range of activity against variety of gram-positive and gram-negative bacteria and are inexpensive. They are an important group of antibiotics and are widely used in livestock and poultry production. TCs are normally administered via injections, feedstuff or drinking water by veterinarians for therapy, prophylaxis and growth promotion in livestock and poultry (Chopra et al., 2001). The total amount of TCs sold or distributed for use in food-producing animals in the United States in 2009 were 4611892 and 515819 kg for domestic and export markets, respectively (FDA, 2009). The efficacy, availability and affordability of TCs have led to widespread misuse which in turn has led to presence of residues beyond acceptable levels in products of animal origin. Presence of excessive levels of antibiotics and other drug residues in products of animal origin has become a matter of considerable debate in food safety. The residue of these molecules has been correlated to the appearance of allergic reactions, development of bacterial resistances, modifications in intestinal flora, and possible mutagenic and/or carcinogenic effects (Demoly and Romano, 2005). Moreover, the long-term presence of TC residues may generate the evolution of microorganisms with resistance to a wider array of antibiotics (Garcia et al., 2004). To protect consumers from possible health related problems, many countries and economic blocks have set up maximum residue limits (MRLs) of some TCs in animal products. According to the European Union (EU), the MRLs of TC, chlortetracycline (CTC), oxytetracycline (OTC) and

*Corresponding author. E-mail: ghzhou@njau.edu.cn. Tel: +86 25 84395376. Fax: +86 25 84395939.

doxycycline (DC) for all animal species have been set at 100, 300 and 600 ngg^{-1} in muscle, liver and kidney tissues, respectively (Council-Regulation, EEC No. 2377/90/EC of 1990). The corresponding values set by Codex Alimentarius Commission are 200 ngg^{-1} in muscle, 600 ngg^{-1} in liver and 1200 ng g^{-1} in both fat and kidney tissues (FAO/WHO, 2004). The US FDA has set the limit of MRLs of TC, CTC, DC and OTC antibiotic residues at 200, 600 and 400 ngg^{-1} in muscle, liver and milk, respectively (US Code of Federal Regulations, 2003).

Drug residues are procedurally measured on uncooked tissues but most foods of animal origin undergo further processing prior to consumption (thermal or food additive treatments or both) for the purpose of increasing palatability and shelf-life. These treatments are mainly done to ensure safety and quality of the food, since heat will reduce or inhibit microbes in food thus, reducing harm to humans. Several studies have been done to study the effect of heat treatment on antibiotics in meat. Studies have demonstrated the effect of heat treatment on antibiotic residues in meat. Antimicrobial drugs undergo degradation in meat during cooking; while net residues in the cooked muscles have been reported to be reduced up to 40% by boiling, roasting in 12 min each, while by microwaving in 1 min (Furusawa and Hanabusa, 2001). Other studies from different cooking processes reveal a reduction in the concentration of DC residue with some of the residue being excreted from the tissue to the cooking fluid during the boiling process (Javadi, 2011). The biological activity of ampicillin, chloramphenicol and OTC has been found to reduce by 12 to 50% in bovine meat after roasting at 50 to 90°C for 20 min. Factors affecting degradation of antimicrobial drugs include drug formulation and pharmacodynamics, cooking temperature and duration, as well as the shape and thickness of cooked tissues (O'Brien et al., 1981). Rose et al. (1996) reported substantial net reductions of 35 to 94% for OTC in beef and mutton, with temperature during cooking having the largest contribution to this loss. Several studies indicate that thermal treatments may reduce the concentration of veterinary drug residues in food and thus, decrease the potential toxic effects of these compounds on the food consumer (Gratacos Cubarsi et al., 2007). The purpose of this study was to examine the net changes in TC, OTC, CTC and DC residues in pig muscles under boiling, deep-frying and microwaving as cooking methods over different periods of time.

MATERIALS AND METHODS

Chemicals

The chemicals used are acetonitrile and methanol of high performance liquid chromatography (HPLC) grade (Merck Company, Germany), analytical grade oxalic acid, disodium ethylene diaminetetraacetate (Na_2EDTA), and sodium hydroxide (NaOH) and standards of OTC, TC, CTC and DC (Sigma–Aldrich, St. Louis, MO, USA).

Equipment

They include an Agilent Technologies model Series 1200 (Waldbronn, Germany) equipped with a model G1322A online vacuum degasser, a model G1311A quaternary pump system, a model G1367A auto sampler and model G1315B photodiode-array detector. The analytical column was reversed-phase (XBridge™ C_{18} 250 □ 4.6 mm I.D., 5 µm, waters, Ireland). Water purification systems (Mul- 9000 series, USA) online GC 200 expansion vessel for potable water (Global water solution company, USA) and a nano pure Model 7150 (Thermo Scientific). For sample preparation, ULTRA-TURRAX T25 Basic homogenizer (IKA works, Staufen, Germany), Centrifuge Allegra 64R (Beckman coulter, USA), Ultrasonic (KQ-300DE, Kun Shan, China). For cooking processes (C-MAG HP10) (IKA works, Staufen, Germany), Microwave oven (800W, 2450MHz, Galanz, China) were used.

Standard solutions

A stock standard solution of each TC compound was prepared by dissolving 10 mg of the compound in 10 ml of methanol to obtain a final concentration of 1 $mgml^{-1}$. Stock standard solutions were then put in amber glasses to prevent photo-degradation and stored at -20°C and left to stabilize for at least 4 weeks. They were then diluted with methanol to give a series of working standard solutions. Finally, chromatographic solutions for each compound were prepared by dilution of the combined working solution with mobile phase.

Samples

Pork samples were extracted from loin muscles from pigs kept in purely organic farms. All samples were analyzed to ensure that none contained TC residues and stored at -20°C until use.

Cooking operations

Antibiotic free pig muscles were homogenized in a bowl cutter (Model GM 200, Retsch, Germany) and fortified with methanolic stock solution of the different TCs. After this, they were immediately analyzed before further treatment to verify the homogeneity of TC addition in the samples. The mixtures were then made into portions of 10 g pig balls.

Boiling

A 10 g sample (pig ball) was first tempered to an initial temperature of 20 ± 2°C and then immersed in a water bath (Jin Tan, Heng Fing, China) at 100°C for 3, 6 or 9 min.

Deep-frying

A 10 g sample (pig ball) was fried in a non-stick frying pan with sunflower cooking oil at 170°C for 3, 6 or 9 min. No juice was collected.

Microwaving

A 10 g sample (pig ball) was tempered to an initial temperature of 20 ± 2°C and placed at the geometric center of a turntable domestic microwave oven. The sample was cooked under full power (800 W, 2450 MHz) for 0.5, 0.75 and 1 min, respectively. No juice was

collected. After treatment, all samples were immediately placed on an ice bath, and stored at 4°C for subsequent analysis within 1 day. All cooking treatments were done in triplicate.

HPLC analysis

The procedure followed for the extraction of the TCs from the prepared samples had been earlier described (Gratacos Cubarsi, et al., 2007). The procedure for the analysis of OTC, TC, CTC, DC residues in cooked or uncooked pig muscle samples (whole quantity, 10 g) was done as follows: An aliquot of 10 g (accuracy, 0.01 g) of pig muscle sample were cut in small pieces and placed in a glass centrifuge tube. 20 ml of McIlvaine buffer-EDTA/MeOH was added and blended for 3 min with cool homogenizer. Probes were rinsed into centrifuge tubes with 3 ml McIlvaine buffer-EDTA/MeOH solution and the accruing rinsate vortexed for 1 min, and sonicated for 10 min. This was followed by centrifugation at 12100 g for 15 min, then supernatant was collected and the precipitate extracted again after adding 20 ml McIlvaine buffer-EDTA/MeOH as previously described. The combined supernatant was filtered through a filter paper and diluted to a final volume of 50 ml with extracting solution. One (1) ml of the final extract was filtered with a nylon filter (porosity: 0.45 µm) and 100 µl injected into the chromatographic system.

The analytical column was reversed-phase (XBridge^{TM} C_{18} 250 □ 4.6 mm I.D., 5 µm, waters, Ireland) set at a flow rate of 1 ml min^{-1}. The column temperature was 35°C. Mobile phase A was methanol, solvent B was acetonitrile, while mobile phase C was 0.01 M oxalic acid in water. The starting mobile phase composition at 0 min was 10:20:70, methanol/acetonitrile/oxalic acid at 1.0 ml/min. It was switched to 15:20:65 after 10 min and going back to the initial conditions in 5 min. The wavelength of ultraviolet (UV) detector was set at 351 nm.

Calibration curves were prepared daily by injecting chromatographic standard solutions in the range between 50 and 2000 ng injected for each compound and estimates of the amount of the analytes in samples were interpolated from these graphs.

Recovery

Sample recovery was determined with blank pig muscle spiked at 0.5 and 1 µgg^{-1} for the raw samples (10 g) or at 0.5 and 1.0 µgg^{-1} for the samples cooked by boiling for 9 min, deep-frying for 9 min and microwaving for 1 min. The spiked samples were analyzed and the recoveries calculated by comparing the peak area of measured concentration to the peak area of the spiked concentration.

Statistical analysis

A descriptive statistical analysis was applied to the validation data, and the influence of the time or cooking method on concentration of TCs was analyzed by one-way analysis of variance (ANOVA) while means were compared using least significant difference (LSD). All data were analyzed at a significance level of 0.05. All analyses were carried out using the SPSS statistics software version 20.

RESULTS AND DISCUSSION

The procedure employed in this work involved four kinds of TC, all of which were extracted efficiently from both uncooked and cooked samples and accurately measured by HPLC. Typical HPLC profiles of the TCs obtained from the standard solutions and the samples are shown in Figure 1, where the four TCs were well separated by the column with elution times ranging from about 3.5 to 11 min. TCs were identified in the samples by their UV spectrums obtained using the photodiode-array detector and retention times. Linearity was evaluated by calibration curves in the range of 10 to 2000 ng for each compound at five points with triplicate analysis. The obtained results are shown in Table 1. The analysis results further revealed that linear regression coefficients (R^2 > 0.9992) were obtained for all tested analytes. The limit of detection (LOD) is considered to be the quantity yielding a detector response approximately equal to thrice the background noise. The limit of quantitation (LOQ) is the lowest amount that can be analyzed within acceptable precision and accuracy at signal to noise ratio of 10 (Biswas et al., 2007). The data shown in Table 1 demonstrates that LOD for the four TCs ranged from 5 to 13 ng, LOQ was 15, 20, 42 and 31 ng for OTC, TC, CTC and DC, respectively.

The spiked concentration for each TC was set at two levels of 0.5 and 1.0 µgg^{-1} and using standard addition method the recoveries of four TCs in the muscle samples were as shown in Table 1. The recoveries of the four TCs in the spiked pig muscle samples were 79.17 to 89.28%. The relative standard deviation (RSD) of the recovery of the four TCs was less than 7.6%. This means that the applied extraction and purification procedure appeared to be efficient, and the HPLC analysis procedure was applicable to detect TC residues in the pig muscle samples. These results are in clear agreement with previous work (Gratacos Cubarsi et al., 2007). The internal temperature in the centre (calculated geometrically) of the cooked sample for each cooking method was monitored. The internal temperature of the meat did not rise above 100°C in any method, and this temperature was not maintained for more than 9 min in boiling and deep-frying or 1 min for microwaving. The highest achieved temperatures were 96.3, 97.0 and 95.5°C during boiling, deep-frying and microwaving, respectively. At 6 min of boiling, 3 min of deep-frying and 0.5 min of microwaving, the samples had a well-done appearance (the internal temperature in center of sample being ≥ 80°C) (Table 2). In these three cooking methods, decreases in measured sample weights ranging from 16 to 23, 14 to 30 and 15 to 28% of the initial weight of 10 g of raw pig muscle were observed during boiling, deep-frying and microwaving, respectively. The net changes of analyte residues in the samples were then analyzed.

The levels of antibiotic residues in pig muscle before and after cooking were compared. The results for each cooking method are shown in Table 2. The results revealed a decrease of all TCs with boiling reducing the TC residues by 27 to 67% after 9 min (Table 2). All the TC residues decreased gradually after the start of cooking. The reductions in OTC, TC, CTC and DC in pig muscles during deep-frying were 32 to 66% in 9 min

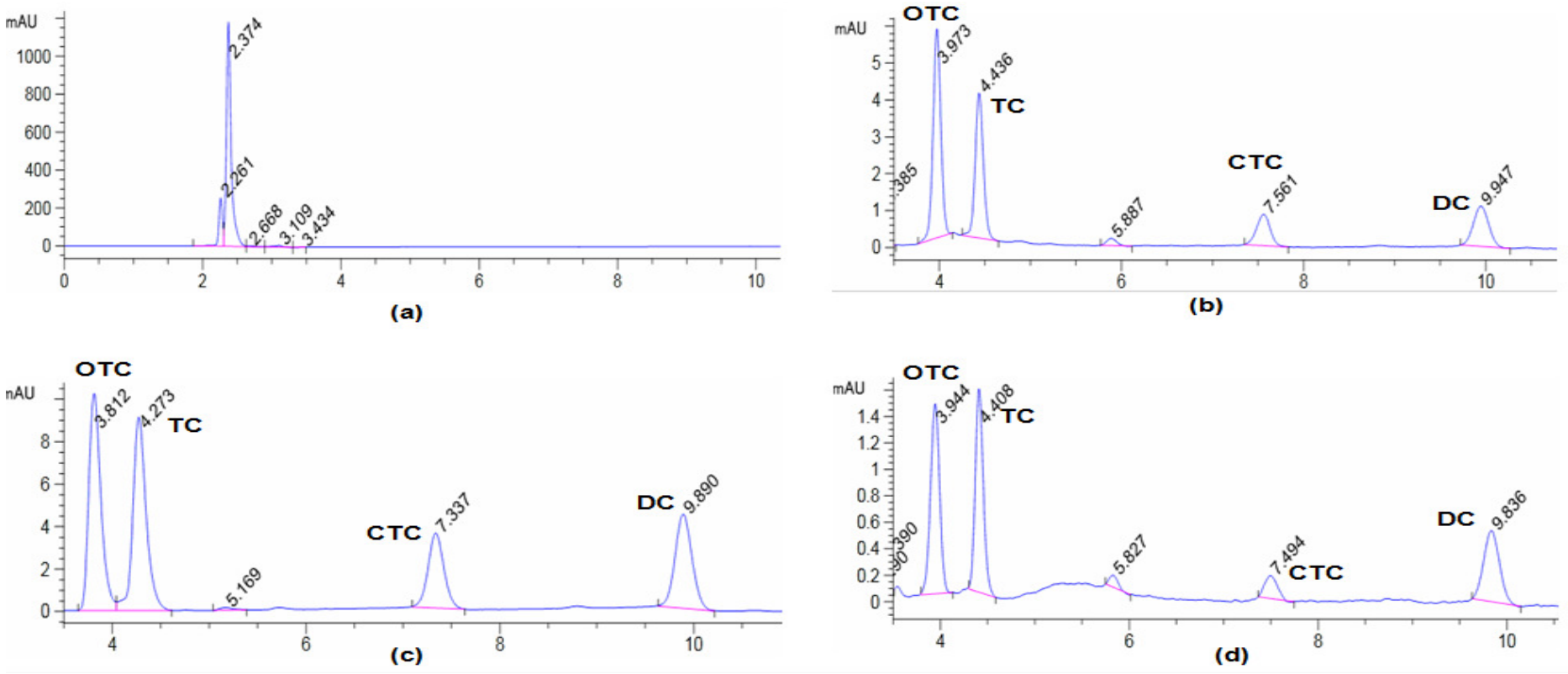

Figure 1. (a), Chromatogram of blank pig muscle samples; (b), chromatogram of spiked pig muscle of each TC; (c), chromatographic standard solution; (d), chromatogram of spiked pig muscle samples of each TC, thermally treated.

(Table 2). Microwaving resulted in 24 to 49% in reduction in TCs levels (Table 2). The statistical analysis (one-way ANOVA) demonstrate a highly significant ($p < 0.05$) difference in the levels of all the TCs between spiked raw and cooked pig muscle samples (Table 2).

The change in TC levels in the tissues depended on the type of TC as well as the method and time of cooking (Table 3). The results showed that CTC had the highest reduction (67, 66 and 48%), while DC showed the lowest reduction (45, 38 and 38%) after cooking by boiling, deep-frying and microwaving, respectively (Table 3). The differences in TC residue under boiling and microwaving were significant for all TCs tested ($p < 0.05$) while OTC was significantly different among all the cooking methods (Table 3).

The results reported here are consistent with those previously reported in studies in which thermal treatments were shown to reduce the concentration of veterinary drug residues in foods, therefore decreasing the possible toxic effects of these compounds to consumers. For example, in investigating the effect of a range of cooking processes including microwaving, boiling, roasting, grilling, braising and frying on OTC residues in animal tissues (Rose et al., 1996) observed substantial net reductions in OTC of 35 to 94%, with temperature during cooking being shown to have the largest impact on the loss. In addition, migration from the tissue into the surrounding liquid or meat juices were observed during the cooking processes. Interestingly, it has been reported that

Table 1. Recoveries (mean, %, n = 5) for raw/cooked TC-fortified pig muscles and linearity, sensitivity, LOD and LOQ of method.

	Cooking method								Linearity, sensitivity, LOD, LOQ method			
	Raw		Boiled		Deep-frying		Microwaving					
TCs added μgg^{-1}	0.5	1	0.5	1	0.5	1	0.5	1	Regression	R^2	LOD ngg^{-1}	LOQ ngg^{-1}
OTC	86.99 (4.91)[A]	87.22 (1.20)	87.72 (1.06)	88.22 (4.95)	87.50 (2.17)	88.82 (1.50)	87.87 (3.48)	89.28 (3.55)	Y = 0.189X - 0.119	0.9996	5	15
TC	81.78 (5.66)	82.68 (2.63)	82.28 (2.55)	84.19 (4.69)	84.93 (4.65)	86.83 (7.56)	84.66 (6.18)	85.62 (5.23)	Y = 0.184X - 0.067	0.9992	7	20
CTC	79.17 (3.69)	81.43 (6.23)	81.59 (1.30)	83.69 (2.29)	82.77 (3.83)	83.88 (6.36)	83.63 (0.80)	85.03 (4.78)	Y = 0.082X - 0.167	0.9992	13	42
DC	82.29 (2.47)	83.38 (2.47)	82.65 (1.84)	84.45 (1.85)	83.17 (4.04)	85.40 (4.71)	83.14 (4.74)	87.10 (4.39)	Y = 0.111X - 0.109	0.9999	10	31

A, Values in parentheses are relative standard deviation of the recovery of the four TCs.

Table 2. Absolute quantities (mean, μg, n = 3) of residual TCs in pig muscles (10 g/raw) cooked by boiling, deep-frying and microwaving.

	Cooking method											
	Boiling				Deep-frying				Microwaving			
Time in cooking (min)	UC*	3	6	9	UC	3	6	9	UC	0.5	0.75	1
Temperature[A] (°C)	20.2	69.5	94	96.3	19.4	93.4	96.5	97.0	19.2	80.4	95.5	93.7
OTC	0.91^{a}	0.61^{b} (33.0)[B]	0.50^{c} (45.4)	0.36^{d} (60.1)	0.91^{a}	0.55^{b} (39.8)[B]	0.45^{c} (50.4)	0.41^{d} (55.1)	0.91^{a}	0.68^{b} (25.2)[B]	0.58^{c} (36.9)	0.47^{d} (48.5)
TC	0.54^{a}	0.37^{b} (31.3)	0.30^{c} (44.2)	0.24^{d} (55.8)	0.55^{a}	0.35^{b} (37.0)	0.31^{c} (44.2)	0.29^{c} (46.7)	0.54^{a}	0.4^{b} (24.8)	0.37^{c} (30.4)	0.32^{d} (41.0)
CTC	0.50^{a}	0.30^{b} (40.4)	0.21^{c} (58.3)	0.17^{d} (66.9)	0.51^{a}	0.33^{b} (35.5)	0.18^{c} (65.1)	0.17^{c} (65.8)	0.51^{a}	0.33^{b} (34.2)	0.32^{b} (37.5)	0.26^{c} (48.0)
DC	0.61^{a}	0.44^{b} (27.3)	0.39^{c} (35.5)	0.33^{d} (45.9)	0.62^{a}	0.42^{b} (31.4)	0.38^{c} (38.4)	0.37^{c} (39.5)	0.58^{a}	0.45^{b} (23.4)	0.44^{b} (25.1)	0.37^{c} (36.0)

A, Internal temperatures in geometric centre of cooked pig muscles; B, values in parentheses are percentages of reduced drug residues from the uncooked samples; [a,b,c,d], values with different letters (a to d) within the same row reduce significantly ($p < 0.05$). *Uncooked meat samples.

Table 3. Effect of different cooking methods on TC residues in pig balls at the end of the heating process.

Cooking process	Temperature/ Power/ time	Percentages of reduced drug residues compared to the uncooked samples			
		OTC	TC	CTC	DC
Raw	Control	100^{a}	100^{a}	100^{a}	100^{a}
Boiling	96.3°C/9	60.16^{b}	55.85^{b}	67.05^{b}	45.35^{b}
Deep-frying	97.0°C /9	55.04^{c}	46.04^{bc}	65.74^{b}	38.17^{c}
Microwaving	93.7°C/800W/1 min	48.47^{d}	41.75^{c}	47.95^{c}	38.17^{c}

[a,b,c,d], Values with different letters (a to d) within the same column reduce significantly ($p < 0.05$).

no individual closely related compound such as 4-epioxytetracycline, α- or β-apooxytetracycline forms a significant proportion of the breakdown products when meat containing TC is cooked by different methods which indicates that the effect of cooking on residues of OTC and other TCs should be considered before data obtained from measurements on raw tissue are used for consumer exposure estimates and dietary intake calculations. In a contrasting report from a study to examine the formation of anhydrotetracycline and 4-epianhydrotetracycline, as toxic degradation products of TC during a heat treatment, it was found that heat treatments led to a significant increase of the amounts of these degradation products (Kuhne et al., 2011) which means that there is need for further studies to provide more insight into the effect of cooking on TCs. Javadi (2011) also reported a great reduction in DC residues in different tissues of broiler chicken under different cooking methods.

A number of studies have demonstrated the formation of 4eATC and ATC in bones containing TCs after a severe thermal treatment Although we did not evaluate the formation of 4eATC and ATC in this study, Gratacos Cubarsi, et al. (2007) have reported that the formation of ATCs is in edible meat samples containing TCs after mild cooking treatments, and they also showed that thermal treatments may reduce the concentration of veterinary drug residues in foods, decreasing the possible toxic effects of these compounds. Microwave heating is the quickest way to reduce TC residues in meat but it also leads to more pronounced production of ATCs probably as a consequence of the higher temperatures quickly reached in meat samples during microwaving compared to other cooking methods. Fedeniuk et al. (1997) showed that some synergy exists when thermal treatments are combined with food additives. They found that additive like sodium nitrite can lead to significant increases in the rate of OTC degradation under thermal treatments. This observation needs further investigation.

Conclusion

When conducting a risk assessment of TC in human health, the presence of these contaminants in meat and other meat products should be considered as a potential source, depending on levels of contaminants and the daily intake of meat. This study was designed to evaluate strategies for reduction of TC in meat before consumption. The results of this study show that the amount of TC residues is significantly affected by cooking whereby both cooking time and methods were found to be important. Though all cooking methods are effective, microwaving exhibited significantly fast reduction of all the four types of TC. Reduction in TC concentrations during boiling and deep-frying was due to migration of the TC from the meat balls to cooking medium (water and oil) while during the microwaving process, reduction was due to juice exuding out from the pig balls. The overall loss of TC residues was due to denaturation of protein - TC compounds. From the safety and toxicological point of view, these findings show an additional advantage of cooking as a food processing method. The cooking methods used in the present study are similar to those widely applied to meat during household cooking. Therefore, the observed findings may be helpful in confirming and selecting the ideal method for cooking so as to effectively reduce TC and probably other antibiotic residues in meat prior to consumption.

ACKNOWLEDGMENTS

The authors are grateful to XiaoBo Yu, Hao Zhao, Guido Fleischer and YunZhi Ge for their assistance in some experiments. The study was funded by 200903012 and the Priority Academic Program Development of Jiangsu Higher Education Institutions.

REFERENCES

Biswas AK, Rao GS, Kondaiah N, Anjaneyulu AR, Mendiratta SK, Prasad R (2007). A simple multi-residue method for determination of oxytetracycline, tetracycline and chlortetracycline in export buffalo meat by HPLC–photodiode array detector. J. Food Drug Anal. 15(3):278–284

Chopra I, Roperts M (2001). Tetracycline antibiotics: mode of action, applications, molecular biology, and epidemiology of bacterial resistance. Microbiol. Mol. Biol. Rev. 6:232–260

Council-Regulation (EEC No. 2377/90/EC of 1990). Laying down a community procedure for the establishment of maximum residue limits of veterinary medicinal products in foodstuffs of animal origin, Brussels, Belgium. Official J. Eur. Community L 224: 1–124

Demoly P, Romano A (2005). Update on Beta - lactam allergy diagnosis. Curr. Allergy Asthma Rep. 1:9–14

FAO/WHO (2004). Residues of some veterinary drugs in animals and foods. Sixty-second report of the Joint FAO/WHO export committee on food additives. WHO Technical Report Series, FAO FNP 41/16.

FDA (2009). Summary report on antimicrobials sold or distributed for use in food-producing animals. Food and Drug Administration Department of Health and Human Services. Available at: http://www.fda.gov/downloads/ForIndustry/UserFees/AnimalDrugUserFeeActADUFA/UCM231851.pdf

Fedeniuk RW, Shand PJ, McCurdy AR (1997). Effect of Thermal Processing and Additives on the Kinetics of Oxytetracycline Degradation in Pork Muscle. J. Agric. Food Chem. 45:2252–2257

Furusawa N, Hanabusa R (2001). Cooking effects on sulfonamide residues in chicken thigh muscle. Food Res. Int. 35:37–42

Garcia I, Sarabia LA, Cruz OM (2004). Detection capability of tetracyclines analysed by a fluorescence technique: comparison between bilinear and trilinear partial least squares models. Analytica Chimica Acta. 501:193–203

Gratacos Cubarsi M, Fernandez Garcia A, Pierre P, Valero-Pamplona A, Garcia-Regueiro J-A, Castellari M (2007). Formation of Tetracycline Degradation Products in Chicken and Pig Meat under Different Thermal Processing Conditions. J. Agric. Food Chem. 55:4610–4616

Javadi A (2011). Effect of roasting, boiling and microwaving cooking method on doxycline residues in edible tissues of poultry by microbial method. Afr. J. Pharm. Pharmacol. 5(8):1034-1037

Kuhne M, Hamscher G, Korner U, Schedl D, Wenzel S (2001). Formation of anhydrotetracycline during a high-temperature treatment of animal-derived feed contaminated with tetracycline. Food Chem. 75:423-429

O'Brien JJ, Campbell N, Conaghan T (1981). Effect of cooking and cold storage on biologically active antibiotic residues in meat. J. Hyg. 87:511-523

Rose MD, Bygrave J, H. FWH, Shearer G (1996). The effect of cooking on veterinary drug residues in food: 4. Oxytetracycline Food Additives and Contaminants: Part A 13(3):275-286

US Code of Federal Regulations (2003). Code of Federal Regulations, Title 21, Part 556, Sections 150, 500, and 720, US.

academicJournals

Vol. 7(22), pp. 1455-1463, 15 June, 2013
DOI 10.5897/AJPP12.1095
ISSN 1996-0816 © 2013 Academic Journals
http://www.academicjournals.org/AJPP

African Journal of Pharmacy and Pharmacology

Full Length Research Paper

Impact of high hydrostatic pressure on gel formation of low methoxylpectin

M. N. Eshtiaghi[1,2]* and J. Kuldiloke[1]

[1]Department of Chemical Engineering, Faculty of Engineering, Mahidol University, Thailand.
[2]Institute of food and bioprocess Engineering, Technical University of Berlin, Germany.

Accepted 30 April, 2013

The effect of different treatment conditions (pressure, treatment time, and temperature), as well as composition of pectin solution (Pectin, Ca^{++} ion and sugar concentration, pH) on gel formation of two types of low methoxylpectins were investigated. The results have shown that with increasing pressure, time or temperature during high hydrostatic pressure (HHP) treatment, the gel hardness increased continuously. Up to 2.5 times higher gel hardness could be achieved after HHP treatment (550 MPa, 35°C, 10 min, and 2% pectin) compared to untreated sample. Higher sugar concentration in pectin solution (about 30 to 60%) resulted in drastically increasing the gel hardness for untreated as well as HHP treated samples but the overall gel hardness was, in the case of HHP treated samples, distinctly higher than the untreated. Similar results could be observed if the Ca^{++} ion concentration increased up to 90 mg/g pectin. Increasing the pH of pectin solution from pH = 3.4 to 5.6 decreased the gel hardness in the case of untreated as well as HHP treated samples. The results of this study confirmed that it is possible to produce firm gel from low methoxylpectin at temperature of ≤ 35°C using high hydrostatic pressure technique.

Key words: Low methoxylpectin, gels, high hydrostatic pressure.

INTRODUCTION

Pectin is a naturally-sourced polysaccharide with wide range of application in food industries as thickener or gelling agent (Lootenes et al., 2003). Pectins are complex mixtures of polysaccharine with linearly connected α (1-4) D-galactronic acid residues interrupted occasionally by 1-2 linked rhamnose residue. Pectin is usually characterized by its degree of methylation (DM) of the carboxyl groups (Thakur et al., 1997). The degree of substitution of methyl esters determines the mechanism of formation of pectin gels and their conformational and rheological properties (Fishman et al., 1984). Pectin with a degree of methylation less than 50%, so-called low-methoxylpectin, forms gel in the presence of Ca++ ions. The gel formation process of low methoxylpectin involves the simultaneous bounding of calcium ion to carbonyl groups of two adjacent pectin molecules and to two hydroxyl groups from one of the molecules (Smidsrod et al., 1972). Grant et al. (1973) suggested an egg-box like model to explain the structure of pectin molecules bound by the calcium ions.

Since the early 1980s, high hydrostatic pressure has been evaluated as an alternative to classical heat treatment food-processing technologies for energy-saving reason. One of the main focuses of high hydrostatic pressure applications has been food preservation at moderate temperatures (Dumoulin et al., 1988). Pressure affects molecules (for example, inactivation/activation of enzymes, protein denaturation), can change the state of molecular organization (for example, crystallization of fat, phase changes of phospholipids, denaturation-induced aggregation and gelation, gelatinization of crystalline starch, depolymerization) (Michel and Autio, 2005). The

*Corresponding author. E-mail: mneshtiaghi@hotmail.com. Tel: ++66815698914

effect of pressure on hydrocolloids has been studied only to a limited extend.

Yen and Lin (1998) reported that hydrocolloid solutions (colloids) are not affected by hydrostatic pressure. Pectin is affected as a mixture of heteropolysaccharides consisting predominantly of partially methoxylated galactronic acid residue (Pilnik, 1990). Michel and Autio (2005) have reported that the degree of methyl esterification of the high methoxylpectin (HMP) (extracted from citrus fruits) did not change when the solutions were pressure treated at pH 5.0; when the pH was 7.0, high hydrostatic pressure treatment caused the degree of methyl esterification to fall from 65% to below 60%. Additionally, they found that the viscosity of a 1.5% HM-pectin solution could be increased up to 10 fold after pressure treatment at 400 MPa and 25°C.

An analysis of the elastic (G′) and viscous moduli (G″) showed that G′ is much greater than G″, indicating that the pectin solution shows a predominantly "solution-like" behavior at all pressure. Pressure increases both the elastic and the viscous moduli. Michel et al. (1998) observed a much more pronounced viscosity increase upon pressure treatment with 1.5% sugar-free high methoxyl apple pectin (degree of methyl esterification 70 to 75%). Those the pressure influenced might be dependent on the pectin source.

The aim of this study was to investigate the effect of different processing conditions (pressure level, treatment temperature and time) during high hydrostatic treatment as well as composition of pectin solutions (Ca^{2+}, sugar, pectin concentration) on the firmness of two different low methoxylpectin gels.

MATERIALS AND METHODS

Raw material

Low methoxylpectin from company Kelco (Genu© Pectin typ LM-102 AS, with degree of esterification of 35% and degree of amidation of 15%) and company Herbstreith and Fox (Pectin classic AB 902, with degree of esterification of 35 to 44% and without amidation) was used as raw material. We used the abbreviation "LM" for 15% amidated low methoxylpectin from company Kelco and "902" for low methoxl pectin without amidation for pectin from company Herbstreith and Fox, respectively.

High-pressure treatments

High hydrostatic pressure treatments were performed in a hydrostatic pressure unit (National forge, St. Niklass, Belgium) with an effective volume of 700 ml and a maximum working pressure of 600 MPa and a maximum working temperature of 90°C. Temperature within the pressure vessel was controlled by an external heat exchanger. The samples were sealed in polyethylene bags and placed in the high-pressure vessel. Pressure buildup was achieved within 2 min (600 MPa) and decompression time was about 10 s. For sample characterization, variation of treatment temperature (up to 65°C), time (0 to 20 min) and pressure (up to 550 MPa) was used.

Texture analysis

Texture (firmness of samples) was measured using a texture analyser (Model TA - XT2, Stable Micro System, Godalming, UK). The maximum deformation force required to compress the sample to a depth of 3 mm on a non-lubricated flat platform using a cylindrical probe (11.3 mm diameter) was recorded by the texture analyser and used as a measure of product firmness. The speed of compression during texture measurement was 1 mm/s. The firmness of gels was calculated as g/cm^2.

Sample preparation

Pectin solution at different concentration of 0.5 to 2.0 was prepared using distilled water and adjusted to pH = 4.0. For investigation of the effect of calcium concentration on gel firmness, different concentration of calcium ion (0 to 90 mg calcium ion/g pectin) as calcium lactate was dissolved in pectin solution. To investigate the effect of sugar concentration of gel firmness, sucrose was mixed with pectin and dissolved in distilled water to achieve 0 to 60% sugar concentration in final pectin solution. For adjusting pH of pectin solution to pH = 3.4 to 5.6, diluted HCl or NaOH was used. The prepared pectin solutions were immediately packed in a polyethylene bag (without air inside the bag) and heat sealed.

Statistics

Statistical analyses were carried out using Plot-It 3.2. Experiments were run in quadruplicates or eight times. Average values were reported.

RESULTS

High hydrostatic pressure (HHP) treatments

Effect of pressure level on firmness of pectin sample

Increasing the pressure at constant treatment temperature (35°C) and treatment time of 10 min increased the firmness of pectin gel distinctively. Both of the investigated pectin solutions showed a linear increase on firmness whereas the "LM" pectin (15% amidated pectin) showed higher firmness value than pectin "902" (without amidation) (Figure 1). In general, the firmness of amidated pectin (pectin "LM") was higher than the pectin without amidation (pectin "902"). It is not clear if the lower firmness of HHP treated "902" pectin compared to "LM" pectin is because of higher esterification degree or because of lack of amidation group in '902' pectin.

Dervisi et al. (2001) have investigated the effect of high hydrostatic pressure (up to 400 MPa) on gel formation of high methoxylpectin. They found that in using high pressure, it is possible to produce jam at room temperature without heating. The best texture for jam was achieved when the pectin concentration was between 2.5 and 5% w/w. In our investigation, we have observed that the HHP treated pectin "LM" and "902" became solid after treatment at 400 MPa and 10 min at

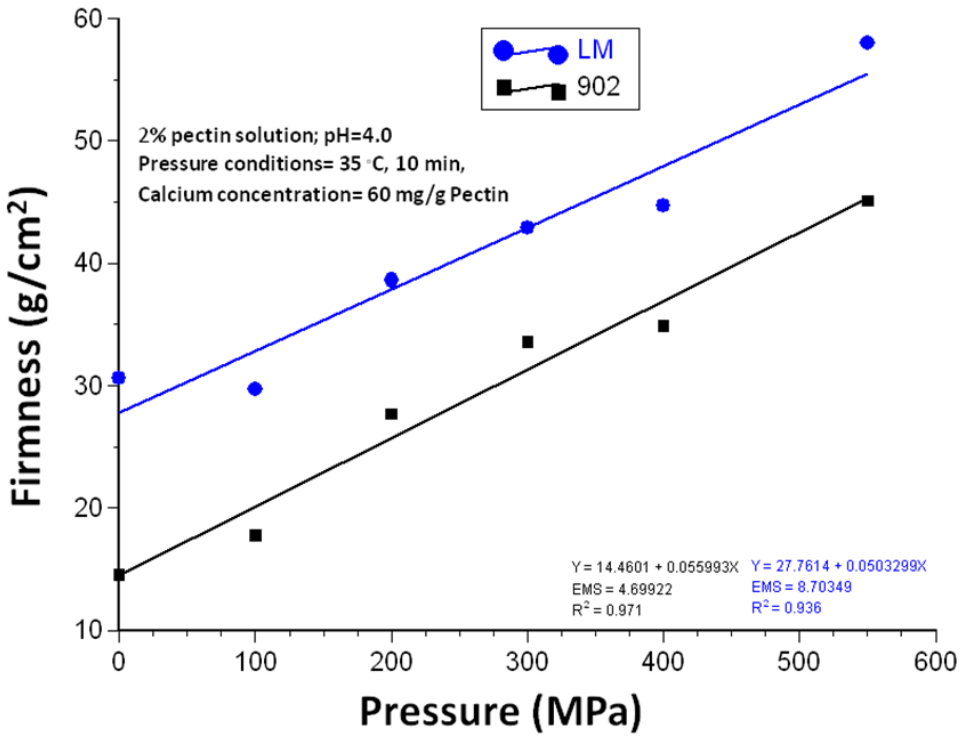

Figure 1. Effect of pressure on firmness of pectin sample

35°C treatment temperature (Figure 2a to d). This indicates the advantage of HHP treatment for production of gels which is suitable for cutting in desired sizes.

Pressure could influence the apparent viscosity of high-methoxylpectin solution. After pressure treatment of 1.5% high-methoxylpectin solution (containing one-third sucrose) at 400 MPa and 25°C, an up to tenfold viscosity increase was observed. This is maybe because of changes in the interactions at the molecular level (Michel and Autio, 2005). Michel et al. (1998) observed a much more higher viscosity increase on 1.5% sugar free high methoxyl apple pectin (degree of methyl esterification 70 to 79%) after high pressure treatment. Thus, the pectin source (apple or citrus) could have effect on pressure induced viscosity increase. The mechanism of viscosity changes during pressure treatment is unknown. It may be because of intermolecular interaction of pectin during pressure treatment. Pressure might influence the hydrophobic interaction between the pectin molecules.

Effect of treatment temperature during high hydrostatic pressure treatment on firmness of pectin sample

In Figure 3 is the effect of different treatment temperatures during high hydrostatic pressure treatment at constant pressure of 550 MPa and 10 min on firmness of pectins demonstrated. A linear increase of gel firmness with increasing treatment temperature was observed. The “LM” pectin showed higher firmness at given temperature compared to ”902” pectin. Increasing the treatment temperature from 35 to 65°C resulted in up to 2 times increase in the gel firmness. Eladouli (2001) and Bakki (2001) investigated the effect of high hydrostatic pressure on gel firmness and heat stability of gels from low methoxylpectin containing fruit puree. It could be stated that the high hydrostatic pressure treatment induced gel with distinct higher firmness compared to sample without high hydrostatic pressure treatment. Again, the firmness of HHP treated “LM” pectin was higher than “902” pectin for all investigated treatment time. Additionally, the high hydrostatic pressure treated gel provides higher heat resistant compared to untreated one. High hydrostatic pressure treated gel retained the shape after autoclave (120°C, 15 min), whereas the untreated gels loss the shape during heat treatment at 120°C (not published data).

Effect of treatment time during high hydrostatic pressure treatment on firmness of pectin sample

The treatment time during high hydrostatic pressure

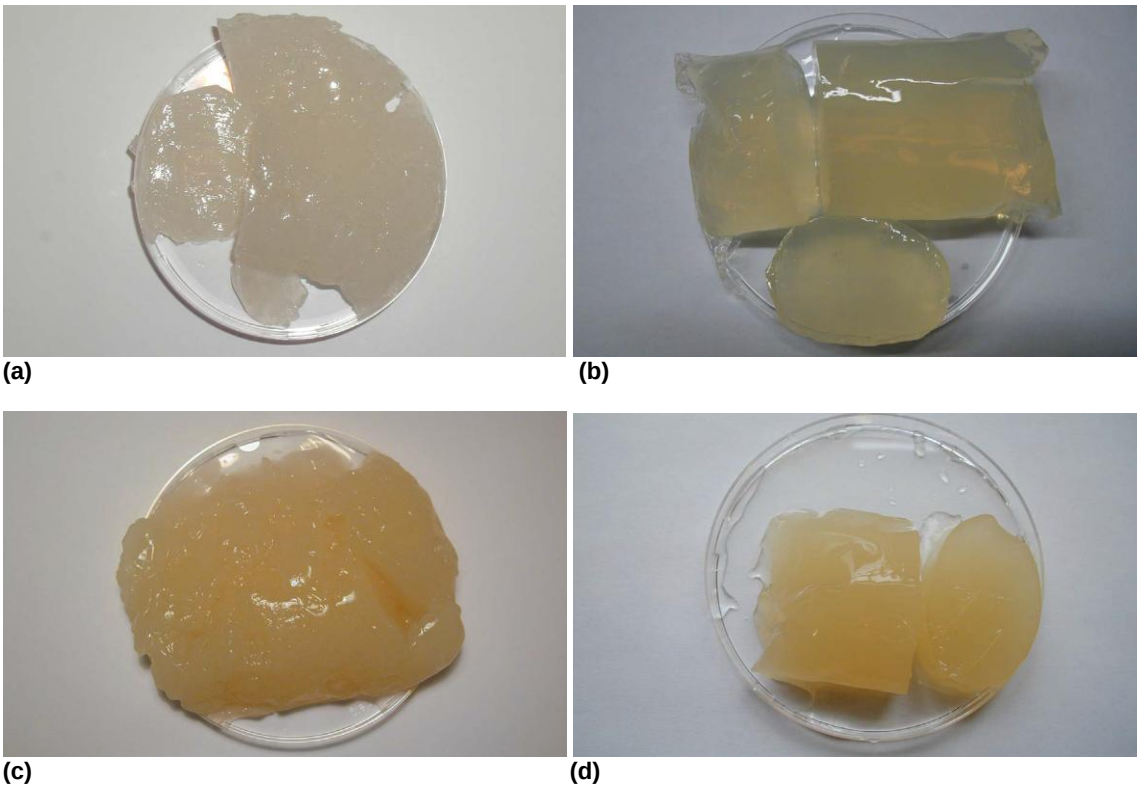

Figure 2. (a) 2% "LM" pectin solution, adjust pH 4.0, Ca^{2+} concentration 60 mg/g pectin, without HHP. (b) 2% "LM" pectin solution, adjust pH 4.0, Ca^{2+} concentration 60 mg/g pectin, after HHP treatment at 400 MPa, 10 min at 35°C. (c) 2% "902" pectin solution, adjust pH 4.0, Ca^{2+} concentration 60 mg/g pectin, without HHP. (d) 2% "902" pectin solution, adjust pH 4.0, Ca^{2+} concentration 60 mg/g pectin, after HHP treatment at 400 MPa, 10 min at 35°C.

treatment (550 MPa, 35°C, 2% pectin solution and calcium concentration of 60 mg/g pectin) showed distinct effect on gel firmness of "LM" pectin as well as "902" pectin (Figure 4). With increasing treatment time, the firmness of high hydrostatic pressure treated pectin was increased. Similar to the effect of pressure and treatment time, the firmness of "LM" pectin was distinctly higher than the "902" pectin.

Effect of pH on firmness of high hydrostatic pressure treated sample

In addition to the effect of process parameters (pressure level, treatment temperature and time), the composition of pectin solution could affect the firmness of high hydrostatic pressure treated pectin solution. As demonstrated in Figure 5, the firmness of pectin gel was rapidly decreased with increased pH from 3.4 to 5.6. This was true for pectin "LM" and "902". The overall firmness of high hydrostatic pressure treated pectin solution was at different pH and distinctly higher compared to untreated pectins. This indicates the positive effect of high hydrostatic pressure on gel formation of low methoxylpectin.

Effect of sugar concentration on firmness of high hydrostatic pressure treated sample

Grosso et al. (2000) reported the effect of sugar on the formation of low methoxylpectin gels. They suggested that pectin and sugar molecules could compete for cations. Depending on the sugar structure, a stable complex can be formed between the sugar and Ca^{2+}. This interaction can be unfavorable to the formation of the gel, due to the decrease of Ca^{2+} available to associate with pectin molecules and therefore, decreasing the gel rigidity. In low methoxylpectin gels, the rigidity is essentially dependent on the capacity of the sugar to compete with the pectin for the calcium ions. The interaction between sugar and water has a secondary effect (Grosso et al., 2000). Similar to the effect of sugar concentration on gel firmness at ambient pressure, the gel firmness of the investigated pectin solution first increased slightly (up to 30% sugar concentration) and then very rapidly (at sugar concentration higher than 30%) with increasing sugar

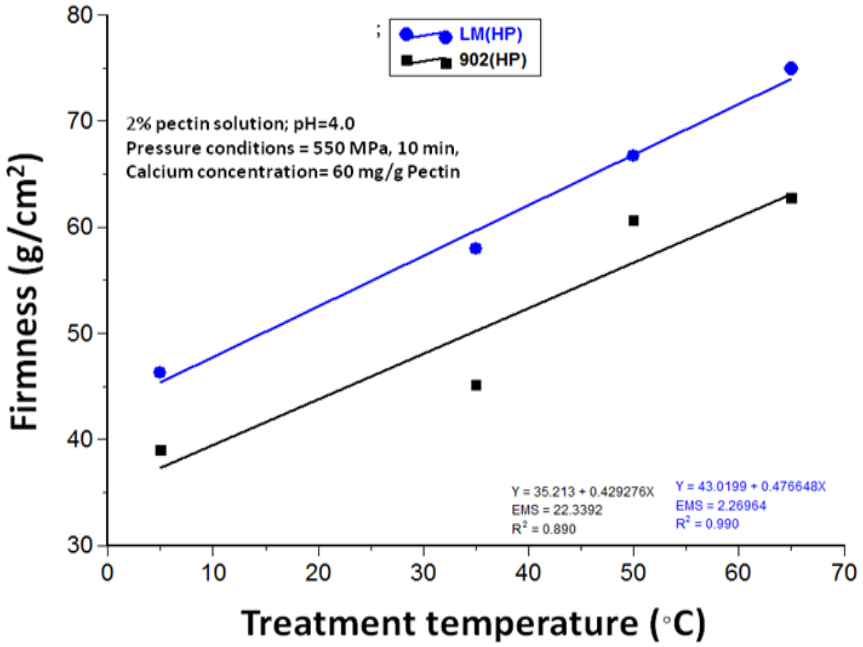

Figure 3. Effect of treatment temperature during high hydrostatic pressure treatment on firmness of pectin solution.

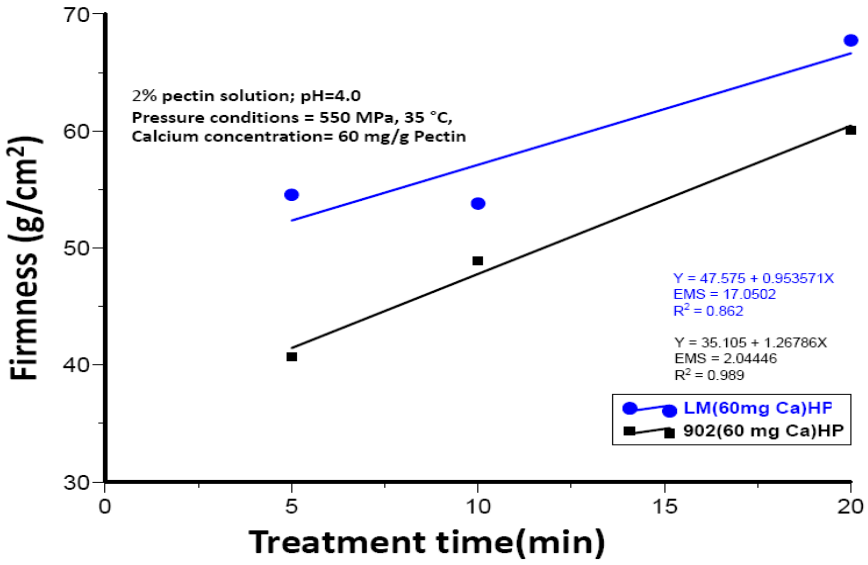

Figure 4. Effect of treatment time during high hydrostatic pressure treatment on firmness of pectin solution.

sugar concentration in pectin solution (Figure 6). The overall firmness of high hydrostatic pressure treated pectin at given treatment conditions (550 MPa, 35°C, 10 min) and composition of pectin solution (2% pectin concentration, 48 mg calcium ion/g pectin) was obviously higher than untreated samples.

Effect of Ca^{++} ion concentration on firmness of high hydrostatic pressure treated sample

Increasing the Ca^{++} ion concentration affected the firmness of high hydrostatic pressure treated pectins (Figure 7). Whereas, the firmness of untreated pectin

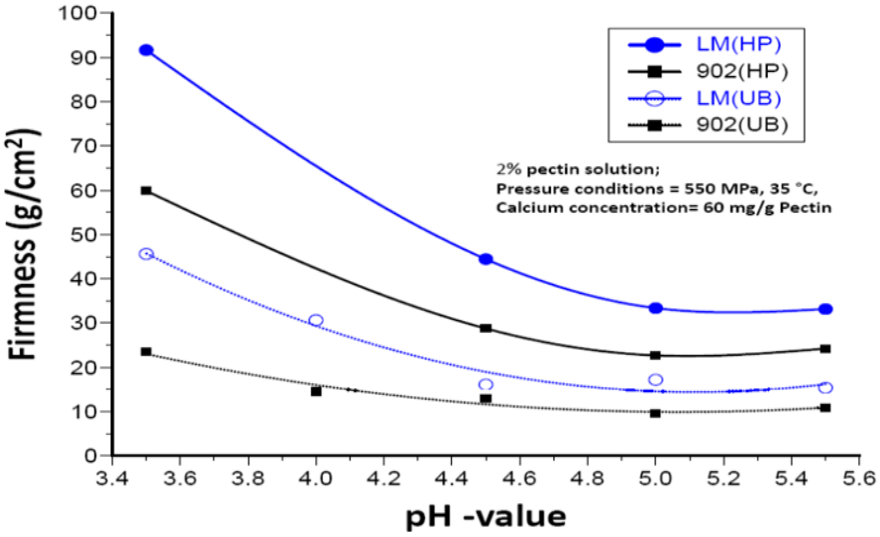

Figure 5. Effect of pH on firmness of untreated and high hydrostatic pressure treatment pectin solution.

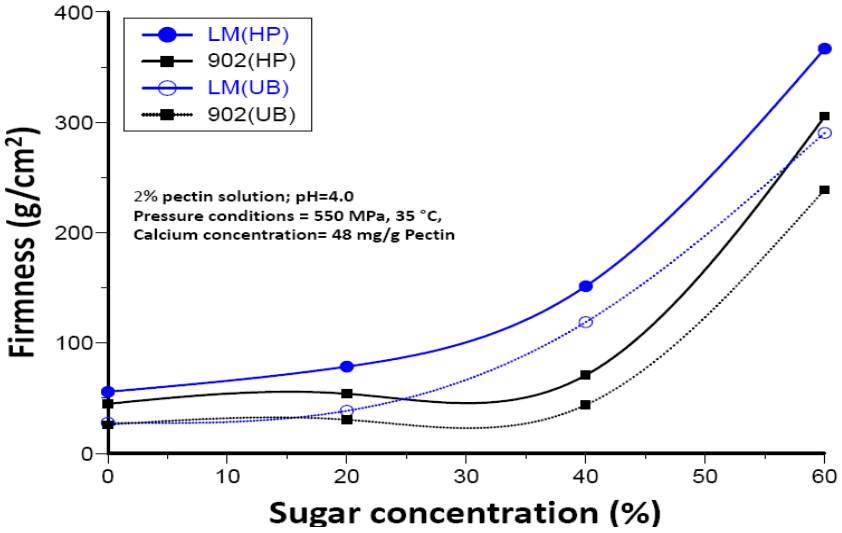

Figure 6. Effect of sugar concentration on firmness of untreated and high hydrostatic pressure treatment

solution (2% pectin solution, pH = 4.0) linear with increasing of the calcium ion concentration up to 30 mg/g pectin increased; the high hydrostatic pressure treated pectin solution showed the linear firmness increasing up to calcium ions concentration of about 48 mg/g pectin. This showed that the high hydrostatic pressure treated pectin could bind higher amount of calcium ions compared to untreated pectin. In addition, the high hydrostatic pressure treated pectin showed distinct higher firmness at constant calcium ion concentration compared to untreated sample (Figure 7).

Lootens et al. (2003) investigated the effect of Ca^{2+} concentration on gelformation of low methoxylpectin. They found that at 20°C and pectin concentration of 10 g/l with increasing Ca^{2+} concentration from 2 mM/g pectin to 7 mM/g pectin, the G″ storage shear modulus increased. The effects of pH, Ca^{2+} concentration, temperature and amidation on the gelation of low methoxylpectin were investigated by Lootens et al. (2003). The shear modulus of pectin solution increased with added Ca^{2+} ion. The shear modulus of partly amidated pectin gels was larger. In contrast, the pH does not strongly influence the shear modulus of pectin gels formed by Ca^{2+} ion for pH > 3.5.

Capel et al. (2006) investigated the effect of calcium ion concentration on gelation of amidated methoxylpectin. Calcium concentration higher than 4 mM induced athermal

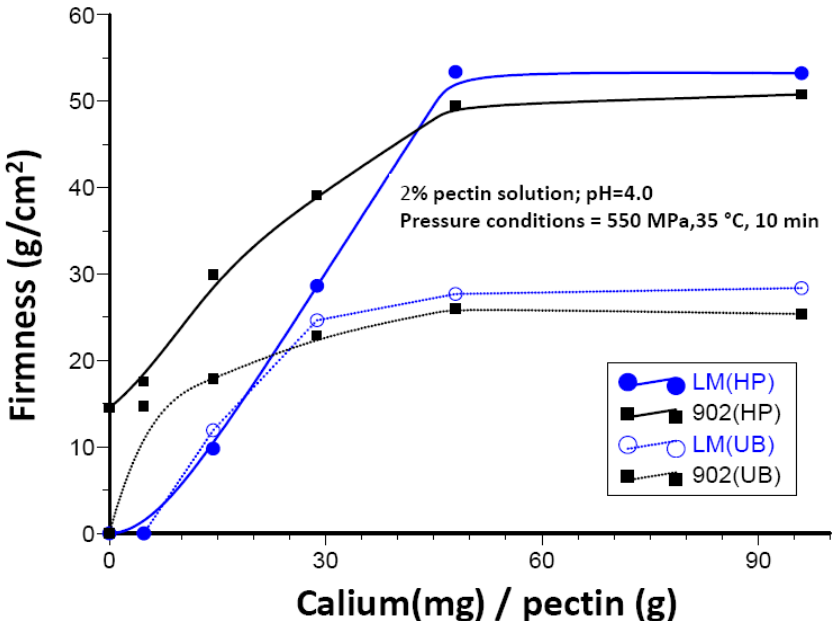

Figure 7. Effect of calcium ion concentration on firmness of untreated and high hydrostatic pressure treatment pectin solution.

gelation of lomethoxylpectin. In our study, the concentration of Ca^{2+} (max. 90 mg/g pectin) was far less than the concentration for athermal gel formation.

Effect of pectin concentration on firmness of high hydrostatic pressure treated sample

With increasing pectin concentration (up to 1% pectin concentration) in pectin solution, the firmness of untreated pectin increased rapidly. Further increase of pectin concentration increased the firmness slightly. This was more obvious for “LM” pectin compared to “902” pectin (Figure 8). In contrast, the high hydrostatic pressure (550 MPa, 35°C, 10 min) treated “LM” pectin did not show any firmness increase at low pectin concentration (up to 1.5% pectin) with increased pectin concentration. Pectin concentration higher than 1.5% led to drastic increase of high hydrostatic pressure treated “LM” pectin. The high hydrostatic pressure (550 MPa, 35°C, 10 min) treated “902” pectin showed increasing firmness with increasing pectin concentration. In general, the high hydrostatic pressure treated pectin showed up to 2 times higher firmness compared to untreated pectin at a given composition of pectin solution. It is well known that pectin solution with viscosities higher than 10 mPas are above the so-called critical entanglement concentration. Pectin solutions with viscosities higher than 30 mPas, even at the highest shear rates, are in the concentration range where entanglements occur. It is assumed that pressure could have influence on the intermolecular entanglement, especially in the hairy regions. If pressure treatment increased the number of entanglements, the viscosity would consequently be higher (Michel and Autio, 2005).

DISCUSSION

There are only limited studies available about the effect of pressure on hydrocolloids. Yen and Lin (1998) reported that hydrocolloid solution could not be affected by hydrostatic pressure. Michel and Autio (2005) have studied the effect of pressure (up to 1000 MPa) on degree of methyl esterification on the high-methoxylpectin (extracted from citrus pectin). They have observed that the degree of methyl esterification did not change when the solution were pressurized at pH 5.0. In contrast, a slight decrease of (from 65% to below 60%) of degree of methyl esterification of the high methoxylpectin was observed at pH 7.0. They suggested that the observed reduction in degree of methyl esterification at pH 7.0 seems to be a purely pH driven demethylation. The demethylation by β-elimination could only occur at high pH and elevated temperature (Albersheim et al., 1960), so that pectin could not be affected chemically by pressure at pH 5.0.

Investigation of Naghshineh et al. (2013) led to the conclusion that high pressure treatment does not have any significant effect on molecular weight of pectin. Therefore,

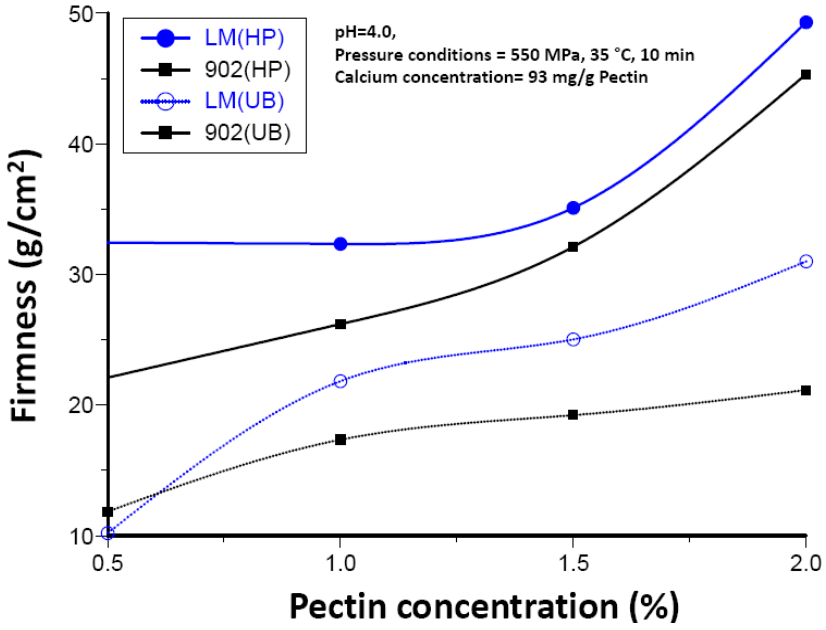

Figure 8. Effect of pectin concentration on firmness of untreated and high hydrostatic pressure treatment pectin solution.

high pressure treatment could not cause pectin polymer chain degradation. Gustin (1995) suggested that the carboxyl group in low methoxhyl group of pectin will be dissociated under pressure. The dissociation of carboxyl group of low methoxylpectin is associated with negative activation volume and could be accelerated under pressure. During pressure release, the carboxyl group will be reorganized. This leads to inducing new connection between carboxyl group and calcium ions and increasing the firmness of low methoxylpectin gels. In addition, the dissociation of water molecules at high hydrostatic pressure decreased the pH in pectin solution.

Hinrichs (2000) have suggested that the salt and acids could be dissociated under high hydrostatic pressure. The induced charged ions are compact and have less volume. The ionization volume of water is about -22.2 ml/mol at 25°C (Kitamura and Itoh, 1987; Neuman et al., 1973) and could be promoted under pressure. This leads to a pH decrease of 0.7 units at 800 MPa (Heinz, 1997). The increasing firmness of low methoxylpectin investigated in this study could also be explained because of dissociation of carboxyl group during high hydrostatic pressure and rearrangement during pressure release as well as because of pH reduction during high hydrostatic pressure treatment.

Conclusion

High hydrostatic pressure treatment could affect the firmness of low methoxylpectin. Generally, high hydrostatic pressure treatment leads to increase in the firmness. The treatment conditions during high hydrostatic pressure treatment (pressure level, treatment time and temperature) can positively affect the firmness. In general, the firmness was of partially amidated pectin (Pectin “LM”) and distinctly higher after HHP treatment compared to pectin “902” at constant HHP processing conditions. Although, increasing of pH decreased the firmness of pectin solution drastically but the high hydrostatic pressure treated pectin solution showed overall higher firmness compared to untreated samples. The positive effect of sugar content (at higher concentration of 30%) in pectin solution was obvious for both untreated and high hydrostatic pressure treated samples. Both investigated low methoxyl “LM” and “902” showed higher Ca^{++} ion tolerance compared to untreated samples, and the firmness after high hydrostatic pressure treatment at given Ca^{++} concentration was up to two times higher for high hydrostatic pressure treated samples than untreated samples.

ACKNOWLEDGEMENT

The authors thanks Technical University of Berlin, Institute of food and Bioprocess Engineering, Germany for providing HHP and texture analyzer equipments.

REFERENCES

Bakki R (2001). Herstellung hitzeresistenter, stückiger Fruchtgelmassen unter Anwendung von hydrostatischem Hochdruck. Master thesis at

Technical University of Berlin, Germany.
Capel F, Nicolai T, Durand D, Nicolai T, Boulenguer P, Langendorf V (2006). Calcium and acid induced gelation of (amidated) low methoxylpectin. Food Hydrocoll. 20:901-907.
Dervisi P, Lamb J, Zabetakis J (2001). High pressure processing in jam manufacture: effects on textural and color properties. Food Chem. 73:85-91.
Dumoulin M, Ozawa S, Hayashi R (1998). Textural properties of pressure-induced gels of food proteins obtained under different temperatures including subzero. J. Food Sci. 63:92-95.
Eladouli K (2001). Hochdruckbehandlung von Polysacchariden zur Herstellung sterilisierfähiger Fruchtgele und deren Einsatz in der Lebensmitteltechnologie. Master thesis at Technical University of Berlin, Germany.
Fishman ML, Pfeffer PE, Barford RA, Doner LW (1984). Studies of pectin solution properties by high performance size exclusion chromatography. J. Agric. Food Chem. 32:372-378.
Grant GT, Morris ER, Rees DA, Smith PJC, Thom D (1973). Biological interactions: the egg box model. FEBS Lett. 32:195-198.
Grosso CRF, Bobbio PA, Airoldi C (2000). Effect of sugar and sorbitol on the formation of low methoxylpectin gels. Carbohydr. Polym. 41:421-424.
Gustin D (1995). Characterization of gel formation and rheological properties of high hydrostatic pressure induced gel. Master thesis, Faculty of Agricultural Sciences of Gembloux, Belgium.
Heinz V (1997). Wirkung hoher hydrostatischer Drücke auf das Absterbe- und Keimungsverhalten sporenbildender Bakterien am Beispiel von Bacillus subtillis ATCC 9372. Dissertation at Technical University of Berlin, Germany.
Hinrichs J (2000). Ultrahochdruckbehandlung von Lebensmitteln mit Schewerpunkt Milk und Milkproddukte. Phenomeme, Kinetik und Methodik.Düsseldorf: VDI-Verlag, Germany. Fortschritt-Berichte VDI, Reihe 3, no. 656.
Kitamura Y, Itoh T (1987). Reaction volume of protonic ionization for buffering agents. Prediction of pressure dependence of pH and pOH. J. Solut. Chem. 16(9):715-725.
Lootens D, Capel F, Durand D, Nicolai T, Boulenguer, Langendorf V (2003). Influence of pH, Ca concentration, temperature and amidation on the gelation of low methoxylpectin. Food Hydrocoll. 17:237-244.
Michel M, Autio K (2005). Effects of high Pressure on Protein-and Polysacharide-Based Structures. In: Hendrickx MEG, Knorr D (eds.), Ultra High Pressure Treatments of Foods. Kluwer Academic Publishers, New York. pp. 195-197.
Michel M, Leser M, Syrbe A, Clerc M-F, Bauwens I, von Schack M-L, Watzke HJ (1998). Structure formation in protein-polysaccharide mixtures upon pressure treatment. In: Autio K. (ed), Fresh Novel Foods by High Pressure. Julkaisija Utgivare, Espoo, Finland. pp. 69-82.
Neuman JR, Kauzmann W, Zipp A (1973). Pressure Dependence of weak Acid Ionization in Aqueous Buffers. J. Phys. Chem. 77(22):2687-2691.
Pilnik W (1990). Pectin-A many splendored thing. In: Phillips GO, Williams PA and Wedlock DJ (Eds.), Gums and Stabilisers for the Food Industry. Oxford University Press, New York, Tokyo. pp. 209-220.
Smidsrod O, Haug A, Whittington SG (1972). The molecular basis for some physical properties of polyuronides. Acta Chem. Scand. 26:2563-2566.
Thakur B, Singh R, Handa A (1997). Chemistry and uses of pectin, a review. Crit. Rev. Food Sci. Nutr. 37(1):47-73.
Yen GC, Lin HT (1998). High pressure and heat treatment effects on pectic substances in guava juice. Adv. Exp. Med. Biol. 434:81-90.

academicJournals

Vol. 7(22), pp. 1464-1470, 15 June, 2013
DOI 10.5897/AJPP2012.0014
ISSN 1996-0816 © 2013 Academic Journals
http://www.academicjournals.org/AJPP

African Journal of Pharmacy and Pharmacology

Full Length Research Paper

Pharmaceutical evaluation of glibenclamide products available in the Jordanian market

Dina El-Sabawi*, Sa'ed Abbasi, Suzan Alja'fari and Imad I. Hamdan

Faculty of Pharmacy, The University of Jordan, Amman, Jordan.

Accepted 21 January, 2013

The pharmaceutical quality of five generics of glibenclamide that are available in the Jordanian market was assessed according to the British Pharmacopoeia (BP) monograph (2009). Similarly, the originator glibenclamide (Daonil®) which was obtained from the Saudi market was subjected to analysis and used as a reference product. All products were found satisfactory in terms of identification and related substances as per the BP requirements. However, the assay results showed that only two products, in addition to the reference (Daonil®) satisfied the BP specifications which required glibenclamide content to be within the range: 95 to 105% of the labeled content. All products, in spite of marginal deviations for two of them, were found to pass the United States Pharmacopoeia (USP) assay specifications (90 to 110%). Significant differences in dissolution behavior were observed between the different generics and the originator (Daonil®). Daonil® exhibited the lowest dissolution profile while some products showed dissolution profiles that were almost twice that of Daonil®.

Key words: Glibenclamide tablets, pharmaceutical equivalency, dissolution testing, quality control.

INTRODUCTION

The absence of quality control measures or effective drug regulatory agencies in many countries led to the production and prevalence of substandard, fake, and counterfeit drugs (World Health Organization (WHO), 1999). Substandard drugs have been defined as those which do not meet quality specifications set for them, as to contain under or over concentration of ingredients, contamination, poor quality ingredients, poor stability and inadequate packaging (Green et al., 2000; Newton et al., 2001). Conventional generics for an orally administered drug are considered to be therapeutically equivalent to a reference, once pharmaceutical equivalence and bioequivalence have been established (Schellekens et al., 2011). In practice, despite the presence of legislations for bioequivalence, generic products can differ significantly from the reference drug and amongst themselves (Genazzani and Pattarino, 2008). Many studies worldwide have shown significant percentages of substandard medicines available in the markets of several countries (Ehianeta et al., 2012; Eichie et al., 2009; Smith et al., 2006; Vial et al., 2008). For example, one of two marketed amoxicillin generics from Italian market was not bioequivalent to the brand leader product (Del Tacca et al., 2009). In another study comparing 13 copies of alendronate, significant differences in dissolution and disintegration of tablets were revealed (Epstein et al., 2003).

Interestingly, some studies have shown that the effect of substandard preparations might not be limited to inadequate physicochemical behavior, but can also be extended to influence the clinical outcome of the use of that preparation (Margolese et al., 2010). According to the current regulations issued by the Jordan Food and Drug Administration (JFDA), only random batches of each product are tested after establishing a record for successful testing results for a particular product. JFDA also requires every generic product to have a valid

*Corresponding author. E-mail: d.sabawi@ju.edu.jo. Tel. +962 6 5355000.

bioequivalence study that demonstrates its equivalence to the originator brand. However, questions are probably still being raised by professionals and the public pertaining to the quality of generics available in the Jordanian market. The result reported by a recent study (Schellekens et al., 2011) is particularly alarming in this regard. According to Schellekens et al. (2011), around 56% of amoxicillin preparations available in regional markets, including the Jordanian market, were out of pharmacopoeial specifications.

In this study, the quality of the oral antidiabetic drug, glibenclamide preparations was assessed through direct purchase of the relevant preparations from local community pharmacies and subjecting them to analysis according to the British Pharmacopoeia (BP). Glibenclamide (Figure 1), also known as glyburide (in the United States), is a sulfonylurea oral hypoglycemic drug which has long been in clinical use (Luzi and Pozza, 1997). In Jordan, five generics are officially registered by the JFDA and are available in the local market. The originator (Daonil®) however, is currently not available in the Jordanian market. In this study, the pharmaceutical qualities of the five generics available locally were compared to that of the originator (Daonil®) which was obtained from the Saudi market.

MATERIALS AND METHODS

Chemicals

Working standards of glibenclamide were obtained from medicine testing laboratories (Amman, Jordan). High-performance liquid chromatography (HPLC) grade acetonitrile and methanol were obtained from TEDIA Company (INC, USA). Potassium dihydrogen orthophosphate was obtained from SD Fine-Chem Limited (Mumbai). Tablets of the five commercially available glibenclamide products were obtained from the local market. The examined tablets were purchased from local community pharmacies in just the same way that the patient might have bought them from such pharmacies. A list of the tested products with their details is shown in Table 1.

Apparatus

The HPLC system employed in this study consisted of a Ultra violet (UV) detector (Merck-Hitachi, model L-7400, Tokyo-Japan), a pump (Merck-Hitachi, model L-7400, Tokyo-Japan) and an integrator unit (Merck-Hitachi, model D-7500, Tokyo-Japan). The employed HPLC column was C18, 5 µm, 200 × 4.6 mm i.d. (Thermo Scientific, USA). Dissolution experiments were carried out using a Copley scientific dissolution apparatus, DIS6000 (UK). Friability testing was carried out using an Erweka TAR Roche Friabilator (Germany). Measurements of pH were made using microprocessor pH meter, HANNA Instruments (Romania).

Tests performed according to BP (2009)

In general, the British pharmacopoeial monograph (British Pharmacopoeia, 2009) was adopted for testing all collected commercial products. Identification test, related substances and assay were performed. The details for each test are described.

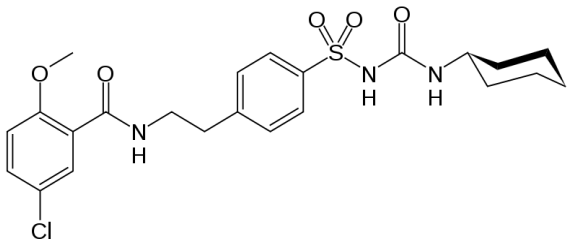

Figure 1. Chemical structure of glibenclamide.

Identification test

According to BP monograph, identification of glibenclamide was performed via thin layer chromatography (TLC). This was achieved by comparing the retention index (R_f values) for the chromatogram of a standard glibenclamide solution to that obtained for the extracted tablets. Further identification was performed by comparing the HPLC retention times of the major peaks for the standard and samples during the conductance of the assay (according to the same pharmacopoeial monograph). The conditions for TLC were those described for the related substances tests.

Related substances

The test sets limits for two specified impurities which are 4-[2-(5-chloro-2-methoxybenzamido)ethyl] benzenesulphonamide (CEBSA) and methyl N-4-[2-(5-chloro-2-methoxybenzamido)ethyl] benzenesulphonyl carbamate (MCEBSC). The test was performed by applying solution 1 representing the extract of commercial tablets containing the equivalent of 0.5% glibenclamide, and solution 4 representing the standard solution of glibenclamide at 0.5% as specified in BP. Solutions 2 and 3 were supposed to be prepared using the two potential glibenclamide impurities. As these impurities were not available, two solutions of standard glibenclamide were prepared at concentrations similar to the concentrations specified for impurities solutions. These glibenclamide standard concentrations were 0.012 and 0.002%, corresponding to CEBSA and MCEBSC, respectively.

Assay

The recommended mobile phase by BP was employed. It comprised a mixture of potassium dihydrogen orthophosphate buffer (pH 3) and acetonitrile in a ratio of 53:47, respectively. The overall chromatographic run time was less than 13 min. The buffer was vacuum filtered through 0.2 µm cellulose acetate membrane and then mixed with acetonitrile. The mobile phase was degassed in an ultrasonic bath. The column was set at room temperature and equilibrated to a stable base line before start of injections. The flow rate was set at 1.5 ml/min.

Preparation of sample solutions according to BP

For each product, 4 tablets were accurately weighed, crushed and the equivalent of the average weight of one tablet was transferred to a 20 ml volumetric flask. The volume was completed to mark with methanol, and additional 2 ml of water was added. The mixture was then sonicated and filtered through a 0.45 µm syringe filter. Three separate preparations were made for each product, and each preparation was injected three times along with three injections of a properly prepared standard solution of glibenclamide.

Dissolution test

The tests were performed according to pharmacopoeial specifications using Apparatus 2 (paddle method). The medium employed was 900 ml of 200 mM phosphate buffer (pH 6.8). Paddle rotation was set at 75 revolutions per minute. Medium temperature was set at 37°C ± 0.5°C. Six tablets of each product were placed in the dissolution apparatus (one in each vessel). Samples (5 ml) were withdrawn at pre-determined time points (10, 20, 30, 45, 60 and 120 min) and the withdrawn samples were replaced with buffer solution. All samples were then filtered before being injected into the HPLC column. The amount of dissolved glibenclamide was determined using the chromatographic conditions recommended in the BP. However, the wavelength was adjusted to 250 nm instead of 300 nm in order to maximize the sensitivity of the method and to enable accurate measurement of the lowest concentration possibly obtained during dissolution testing. The linearity of the method was ensured by injecting standard solutions of glibenclamide in the concentration range 1.135 to 5.675 µg/ml which covers 20 to 115% of the anticipated concentration resulting from the dissolution of the 5 mg tablet in 900 ml of buffer. A good correlation coefficient for the average calibration equation was obtained (0.9972). The percentage release of glibenclamide was determined by using the following equation:

$$\text{Released (\%)} = [Cs \times (0.9) / 5] \times 100$$

Where Cs is the calculated concentration of glibenclamide in the sample (µg/ml). Dissolution profile for each generic product was obtained by plotting the percentage released against time of sampling.

Friability

Twenty tablets were accurately weighed then tumbled at 25 rounds per minute for a period of 4 min. The tablets were then removed from the tumbling chamber, de-dusted on a sieve and re-weighed. The loss in weight due to the tumbling action was recorded as percentage weight loss according to:

$$\text{Friability (\%)} = [\text{Initial weight - Final weight / Initial weight}] \times 100$$

RESULTS AND DISCUSSION

Identification

According to BP monograph, identification of glibenclamide can be achieved using two chromatographic tests. The first chromatographic test employs the same HPLC conditions that are recommended for the assay of glibenclamide in this monograph. The test is based on comparing the retention time (t_r) of the analyte (glibenclamide) from commercial tablets to that of a standard preparation of glibenclamide. The second identification test is based on TLC which utilizes the same chromatographic conditions that are used for related substances test in the same monograph. According to the test, the substance is positively identified if it exhibits a similar $R_{f\ value}$ of a standard solution. All commercial preparations tested exhibited practically similar R_f and t_r values when compared to standard glibenclamide. Thus, all the tested preparations can be said to contain the correct active ingredient as per the pharmacopoeial specifications.

Related substances

The BP test for related substances in glibenclamide tablets is a semi-quantitative test that is based on TLC. The test states that the spots corresponding to the mentioned impurities in sample should not exceed in intensity that for a standard preparation for each of them, which means that the maximum allowed limit for CEBSA and MCEBSC were 0.012 and 0.002%, respectively. The results indicated that, in all of the tested preparations, only one major spot could be seen in the extracted preparations (solution 1) which corresponds to glibenclamide as confirmed by the spot in the standard solution (solution 4). This suggests that all of the tested preparations met the pharmacopoeial specifications pertaining related substances.

Assay

All of the obtained generic tablets of glibenclamide were assayed as recommended by BP. The peak of the analyte in the chromatogram of the solution prepared from tablets was confirmed by comparing the retention time (11.3 min) with that of a standard solution of glibenclamide. A reasonable peak shape was obtained for the analyte (Figure 2). Before the start of analysis, standard solutions of glibencalmide were injected every day in triplicate and relative standard deviation (RSD) values for peak areas were calculated. Three injections were applied to HPLC from each of the three preparations prepared for each product. RSD for triplicate injections of either standard glibenclamide solution or solutions prepared from tablets were always less than 2%. Summary of the obtained assay results expressed as percentage per label for all generics tested, together with RSD values, are presented in Table 2.

In general, the precision of analysis was satisfactory as judged by the obtained RSD values of less than 2%. Strictly speaking, only two preparations can be said to pass the BP assay requirements which are Glucomid® (97.2%) and Glunil® (105%). This is because the BP (British Pharmacopoeia, 2009) requires glibenclamide tablets to contain not less than 95% and not more than 105% of the claimed amount. However, if the USP (United States Pharmacopoeia, 2005) specifications were to be considered, which allows percentage per label to be in the range 90 to 110%, then all of the tested preparations would pass the assay requirements with two preparations being on the borderline (Melix®,110.3% and Glibemide®, 111.5%).

Since the manufacturers of the assayed products might have adopted the USP specifications rather than the BP ones, it could be concluded that the assayed products

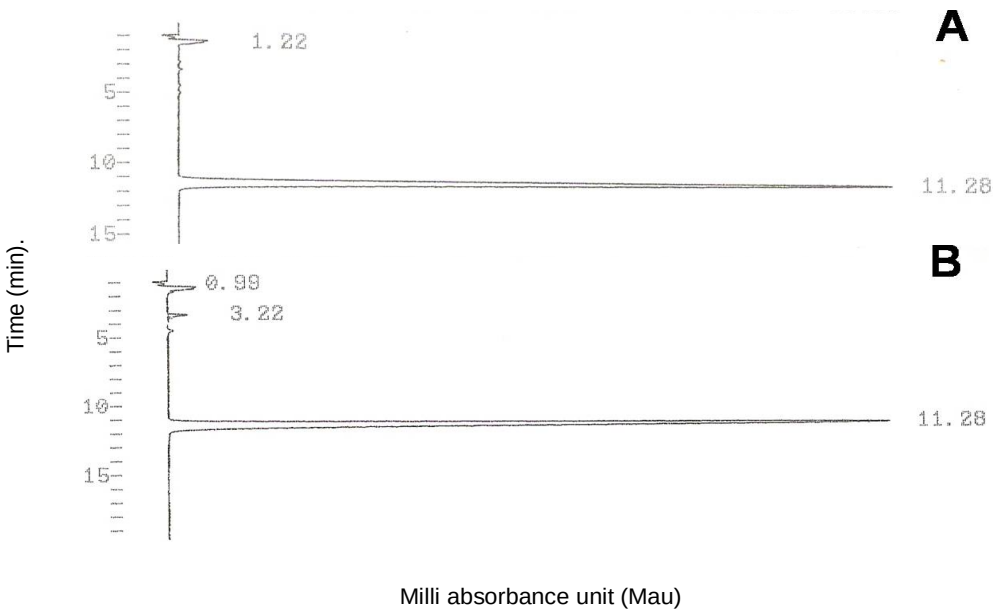

Figure 2. (A) Sample chromatograms for standard glibenclamide and (B) a solution prepared from commercial tablets of Daonil®.

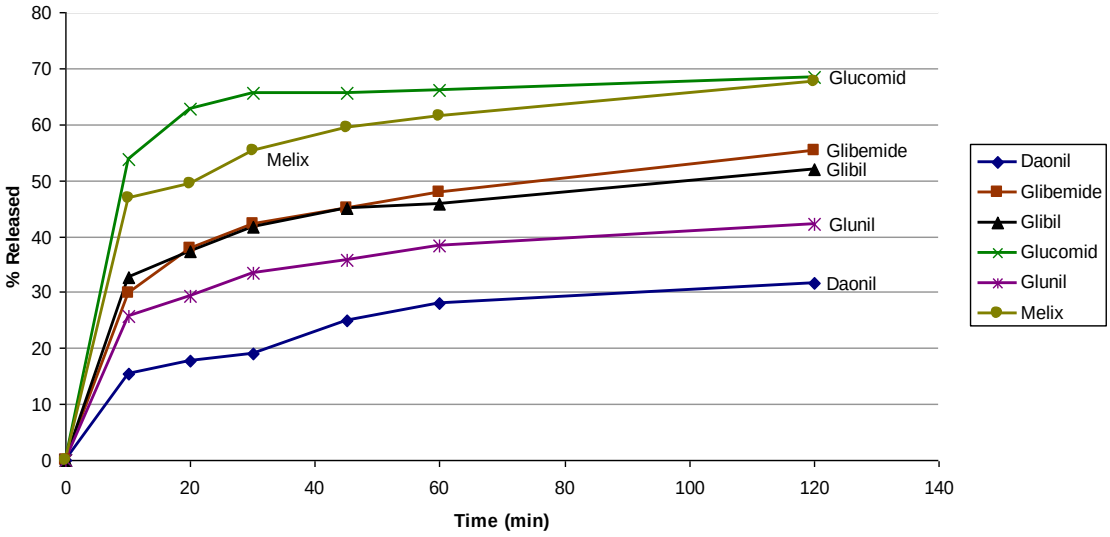

Figure 3. Average dissolution profile for the various commercial products tested in phosphate buffer pH 6.8.

demonstrated generally satisfactory assay results.

Dissolution test

A simple medium of phosphate buffer at pH 6.8 was adopted to carry out the dissolution studies. A complete dissolution profile for each product was obtained. Dissolution profiles are believed to better reflect (than single point determination) the *in vivo* bioavailability of drugs, particularly for those drugs which are classified as class II in the bioclassification system (Dressman et al., 1998). Such drugs are generally known as low solubility high permeability drugs (Dressman et al., 2001). Glibenclamide is known to be classified as a class II drug (Dressman et al., 2001), therefore its *in vitro* dissolution profile could be expected to reflect the *in vivo* performance of the formulation.

The average dissolution profile obtained for each of the tested commercial preparations is shown in Figure 3. From

Table 1. List of the tested generics and reference tablets containing glibenclamide.

Brand name	Manufacturer	Batch No.	Manufacture date	Expiry date
Daonil®	Sanofi-Aventis France	0CH9A	04/2010	04/2012
Melix®	Bio-Strata Pharmaceuticals	6074	08/2006	08/2011
Glunil®	Ram Pharmaceuticals, Jordan	L09	09/2009	09/2011
Glibil®	Hikma Pharmaceuticals, Jordan	6222	10/2010	10/2013
Glibemide®	United Pharmaceuticals, Jordan	7720	08/2010	08/2013
Glucomid®	APM, Jordan	756076	02/2007	02/2012

Table 2. Average percentage per label obtained for each of the tested products.

Product	Percentage per label	RSD% (n = 3)
Daonil®	104.2	0.56
Melix®	110.3	0.93
Glunil®	105	1
Glibil®	110	0.75
Glibemide®	111.5	1.1
Glucomid®	97.2	0.86

RSD: relative standard deviation.

the figure, it can be seen that all products, including the originator (Daonil®) did not release significant percentage of the drug within the first 30 min. In fact, Daonil® exhibited the lowest percentage release within the first 30 min (20%) while other products varied in the range of 35 to 65%. This might be unexpected but indeed explainable. The pharmacopoeia did not specify a dissolution medium for glibenclamide tablets and left the choice of the medium to the manufacturer, so if the medium was different (for example, simulated gastric or intestinal fluid), a significant increase in the dissolution of glibenclamide may be anticipated. In fact previous reports on the dissolution of Daonil® in simple phosphate buffer (pH 6.8) obtained almost identical results to those obtained in this study that is, no more than 40% of glibenclamide in Daonil® was released within 120 min (Lee et al., 1999). Moreover, the dissolution of Daonil® was shown to significantly increase (from ~40 to ~90%) by changing the pH by one unit only (from 6.8 to 7.8), which indicates the high sensitivity of glibenclamide solubility to pH of the medium.

A previous study on the originator Euglucon N® which is the trade name of glibenclamide in Britain (made by Boehringer Mannheim/Hoechst, Germany), showed that no more than ~20% of the drug was released over 30 min in simple phosphate buffer (pH 6). However, significantly higher dissolution rates were obtained when dissolution was studied in simulated fluids (Löbenberg et al., 2000). Yet another confirmation came from a study that compared the performance of Daonil® (Hoechst) to other two suggested formulations of glibenclamide. The results showed that the percentage release of glibenclamide from Daonil® in phosphate buffer (pH 7.4) was just below 40% over 1 h (Tashtoush et al., 2004).

More importantly, the obtained dissolution profiles in this study for the tested commercial products were obviously different, with Daonil® showing the least percentages released over the entire dissolution curve. For some products, the percentages dissolved over the time range 60 to 120 min were almost twice that of Daonil®. For better evaluation of similarity of dissolution profiles, the similarity factor (f2) value was calculated for each dissolution curve in comparison to Daonil® and they were 34.5, 35.3, 19.3, 47 and 23.5 for Glibemide®, Glibil®, Glucomid®, Glunil®, and Melix®, respectively.

According to the estimated f2 values, none of the profiles could be considered similar to that of Daonil® which is quite alarming. In principle, it should not be taken that the products with higher percentage dissolution are better performing than Daonil® because Daonil® is the originator on which relevant clinical, pharmacokinetics and toxicity studies were performed before authorization. Therefore, if a generic of glibenclamide released double the percentages of Daonil®, and that was highly correlated with *in vivo* performance, then that generic would provide almost double the dose of Daonil® which essentially should not be acceptable. However, the question here is whether the obtained dissolution profiles correlate directly with *in vivo* bioavailability profiles for the products. An answer to this question could be found in relevant literature.

A study (Löbenberg et al., 2000) has shown very strong *in vitro*/*in vivo* correlation for glibenclamide preparations when investigated in fasted simulated intestinal fluid, and

some weak correlations in other dissolution media. Yet another study has shown that some *in vitro/in vivo* correlation exist for different glibenclamide preparations even in simple dissolution media such as phosphate buffer at pH 7.4 (Dressman et al., 1998). Therefore, it is quite likely that the observed differences in the dissolution profiles of glibenclamide generics might be reflected on *in vivo* bioavailability performance with potential ramifications in their clinical effects. This is particularly true for those products whose dissolution profiles were significantly different from that of Daonil® (Melix® and Glucomid®). Other commercial products of glibenclamide in different countries with dissolution profiles that are not similar to that of the originator (Daonil®) have been previously reported (Lee et al., 1999).

Friability of tablets is a criterion that measures the tendency of tablets to shed powder, so that more friable tablets could be anticipated to be more easily crushable and disintegrated, which in turn may influence their dissolution. Due to the observation that some of the tested generics appeared to have higher levels (than the originator) of shed fine powder; while in their blister packs and in attempts to explain the difference in dissolution behavior of the generics studied, friability tests were performed according to the pharmacopoeial requirements. The obtained percentage friability [weight loss (%)] were: 0.094, 0.079, 0.228, 0.075, 0.125 and 0.262 for Daonil®, Melix®, Glunil®, Glibil®, Glibemide® and Glucomid®, respectively. Although all of the tested commercial products were of satisfactory limits for friability, different generics exhibited slightly different values of percentage weight loss. However, no obvious correlation was obtained between the percentage loss and percentage release of the drug. Together with the observation that all preparations reached their maximum percentage release within 50 min or less (no further release occurred up to 120 min), the observed differences in dissolution behavior of the tested generics can not be attributed to factors such as friability and disintegration rate.

Overall, the study demonstrated that generics of glibenclamide available in Jordan market were of satisfactory quality attributes pertaining to identification, related substances and content of the active substance. However, the studied generics exhibited dissolution profiles that are significantly different from each other and from that of the originator Daonil®. In light of the relevant literature, it could be anticipated that the observed *in vitro* dissolution inequivalence of the different products, is likely to be reflected as *in vivo* bio-inequivalance. Therefore, further *in vivo* bio-equivalence studies are essential to confirm or refute these *in vitro* findings.

Conclusion

In general, all tested commercial glibenclamide generic tablets from the Jordanian market were within the BP specifications in terms of identification and related substances. All tested products can be said to pass the USP requirements of percentage per label. The tested generics differed mostly in their dissolution behavior when tested in phosphate buffer (pH 6.8). Daonil® showed the lowest dissolution profile of all the products tested. Some generics showed a percentage release of the drug, almost twice that of Daonil®. The differences in dissolution profiles are likely to reflect potential differences in clinical performance of the tested generics. Properly controlled bio-equivalence studies are strongly recommended to further investigate the potential inequivalence of the tested products.

ACKNOWLEDGEMENT

The authors would like to thank the Deanship of Academic Research at The University of Jordan for their financial support.

REFERENCES

British Pharmacopoeia (2009). Glibenclamide (and tablet) monograph Volume 1 and 2. London: The stationary office.

Del Tacca M, Pasqualetti G, Di Paolo A, Virdis A, Massimetti G, Gori G, Versari D, Taddei S, Blandizzi C (2009). Lack of pharmacokinetic bioequivalence between generic and branded amoxicillin formulations. A post-marketing clinical study on healthy volunteers. Br. J. Clin. Pharmacol. 68:34-42.

Dressman JB, Amidon GL, Reppas C, Shah VP (1998). Dissolution testing as a prognostic tool for oral drug absorption: immediate release dosage forms. Pharm. Res. 15:11-22.

Dressman J, Butler J, Hempenstall J, Reppas C (2001). The BCS: where do we go from here? Pharm. Tech. 25:68-76.

Ehianeta T, Williams B, Surakat J, Mohammed N, Anyakora C (2012). Quality survey of some brands of artesunate-amodiaquine in Lagos drug market. Afr. J. Pharm. Pharmacol. 6:636-642.

Eichie FE, Arhewoh IM, Ezeobi OC (2009). *In-vitro* evaluation of the pharmaceutical quality of some ibuprofen tablets dispensed in Nigeria. Afr. J. Pharm. Pharmacol. 3:491-495.

Epstein S, Cryer B, Ragi S, Zanchetta JR, Walliser J, Chow J, Johnson MA, Leyes AE (2003). Disintegration / dissolution profiles of copies of Fosamax (alendronate). Curr. Med. Res. Opin. 19:781-789.

Genazzani AA, Pattarino F (2008). Difficulties in the production of identical drug products from a pharmaceutical technology viewpoint. Drugs R&D 9:65-72.

Green MD, Mount DL, Wirtz RA, White NJ (2000). A Colorimetric field method to assess the authenticity of drugs sold as antimalarial artesunate. J. Pharm. Biomed. Anal. 24:65-70.

Lee MS, Chang YC, Shih CC, Chen CJ, Chang BL (1999). Study on dissolution profile of commercial glyburide tablets. J. Food Drug Anal. 7:82-93.

Löbenberg R, Krämer J, Shah VP, Amidon GL, Dressman JB (2000). Dissolution testing as a prognostic tool for oral drug absorption: dissolution behavior of glibenclamide. Pharm. Res. 17:439-444.

Luzi L, Pozza G (1997). Glibenclamide: an old drug with a novel mechanism of action? Acta. Diabetol. 34:239-244.

Margolese HC, Wolf Y, Desmarais JE, Beauclair L (2010). Loss of response after switching from brand name to generic formulations: three cases and a discussion of key clinical considerations when switching. Int. Clin. Psychopharmacol. 25:180-182.

Newton P, Proux S, Green M, Smithuis F, Rozendaal J, Prakongpan S, Chotivanich K, Mayxay M, Looareesuwan S, Farrar J, Nosten F, White NJ (2001). Fake artesunate in South-east Asia. Lancet

357:1948-1950.
Schellekens H, Klinger E, Mühlebach S, Brin JF, Storm G, Crommelin DJ (2011). The therapeutic equivalence of complex drugs. Regul. Toxicol. Pharmacol. 59:176-183.
Smith JC, Tarocco G, Merazzi F, Salzmann U (2006). Are generic formulations of carvedilol of inferior pharmaceutical quality compared with the branded formulation? Curr. Med. Res. Opin. 22:709-720.
Tashtoush BM, Al-Qashi ZS, Najib NM (2004). In vitro and in vivo evaluation of glibenclamide in solid dispersion systems. Drug Dev. Ind. Pharm. 30:601-607.
United States Pharmacopoeia (2005). The official compendia of standards. United States Pharmacopoeia Convention, INC. 12601, Twinbrook parkway, Rockville, MD 20852.
Vial J, Cohen M, Sassiat P, Thiébaut D (2008). Pharmaceutical quality of docetaxel generics versus originator drug product: a comparative analysis. Curr. Med. Res. Opin. 24:2019-2033.
WHO (1999). Counterfeit drugs: guidelines for the development of measures to combat counterfeit drugs, department of essential drugs and other medicines. Geneva: WHO.

academicJournals

Vol. 7(22), pp. 1471-1481, 15 June, 2013
DOI 10.5897/AJPP2013.2977
ISSN 1996-0816 © 2013 Academic Journals
http://www.academicjournals.org/AJPP

African Journal of Pharmacy and Pharmacology

Full Length Research Paper

Acetylcholinesterase inhibitors used or tested in Alzheimer's disease therapy; their passive diffusion through blood brain barrier: *In vitro* study

Jana Zdarova Karasova[1,2]*, Jan Korabecny[2], Filip Zemek[3], Vendula Sepsova[3] and Kamil Kuca[2]

[1]Department of Public Health, Faculty of Military Health Sciences, University of Defence, Hradec Kralove, Czech Republic.
[2]Biomedical Research Center, University Hospital, Hradec Kralove, Czech Republic.
[3]Department of Toxicology, Faculty of Military Health Sciences, University of Defence, Hradec Kralove, Czech Republic.

Accepted 27 May, 2013

Although the information about Alzheimer's disease (AD) etiology is still unclear; acetylcholinesterase inhibitors still play a major role in symptomatic treatment of AD. Unfortunately, a relevant argumentation is complicated since information about real drug concentration in the brain or time-dependent blood-brain barrier (BBB) distribution studies are still quite rare. In this *in vitro* study, high-performance liquid chromatography (HPLC) method with special (IAM – immobilized artificial membrane) column was used to determine the ability of cholinesterase inhibitors to penetrate through BBB. Set of 8 structurally different cholinesterase inhibitors applicable to AD treatment was evaluated throughout this study. According to our method, all molecules are able to penetrate BBB by passive transport. However, some molecules such as huperzine A and galanthamine have lower ability to penetrate the BBB directly. These molecules may be delivered into the brain via active transport. Other molecules probably use passive transport to permeate into the central nervous system; tacrine and 7-methoxytacrine exert the highest passive permeation from this set of compounds.

Key words: Blood-brain barrier, central nervous system, acetylcholinesterase, Alzheimer disease.

INTRODUCTION

Alzheimer's disease (AD) is the most common age-related neurodegenerative disease with many cognitive and neuropsychiatric manifestations that result in progressive disability (Grossberg, 2003; Schwarz et al., 2012). Loss of basalocortical cholinergic neurons in the hippocampus and the presence of β-amyloid protein in extraneuronal plaques and tau protein in neurofibrillary tangles are the characteristic histopathological features of AD (Bi, 2010; Braak and Del Tredici, 2013). Cholinergic neurons are slowly depleted, and consistent deficit of acetylcholine (ACh) is responsible for insufficient cholinergic neurotransmission (Castellani et al., 2010; Van der Zee et al., 2011).

Two enzymes are closely involved in ACh fate: human choline acetyltransferase (hChAT; EC 2.3.1.6) partaking in ACh synthesis and human acetylcholinesterase (hAChE; EC 3.1.1.7)) in the degradation of ACh in neurons (Racchi et al., 2004). Interestingly, hAChE activity decreases progressively in certain brain regions from mild to severe stages of AD to reach 10 to 15% of normal values. While butyrylcholinesterase (BChE; EC 3.1.1.8) activity is unchanged or even increased by 20%, therefore a large pool of BChE is available in glia, neurons and neuritic plaques (Becker and Giacobini, 1997).One way to improve cholinergic transmission in AD patients is inhibition of hAChE. Lower degradation leads to increased

*Corresponding author. E-mail: karasova@pmfhk.cz. Tel: +420-973-251-534. Fax: +420-495-518-094.

availability of ACh to stimulate nicotinic and muscarinic recaptors within the brain. Although the cholinesterase inhibitors (ChEI) application may be considered as simple symptomatic treatment, they still represent the cornerstone of AD therapy (Giacobini, 2004).

The effectiveness of ChEI in AD treatment is limited by their ability to penetrate through the blood-brain barrier (BBB). BBB is dynamics and complex interface between blood substances and central compartment that play a key role in brain protection and homeostasis (Tsukita et al., 2001; Turksen and Troy, 2004). BBB is not only physical but also a metabolic barrier where imbedded enzymes are involved in the catabolism of xenobiotics (Lorke et al., 2008). Smaller lipophilic substances have some access to the central nervous system by diffusion, whereas other substances can cross the BBB by carrier-mediated influx transport, receptor mediated transcytosis and absorptive-mediated transcytosis (Terasami and Ohtsuki, 2005; Edvinsson and Tfelt-Hansen, 2008).

Tacrine, donepezil, rivastigmine and galanthamine were found among the commonly used ChEI for the symptomatic treatment of patients suffering from mild to moderate AD (Moussa et al., 2005). The other potential compounds are huperzine A and 7-methoxytacrine (7-MEOTA) (Zhao et al., 2002). The penetration into central nervous system (CNS) is commonly confirmed by their therapeutic effect (improved cognitive and memory functions, improved behavioral deficits) or by their potency to inhibit cholinesterase in brain (de los Rios, 2012).

The aim of this study is to experimentally characterise and predict the ability of some ChEI to penetrate the BBB. For this purpose, we have chosen *in vitro* high-performance liquid chromatography (HPLC) method, which employs immobilized artificial membrane (IAM) (Karasova et al., 2010a). The IAM chromatography was used earlier for the prediction of the passive drug transport across biological barrier and for that reason it could be also used as a screening method for the prediction of BBB permeation (Yoon et al., 2006; Karasova et al., 2010b).

This method was validated on a set of twenty-one therapeutic compounds (Table 1) (Yoon et al., 2006) and consequently used for a set of eight structurally varying ChEI. Set of these ChEI consists of commonly used anti-AD drugs (donepezil, rivastigmin, galanthamine) and also some other aqiured drugs with promising central inhibition potency (tacrine, huperzine A, 7-MEOTA). The last tested compounds was quaternary pyridostigmine. All structures are depicted in Table 2.

MATERIALS AND METHODS

The experimental part such as used chemicals, apparatus and chromatographic conditions were published and reviewed previously (Karasova et al., 2010a, b). The results of validation process were slightly changed as described below.

Chemicals

Atenolol, β-estradiol, caffeine, cefuroxime, chlorpromazine, cimetidine, corticosterone, desipramine, enalapril, hydrocortisone, ibuprofen, imipramine, lomefloxacin, loperamide, nadolol, piroxicam, progesterone, promazine, propranolol, and testosterone were purchased from Sigma Aldrich (Prague branch, Czech Republic). Acetonitrile gradient grade LiChrosolv was purchased from Merck (Darmstadt, Germany). KH_2PO_4, Na_2HPO_4, KCl, and NaCl were purchased from Lachema (Neratovice, Czech Republic). AChE reactivators were synthetized previously in our laboratory. Their structures are shown in Table 1. Water was reverse osmosis pure.

Apparatus and chromatographic condition

The HPLC system consisted of a P200 gradient pump (Spectra-Physics Analytical, Fremont, USA), a 7125 injection valve – 10 ul loop (Rheodyne, Cotati, USA), an UV1000 detector (Spectra-Physics Analytical, Fremont, USA) and a CSW Chromatography Station 1.5 software (DataApex, Praha, Czech Republic). For analyses an IAM.PC.DD 2 (150 × 4.6 mm; 12 µm) column (Regis Technologies, Morton Grove, IL) was used. The mobile phase was 80% phosphate buffered saline (PBS) and 20% acetonitrile (v/v) with pH 7.4 using Na_2HPO_4. The PBS was prepared with 2.7 mM KCl, 1.5 mM KH_2PO_4, 137 mM NaCl, and 8.1 mM Na_2HPO_4. The flow rate was 1.2 ml/min. The absorbance was measured at 210 nm. All chromatograms were obtained at 37°C.

Procedure

In this study, we determined k_{IAM} (capacity factor of this special column) for AChE reactivators. The capacity factor was calculated according to below mentioned formula.

$$k_{IAM} = \frac{t_r - t_0}{t_0}$$

t_r is the retention time of the drug and t_0 is the hold-up time of the column.

The k_{IAM} was determined for twenty-one reference drugs mentioned before. The knowledge about penetration of these drugs through the BBB was compared with measured k_{IAM}. The last step was correction of result by power function of molecular weight according to below mentioned formula.

$$X = \frac{k_{IAM}}{MW^4}$$

The obtained results of standards were correlated with known physico-chemical constants – logarithm of partition coefficient (LogP), molecular polar surface area (PSA) and molecular weight (MW) of standards (Table 1). These constants were also calculated for tested AChE inhibitors (Table 2) (Yoon et al., 2006). The calculated physico-chemical parameters were used for correlation standard compounds results (X) (Table 1) and showed the validity of this method (Figures 1 and 2).

Statistical analysis

Statistical analysis was performed using GraphPad Prism, version

Table 1. Structures and descriptors of standards.

S/No	Compound name	MW	Structure	pKa	log P	PSA (Å^2)	t_r (min)	Result (X)
1	Cefuroxime CNS-	424	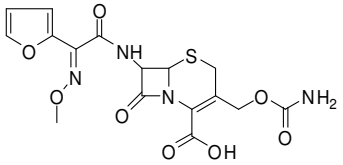	3.15	-1.44	201.89	1.64	0.38
2	Enalapril CNS-	376	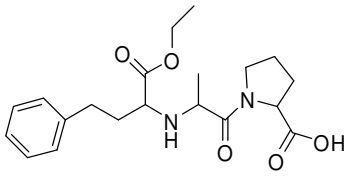	3.18/5.19	2.10	98.77	1.77	0.71
3	Lomefloxacine CNS-	352	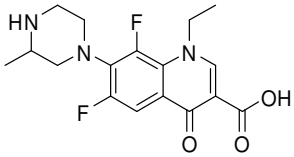	5.65/8.70	2.06	80.29	3.09	2.11
4	Piroxicame CNS-	331	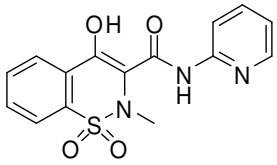	4.27	1.02	110.81	1.87	1.31
5	Nadolol CNS-	309	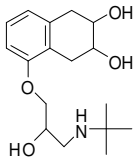	9.76	0.37	86.53	8.56	11.78

Table 1. Contd.

6	Atenolol CNS-	266	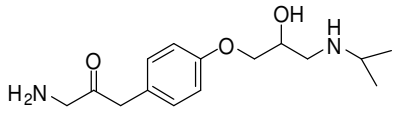	9.67	0.26	84.58	4.81	11.19
7	Hydrocortisone CNS-	362	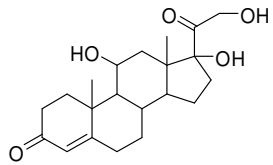	12.74	1.47	94.83	5.90	4.13
8	Cimetidine CNS-	252	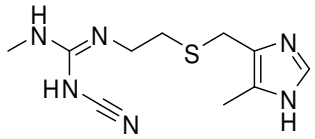	6.92	0.24	114.19	2.66	6.57
9	Corticosterone CNS-	346	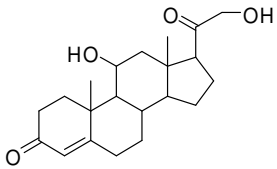	-	2.48	74.60	9.33	8.23
10	Loperamide CNS-/CNS+	477	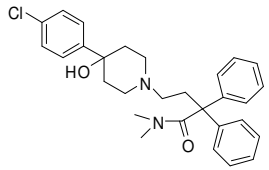	9.41	4.71	44.98	359.06	94.95

Table 1. Contd.

11	Caffeine CNS+	194	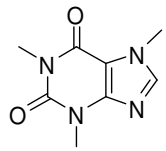	1.50	-0.79	58.44	2.06	12.85
12	Ibuprofene CNS+	206	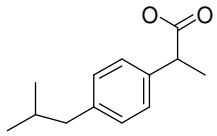	4.86	3.83	40.13	2.81	15.83
13	Propranolol CNS+	259	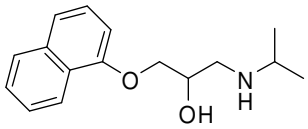	9.67	2.50	46.07	99.61	301.41
14	Progesterone CNS+	314	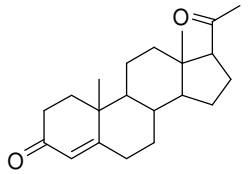	-	4.63	34.14	61.74	86.10
15	Testosterone CNS+	288	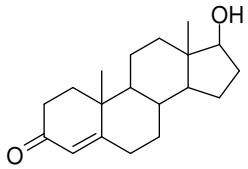	-	3.54	37.30	26.24	50.87

Table 1. Contd.

16	Imipramine CNS+	280	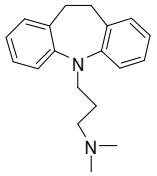	9.19	4.01	7.68	229.98	511.62
17	Desipramine CNS+	266	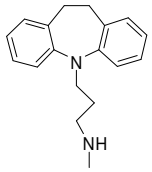	10.02	3.64	19.85	240.37	656.61
18	p-Toluidine CNS+	107	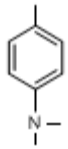	5.46	2.78	3.24	4.10	352.56
19	Promazine CNS+	284	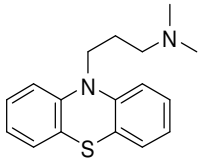	9.20	4.04	32.98	313.41	659.96
20	Chlorpromazine CNS+	319	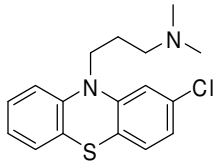	9.19	4.56	32.98	644.08	863.00

Table 1. Contd.

21	β-estradiol CNS+	272	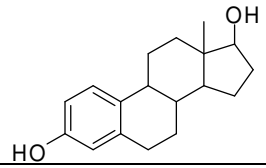	10.33	3.71	40.46	94.39	218.23

Table 2. Structures of AChE inhibitors.

No.	Compound name	MW	Structure	pKa	log P	PSA (Å^2)	t_r (min)	Result (X)
1	Huperzine A	242	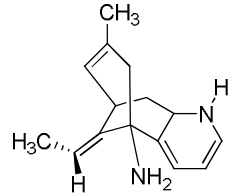	9.10 11.40	0.62	56.74	4.02	13.15
2	Galanthamine	287	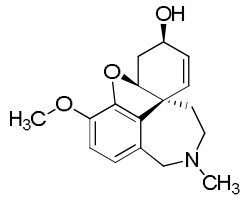	8.90	1.16	43.13	7.26	13.20
3	Donepezil	379	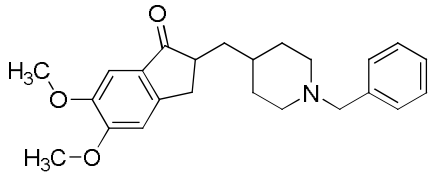	8.60	4.21	39.97	29.48	19.11
4	Physostigmine	275	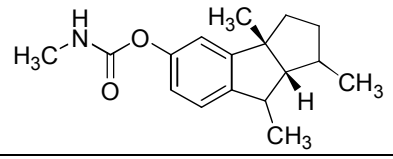	6.60	2.23	44.81	9.28	20.50

Table 2. Contd.

5	Pyridostigmine	181	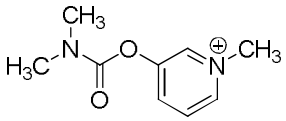	-	-3.47	33.42	3.866	40.09
6	Rivastigmine	250	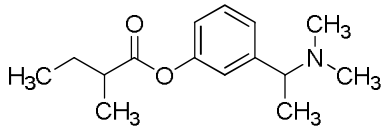	8.90	2.41	33.98	14.15	47.14
7	7-MEOTA (7-mehtoxytacrine)	228	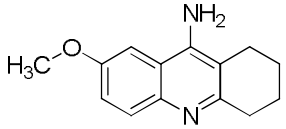	8.90	1.88	49.39	59.11	296.37
8	Tacrine	198	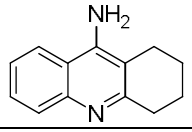	8.95	2.63	40.16	34.436	300.84

5.0 (GraphPad Software, San Diego, California). Marvin was used for drawing, displaying and characterizing chemical structures, substructures and also for calculating of physico-chemical properties (pKa, log P, PSA), Marvin 5.1.0, 2008, ChemAxon (http://www.chemaxon.com).

RESULTS

Over the last decade polar surface area (PSA) has become a ubiquitous term in medicinal and computational chemistry. As shown previously, it correlated with human intestinal and other biological barrier permeation, especially BBB (Palm et al., 1998; Zhu et al., 2002; Clark, 2011). However, good correlation was observed between PSA and k_{IAM}/MW^4 for drugs used in calibration in this study. Correlation being 0.741 at the mobile phase of pH 7.4 (Figure 2) was found. The correlation between log P, the standard pharmacokinetics descriptor, and k_{IAM}/MW^4 was 0.706. Both results show stronger dependency between respected physicochemical descriptors and drug ability to penetrate through the BBB. Based on this result this method may be accepted for *in vitro* prediction of BBB permeation. On the other hand, the results of standards were also used for determination of border between CNS- and CNS+ compounds. For this, the known data about BBB penetration of standards from human studies were used.

According to the reported method, the CNS^- drugs (drugs with low passive penetration through the BBB) showed evident inability to bound to the phosphatidylcholine column and have permeability values less than 9.48, whereas the CNS^+ drugs (drugs with higher passive penetration through the BBB) proved to bound much better and their permeability values were higher than 17.6. If compounds reach values over 17.6, they can penetrate the BBB. However, values below 9.48 predict that compounds stay in the periphery. These conclusions were achieved during the correlation of physical parameters with the results of assay of twenty-one structurally different therapeutics set. After the method validation, a set of eight structurally different ChEIs was measured three times using similar conditions. K_{IAM} values were calculated from the

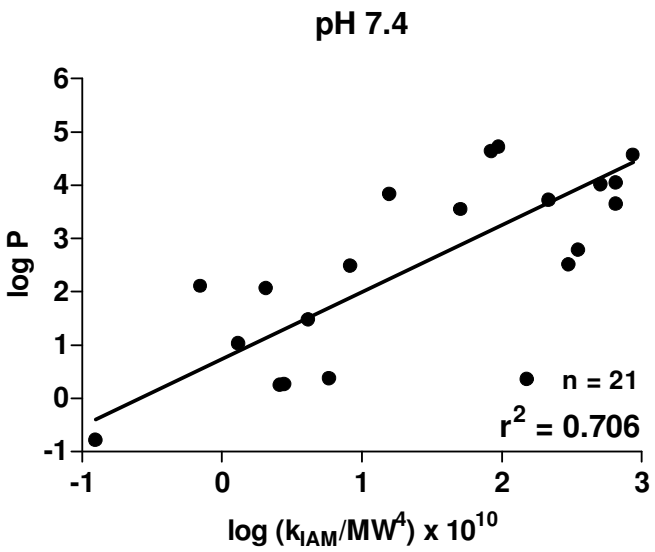

Figure 1. Correlation between log P and k_{IAM}/MW^4 for tested 21 drugs. Good correlation was found with the correlations coefficient (r^2) being 0.706 at pH 7.4.

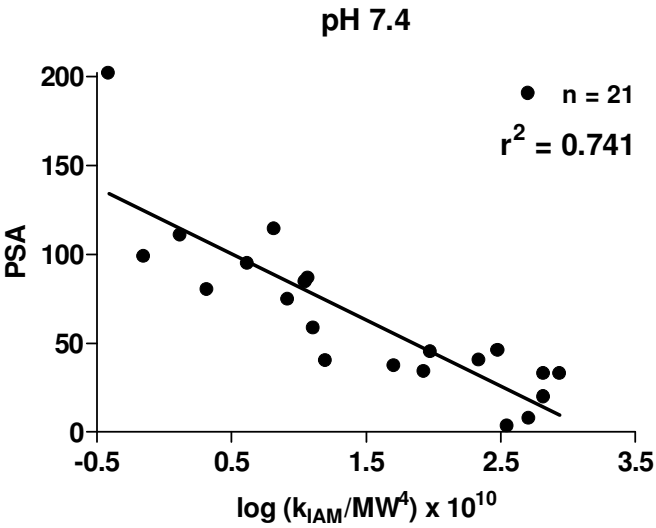

Figure 2. Correlation between polar surface area (PSA) and k_{IAM}/MW^4 determined at the mobile phase pH of 7.4 for the tested drugs.

retention times of ChEIs and after that, results were correlated by molecular weights. Using this approach, the permeability values for tested drugs were found.

In accordance with the acquired values characterizing tested compounds BBB permeability, we can discuss features influencing this process. All results obtained in this study are shown in Table 2. The structure of the tested ChEIs and also molecular weight are the most important factors, which may influence passive transport of these molecules into the brain. According to our methodology, the molecules such as huperzine A and galanthamine have lower ability to go through the BBB directly, which points to the possibility that these molecules could be delivered into the brain via active transport. Donepezil and physostigmine are able to use passive transport to permeate into CNS. Interestingly, rivastigmine is able to penetrate throught the BBB 2.5 fold more than donepezil. The key role in this discrepancy probably plays molecular weight.

The passive penetration into the CNS is strongly influenced by the presence of charge in molecule. It can be seen as a surprise that molecule as pyridostigmin is able to pass the BBB by passive penetration. The last two ChEIs molecules, tacrine and 7-MEOTA seem to mainly exploit the passive penetration to overcome the BBB.

DISCUSSION

All drugs that are successfully used in the therapy of AD should be considered as CNS+ targeted. There are many markers that may help us to estimate their ability to penetrate through the BBB. Physico-chemical descriptors are the most recent and most convenient prediction indicators used at the moment. Among them, lipophilicity (expressed by logP) was the first suitable parameter. The optimal BBB penetration value of logP is in 1.5 to 2.7 range (Hansch and Leo, 1979). From the group of tested ChEIs, physostigmine, rivastigmine, tacrine and 7-MEOTA fulfil this condition.

MW also plays important role in passive penetration through the BBB. Smaller molecules (MW < 400 Da) have significantly better passive lipid-mediated transport into CNS. The commonly used centrally active drugs have the mean value of MW 310 Da (Leeson and Davis, 2004). Better descriptor than MW is PSA; PSA is the sum of surfaces of polar atoms such as oxygens, nitrogens and attached hydrogens, in a molecule (Chen et al., 2009; Lanevskij et al., 2009); and is successfully used as a predictor for BBB passive penetration which is successfully used as a predictor for BBB passive penetration by many investigators (Yoon et al., 2006; Feng, 2002). Drugs aimed at the central compartment tend to have lower PSA than peripherally acting therapeutics. The higher PSA value convenient for CNS penetration was estimated at 60 to 70 $Å^2$. The upper limit of PSA for molecule to penetrate the brain is around 90 $Å^2$ (Kelder et al., 1999). All tested ChEIs ranged from 34.0 (rivastigmine) to 56.7 $Å^2$ (huperzine A).

Although these descriptors are able to confirm ability of tested drugs to penetrate through the BBB, it is still necessary to compare them with *in vivo* studies (Amourette et al., 2009; Geerts et al., 2005; Karasova et al., 2011; Polinsky, 1998; Wilson et al., 2008; Yue et al., 2007). Previously published *in vivo* data show many contradictory results. Many of them confirmed the BBB

penetration by certain indirect methods such as decrease of cholinesterase level (Ellman's method) in chosen brain parts. These studies may be loaded by numerous mistakes. A better way on how to follow this pharmacokinetic parameter is to measure the real brain concentrations directly (mainly by HPLC) (Geerts et al., 2005; Wilson et al., 2008; Yue et al., 2007).

It is peculiar that results of this kind of studies are so rare. One of the useful studies was published by Geerts et al. (2005) where author suggested that donepezil had a better brain penetration than galanthamine. The donepezil distribution curves in the brain have tendency to decrease more slowly that the galanthamine levels, suggesting a higher retention rate.

In another study, peak brain concentration was reached 15 (donepezil) and 30 min (galanthamine) after s.c. administration (Geerts et al., 2005).

According to our results, donepezil and galanthamine have lower ability to penetrate BBB under passive diffusion like molecules of Huperzine A and physostigmine. The real concentration of Huperzine A in brain was also measured (Yue et al., 2007). According to these results, it was demonstrated that Huperzine A is capable to cross the BBB readily under passive diffusion mechanism. The maximal concentration was reached after 5 min (intravenous application) and 30 min (intranasal application). This rapid permeation may also confirm integration of some BBB active transport system into this process.

Molecules such as rivastigmine and pyridostigmine were evaluated to have better potency to pass through the BBB via passive transport. According to *in vivo* results (Polinsky, 1998), rivastigmine is noted in cerebrospinal fluid (CSF) 30 min after application and its concentration quickly grew up till the maximal concentration was achieved (120 min after administration). Rivastigmine elimination from CSF was slow. The brain action of pyridostigmine is still unclear. Some results exist but they are based only on changes in ChE activities. Although pyridostigmine is a quaternary molecule, some evidence about BBB penetration for this type of molecules exist. The application of this ChE inhibitor dose induced a 7% depression in brain ChE activity. This was subsequently confirmed by radioactivity measurement in selected brain areas (Amourette et al., 2009). It is not the first evidence of quaternary molecules penetrating into the central nervous system (Karasova et al., 2011). Among the tested molecules, tacrine and 7-MEOTA were evaluated as structures with highest potency to penetrate through the BBB by passive diffusion. According to our results, we found out their ability to pass into central nervous system in comparable concentrations. Some *in vivo* results with tacrine were published by Wilson et al. (2008). The tacrine BBB penetration was confirmed, the real concentration was in 10^{-8} order (g/ml of brain homogenate). The brain concentration of 7-MEOTA and other pharmacokinetics data are still missing.

Conclusions

All tested ChEIs are able to penetrate the BBB. This ability is the cornerstone in AD therapy. Some of them should mainly use passive transport system; others may partially pass under active transport. Unfortunately, a relevant argumentation is complicated since information about real drug concentration in the brain or time-dependent BBB distribution studies are still quite rare; especially *in vivo* studies.

ACKNOWLEDGEMENTS

Authors would like to thank the Grant Agency (Czech Republic) No. P303/11/1907 and No. P303/12/0611 and a long-term organization development plan 1011.

REFERENCES

Amourette Ch, Lamproglou I, Barbier L, Fauquette W, Zoppe A, Viret R, Diserbo M (2009). Gulf War illness: Effect of repeated stress and pyridostigmine treatment on blood-brain barrier permeability and cholinesterase activity in rat brain. Behav. Brain Res. 203:207-214

Becker R, Giacobini E (1997). Alzheimer Disease: From molecular biology to therapy. Birkhauser, Boston.

Bi X (2010). Alzheimer disease: update on basic mechanism. J. Am. Osteopath. Assoc. 110:S8:3-9

Braak H, Del Tredici K (2013). Evolutional aspects of Alzheimer´s Disease pathogenesis. J Alzheimer Dis 33 : S155-161

Castellani RJ, Rolston RK, Smith MA (2010). Alzheimer Disease. Disease-a-month 56:484-546

Chen Y, Zhu QJ, Pan J, Yang Y, Wu XP (2009). A prediction model for blood-brain barrier permeation and analysis on its parameter biologically. Computh. Met. Prog. Biol. 95:280-287

Clark DE (2011). What has polar surface area ever done for drug discovery? Future Med. Chem. 3:469-484.

De los Rios C (2012). Cholinesterase inhibitors: a patent review (2007-2011) Expert Opin. Ther. Pat. 22:853-869

Edvinsson L, Tfelt-Hansen P (2008). The blood-brain barrier in migraine treatment. Cephalalgia 28:1245-1258

Feng RM (2002). Assessment of blood-brain barrier penetration: in silico, in vitro and in vivo. Curr. Drug Metab. 3:647-657

Geerts H, Guillaumat PO, Grantham CH, Bode W, Anciaux K, Sachak S (2005). Brain levels and acetylcholinesterase inhibition with galantamine and donepezil in rats, mice, and rabbits. Brain Res. 1033: 86-193

Giacobini E (2004). Cholinesterase inhibitors: new role and therapeutic alternatives. Pharm. Res. 50:433-440

Grossberg GT (2003). Cholinesterase inhibitors for the treatment of Alzheimer's Disease: Getting on and staying on. Curr. Ther. Res. 64:216-235

Hansch C, Leo AJ (1979). Substituent constant for correlation analysis in chemistry and biology. Wiley, New York.

Karasova JZ, Stodulka P, Kuca K (2010a). In vitro screening of blood-brain barrier penetration of clinically used acetylcholinesterase reactivators. J. Appl. Biomed. 8:35-40

Karasova JZ, Pohanka M, Musilek K, Zemek F, Kuca K (2010b). Passive diffusion of acetylcholinesterase oxime reactivators throught the blood–brain barrier: Influence of molecular structure. Toxicol. in Vitro 24:1838-1844

Karasova JZ, Zemek F, Bajgar J, Vasatova M, Prochazka P, Novotny L, Kuca K (2011). Partition of bispyridinium oximes (trimedoxime and K074) administered in therapeutic doses into different parts of the rat brain. J. Pharm. Biomed. Anal. 54:1082-1087

Kelder J, Grootenhuis PDJ, Bayada DM, Delbressine LPC, Ploemen JP

(1999). Polar molecular surface as a dominating determinant for oral absorbtion and brain penetration of drugs. Pharmacol. Res. 16:1514-1519

Lanevskij K, Japertas P, Didziapetris R, Petrauskas A (2009). Ionization-specific prediction of blood-brain permeability. J. Pharm. Sci. 98:122-134

Leeson PD, Davis AM (2004). Tine-related differences in the physical property profiles of oral drugs. J. Med. Chem. 47:6338-6348

Lorke DE, Kalasz H, Petroianu GA, Tekes K (2008). Entry of oximes into the brain: a review. Curr. Med. Chem. 15:743-753

Moussa BH, Buccaflusco Y, Buccafusco JJ (2005). Multi-functional drugs for various CNS targets in the treatment of neurodegenerative disorders. Trends Pharmacol. Sci. 26:27-35

Palm K, Luthman K, Ungell AL, Strandlung G, Beigi F, Lundahl P (1998). Evaluation of dynamic polar molecular surface area as predictor of drug absorption: comparison with other computational and experimental predictors. J. Med. Chem. 41:5382-5392

Polinsky RJ (1998). Clinical pharmacology of Rivastigmine: A new-generation acetylcholinesterase inhibitor for the treatment of Alzheimer's disease. Clin. Ther. 20:634-647

Racchi M, Mazzucchelli M, Porrello E, Lanni C, Govoni S (2004). Acetylcholinesterase inhibitors: novel activities of old molecules. Pharm. Res. 50:441–451

Schwarz S, Froelich L, Burns A (2012). Pharmacological treatment of dementia. Curr. Opin. Psychiatr. 25:542-550.

Terasami T, Ohtsuki S (2005). Brain-to-blood transporters for endogenous substrates and xenobiotics at the blood-brain barrier: an overview of biology and methodology. Neurotherapeutics 2:63-72

Tsukita S, Furuse M, Itoh M (2001). Multifunctional strands in tight junctions. Nature Rev. Mol. Cell. Biol. 2:285-293

Turksen K, Troy TC (2004). Barriers built on claudins. J. Cell Sci. 117:2435-2447

Van der Zee EA, Platt B, Riedel G (2011). Acetylcholine: Future research and perspectives. Behav. Brain Res. 221:583-586

Wilson B, Samanta MK, Santhi K, Kumar KPS, Paramakrishnan N, Suresh B (2008). Targeted delivery of tacrine into the brain with polysorbate 80-coated poly(n-butylcyanoacrylate) nanoparticles. Eur. J. Pharm. Biopharm. 70:75–84

Yoon HCh, Kim SJ, Shin BS, Lee KCh, Yoo SD (2006). Rapid screening of blood-brain barrier penetration of drugs using the immobilized artificial membrane phosphatidylcholine column chromatography. J. Biomol. Screen 11:13-20

Yue P, Tao T, Zhao Y, Ren J, Chai X (2007). Huperzine A in rat plasma and CSF following intranasal administration. Int. J. Pharm. 337:127-132

Zhao Q, Tang XC (2002). Effects of huperzine A on acetylcholinesterase isoforms in vitro: comparison with tacrine, donepezil, rivastigmine and physostigmine. Eur. J. Pharm. 455:101–107

Zhu C, Juany L, Chen TM, Hwang KK (2002). A comparative study of artificial membrane permeability assay for high throughput profiling of drug absorption potential. Eur. J. Med. Chem. 37:399-407

academicJournals

Vol. 7(22), pp. 1482-1500, 15 June, 2013
DOI 10.5897/AJPP2013.2987
ISSN 1996-0816 © 2013 Academic Journals
http://www.academicjournals.org/AJPP

African Journal of Pharmacy and Pharmacology

Full Length Research Paper

Design and optimization of self-nanoemulsifying drug delivery systems of simvastatin aiming dissolution enhancement

Hanaa Mahmoud, Saleh Al-Suwayeh and Shaimaa Elkadi*

Department of Pharmaceutics, Collage of Pharmacy, King Saud University, Riyadh 11472, Saudi Arabia.

Accepted 18 April, 2013

The aim of this work was to improve the *in vitro* dissolution of simvastatin through development of self-nanoemulsifying tablets. Various modified oils, surfactant and co-surfactant mixtures were used to prepare different self-nanoemulsifying drug delivery systems (SNEDDS) whose composition was optimized using drug-solubility, ternary phase diagram, system stability and droplet size distribution studies. Optimized SNEDDSs, with acceptable surfactant ratio, stability and particle size (nano-range) upon dilution with simulated gastric fluid (SGF, pH 1.2) under gentle agitation conditions, were loaded onto microcrystalline cellulose and nano-size colloidal silicon dioxide powders using loading factor (L_f) = 0.2 and excipient ratio (R) = 20. Prepared powders were compressed into tablets and the *in vitro* performance of the prepared self-nanoemulsifying tablets was investigated. Results revealed that systems with 10% relatively polar oils (C_8), 60% Cremophore® RH 40 (surfactant), and 30% Transcutol® HP (co-surfactant), acquired good self-nanoemulsification properties either in liquid or tableted forms. Prepared self-nanoemulsifying tablets demonstrated significantly higher dissolution rates, compared to direct compression tablets (DCT) and marketed tablet (Zocor®). In conclusion, self-nanoemulsifying tablets were able to introduce simvastatin successfully in a unique immediate-release solid dosage form.

Key words: Simvastatin, self-nanoemulsifying tablets, self-nanoemulsifying drug delivery systems (SNEDDS), droplet size.

INTRODUCTION

Oral route is the major route of drug delivery for the chronic treatment of many diseases due to the convenience and improved patient safety (Wang et al., 2009). To achieve successful therapeutic outcomes, orally-administered drugs should be well absorbed across the gastrointestinal tract (GIT) and should also provide good oral exposure. Thus, improvement of the aqueous solubility of poorly-water soluble drugs presents one of the most important challenges in field of pharmaceutics, because low aqueous solubility will show dissolution rate-limited absorption *in vivo* and hence poor absorption, distribution, and targeted-organ delivery (Patel and Patel, 2007). Much attention has been focused on techniques used to increase the drug solubility and dissolution properties, such as solid dispersion (Serajuddin, 1999), anti-solvent (Muhrer et al., 2006), complexation with cyclodextrin (Ammar et al., 2006), and lipid-based formulations (Hauss, 2007). In the recent years, there is a growing interest in the lipid-based formulations for the oral delivery of poorly water-soluble drugs. In fact, the most popular approach is the incorporation of the drug compound into inert lipid vehicles such as oils, surfactant

*Corresponding author. E-mail: elkadishaimaa@yahoo.com. Tel: +966-532858367. Fax: +966-1-2913739.

dispersion (Nielsen et al., 2008), liposomes (Schwendener and Schott, 1996), microemulsions (Araya et al., 2005), nanoemulsions (Shafiq et al., 2007), self-emulsifying formulations (Kommuru et al., 2001), self-microemulsifying formulations (Wu et al., 2006), and self-nanoemulsifying formulations (Villar et al., 2012). Most of them advantageously increase surface area of the drugs to improve solubilization behavior, as well as permeation (Shafiq et al., 2007).

Self-nanoemulsifying drug delivery systems (SNEDDS) are isotropic mixtures of natural or synthetic oils, surfactants, and co-surfactants. These systems spontaneously emulsify when exposed to gastrointestinal fluids to form oil in water nanoemulsion with nanometric droplet size (Elnaggar et al., 2009), while the digestive motility of the stomach and intestine provides the agitation necessary for self-emulsification–dispersion process (Neslihan Gursoy and Benita, 2004). Drug substances with adequate solubility in lipid/surfactants/co-surfactant blends are candidates for this formulation concept (Rane and Anderson, 2008). SNEDDS exhibited privileges over other delivery systems. They are characterized by ease of manufacture, high solvent capacity, small particle size, and excellent physical stability. In addition, they can enhance permeation across the intestinal membrane, reduce or eliminate food effect and enhance drug bioavailability (Rane and Anderson, 2008; Wasan et al., 2009). However, only very specific pharmaceutical excipient combinations will lead to efficient self-emulsifying systems. This could explain that although many studies have been carried out in this field, there are few drug products on the pharmaceutical market formulated as self-emulsifying formulations (Elnaggar et al., 2009). For selection of a successful self-nanoemulsifying vehicle, it is important to assess the drug solubility in various components, the area of self-emulsifying region in the phase diagram, and droplet size distribution following self-emulsification (Kommuru et al., 2001).

Simvastatin is a poorly-water soluble cholesterol-lowering agent; widely used to treat hypercholesterolemia in animals and humans. When given orally, simvastatin (a lactone) undergoes hydrolysis and is converted to the β-hydroxyacid form, a potent competitive inhibitor of 3-hydroxy-3-methylglutaryl coenzyme A (HMG-CoA) reductase; the enzyme that catalyzes the rate-limiting step of cholesterol biosynthesis (Carlucci et al., 1992; Lin et al., 2012). It is a white to off-white, non-hygroscopic, crystalline powder (Ambike et al., 2005). Water solubility of simvastatin is low, approximately 30 µg/ml (Margulis-Goshen and Magdassi, 2009). Several systems for improving simvastatin solubility have been reported in the literature (Kang et al., 2004; Ambike et al., 2005; Patel and Patel, 2007; Patil et al., 2007; Margulis-Goshen and Magdassi, 2009; Thomas et al., 2013).

In this study, self-nanoemulsifing drug delivery systems (SNEDDS) containing simvastatin were formulated with the objective of improving solubility and dissolution rate of the drug. To obtain such formula, the following steps were conducted; (a) preparation and evaluation of self-emulsifying drug delivery systems (SEDDS) composed of different selected oils, surfactants and co-surfactants, (b) incorporation of simvastatin into optimized SNEDDS composed of different ternary systems, (c) identifying optimal drug loaded SNEDDSs through screening the factors influencing droplet size of the generated emulsions after systems' dilution, (d) incorporation of optimal drug loaded SNEDDSs into tablets. The *in vitro* release profiles of simvastatin from different self-nanoemulsifying tablets and the tablets prepared by direct compression (DCT) as well as the marketed tablets (Zocor®) were compared. Additionally, the relationship between the simvastatin dissolution rate from self-nanoemulsifying tablets and droplet size of resulting emulsions was investigated.

MATERIALS AND METHODS

Materials

Simvastatin was kindly provided by Amriya Pharm. Ind. (Alexandria, Egypt). Propylene glycol monocaprylates (Capryol™ 90 and Capryol™ PGMC), propylene glycol dicaprylocaprate (Labrafac™ PG), medium chain triglycerides (Labrafac™ Lipophile WL 1349), polyoxylglycerides (Labrafil® M 1944 CS and Labrafil® M 2125 CS), propylene glycol monolaurates (Lauroglycol™ 90 and Lauroglycol™ FCC), glycerol monolinoleate (Maisine™ 35-1), glycerylmonooleate (Peceol™), and diethylene glycol monoethyl ether (Transcutol® HP) were kindly donated by Gattefosse Co. (France). Polyoxy 40 hydrogenated castor oil (Cremophor® RH 40), and polyoxy 35 castor oil (Cremophor® EL) were kindly gifted by BASF Co. (Germany). Nano-size colloidal silicon dioxide (Cab-o-sil® H-5) was obtained from Cabot Corporation (Germany). Microcrystalline cellulose (Vivapur® PH 102, MCC), and crosscarmellose sodium (Ac-Di-Sol®) were kindly supplied by Al Jazeera Pharmaceutical Industries (Riyadh, Saudi Arabia). All other chemicals used were of analytical grade.

Solubility studies

Screening of the liquid vehicles was done by determining the equilibrium solubility of simvastatin in different oils, surfactants, and co-solvents/co-surfactants. An excess quantity of simvastatin was added to each (1.5 ml capacity) capped microfuge tube containing 1 g of each of the selected vehicles. After sealing the tubes, vortex mixer was used to facilitate solubilization of the formed mixtures. Formed suspensions were then shaken at 37°C for 48 h in an isothermal shaking water bath, followed by equilibrium for 24 h. Mixtures were then centrifuged at 12,000 rpm for 15 min at 25°C to remove the undissolved simvastatin. The supernatant was separated and adequately diluted with methanol. Tests were repeated in triplicates and the concentration (w/w) of simvastatin in each vehicle was then quantified spectrophotometrically using UV-visible spectrophotometer (Ultraspec 2100 pro, England) at λ_{max} 238 nm based on a pre-constructed calibration curve ($R^2 = 0.999$).

Preliminary screening of ternary liquid formulae

This method was used to investigate relative efficacy of different (oil, surfactant, and co-solvent/co-surfactant) combinations to form

microemulsion or nanoemulsion upon dilution. Homogenous ternary mixtures of selected oils, surfactants, and co-solvents/co-surfactants at mass fraction of 1:2:2, respectively, were blended for all the samples. These mixtures were gently heated at 40°C to facilitate homogenizing the components using vortex mixer. From each isotropic mixture, 100 mg were accurately weighed and diluted 200-folds with simulated gastric fluid without pepsin (SGF, pH 1.2), pre-equilibrated at 37°C, and gently mixed by a magnetic stirrer. The clarity of the formed aqueous dispersion was visually assessed. All experiments were repeated in duplicates, with similar observations being made between repeats.

Construction of ternary phase diagrams

The existence of self-nanoemulsifying formulation fields; that could self-emulsify under dilution and gentle agitation to give SNEDDS, were identified from ternary phase diagrams for formulae containing oil, surfactant, and co-surfactant; each of them, representing an apex of the triangle. Ternary phase diagrams with varying compositions of oil, surfactant, and co-surfactant were constructed. For each diagram, thirty-six ternary systems (S1 to S36) with varying concentrations (10 to 80% w/w) of oil, surfactant, and co-surfactant were prepared such that for any system, the total of three components' concentration were always added to 100%. The oily phase was mixed with the surfactant/co-surfactant mixture and the ternary system was gently heated at 40°C to facilitate homogenizing the components using vortex mixer. From each system, 100 mg were accurately weighed and diluted 200-folds with SGF (pH 1.2, pre-filtered through 0.22-µm membrane filter (Durapore GVWP, Millipore Corp., USA) and pre-equilibrated at 37°C) and gently mixed by a magnetic stirrer.

The clarity of the formed aqueous dispersion was visually assessed using the A, B, C, D, or E grading (Figure 1) to identify the type of tested systems (Mahmoud et al., 2009). All experiments were established in triplicates, with similar observations being made between repeats. Type (A) systems are most likely expected to have particle size less than 50 nm and referred as SNEDDS (Khoo et al., 1998).

Determination of simvastatin saturated solubility in different systems

Excess quantity of simvastatin was added to the obtained type (A) ternary systems, for all ternary formulae (P1 to P8) and mixed using vortex mixer. Formed suspensions were then shaken at 37°C, for 48 h in an isothermal shaking water bath, followed by equilibrium for 24 h. Mixtures were then centrifuged at 12,000 rpm for 15 min at 25°C to remove the undissolved simvastatin. The supernatant was separated and adequately diluted with methanol. Tests were repeated in triplicates and the concentration of simvastatin was then quantified spectrophotometrically at λ_{max} 238 based on a pre-constructed calibration curve (R^2 = 0.999).

Preparation of simvastatin-loaded SNEDDS

Simvastatin (5% w/w) was added to pre-prepared and homogenized type (A) systems for all ternary formulae (P1 to P8), and mixed using vortex mixer till the appearance of a clear system. Systems containing simvastatin were then shaken at 37°C for 24 h in an isothermal shaking water bath to ensure complete solubilization, then stored at ambient temperature (25°C).

Evaluation of simvastatin-loaded SNEDDS

Droplet size distribution was used to characterize simvastatin-loaded SNEDDS (drug-loaded type (A) systems). From each system, 100 mg were accurately weighed and diluted as mentioned earlier. The droplet size of resulting emulsions was determined by dynamic light scattering (DLS) at a scattering angle of 173° (Zetasizer Nano-ZS, Malvern, UK) at 25°C, employing an argon laser (λ = 633 nm). Formulations that showed immediate precipitation of the drug or cracking were rejected.

Stability was determined by visual inspection of the resultant nanoemulsions for 12 h. Formulations were considered unstable if they showed any drug precipitation or phase separation within this period of time.

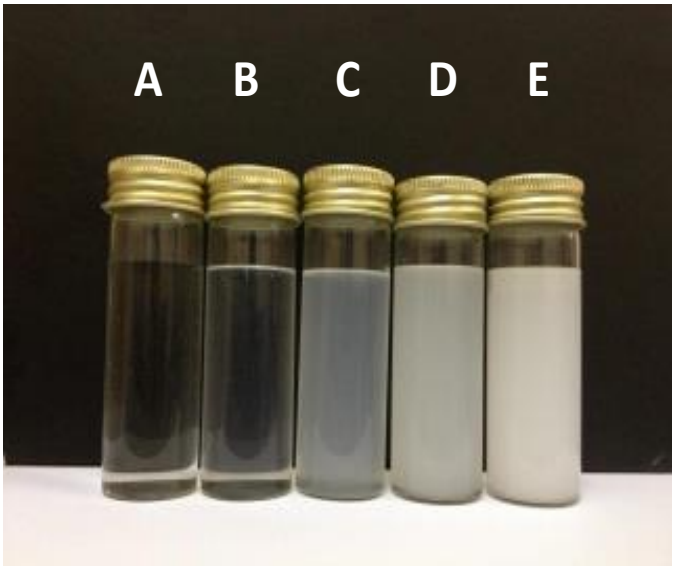

Figure 1. Typical appearance of the visual grades used to assess the clarity of the diluted systems. (A, denoting the formation of clear microemulsion or nanoemulsion; B, denoting the formation of translucent microemulsion; C, denoting the formation of less clear bluish white emulsion; D, denoting the formation of bright white emulsion and E, denoting that poor emulsion with large oil droplets on the surface or even no emulsion was formed).

Preparation of self-nanoemulsifying tablets

Calculated quantities *(Q)* of microcrystalline cellulose (Vivapur® PH 102) were loaded with specific weight *(W)* of the selected liquid simvastatin-loaded SNEDDS using loading factor (L_f) = 0.2 (Equation 1) (Spireas and Bolton, 1999).

$$L_f = \mathrm{W/Q} \quad (1)$$

After mixing, the resulting wet mixture was blended with the pre-calculated quantities (q) of nano-size colloidal silicon dioxide (Cab-o-sil® H-5) to obtain free flowing dry powder, using excipient ratio (*R*) = 20 (Equation 2) (Spireas and Bolton, 1999).

$$R = \mathrm{Q/q} \quad (2)$$

Finally, 5% w/w of disintegrant (Ac-Di-Sol®) was added to the mixture and mixed for 10 min. Prepared powders were compressed into oval, curve faced tablets of desired weight, using medium-oval convex punches (17.5 mm length × 9 mm width) in a rotary tablet press machine (Rimek Mini Press, Model RSB-4, Kanavati Engineering

Ltd., India). The applied compression force was adjusted to achieve tablet hardness of 40 to 70 N. Batches of 100 tablets, containing 5 mg of simvastatin per tablet, were obtained and exposed to further investigations.

Additionally, direct compression tablets (DCT) were prepared for better comparison, where physical mixtures of drug with all excipients without liquid vehicle were prepared and tableted under the same conditions that were used for the preparation of self-nanoemulsifying tablets.

Evaluation of self-nanoemulsifying tablets

Content uniformity

The uniformity of drug content in different self-nanoemulsifying tablet formulation was determined by accurately weighing 10 tablets of each formula individually. Each tablet was then crushed and dissolved in methanol, then the solution was filtered through 0.45-µm filter (Durapore HVHP, Millipore Corp., USA), properly diluted, and then simvastatin content was quantified spectrophotometrically at λ_{max} 238 (USP, 2006) based on a pre-constructed calibration curve (R^2 = 0.999).

Reconstitution properties (droplet size analysis)

Droplet size of the formed nanoemulsions was investigated after tablets' reconstitution. Each self-nanoemulsifying tablet was gently mixed with 20 ml of SGF (pH 1.2), filtered, and was subjected to droplet size analysis test using Zetasizer Nano-ZS. Z-average of generated nanoemulsions was compared to that of nanoemulsions generated from dilution of liquid simvastatin-loaded SNEDDS with SGF (pH 1.2).

In vitro dissolution test

The dissolution of simvastatin from self-nanoemulsifying tablets was performed in 500 ml of SGF (pH 1.2) at 37 ± 0.5°C using the USP Dissolution Tester (Erweka, model DT 600 HH, Germany), Apparatus II (rotating paddle), at a rotation of 100 rpm. Aliquots from the dissolution medium were withdrawn at 5, 10, 15, 20, 30, 45, 60, 75, 90, 105, and 120 min. The withdrawn samples were replaced by equal amounts of dissolution medium to maintain a constant volume. The samples were then filtered through 0.45-µm filter (PVDF membrane, Millipore Corp., USA) and were adequately analyzed, after proper dilution, for simvastatin content spectrophotometrically at λ_{max} 238 nm based on a pre-constructed calibration curve (R^2 = 0.999).

RESULTS AND DISCUSSION

Solubility studies

Self-emulsifying formulation consisting of oil, surfactant, co-solvent/co-surfactant and drug should be a clear and monophasic liquid at ambient temperature when introduced to aqueous phase and should have good solvent properties to allow presentation of the drug in solution after *in vivo* dilution (Singh et al., 2010). Therefore, appropriate vehicles should have good solubilizing capacity of the drug substance. Also, solubility of drug in such vehicles plays an important role in determining stability of formulation, as many formulations undergo precipitation before undergoing in situ solubilization (Parmar et al., 2011).

Solubilizing capacity of an oily phase is the perspective consideration regarding oil selection (Pouton and Porter, 2008). Figure 2 shows the results of simvastatin solubility tested in ten different oily phases that were commonly utilized in SEDDS and SNEDDS formulations (Chen, 2008). The obtained results showed higher drug solubility in Capryol™ PGMC, Capryol™ 90, Lauroglycol™ 90, Peceol™, Maisine™ 35-1, and Lauroglycol™ FCC, compared to Labrafil® M 2125 CS, Labrafil® M 1944 CS, Labrafac™ PG, and Labrafac™ Lipophile WL 1349; therefore the former ones were chosen for further investigations.

Four nonionic hydrophilic surfactants with hydrophilic-lipophilic balance (HLB) greater than 10; Cremophor® EL (HLB 12-14), Cremophor® RH 40 (HLB 14-16), Tween® 80 (HLB 15), and Tween® 20 (HLB 16.7), were employed in this study. Results represented in Figure 3 show that Cremophor® EL, Tween® 80, and Tween® 20 exhibited better solubility for simvastatin than Cremophor® RH 40, however, it was reported that Cremophor® RH 40 have a high self-emulsification properties with a wide range of oils and also the use of Cremophor® RH 40 for oral ingestion appeared to be more advantageous than Cremophor® EL (Elnaggar et al., 2009). Therefore, the four surfactants were subjected to further screening.

The presence of co-solvent/co-surfactant helps in increasing the solvent capacity of the formulation for the drug (Pouton and Porter, 2008). Acting as co-surfactants, they could also decrease the bending stress of interface and allow the interfacial film sufficient flexibility to take up different curvatures required to form nanoemulsion over a wide range of compositions. Also, low or negative interfacial tension and fluidization of the hydrocarbon region of the interfacial film is rarely achieved by the use of surfactant alone, therefore usually necessitating the addition of a co-surfactant (Eccleston, 1994; Kawakami et al., 2002). In this study, solubility of drug in co-solvents/co-surfactants (PEG 400, 1, 2-Propylene glycol, Transcutol® HP, and Span® 20) was examined. From the results depicted in Figure 3 it is clear that amongst all the examined vehicles, Transcutol® HP showed the highest capacity to dissolve simvastatin (212 ± 7 mg/g).

Final selection among different oils would secondly be confirmed according to their self-emulsification properties with other ingredients. Regarding surfactants and co-solvents/co-surfactants selection, drug solubility would come second to the main selection perspective: self-emulsification efficiency (Date and Nagarsenker, 2007).

Preliminary screening of ternary liquid formulae

The objective of screening different ternary combinations of oils, surfactants, and co-solvents/co-surfactants was to investigate their ability to form large efficient self-nanoemulsification regions on their ternary phase

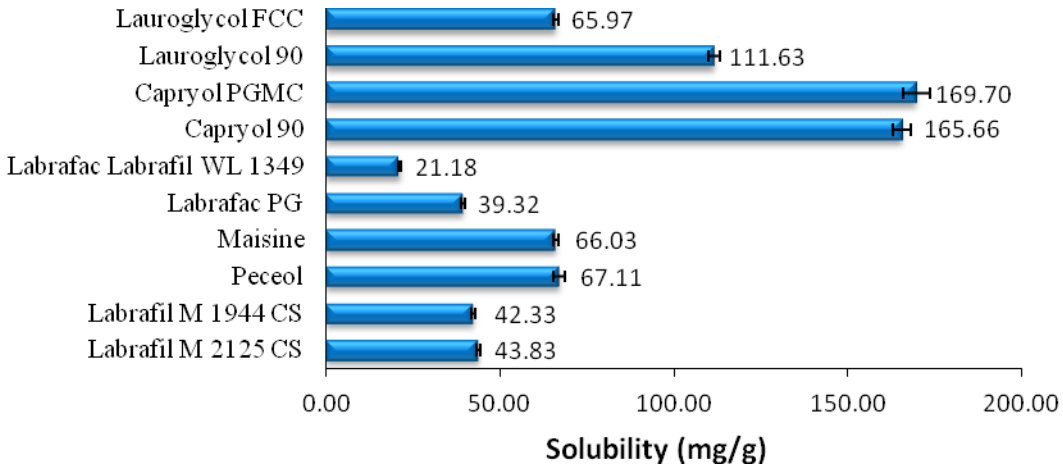

Figure 2. Solubility of simvastatin in various oils. Data are expressed as mean ± SD (n = 3).

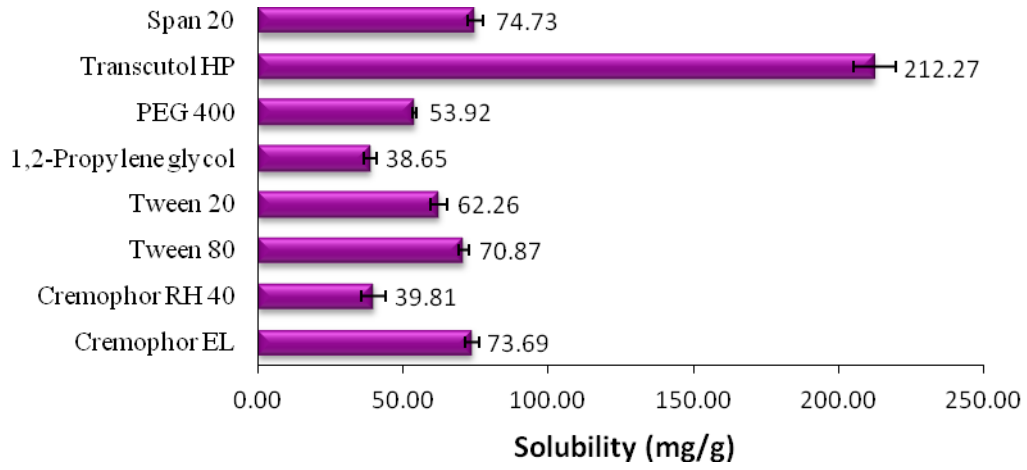

Figure 3. Solubility of simvastatin in various surfactants and co-solvents/co-surfactants. Data are expressed as mean ± SD (n = 3).

diagrams (Zhang et al., 2008). This ability could be expected for the ternary mixtures (oil: surfactant: co-solvent/co-surfactant, mass fraction 1: 2: 2) that form clear transparent or translucent emulsion after dilution; denoting the formation of self-nanoemulsion or self-microemulsion.

The efficiency of self-nonoemulsification is controlled by multiple variables including, HLB value of surfactant, lipid–surfactant affinity, and viscoelasticiy of the emulsion base (Sánchez et al., 2001). Results in Table 1 show that Cremophor® EL, Cremophor® RH 40, and Tween® 80 surfactants exhibited better self-emulsification efficiency than Tween® 20 due to its higher HLB value (HLB 16.7). Cremophor® EL, Cremophor® RH 40, and Tween® 80 also showed different self-emulsification efficiencies with different lipids used in this study; Cremophor® RH 40 showed high self-emulsification efficiency with Capryol™ 90, Capryol™ PGMC, and Maisine™ 35-1, while Cremophor® EL showed good self-emulsification efficiency with Capryol™ 90, Capryol™ PGMC, and Lauroglycol™ FCC; however, Tween® 80 showed good self-emulsification efficiency only with Capryol™ PGMC and Lauroglycol™ FCC which could be attributed to the difference in lipid-surfactant affinity that led to increased adsorption of surfactants onto droplets of specific oily phases rather than others (Sánchez et al., 2001).

As for the selection of co-solvents/co-surfactants, 1, 2-Propylene glycol, PEG-400 and Span® 20 (HLB 8.6) showed

poor self-emulsifying efficiency compared to Transcutol® HP (HLB 4.2) (Table 1) which could be due to their relatively higher hydrophilic properties, which increase the risk of destroying the emulsion (Zhang et al., 2008). These hydrophilic co-solvents/co-surfactants, being soluble in water, was anticipated to enter the water phase upon dilution and redistribute between the water phase and the emulsion-water interface, resulting in a loss of solvent capacity of the vehicle (Patel and Vavia, 2007). In addition, Transcutol® HP provided the highest drug solubility among all vehicles tested in this study (Figures 2 and 3) and was reported to give optimal SNEDDS formulations (Dixit and Nagarsenker, 2008; Basalious et al., 2010). Therefore, Transcutol® HP was selected as a co-surfactant in development of all SNEDDS formulations aiming to improve the drug loading capabilities and form spontaneous fine nanoemulsions.

Results represented in Table 1 also inferred that the oily phase Capryol™ PGMC exhibited the highest emulsification efficiency with all the surfactants employed (except Tween® 20). On the other hand, Lauroglycol™ 90 and Peceol™ showed very poor emulsification properties with all the surfactants employed. Capryol™ 90 and Lauroglycol™ FCC exhibited variable emulsification tendency with different surfactants, while Maisine™ 35-1 formed emulsion with only one surfactant (Cremophor® RH 40). Generally, the polarity of the lipids decreases with an increase in the number and length of the fatty acid chain (Shen and Zhong, 2006). It was reported that lipids with high polarity seem to be adequate to form a nanoemulsion (Kawakami et al., 2002), also oils of medium carbon chain length and higher HLB values are better than longer chain length and lower HLB values to form SNEDDS (Elnaggar et al., 2009). This could interpret the observed higher self-emulsification properties of Capryol™ 90 (C_8, HLB 6), Capryol™ PGMC (C_8, HLB 5), and Lauroglycol™ FCC (C_{12}, HLB 4) compared to Maisine™ 35-1 (C_{18}, HLB 4) and Peceol™ (C_{18}, HLB 3). Thus, the poor self-emulsification ability of Peceol™ reflected its high hydrophobic property. However, this could not explain the poor self-emulsification ability of Lauroglycol™ 90 (C_{12}, HLB 5) that could be attributed to the dependence of self-emulsification properties on the lipid-surfactant affinity, as explained earlier. Moreover, the observed higher self-emulsification ability of Lauroglycol™ FCC (with monoesters 45 to 70%) compared to Lauroglycol™ 90 (with monoesters > 90%) could be due to the branching; as a result of the presence of higher percentage of diesters, that gave more flexible interfacial films (Wang et al., 2009). This could also explain the observed higher self-emulsification ability of Capryol™ PGMC (with monoesters > 60%) compared to Capryol™ 90 (with monoesters > 90%) with Cremophor® EL and Tween® 80 as surfactants in the presence of Transcutol® HP as co-surfactant. Thus, Capryol™ 90, Capryol™ PGMC, Lauroglycol™ FCC, and Maisine™ 35-1 were selected as oily vehicles due to their good solubility and good self-emulsification efficiency with selected surfactants and co-surfactants upon dilution.

Based on the results of preliminary screening, eight distinct ternary formulae were selected (Table 2) according to their visual assessment grades, which were either A or B (Table 1). Detailed study of these eight ternary formulae; possessing various components in eight different combinations, was carried out via ternary phase diagrams.

Construction of ternary phase diagrams

Based on the results of solubility studies and preliminary screenings, ternary phase diagrams of the selected ternary formulae namely; P1, P2, P3, P4, P5, P6, P7, and P8 (Table 2) were constructed in the absence of simvastatin. These phase diagrams are depicted in Figures 4 and 5. In this study, the effect of the aqueous phase was ignored and considered as a constant factor for simplicity, where only the oil, surfactant and co-surfactant components were used to identify the self-nanoemulsifying region, after dilution of 200-folds with SGF (pH 1.2), on the ternary phase diagrams.

From the results depicted in Figures 4 and 5, it can be seen that, for ternary formulae having the same oil component, according to the size of the self-nanoemulsifying and self-microemulsifying region of the formulations, the self-nanoemulsifying or microemulsifying efficiency of surfactants was suggested to be in the following order: Cremophor® RH 40 > Tween® 80 > Cremophor® EL which could be due to increasing the HLB value of the surfactant being required for forming a good oil-water emulsion (Kommuru et al., 2001). The wider self-nanoemulsifying region observed with ternary formula P4 compared to others could be attributed to the high polarity of the lipid content (Capryol™ 90, HLB 6) and its high lipid-surfactant affinity. However, results obtained with ternary formula P8 indicated that apart from HLB value and type of surfactant, other factors such as structure and relative length of hydrophobic chains of lipid (Maisine™ 35-1, C_{18} glyceryl monolinoleate) had influence on emulsification efficiency and thereby self-nanoemulsifying and/or self- microemulsifying regions on the phase diagram (Elnaggar et al., 2009).

Results also deduced that varying ratios of oil provides the largest contribution to self-emulsifying efficiency of the systems. It is noteworthy that oil concentration more than 40% resulted in turbid and crude emulsions that were attributed to increase in the emulsion particle size upon increasing oil content (Hong et al., 2006). Also, the increase in surfactant content increased the clarity of the produced emulsion (Nazzal et al., 2002). This could be explained by the fact that the surfactant stabilizes the oil-water interface and its concentration increased at the interface upon decreasing the oily content in the ternary system, thus decreasing the generated emulsion particle size (Levy and Benita, 1990). However, the existence of

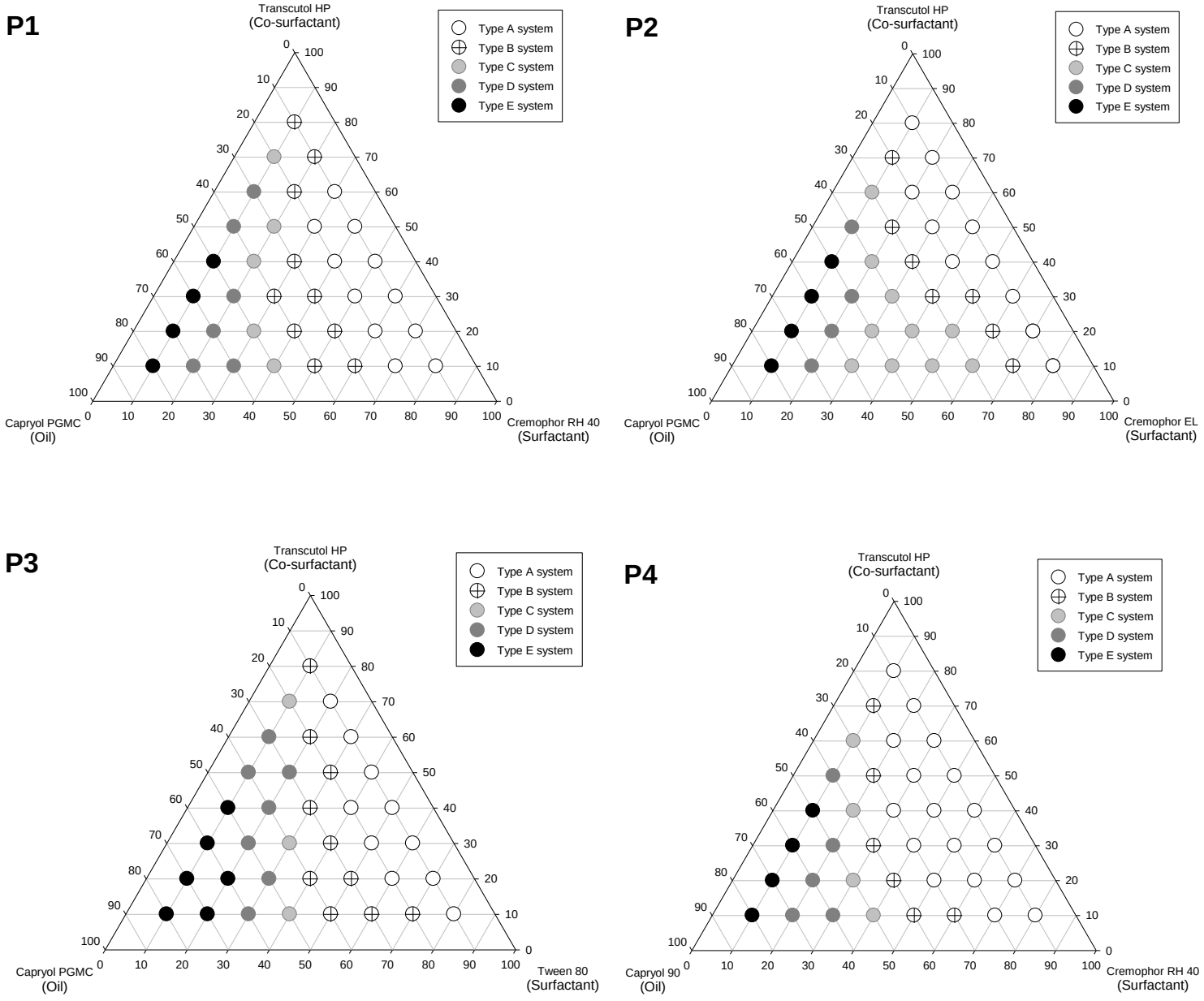

Figure 4. Ternary phase diagrams; P1,P2, P3, and P4.

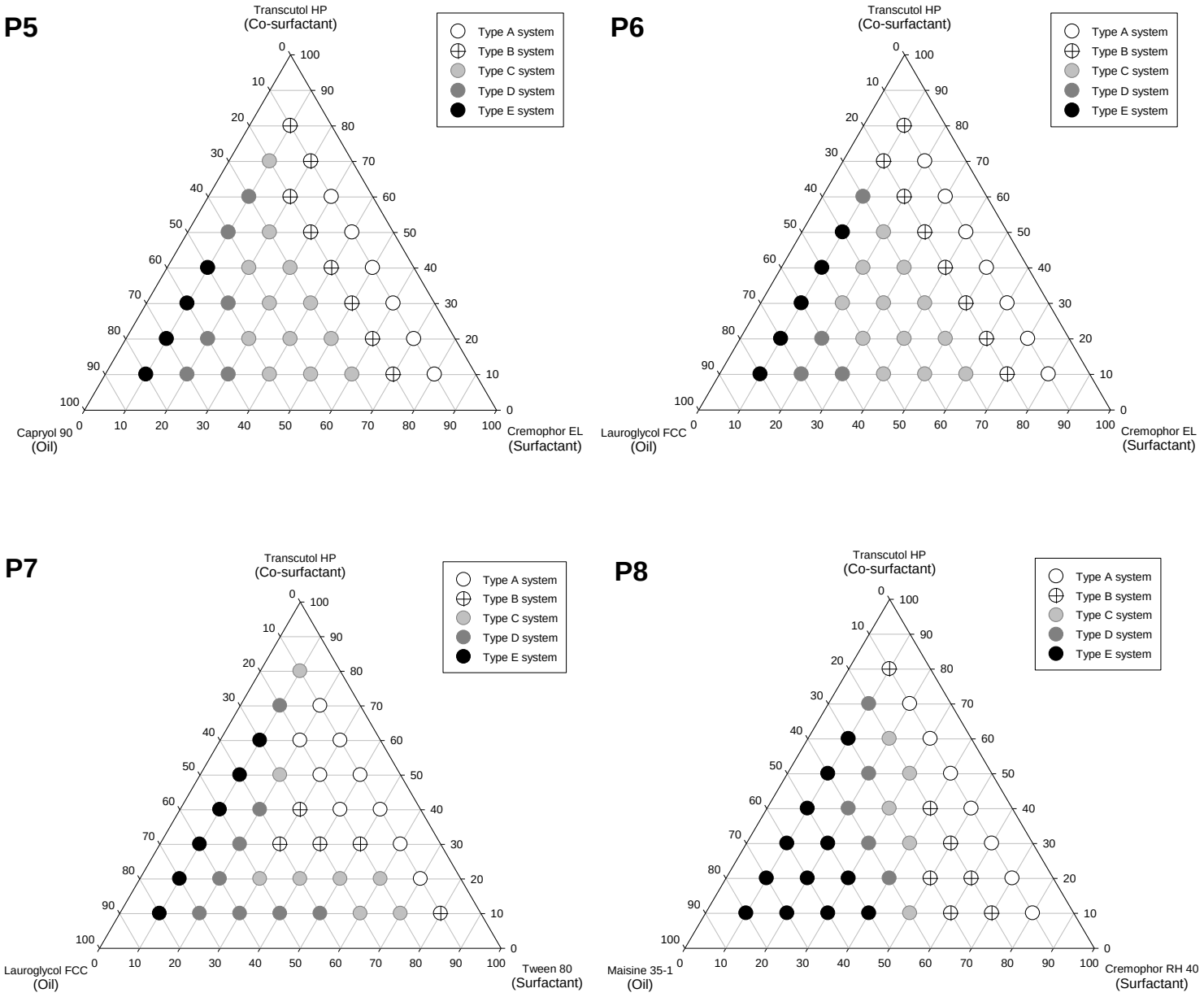

Figure 5. Ternary phase diagrams; P5, P6, P7, and P8.

Table 1. Classification of systems composed of (oil:surfactant:co-solvent/co-surfactant) at mass fraction of (1:2:2) as grade A, B, C, D, or E upon dilution ("200-folds") with SGF (pH 1.2).

Surfactant	Co-surfactant	Oil					
		Capryol 90	Capryol PGMC	Lauroglycol 90	Lauroglycol FCC	Peceol	Maisne 35-1
Cremophor EL	1,2-Propylene glycol	C	C	C	C	C	C
	PEG -400	C	C	C	C	C	C
	Transcutol HP	B	A	C	B	C	C
	Span 20	D	D	D	D	D	D
Cremophor RH 40	1,2-Propylene glycol	C	C	C	C	C	C
	PEG -400	C	C	C	D	D	D
	Transcutol HP	A	A	C	C	C	B
	Span 20	D	D	D	D	D	D
Tween 80	1,2-Propylene glycol	C	C	C	C	C	C
	PEG -400	C	C	C	C	C	D
	Transcutol HP	C	A	C	A	C	C
	Span 20	D	D	D	D	D	D
Tween 20	1,2-Propylene glycol	D	C	D	D	D	D
	PEG -400	D	C	D	D	D	D
	Transcutol HP	C	C	C	D	C	C
	Span 20	E	E	E	E	E	E

*Visual grading system: A, denoting the formation of clear microemulsion or nanoemulsion; B, denoting the formation of transluscent microemulsion; C, denoting the formation of less clear bluish white emulsion; D, denoting the formation of bright white emulsion and E, denoting that poor emulsion or even no emulsion was formed.

Table 2. Oils, surfactants and co-surfactants grouped in different combinations for construction of ternary phase diagrams.

Ternary phase diagram formula	Oil	Surfactant	Co-surfactant
P1	Capryol PGMC	Cremophor RH 40	Transcutol HP
P2	Capryol PGMC	Cremophor EL	Transcutol HP
P3	Capryol PGMC	Tween 80	Transcutol HP
P4	Capryol 90	Cremophor RH 40	Transcutol HP
P5	Capryol 90	Cremophor EL	Transcutol HP
P6	Lauroglycol FCC	Cremophor EL	Transcutol HP
P7	Lauroglycol FCC	Tween 80	Transcutol HP
P8	Maisine 35-1	Cremophor RH 40	Transcutol HP

more turbid diluted systems upon increasing the surfactant concentration to a certain extent was observed in phase diagrams P2, P3, and P7 (Figures 4 and 5), where similar trends were reported in studies for various self-emulsifying systems (Kommuru et al., 2001; Wang et al., 2009; Parmar et al., 2011). This phenomenon could be attributed to the interfacial disruption elicited by enhanced water penetration into the oil droplets mediated by the increased surfactant concentration and leading to ejection of oil droplets into the aqueous phase (Pouton, 1997).

Ternary phase diagrams also corroborated the effect of co-surfactant on the nanoemulsifying area. SNEDDS were easily obtained, using the proper ratio and kind of surfactant and co-surfactant as it was reported that the development of a successful self-emulsifying formulation requires a right blend of low and high HLB surfactant necessary for the formation of a stable microemulsion (Craig et al., 1995; Pouton, 2000). Therefore, using a high HLB surfactant; Cremophor® EL (with an average HLB of 13), Cremophor® RH 40, or Tween® 80 (with average HLB of 15), with a low HLB co-surfactant; Transcutol® HP (with an average HLB of 4.2), have proven to give successful self-nanoemulsifying formulations. Furthermore, co-surfactant (Transcutol® HP) was likely to increase interfacial fluidity of surfactant boundaries in the micelles by penetrating into the surfactant film creating void space among surfactant molecules (Constantinides and Scalart, 1997).

Finally, from the results observed during construction of the ternary phase diagrams that were discussed earlier, it was concluded that:

(1) Optimum self-nanoemulsifying and self-microemulsifying performance of ternary formulae (oil, surfactant, and co-surfactant) require the employment of surfactants with high HLB values and oils with high polarity and relatively short hydrophobic chain length, provided that the employed oil and surfactant possess a high lipid-surfactant affinity towards each other.
(2) Increasing the oil content in the formed systems results in decreasing the self-nanoemulsifying and self-microemulsifying efficiency of the systems (oil concentration > 40% resulted in turbid and crude emulsions), while in most cases, increasing the surfactant content increased the clarity of the produced emulsion.
(3) Using a high HLB surfactant with a low HLB co-surfactant in proper ratio, have proven to give successful self-nanoemulsifying formulations.

From each constructed phase diagram, SNEDDS or type (A) systems were identified and selected for further investigation.

Determination of simvastatin solubility in different SNEDDS

Simvastatin-loaded SNEDDS should have stability such that it does not undergo precipitation, creaming or cracking upon dilution. However, in many cases, drug tends to precipitate from the formed nanoemulsion; seed crystals start to appear and might grow to large crystalline materials that will precipitate out at the bottom of the vessel (Parmar et al., 2011). Whether nucleation and crystallization would subsequently occur or not in such a system depends on relative levels of drug solubilized versus its saturation concentration in the system (Narang et al., 2007).

Therefore, simvastatin concentration in the prepared systems should be much less than the saturation concentration of simvastatin in these systems. Accordingly, a fixed simvastatin concentration (5% w/w) was selected to be loaded on all type (A) systems as this concentration was less than the minimal simvastatin saturated solubility observed for type (A) systems (approximately 6.5% w/w) (results not shown) and was expected to provide spontaneous emulsification of SNEDDS with lower possibility of drug precipitation upon aqueous dilution. Using fixed simvastatin concentration for all systems was proposed to exclude the effect of varying the drug concentration on the self-emulsifying efficiency of the systems.

It was also noticed that, when simvastatin was used in concentrations above 5% w/w, mixtures showed a bluish white appearance or even phase separation upon aqueous dilution. This observation agreed with the earlier investigations reported by Wang et al. (2009) who have concluded that above specific drug concentration, the nanoemulsion displays a notable increase in droplet size. It has been also suggested that at high drug concentrations, there is a possibility of precipitation of drug particles in the oil in water interface, where these precipitated drug particles could reduce the flexibility of the surfactant film (Park and Kim, 1999) and result in more compact interfacial films hindering the spontaneous emulsification of SNEDDS (Wang et al., 2009). Therefore, systems formulated to have drug solubilization capacity much higher than the required optimum concentration would be expected to show the least propensity for precipitation (Narang et al., 2007).

Characterization of simvastatin loaded SNEDDS

Droplet size analysis

The droplet size is a crucial factor in self-emulsification performance, because it predicts the rate and extent of drug release as well as *in vivo* absorption (Constantinides et al., 1994). The smaller droplet size permits a faster release rate and provides a larger interfacial surface area for drug absorption (Liu et al., 2009).

Table 3 shows the z-average diameter and polydispersity index (PDI) of various emulsions generated from simvastatin-loaded SNEDDS (drug-loaded type (A) systems) from the eight studied formulae (P1 to P8).

Table 3. Ternary composition (%w/w), z-average (Z-av) and polydispersity index (PDI) of simvastatin (5% w/w) loaded type (A) systems for ternary formulae (P1 to P8).

Parameter		Type (A) systems loaded with 5% w/w simvastatin *																
		S1	**S2**	**S3**	**S4**	**S5**	**S6**	**S7**	**S8**	**S9**	**S10**	**S11**	**S12**	**S13**	**S14**	**S17**	**S18**	**S19**
Oil (% w/w)		10	10	10	10	10	10	10	10	20	20	20	20	20	20	30	30	30
SAA (% w/w)		80	70	60	50	40	30	20	10	70	60	50	40	30	20	50	40	30
Co-SAA (% w/w)		10	20	30	40	50	60	70	80	10	20	30	40	50	60	20	30	40
P1	Z-av (d. nm)	15.07	15.43	15.84	15.84	20.69	18.20	—	—	31.63	29.96	29.24	22.67	22.59	—	—	—	—
	PDI	0.050	0.065	0.171	0.049	0.235	0.075	—	—	0.655	0.583	0.532	0.217	0.037	—	—	—	—
P2	Z-av (d. nm)	31.00	37.14	37.55	62.13	86.89	115.80	94.06	86.88	—	—	—	142.00	80.48	52.49	—	—	—
	PDI	0.663	0.614	0.757	0.489	0.410	0.472	0.414	0.193	—	—	—	0.409	0.290	0.110	—	—	—
P3	Z-av (d. nm)	61.85	66.17	67.94	78.49	104.40	**	**	—	—	118.90	87.63	60.35	—	—	—	—	—
	PDI	0.538	0.536	0.491	0.452	0.435	**	**	—	—	0.622	0.639	0.593	—	—	—	—	—
P4	Z-av (d. nm)	6.89	7.14	14.48	15.10	17.15	35.01	36.11	123.80	42.06	38.54	33.46	19.76	27.06	33.09	35.63	21.76	25.45
	PDI	0.130	0.070	0.105	0.147	0.282	0.831	0.638	0.392	0.707	0.769	0.780	0.202	0.166	0.410	0.690	0.146	0.078
P5	Z-av (d. nm)	54.51	51.21	59.16	76.98	94.95	151.54	—	—	—	—	—	—	—	—	—	—	—
	PDI	0.415	0.290	0.256	0.280	0.359	0.762	—	—	—	—	—	—	—	—	—	—	—
P6	Z-av (d. nm)	54.19	27.71	26.95	43.40	65.79	99.91	155.10	—	—	—	—	—	—	—	—	—	—
	PDI	0.919	0.564	0.331	0.427	0.286	0.425	0.497	—	—	—	—	—	—	—	—	—	—
P7	Z-av (d. nm)	—	102.70	88.30	97.42	117.20	146.10	149.40	—	—	—	—	157.30	130.60	59.41	—	—	—
	PDI	—	0.445	0.463	0.381	0.228	0.387	0.517	—	—	—	—	0.453	0.562	0.401	—	—	—
P8	Z-av (d. nm)	16.08	16.19	16.39	17.02	26.37	53.47	141.10	—	—	—	—	—	—	—	—	—	—
	PDI	0.091	0.044	0.047	0.033	0.328	0.381	0.459	—	—	—	—	—	—	—	—	—	—

Surfactant is denoted as SAA, and Co-surfactant is denoted as Co-SAA. *For each formula (P1 to P8), systems whose z-average and PDI are represented as (—) were not type (A) systems, and those represented as (**) showed phase separation and were not able to be examined.

The relationship between HLBmix and the droplet size of the generated emulsions at different oil concentrations: For each formula, there is an optimum HLBmix value of the surfactant/co-surfactant mixtures that should be achieved to obtain nanoemulsions with the smallest droplet size (Wang et al., 2009). Accordingly, proper ratio of surfactant and co-surfactant results in production of formulation in nano-range droplet size (Taha et al., 2004).

The HLBmix values of the surfactant/co-surfactant mixtures could be calculated from the following equation:

$$HLBmix = f_A HLB_A + f_B HLB_B \quad (3)$$

where HLB_A, HLB_B are the HLB values and f_A, f_B are the weight fractions of surfactant and co-surfactant, respectively. This equation shows that the increase in HLBmix was due to the increase in surfactant (high HLB) concentration with simultaneous decrease in co-surfactant (low HLB) concentration.

Figure 6a and b depicts the relationship between the HLBmix and the z-average diameters of the emulsions generated after dilution of simvastatin-loaded type (A) systems. From Figure 6a, it is clear that, at 10% w/w oil, increasing HLBmix in different SNEDDS formulae decreased the z-average diameter of emulsion formed. However, increasing HLBmix above the value of 10 with ternary formulae P6 and P7 containing Lauroglycol™ FCC (oil), cause a slight increase in the z-average diameter. The decrease in droplet size may be the result of more surfactant being available for adsorption and the formation of a more closely packed surfactant film at the oil–water interface, thereby providing stable and condense interfacial film (Zhao et al., 2010; Gupta et al., 2011), as well as the decrease interfacial tension in the system, both of which in favor of the formation of nanoemulsions with smaller droplet size (Wang et al., 2009; Cui et al., 2011). This decrease in droplet size could be also attributed to the decrease in co-surfactant concentration with subsequent decrease in the expansion of the interfacial film supported by the presence of co-surfactant (Gao et al., 1998).

On the other hand, it is clear from Figure 6b that, systems with higher oil content (20 or 30% w/w) exhibited a very different pattern. Where, an increase in z-average diameter was observed with the increase of HLBmix. Similar trends of increasing the emulsion droplet size with increasing the surfactant concentration were reported in studies for various self-emulsifying systems (Kommuru et al., 2001; Wang et al., 2009; Parmar et al., 2011). This could be attributed to that in the presence of this relatively higher oil content, the decrease of co-surfactant ratio increased the bending stress and rigidity of interface and decreased the flexibility of the interfacial film thus lost its ability to take up different curvatures required to form nanoemulsion (Eccleston, 1994; Kawakami et al., 2002), resulting in emulsions with larger droplet size.

These results inferred an important influence of the HLBmix values and the relative proportion of surfactant to co-surfactant on the droplet size of nanoemulsions generated from drug-loaded SNEDDS. However, from the results depicted in Figure 6a and b, it was observed that both the decrease and the increase in z-average diameter (at 10% w/w oil and at 20 to30% w/w oil, respectively) were much less prominent with increasing Cremophor® RH 40 in formulae (P1, P4, and P8) compared to increasing Cremophor® EL in formulae (P2, P5, and P6) or Tween® 80 in formulae (P3 and P7).

Effect of surfactants and oils structures on the droplet size of the generated emulsions: Selection of surfactant based on their structural features over the HLB has also been a subject of discussion. Wang et al. (2009) observed that surfactant molecular structure had a significant effect on the final emulsion droplet size. This observation is in line with the investigations reported by Dai et al. (1997), Malcolmson et al. (1998) and Warisnoicharoen et al. (2000).

From Figure 6a and b, it was also observed that, apart from the effect of HLB value on the droplet size of the formulation, there is a significant difference ($p < 0.05$) in the emulsion droplet size as a function of surfactant molecular structure. Nanoemulsions with the smallest droplet size were prepared from systems of ternary formulae (P1, P4, and P8); containing Cremophor® RH 40 surfactant, while those with the largest droplet sizes were prepared from systems of ternary formulae (P3 and P7); containing Tween® 80 surfactant even though both surfactants possess the same HLB value. Such small droplet size observed for systems containing Cremophor® RH 40 surfactant may be due to the proper arrangement of co-surfactants specifically along with Cremophor® RH 40 in mixed film around oil–water interface which, in turn, is dependent on molecular structure of both surfactant and co-surfactant (Nepal et al., 2010). It was reported that, effective arrangement of co-surfactant in the films would bring marked reduction in interfacial tension and emulsion droplet size (Nepal et al., 2010). Also, it was observed that ternary formulae containing Cremophor® RH 40 surfactant were able to generate nanoemulsions with almost invariable z-average values over a wide range of HLBmix values and surfactant concentrations (Table 3 and Figure 6a and b).

It was reported that the nature of the oil affects emulsion properties as well (Wang et al., 2009). In this study, although Maisine™ 35-1 (C_{18} glycerol monolinoleate, HLB 4) is less polar compared to other used oils, however, it was able to give nanoemulsions with small droplet size in combination with Cremophor® RH 40 (ternary formula P8). This could be attributed to the presence of unsaturated linoleic acid backbone (two double bonds), as it was reported that lipids with unsaturated chain would increase the fluidity of surfactant film, and reduce the tendency for chance to crystallize or form liquid crystalline mesophases (Trotta et al., 1999).

Stability of diluted systems

SNEDDS possess the risk of *in vivo* drug precipitation upon dilution in GIT which can lead to failure in bioavailability enhancement (Narang et al., 2007). Moreover, the two phases of the formed nanoemulsion have a tendency for separation to reduce the interfacial area, and hence, free energy of the system (Craig et al., 1995). Hence, stability of the drug loaded SNEDDS was evaluated by keeping it under visual inspection for 12 h after aqueous dilution (200 folds with SGF, pH 1.2) for

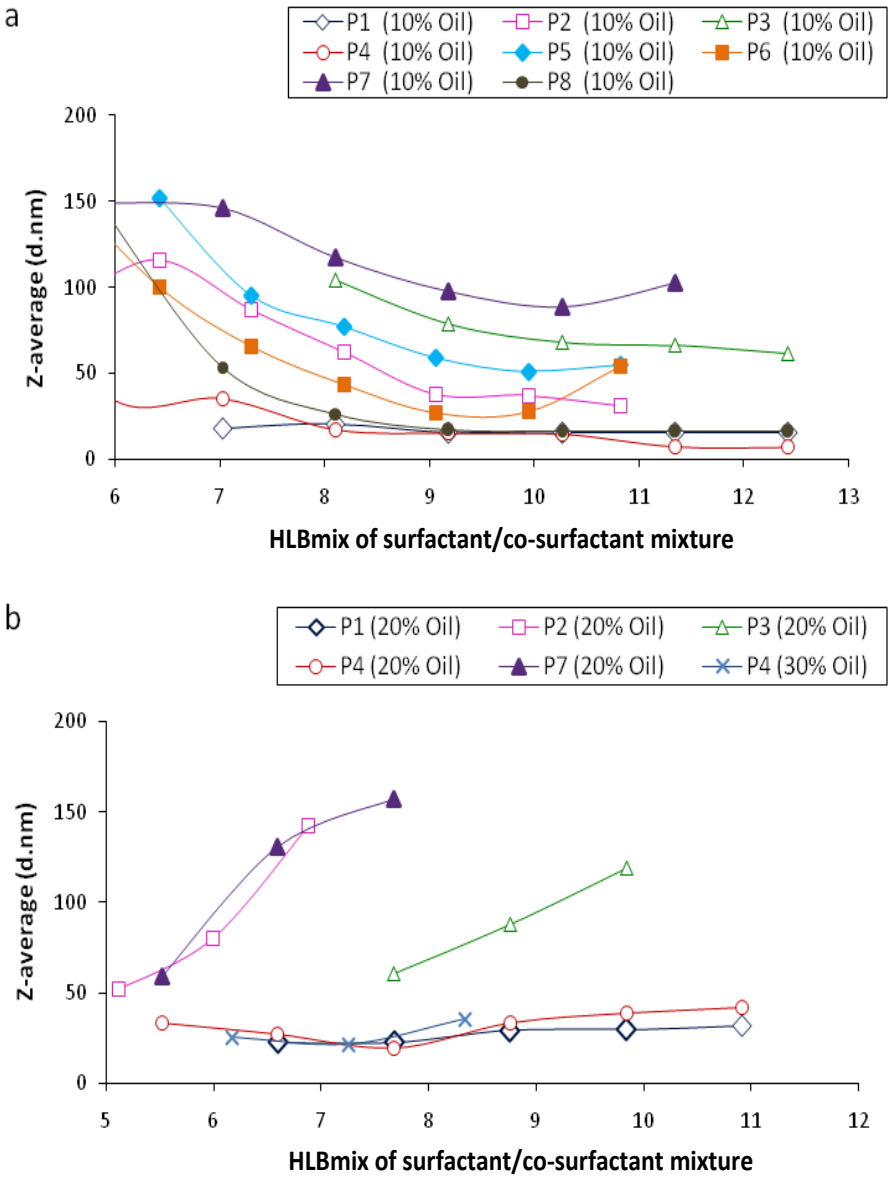

Figure 6. Z-average of diluted SNEDDS (200-folds with SGF, pH 1.2) from formulae (P1-P8), as a function of HLB of surfactant/co-surfactant mixture for each simvastatin (5% w/w) loaded SNEDDS: (a) for systems containing 10% oil and (b) for systems containing 20 and 30% oil.

detection of any drug precipitation, phase separation or cracking. It was observed that, systems with surfactant concentration less than 40% were unable to give stable nanoemulsions over the period of 12 h.

Rational of selecting SNEDDS to be formulated as self-nanoemulsifying tablets

Selection of different SNEDDS formulations from different ternary formulae was based on the following criteria:

1) SNEDDS from ternary formulae (P1, P4, and P8) containing Cremophor® RH 40 surfactant were provoked to be selected due to the preferential properties of Cremophor® RH 40 including that: (a) Cremophor® RH 40 exhibited the highest self-nanoemulsification efficiency and the smallest nanoemulsion droplet size throughout this study. Also, the change in Cremophor® RH 40 concentration had insignificant effect on the droplet size of the generated nanoemulsion over a wide range of surfactant concentration; (b) The use of Cremophor® RH 40 (polyoxy 40 hydrogenated castor oil) for oral ingestion appeared to be advantageous as it was reported that Cremophor® RH 40 is less readily digested and hydrolyzed, thus, masking the approach of pancreatic

Table 4. Composition of systems selected to be formulated as self-nanoemulsifying tablets.

SNEDDS[a]	Composition (% w/w)				
	Oil			Surfactant	Co-surfactant
	Capryol PGMC	Capryol 90	Maisine 35-1	Cremophor RH 40	Transcutol HP
P1-S3	10	—	—	60	30
P1-S12	20	—	—	40	40
P4-S3	—	10	—	60	30
P4-S12	—	20	—	40	40
P4-S18	—	30	—	40	30
P8-S3	—	—	10	60	30

[a]SNEDDS are denoted as (Ternary formula symbol – System symbol).

enzymes and preventing drug precipitation and decreased solubilization. This effect may be attributed to the low reactivity of the saturated backbone of Cremophor® RH 40, the high polyethylene oxide content, and the low residual of digestible glycerides content (Elnaggar et al., 2009); (c) This surfactant was supposed to increase lipophilic drug bioavailability not only via solubilization theory but also due to bioactive respects. It is a known inhibitor of cytochrome-3A (CYP3A) (Elnaggar et al., 2009), the enzyme incorporated in dimensioned bioavailability of many drug substrates, including simvastatin (De Angelis, 2004); (d) Cremophor® RH 40 was reported to have a role in improving bioavailability of some drugs formulated as self-emulsifying formulations, such as atorvastatin (Shen and Zhong, 2006), probucol (Nielsen et al., 2008) and tamoxifen citrate (Elnaggar et al., 2009), and was utilized in one of the few marketed SNEDDS products; Neoral® (Elnaggar et al., 2009).

2) Generated nanoemulsions from diluted simvastatin loaded SNEDDS should have z-average diameter less than 50 nm and polydispersity index (PDI) in the range of 0.25 ± 0.05 which indicates that the system had narrow size distribution. It was reported that a poor formulation can be distinguished from an adequate formulation by determining PDI (Pouton and Porter, 2008).

3) The surfactant concentration should range between 40% and 60% (w/w) as it was reported that surfactant concentration (30 to 60%) are necessary to form stable SNEDD (Neslihan Gursoy and Benita, 2004; Tang et al., 2008) and as observed in this study, systems with surfactant concentration less than 40% were unstable over 12 h period after dilution.

4) Surfactant to co-surfactant ratios of 2:1 and 1:1 were selected as these ratios were reported to be optimal and found to yield the desired SNEDDS in previous studied (Taha et al., 2004; Zhang et al., 2008). System P4-S18 (oil: surfactant: co-surfactant, of ratio 30:40:30) was also selected for comparative aspects.

5) Systems should be stable and still have the required properties when the formed quantity was scaled up.

Accordingly, six different simvastatin-loaded SNEDDS as shown in Table 4 were found to match these criteria and were selected for further studies.

Evaluation of self-nanoemulsifying tablets

Content uniformity

In this study, a dose of 5 mg simvastatin per tablet was selected for formulating the self-nanoemulsifying tablets. The rational for using such a low dose was the possible higher bioavailability expected by these self-nanoemulsifying formulations (Kang et al., 2004).

It was observable that all tablet formulae complied with the test of simvastatin content uniformity according to the United States Pharmacopoeia, where none of the individual tablets is outside limits of 90 to 110% of the labeled amount of simvastatin (5 mg per tablet) (USP, 2006). It was claimed that usually the processes involved adsorption of liquid formulation onto carriers give uniform drug distribution; therefore, promote good content uniformity (Fahmy and Kassem, 2008). It was also observed that, there was no distinct difference in drug content uniformity between self-nanoemulsifying tablets and direct compression tablets (DCT) observed in this study.

Reconstitution properties (droplet size analysis)

Self-nanoemulsification efficiency of prepared tablets was estimated by determining the droplet size distribution of emulsions generated after tablet reconstitution in SGF (pH 1.2). The *z*-average diameters and PDI of the diluted liquid SNEDDS and reconstituted tablets are presented in Table 5 which reveals that all self-nanoemulsifying tablets were able to generate nanoemulsions in an acceptable droplet size range (<50 nm). As shown in Table 5 and Figure 7, there was no significant difference ($p > 0.05$) between droplet sizes of nanoemulsions generated from P4-S3 (14.48 nm) liquid SNEDDS and those generated from their corresponding tablet formulations SNT-14 (15.80 nm), also the difference between droplet sizes of nanoemlsions generated from P1-S3 (15.84 nm) liquid SNEDDS and those generated from their corresponding tablet formulations SNT-4 (22.08 nm) was small compared to other formulations. In addition, their low PDI values indicated uniform droplet size distribution of the

Table 5. Z-average (mean emulsion droplet size) and polydispersity index (PDI) of diluted liquid SNEDDS and their corresponding reconstituted self-nanoemulsifying tablets.

Liquid SNEDDS	P1-S3	P1-S12	P4-S3	P4-S12	P4-S18	P8-S3
Z- average (d nm)	15.84	22.67	14.48	19.76	21.76	16.39
PDI	0.171	0.217	0.105	0.202	0.146	0.047
Self-nanoemulsifying tablets	**SNT-4**	**SNT-9**	**SNT-14**	**SNT-19**	**SNT-24**	**SNT-29**
Z- average (d nm)	22.08	62.36	15.80	53.27	45.96	39.58
PDI	0.377	0.487	0.198	0.577	0.561	0.557

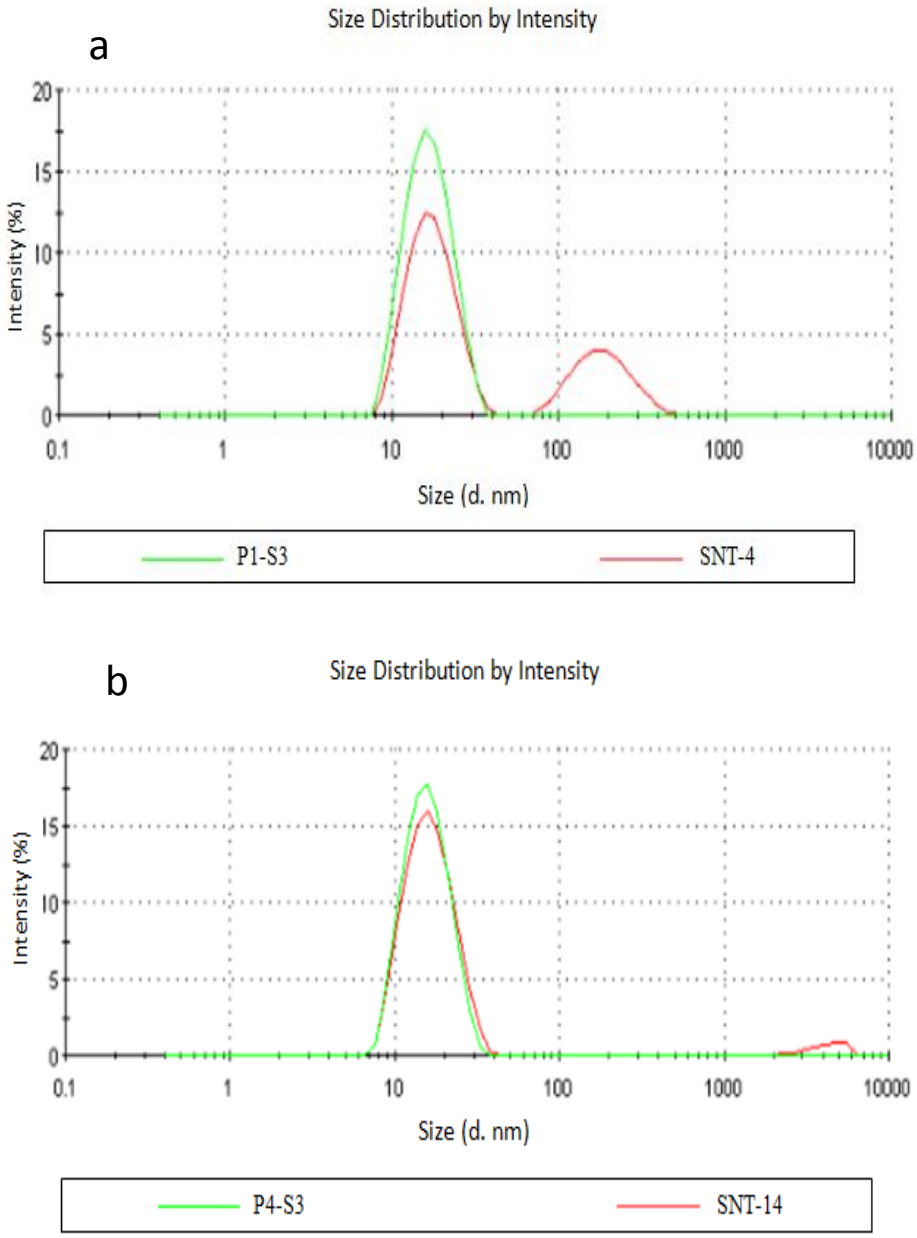

Figure 7. Droplet size distribution of nanoemulsions generated from: (a) dilution of liquid P1-S3 SNEDDS and reconstitution of SNT-4 tablet; (b) dilution of liquid P4-S3 SNEDDS and reconstitution of SNT-14 tablet measured using (Zetasizer Nano-ZS).

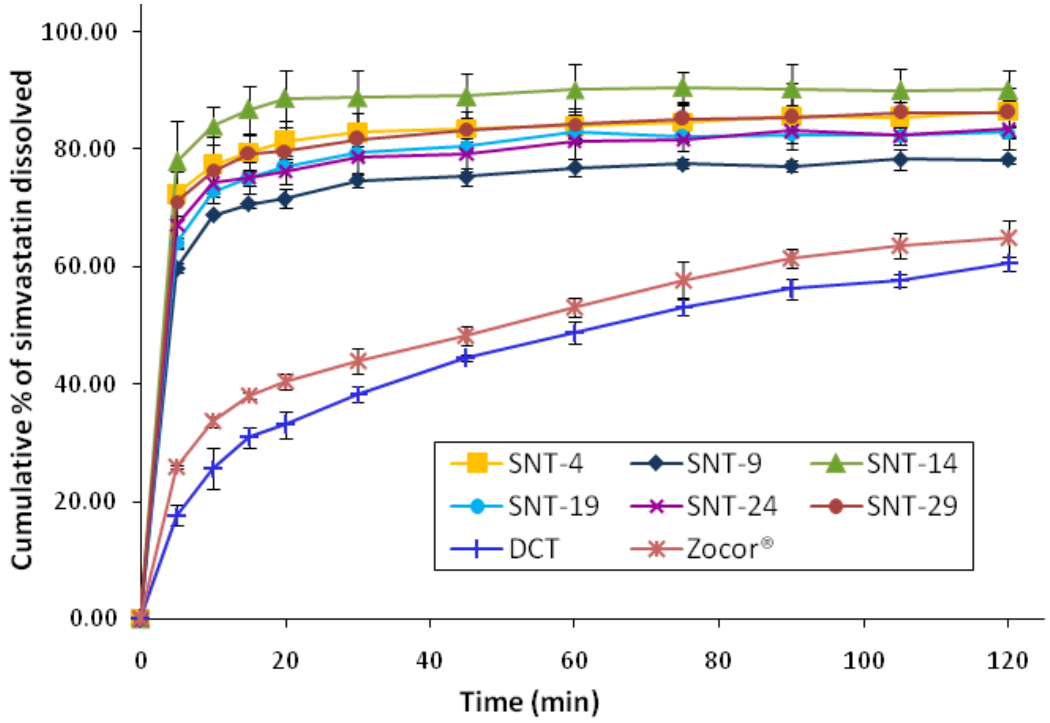

Figure 8. Dissolution profiles of simvastatin from different liquisolid tablets, DCT, and marketed tablets in SGF (pH 1.2). Data are expressed as mean ± SD (n = 3).

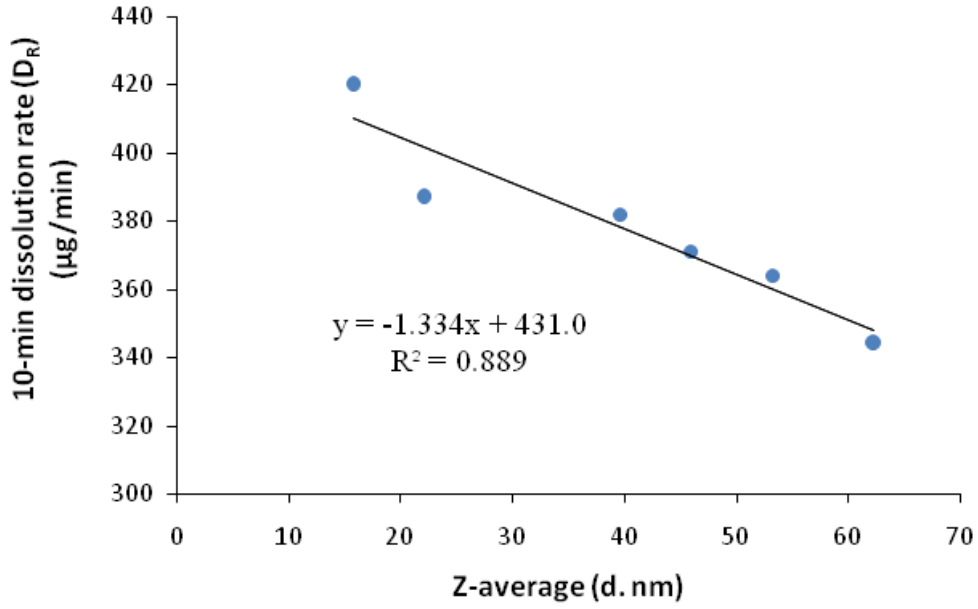

Figure 9. Correlation between z-average of generated nanoemlsions after reconstitution of self-nanoemulsifying tablets and the 10-min dissolution rate of simvastatin from these tablets.

nanoemulsions generated from reconstitution of these tablets. Form these results; it was clear that the self-nanoemulsifying tablets SNT-4 and SNT-14 were able to preserve the good self-nanoemulsifying efficiency of their loaded liquid SNEDDS. This could be probably attributed to the low oil content (10%), high surfactant content (60%), and surfactant to co-surfactant ratio (2:1) of the loaded liquid SNEDDS, as well as the nature of their oils content (Capryol™ PGMC and Capryol™ 90) that possess high polarity and relatively short hydrophobic

chain length (C_8). Therefore, these SNEDDS have proven to be able to retain their self-nanoemulsification properties irrespective of physical form change compared to other liquid SNEDDS due to their optimized properties.

In vitro dissolution test

The dissolution profiles of different simvastatin self-nanoemulsifying tablets together with the dissolution profile of simvastatin directly compressed tablets (DCT), and that of simvastatin marketed tablets (Zocor®) are presented in Figure 8. Simulated gastric fluid without pepsin (SGF, pH 1.2) was chosen as a dissolution medium to eliminate the possibility of partial conversion of simvastatin into the more soluble open-ring form that may occur at high pH (Margulis-Goshen and Magdassi, 2009). Also, no dissolution-accelerating components or surfactants, such as sodium lauryl sulfate, were added to the media, because these components result in failure to discriminate between different dissolution profiles as the surfactant is the key element in improving dissolution of SEDDS dosage forms (Atef and Belmonte, 2008; Margulis-Goshen and Magdassi, 2009).

Figure 8 signifies that dissolution profiles of simvastatin from self-nanoemulsifying tablets produced constantly superior drug dissolution rate ($p < 0.01$) compared to that of DCT and that of marketed tablets (Zocor®). Within 10 min, only 26 ± 3 and 33 ± 1% of simvastatin was dissolved from DCT and marketed tablets, respectively; however, simvastatin dissolved from self-nanoemulsifying tablets within the same time period reached 84 ± 3% for SNT-14 tablets. This enhancement in simvastatin dissolution rate and extent could be attributed to the formation of nanoemulsion during dissolution process with droplet size in submicron range induced the presentation of simvastatin at a molecular level in the form of nanoemulsion which lead to an increased solubilization and enhanced drug dissolution rate and extent. However, the comparatively slow simvastatin dissolution from DCT and the marketed tablets can mainly be explained by the poor water solubility of the drug (Dixit and Nagarsenker, 2008; Balakrishnan et al., 2009). This finding also supported the hypothesis that nano-sized droplets of emulsion can enhance the release of poorly soluble drugs (Ghai and Sinha, 2011). Also, as shown in Figure 9, there was a good correlation between z-average of generated nanoemulsions after reconstitution of self-nanoemulsifying tablets and the 10-min dissolution rate of simvastatin from these self-nanoemulsifying tablets (R^2 = 0.889, slop = -1.334). This indicates that the amount of drug dissolved in the aqueous phase at time *t*, is inversely proportional to the droplet size of the generated nanoemulsions after tablet reconstitution (Atef and Belmonte, 2008). Thus, this rapid drug release was promoted by the larger interfacial areas present in emulsions with smaller drops (Wang et al., 2009).

Conclusion

In this study, formulation factors had a distinct influence on the mean droplet size of nanoemulsions generated from SNEDDS upon dilution. Cremophore® RH 40 (surfactant) and Transcutol® HP (co-surfactant) have proven to acquire excellent self-nanoemulsifying efficiency. Oil concentration had a great influence on the pattern by which the surfactant and co-surfactant concentrations affect the droplet size of generated nanoemulsions. In addition, self-nanoemulsifying tablets were able to successfully introduce the SNEDDS into the dissolution media where it was efficiently transformed into nanoemulsion by the gentle agitation provided in the dissolution experiment. Prepared self-nanoemulsifying tablets demonstrated significantly higher dissolution rates, compared to DCT and marketed tablets (Zocor®) and expected to increase simvastatin bioavailability. SNEDDS with low oil content (10%), high surfactant content (60%), and surfactant to co-surfactant ratio (2:1), and with relatively polar and short hydrophobic chain length of oils content (C_8) were able to retain their self-nanoemulsification properties irrespective of physical form change (either liquid or tableted form).

ACKNOWLEDGEMENT

This research project was supported by a grant from the "Research Center of the Center for Female Scientific and Medical Colleges", Deanship of Scientific Research, King Saud University.

ABBREVIATIONS

d. nm, Diameter in nanometer; **DCT,** directly compressed tablets; **DLS,** dynamic light scattering; **PDI,** polydispersity index; **SEDDS,** self-emulsifying drug delivery systems; **SNEDDS,** self-nanoemulsifying drug delivery systems; **SNT,** self-nanoemulsifying tablet formula; **Z-av,** z-average (cumulants mean droplet size).

REFERENCES

Ambike AA, Mahadik KR, Paradkar A (2005). Spray-dried amorphous solid dispersions of simvastatin, a low tg drug: in vitro and in vivo evaluations. Pharm. Res. 22:990-998.

Ammar HO, Salama HA, Ghorab M, Mahmoud AA (2006). Implication of inclusion complexation of glimepiride in cyclodextrin–polymer systems on its dissolution, stability and therapeutic efficacy. Int. J. Pharm. 320:53-57.

Araya H, Tomita M, Hayashi M (2005). The novel formulation design of O/W microemulsion for improving the gastrointestinal absorption of poorly water soluble compounds. Int. J. Pharm. 305:61-74.

Atef E, Belmonte AA (2008). Formulation and *in vitro* and *in vivo* characterization of a phenytoin self-emulsifying drug delivery system (SEDDS). Eur. J. Pharm. Sci. 35:257-263.

Balakrishnan P, Lee BJ, Oh DH, Kim JO, Hong MJ, Jee JP, Kim JA, Yoo BK, Woo JS, Yong CS, Choi HG (2009). Enhanced oral

bioavailability of dexibuprofen by a novel solid self-emulsifying drug delivery system (SEDDS). Eur. J. Pharm. Biopharm. 72:539-545.
Basalious EB, Shawky N, Badr-Eldin SM (2010). SNEDDS containing bioenhancers for improvement of dissolution and oral absorption of lacidipine. I: development and optimization. Int. J. Pharm. 391:203-211.
Carlucci G, Mazzeo P, Biordi L, Bologna M, (1992). Simultaneous determination of simvastatin and its hydroxy acid form in human plasma by high-performance liquid chromatography with UV detection. J. Pharm. Biomed. Anal. 10:693-697.
Chen ML (2008). Lipid excipients and delivery systems for pharmaceutical development: a regulatory perspective. Adv. Drug Deliv. Rev. 60:768-777.
Constantinides PP, Scalart JP (1997). Formulation and physical characterization of water-in-oil microemulsions containing long- versus medium-chain glycerides. Int. J. Pharm. 158:57-68.
Constantinides PP, Scalart JP, Lancaster C, Marcello J, Marks G, Ellens H, Smith PL (1994). Formulation and intestinal absorption enhancement evaluation of water-in-oil microemulsions incorporating medium-chain glycerides. Pharm Res. 11:1385-1390.
Craig DQM, Barker SA, Banning D, Booth SW (1995). An investigation into the mechanisms of self-emulsification using particle size analysis and low frequency dielectric spectroscopy. Int. J. Pharm. 114:103-110.
Cui Y, Li L, Gu J, Zhang T, Zhang L (2011). Investigation of microemulsion system for transdermal delivery of ligustrazine phosphate. Afr. J. Pharm. Pharmacol. 5:1674-1681.
Dai L, Li W, Hou X (1997). Effect of the molecular structure of mixed nonionic surfactants on the temperature of miniemulsion formation. Colloids Surf. A Physicochem. Eng. Asp. 125:27-32.
Date AA, Nagarsenker MS (2007). Design and evaluation of self-nanoemulsifying drug delivery systems (SNEDDS) for cefpodoxime proxetil. Int. J. Pharm. 329:166-172.
De Angelis G (2004). The influence of statin characteristics on their safety and tolerability. Int. J. Clin. Pract. 58:945-955.
Dixit RP, Nagarsenker MS (2008). Self-nanoemulsifying granules of ezetimibe: design, optimization and evaluation. Eur. J. Pharm. Sci. 35:183-192.
Eccleston J (1994). Microemulsions. In: Swarbrick J, Boylan JC (eds.), Encyclopedia of pharmaceutical technology. Marcel Dekker, New york, pp 375-421.
Elnaggar YS, El-Massik MA, Abdallah OY, (2009). Self-nanoemulsifying drug delivery systems of tamoxifen citrate: design and optimization. Int. J. Pharm. 380:133-141.
Fahmy RH, Kassem MA (2008). Enhancement of famotidine dissolution rate through liquisolid tablets formulation: in vitro and in vivo evaluation. Eur. J. Pharm. Biopharm. 69:993-1003.
Gao ZG, Choi HG, Shin HJ, Park KM, Lim SJ, Hwang KJ, Kim CK (1998). Physicochemical characterization and evaluation of a microemulsion system for oral delivery of cyclosporin A. Int. J. Pharm. 161:75-86.
Ghai D, Sinha VR (2011). Nanoemulsions as self-emulsified drug delivery carriers for enhanced permeability of the poorly water-soluble selective β1-adrenoreceptor blocker Talinolol. Nanomedicine 8(5):618-626
Gupta S, Chavhan S, Sawant KK (2011). Self-nanoemulsifying drug delivery system for adefovir dipivoxil: Design, characterization, in vitro and ex vivo evaluation. Colloids and Surfaces A: Physicochemical and Engineering Aspects. 392:145-155.
Hauss DJ, (2007). Oral lipid-based formulations. Adv. Drug Deliv. Rev. 59:667-676.
Hong JY, Kim JK, Song YK, Park JS, Kim CK, (2006). A new self-emulsifying formulation of itraconazole with improved dissolution and oral absorption. J. Control Release. 110:332-338.
Kang BK, Lee JS, Chon SK, Jeong SY, Yuk SH, Khang G, Lee HB, Cho SH (2004). Development of self-microemulsifying drug delivery systems (SMEDDS) for oral bioavailability enhancement of simvastatin in beagle dogs. Int. J. Pharm. 274:65-73.
Kawakami K, Yoshikawa T, Moroto Y, Kanaoka E, Takahashi K, Nishihara Y, Masuda K (2002). Microemulsion formulation for enhanced absorption of poorly soluble drugs. I. Prescription design. J. Control Release 81:65-74.
Khoo SM, Humberstone AJ, Porter CJH, Edwards GA, Charman WN (1998). Formulation design and bioavailability assessment of lipidic self-emulsifying formulations of halofantrine. Int. J. Pharm. 167:155-164.
Kommuru TR, Gurley B, Khan MA, Reddy IK (2001). Self-emulsifying drug delivery systems (SEDDS) of coenzyme Q10: formulation development and bioavailability assessment. Int. J. Pharm. 12:233-246.
Levy MY, Benita S, (1990). Drug release from submicronized o/w emulsion: a new in vitro kinetic evaluation model. Int. J. Pharm. 66:29-37.
Lin Y, Cai M, Lin Y, Teng H, (2012). Combination therapy with simvastatin and xuezhikang improves the lipid-lowering efficacy in hyperlipidemic rats. Afr. J. Pharm. Pharmacol. 6:2318-2321.
Liu Y, Zhang P, Feng N, Zhang X, Wu S, Zhao J (2009). Optimization and in situ intestinal absorption of self-microemulsifying drug delivery system of oridonin. Int. J. Pharm. 365:136-142.
Mahmoud EA, Bendas ER, Mohamed MI (2009). Preparation and evaluation of self-nanoemulsifying tablets of carvedilol. AAPS Pharm. Sci. Tech. 10:183-192.
Malcolmson C, Satra C, Kantaria S, Sidhu A, Lawrence MJ (1998). Effect of oil on the level of solubilization of testosterone propionate into nonionic oil-in-water microemulsions. J. Pharm. Sci. 87:109-116.
Margulis-Goshen K, Magdassi S (2009). Formation of simvastatin nanoparticles from microemulsion. Nanomedicine 5:274-281.
Muhrer G, Meier U, Fusaro F, Albano S, Mazzotti M, (2006). Use of compressed gas precipitation to enhance the dissolution behavior of a poorly water-soluble drug: Generation of drug microparticles and drug–polymer solid dispersions. International Journal of Pharmaceutics. 308:69-83.
Narang AS, Delmarre D, Gao D (2007). Stable drug encapsulation in micelles and microemulsions. Int. J. Pharm. 345:9-25.
Nazzal S, Nutan M, Palamakula A, Shah R, Zaghloul AA, Khan MA (2002). Optimization of a self-nanoemulsified tablet dosage form of Ubiquinone using response surface methodology: effect of formulation ingredients. Int. J. Pharm. 240:103-114.
Nepal PR, Han HK, Choi HK (2010). Preparation and in vitro-in vivo evaluation of Witepsol H35 based self-nanoemulsifying drug delivery systems (SNEDDS) of coenzyme Q(10). Eur. J. Pharm. Sci. 39:224-232.
Neslihan GR, Benita S (2004). Self-emulsifying drug delivery systems (SEDDS) for improved oral delivery of lipophilic drugs. Biomedicine & Pharmacotherapy. 58:173-182.
Nielsen FS, Petersen KB, Mullertz A (2008). Bioavailability of probucol from lipid and surfactant based formulations in minipigs: influence of droplet size and dietary state. Eur. J. Pharm. Biopharm. 69:553-562.
Park KM, Kim CK (1999). Preparation and evaluation of flurbiprofen-loaded microemulsion for parenteral delivery. Int. J. Pharm. 181:173-179.
Parmar N, Singla N, Amin S, Kohli K (2011). Study of cosurfactant effect on nanoemulsifying area and development of lercanidipine loaded (SNEDDS) self nanoemulsifying drug delivery system. Colloids Surf. B Biointerfaces. 86:327-338.
Patel AR, Vavia PR, (2007). Preparation and in vivo evaluation of SMEDDS (self-microemulsifying drug delivery system) containing fenofibrate. AAPS J. 9: E344-352.
Patel RP, Patel MM (2007). Physico-Chemical Characterization & In Vitro Dissolution Behavior of Simvastatin-Cyclodextrin Inclusion Compounds Drug Deliv. Technol. 7:50-56.
Patil P, Patil V, Paradkar A, (2007). Formulation of a self-emulsifying system for oral delivery of simvastatin: in vitro and in vivo evaluation. Acta Pharm. 57:111-122.
Pouton CW (1997). Formulation of self-emulsifying drug delivery systems. Adv. Drug Deliv. Rev. 25:47–58.
Pouton CW (2000). Lipid formulations for oral administration of drugs: non-emulsifying, self-emulsifying and 'self-microemulsifying' drug delivery systems. Eur. J. Pharm. Sci. 11(Suppl 2):S93-S98.
Pouton CW, Porter CJ (2008). Formulation of lipid-based delivery systems for oral administration: materials, methods and strategies. Adv. Drug. Deliv. Rev. 60:625-637.
Rane SS, Anderson BD (2008). What determines drug solubility in lipid vehicles: Is it predictable? Adv. Drug Deliv. Rev. 60:638-656.
Sánchez MC, Berjano M, Guerrero A, Gallegos C (2001). Emulsification

Rheokinetics of Nonionic Surfactant-Stabilized Oil-in-Water Emulsions. Langmuir. 17: 5410-5416.
Schwendener RA, Schott H (1996). Lipophilic 1-beta-d-arabinofuranosyl cytosine derivatives in liposomal formulations for oral and parenteral antileukemic therapy in the murine L1210 leukemia model. J. Cancer Res. Clin. Oncol. 122:723–726.
Serajuddin AT (1999). Solid dispersion of poorly water-soluble drugs: early promises, subsequent problems, and recent breakthroughs. J. Pharm. Sci. 88:1058-1066.
Shafiq S, Shakeel F, Talegaonkar S, Ahmad FJ, Khar RK, Ali M (2007). Development and bioavailability assessment of ramipril nanoemulsion formulation. Eur. J. Pharm. Biopharm. 66:227-243.
Shen H, Zhong M (2006). Preparation and evaluation of self-microemulsifying drug delivery systems (SMEDDS) containing atorvastatin. J. Pharm. Pharmacol. 58:1183-1191.
Singh SK, Verma PR, Razdan B (2010). Development and characterization of a lovastatin-loaded self-microemulsifying drug delivery system. Pharm. Dev. Technol. 15:469-483.
Spireas S, Bolton SM (1999). Liquisolid systems and methods of preparing same. US Patent, No. 5:968, 550.
Taha EI, Al-Saidan S, Samy AM, Khan MA (2004). Preparation and in vitro characterization of self-nanoemulsified drug delivery system (SNEDDS) of all-trans-retinol acetate. Int. J. Pharm. 285:109-119.
Tang B, Cheng G, Gu JC, Xu CH (2008). Development of solid self-emulsifying drug delivery systems: preparation techniques and dosage forms. Drug Discov. Today 13:606-612.
Thomas N, Holm R, Garmer M, Karlsson J, Müllertz A, Rades T (2013). Supersaturated Self-Nanoemulsifying Drug Delivery Systems (Super-SNEDDS) Enhance the Bioavailability of the Poorly Water-Soluble Drug Simvastatin in Dogs. AAPS J. 15:219-227.
Trotta M, Gallarate M, Pattarino F, Carlotti ME (1999). Investigation of the phase behaviour of systems containing lecithin and 2-acyl lysolecithin derivatives. Int. J. Pharm. 190:83-89.
United States Pharmacopeia (2006). In: USP 29, NF 24, Rockville, Maryland, USA.
Villar AMS, Naveros BC, Campmany ACC, Trenchs MA, Rocabert CB, Bellowa LH (2012). Design and optimization of self-nanoemulsifying drug delivery systems (SNEDDS) for enhanced dissolution of gemfibrozil. Int. J. Pharm. 431:161-175.
Wang L, Dong J, Chen J, Eastoe J, Li X, (2009). Design and optimization of a new self-nanoemulsifying drug delivery system. J. Colloid Interface Sci. 330:443-448.
Warisnoicharoen W, Lansley AB, Lawrence MJ (2000). Nonionic oil-in-water microemulsions: the effect of oil type on phase behaviour. Int. J. Pharm. 198:7-27.
Wasan EK, Bartlett K, Gershkovich P, Sivak O, Banno B, Wong Z, Gagnon J, Gates B, Leon CG, Wasan KM (2009). Development and characterization of oral lipid-based Amphotericin B formulations with enhanced drug solubility, stability and antifungal activity in rats infected with *Aspergillus fumigatus* or *Candida albicans*. Int. J. Pharm. 372:76-84.
Wu W, Wang Y, Que L (2006). Enhanced bioavailability of silymarin by self-microemulsifying drug delivery system. Eur. J. Pharm. Biopharm. 63:288-294.
Zhang P, Liu Y, Feng N, Xu J (2008). Preparation and evaluation of self-microemulsifying drug delivery system of oridonin. Int. J. Pharm. 355:269-276.
Zhao Y, Wang C, Chow AHL, Ren K, Gong T, Zhang Z, Zheng Y (2010). Self-nanoemulsifying drug delivery system (SNEDDS) for oral delivery of Zedoary essential oil: Formulation and bioavailability studies. Int. J. Pharm. 383:170-177.

academicJournals

Vol. 7(22), pp. 1501-1511, 15 June, 2013
DOI 10.5897/AJPP2013.3523
ISSN 1996-0816 © 2013 Academic Journals
http://www.academicjournals.org/AJPP

African Journal of Pharmacy and Pharmacology

Full Length Research Paper

Investigation of factors effected dissolution variations of hydroxypropyl methylcellulose capsule

Chuanfeng Tong[1]*, Zhiquan Wang[1], Ya Zhong[1] and Min Zhen[2]

[1]Department of Cardiology, Zhongnan Hospital, Wuhan University, Wuhan 430071, China.
[2]Department of Pharmacology, Medical College, Xianning University, China.

Accepted 10 May, 2013

The objective of this study was to identify if the root cause of dissolution was from the HPMC shell differences and/or the insufficient robustness of dissolution method. Studying the dissolution behavior of 40 and 150 mg granules (with and without shells), followed by capsule dissolution with switched shells, the sink condition can be verified by the extent of granule dissolutions with switch shells. The effect of the apparatus, agitation speed and medium deaeration on dissolution variations was also studied. The surface dissolution behavior for shells with different moisture levels was probed in an aqueous medium utilizing an ActiPix SDI300 surface dissolution imaging system. The inter-vessel variability of 150 mg granules was low, while for 40 mg granules, the inter-vessel variability of the 40 mg granules was slightly higher. Basket method exhibited much slower dissolution and higher percent relative standard deviation (RSD) at early sampling-points when comparing the paddle apparatus. Degassed medium reduced the capsule-to-capsule variations at early sampling-points and improved the dissolution rate. The 40 mg granule with the 150 mg capsule shell had an average dissolution release of 88% at 20 min with 7.4% RSD for n = 6 samples. It was slower and more variable as compared to 96% release with 2.8% RSD from the original 40 mg capsules (40 mg granule in 40 mg capsule shell). Capsules with un-dried shells exhibited a slower and variable dissolution at early sampling-points, whereas a faster and consistent dissolution was obtained for capsules with dried shells. The root cause of the undesirable dissolution variations at early sampling-points and the intermittent failure for stage 1 specification was the higher moisture content in the HPMC shells of the high strength capsules. Insufficient hydrodynamics in dissolution vessels contributed to the intermittent low drug release, higher agitation speed and medium deaeration can improve dissolution rate and reduce dissolution variations for HPMC shells.

Key words: Hypromellose capsule, dissolution, hydrodynamics, medium deaeration.

INTRODUCTION

Hydroxypropyl methylcellulose (HPMC), now commonly known as hypromellose, is produced by synthetic modification of the naturally occurring polymer cellulose and is considered safe for normal consumption in humans. Due to its vegetable source, proof of cross-linking and inherent lower equilibrium moisture content as compared to the gelatin counterpart, the HPMC capsule shells are often used to improve drug product stability (for moisture moisture sensitive drug) and become the second only to gelatin capsules in terms of frequency of usage in pharmaceutical development.

However, the in vitro dissolution method development for HPMC capsules is of challenge as the dissolution performance of HPMC capsules varies from vendor to vendor and from process to process. For example, HPMC capsules made with gellan gum as a gelling aid or

*Corresponding author. E-mail: tongchuanfeng@hotmail.com. Tel: +86 (0)2767813073.

carrageenan as the gelling system have different dissolution rates in the physiological pH range of pH 1.2 to 6.8 (Moawia, 2010). Study has proved that the acid conditions and the presence of potassium cations hindered the opening of $HPMC_{gell}$ (Gellan gum as gelling aid) capsules due to the nature of the gel network that was formed in the presence of cations (Ewart et al., 2004). $HPMC_{carr}$ (carrageenan as gelling aid) solubility on the other hand was independent of pH (Robert et al., 2001). In pH 6.8 buffer, $HPMC_{carr}$ capsule showed significant difference in dissolution release when a potassium phosphate buffer was replaced by a sodium phosphate buffer; however, this effect was absent in the VCaps Plus® HPMC shells which did not use a gelling promoter (Sherry et al., 2010). The HPMC capsule dissolution was prolonged when stored under the high heat and high humidity (Irene et al., 2000). However, this observation was not confirmed in model drugs filled in Quali-V® HPMC capsules stored at 40°C/75% relative humidity for six month (Nagata, 2002).

The *in vitro-in vivo* correlation of HPMC capsule dissolution was also studied and reported in literatures. The HPMC shells made both with and without a gelling agent showed comparable *in vivo* performances in spite of the rupture time differences, demonstrating the rapid dissolution in animal and human pharmacokinetics studies (Sherry et al., 2010). The *in vivo* opening times for HPMC shells were longer than their gelatin counterparts but the differences in the regulatory important pharmacokinetics metrics of maximum observed concentration (Cmax) and area under the curve (AUC) were not significant for a Biopharmaceutical Classification System (BCS) class II compound (Irene et al., 2000). The composition of the dissolution media has been reported to influence the disintegration time of the HPMC capsules; however, the rate of disintegration may not correlate with the drug product *in vivo* bioavailability (Tuleu et al., 2007; El-Malah et al., 2007).

To date, the inconsistent dissolution performance of the HPMC capsules and a lack of understanding of the correlation between the shell properties and shell disintegration/dissolution remain challenges for dissolution scientists. It is advantageous to develop a systematic approach in solving dissolution variations for formulations with HPMC shells and share the knowledge among formulators and dissolution scientists. A highly variable dissolution may cause product to fail quality control (QC) specification and requires stage 2 or 3 test which may not be operational effective. It is desirable that a dissolution method is discriminating yet sufficiently rugged and reproducible for the day-to-day operation (Michael, 2011).

EXPERIMENTAL

Reagents and materials

The low density lipoprotein (LDL) and high density lipoprotein (HDL) capsules under the investigation were made internally by Hekelishi the chemical limited company (Luzhou City, Sichuan province). Drug substance reference standard was qualified and provided by the reference standard material group in Hekelishi the chemical limited company. A concentrated hydrochloride acid was purchased from Urumqi chemical reagent factory (China). Ultra-pure water (Urumqi chemical reagent factory, China) was used for the dissolution medium throughout the analysis. The HPMC capsule shells (Size 1, Lot E0905048N) used in the capsule formulations were purchased from Qualicap®, Inc. 0.01 N HCl was prepared by dissolving 0.85 ml of concentrated hydrochloride acid into each liter of the Mili-Q purified deionized water. Degassed 0.01 N HCl media was prepared by purging the medium with helium.

Equipment

A Leap UV-Fiber Optical OPT-DISS™ Dissolution testing system with a Distek Evolution 6100 dissolution bath was used throughout the study. The dissolution samples were analyzed by using UV detection at 258 nm with a background subtraction wavelength of 300 nm. Six 1-mm and six 10-mm arch™ probes were used aimed at achieving the optimal UV response for *in-situ* dissolution measurement for the HDL and LDL capsules, respectively.

Dissolution testing

The validated dissolution method employed the USP apparatus 2 (paddle) at 75 rpm and1000-ml of 0.01 N HCl as the dissolution medium operated at 37 ± 0.5°C. The *in-situ* dissolution measurement was performed in six vessels simultaneously in 1 min interval by UV-fiber optical probes.

Moisture content determination

A Mettler-Toledo Halogen Moisture Analyzer HR83 was used to determine the moisture content in capsule shells via thermogravimetric measurement. The emptied shells were weighed and heated at 120°C with an infrared radiator (halogen lamp). The moisture content was automatically calculated based on the difference in weight. Eight empty shells were used for each measurement and duplicate measurements were made for each type of the shells.

Surface dissolution characterization

An ActiPix SDI 300 UV area imaging system was used to enable the quantitative imaging of surface erosion and dissolution of HPMC capsule shell in dissolution media. Samples were prepared by pressing a parafilm into a sample cup to form a surface on which the sample can be pressed, followed by cutting a 2.0-mm diameter disc from a shell and pressed onto the parafilm surface in the sample press using 50 cNm torque. After establishing background absorbance at all pixels in the imaged area using appropriate dissolution medium in the flow cell, the sample was inserted into the flow cell and the cell was refilled with the dissolution medium. The flow rate was then increased in steps from 0.3 ml/min for 15 min, stopped for 5 min and followed by 2.0 ml/min for 2 min. A sequence of images was taken during this time using a 254 nm wavelength filter.

RESULTS AND DISCUSSION

Typical dissolution variation of the highly variable batch is

presented in Table 1, 2 and Figure 1. About 10% of the stability samples from this high strength batch encountered the stage 1 dissolution failures in six month test period which either required stage 2 or 3 testing or demanded significant investigation effort. Considering the rapid and consistent dissolution for the low strength batch, formulation variables and dissolution method variables that could contribute to the differences in rate and inter-vessel variability were examined.

A possible variable that could contribute to the slower and variable dissolution of the high strength batch was the lower microcrystalline cellulose (MCC)/drug ratio due to the 75% drug loading in this formulation. On the other hand, the low strength batch has a higher MCC/drug ratio due the 25% drug loading. MCC was used as a filler and also it acted as a disintegrant. The lower MCC/drug ratio would provide less disintegration capacity when inadequate dissolution surface area was presented due to a slow erosion of the capsule shells. The first in human (FIH) batch that exhibited this behavior was a 150 mg capsules formulated with a BCS class III compound as shown in Table 3. It has a 75% drug loading (HDL), contains MCC, silicon dioxide and magnesium stearate as the excipients, and uses Quali-V® HPMC capsule shells. The Quali-V® HPMC capsule shells were selected based on available supply and the consideration of low equilibrium moisture content in capsule shells (4 to 6% as per manufacturer specification) that could prevent the undesirable drug degradation. The other FIH batch (40 mg capsules) that was manufactured at the same time has a 25% drug loading (LDL), and contains the same type of excipients and uses the same lot of the HPMC shells. The HPMC shells used for the 40 mg capsule manufacturing were stored in a package that was previously opened, whereas the shells for the 150 mg capsule batch were acquired from an un-opened package

Effect of the sink condition on the rate and extent of the drug release

The capsule formulations under the investigation contained a BCS class III compound (high solubility and low permeability) with an aqueous solubility of approximately 0.6 g/ml across physiological pH range of 1.2 to 6.8. The validated dissolution method employed a dissolution medium (0.01 N HCl) based on the consideration of the physiological relevance of the medium, the solubility of the active pharmaceutical ingredients (API) as well as the Quali-V® HPMC shell and the stability of the API. Dissolution sink factor for a 150 mg strength in1000 ml of 0.01 N HCl can be obtained by using Equation 1:

$$\text{Sink factor} = V \times C_S / \text{Maximum dissolvable dose}$$

where V is the dissolution medium volume, C_S is the saturated solubility of the compound, maximum dissolved dose is the capsule strength (Cynthia et al., 2004).

The dissolution sink condition is dictated by the solubility of the API and the dissolution volume. For a 150 mg dose, the sink is calculated as 4000, which is significantly higher than the recommended 3 to 10×, which is the volume required to completely solubilize the dose. For the 40 mg strength, the sink factor is 15000, which is approximately four times of that of the 150 mg dose. The effect of the sink on the dissolution rate and extent was accessed by performing dissolution using only stock granulations. Samples from both stock granulations were made by opening and transferring entire content of one capsule into a vessel that contains 1000 ml of 0.01 N HCl. Dissolutions were performed on n = 3 LDL and HDL granulations as per method and the results are plotted in Figure 2. The dissolution release for both granulations was rapid with approximately 95% released in 2 min. The inter-vessel variability of 150 mg granules was low, with a relative standard deviation (RSD) of approximately 1% across all sampling-points. For 40 mg granules, the RSD is approximately 4%. The slightly higher inter-vessel variability of the 40 mg granules was due to a low percent drug release in a 40 mg vessel caused by incomplete emptying of the capsule or lose of the capsule content during sample transferring. When adequate API solubility (sink factor) and the dissolution surface area (without shell) were presented, both granulations exhibited rapid and complete release. On the basis of these results, we concluded that the drug release rate and extent for both granulations are the same. The slower and variable dissolution of the 150 mg capsules was not due to the granules.

Effect of USP apparatus, agitation speed and medium deaeration to dissolution rate and dissolution variations

Factors controlling the dissolution rate can be described by Equation 2 based on Noyes-Whitney equation:

$$dm/dt = D/V \times S/h\ (Cs-Ct)$$

where dm/dt is the dissolution rate; D is the diffusion coefficient; S is the surface area; h is the thickness of the diffusion film adjacent to the dissolving surface; Cs is the saturation solubility of the drug molecule; Ct is the concentration of the dissolved solute; and V is the volume of the dissolution medium (Aristides and Panos, 2006).

From Equation 2, one can conclude that increasing the diffusion coefficient or increasing the surface area or decreasing the diffusion layer would enhance the dissolution rate and reduce the variations. The diffusion coefficient is affected by the solvent viscosity and the molecular size of the solute which in our case is considered the same for the low strength and high strength

Table 1. Example of the dissolution profile of a highly variable batch (HDL) that failed internal specification.

Sampling point	1	2	3	4	5	6	Mean	% RSD
10	55	45	28	6	17	55	35	62.9
20	94	98	70	64	45	86	78	25.1
30	97	99	90	86	72	94	93	11.9
45	97	98	96	99	93	100	99	3.8
60	97	97	97	99	95	98	97	1.6

Figure in red represent result which failed the proposed specification of 75%(Q)+5% at stage I (1000 ml of 0.01 N HCl and USP apparatus II (Paddle) at an agitation speed of 75 rpm).

Table 2. Dissolution profile of a low strength batch (LDL) (n = 6).

Sampling point	1	2	3	4	5	6	Mean	% RSD
10	27	56	94	98	92	47	68	42.0
20	96	100	96	98	101	95	99	3.8
30	97	101	96	96	102	96	99	3.9
45	96	102	97	95	101	98	99	3.9
60	97	101	96	96	104	95	98	4.0

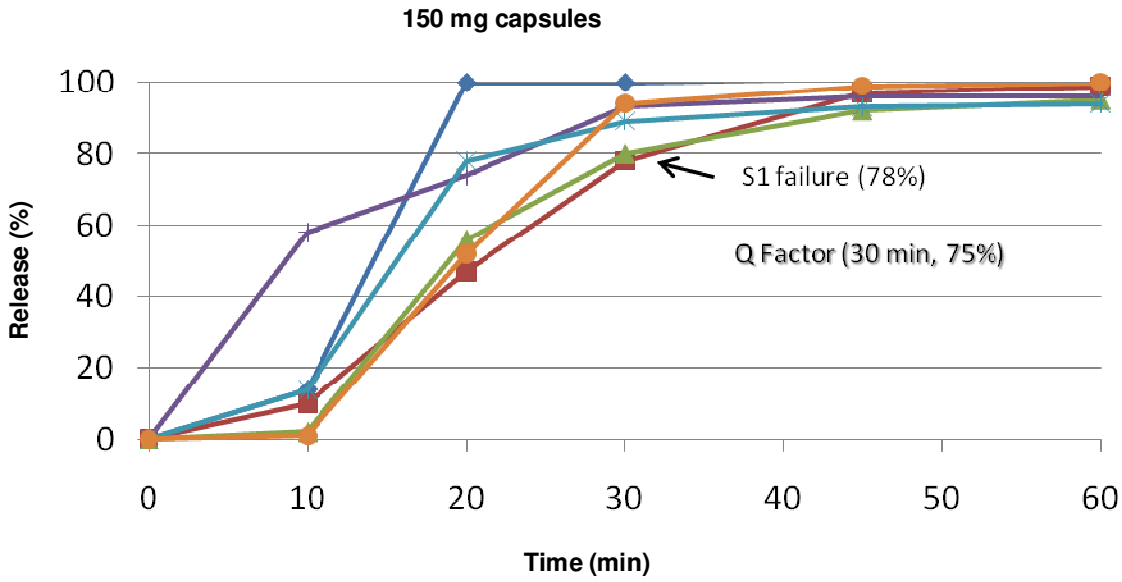

Figure 1. Dissolution profile of a highly variable batch (HDL) that failed internal specification (n = 6).

Table 3. Formulation composition.

40 mg capsules	150 mg capsules
25% drug loading	75% drug loading
MCC	MCC
Silicon dioxide	Silicon dioxide
Magnesium stearate	Magnesium stearate
Quali-V® HPMC capsule shells	Quali-V® HPMC capsule shells

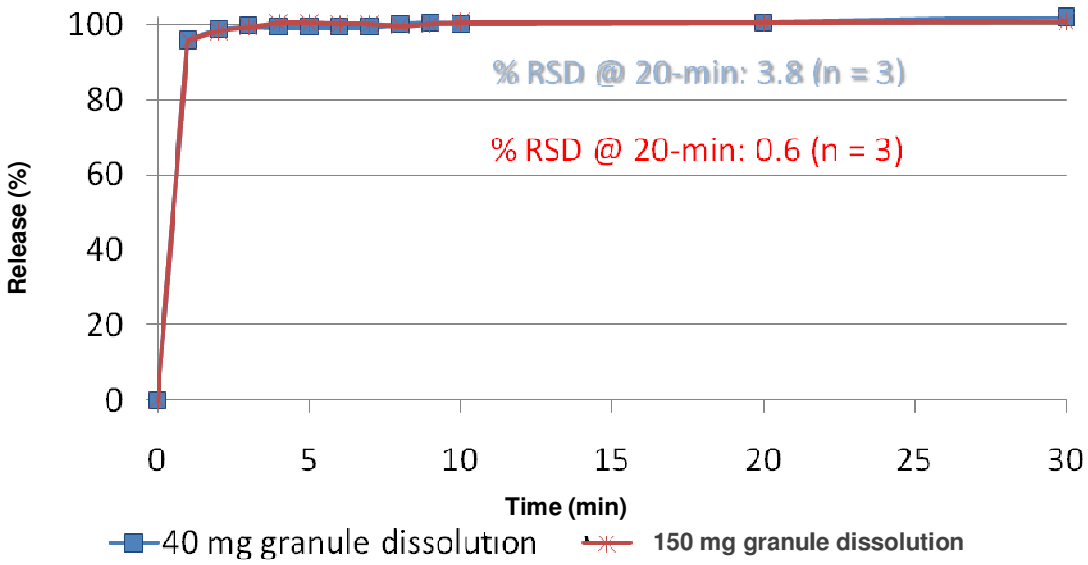

Figure 2. Granule dissolution 40 mg and 150 mg stock granulations. 40 mg granule dissolution: % RSD at 20min: 3.8 (n = 3); 150 mg granule dissolution: % RSD at 20 min: 0.6 (n = 3).

Table 4. Effect of apparatus I and II on dissolution.

Sampling point (min)	Mean % release		% RSD	
	Basket at 100 rpm	Paddle at 75 rpm	Basket at 100 rpm	Paddle at 75 rpm
10	2	45	45.5	42
20	24	80	75.5	10.8
30	69	95	10.5	7.7
45	95	97	2.9	4.4
60	97	97	2.1	3.3

formulations. The dissolution surface area and the diffusion layer are dictated by the disintegration rate of the capsule shells and the dissolution apparatus and agitation speed. The API dissolution surface area in a HPMC capsule formulation is affected by the rate of the disintegration of capsule shells and API particle size. The disintegration of the HPMC shells is affected by the water penetration through the shell walls and the hydrodynamics in dissolution vessels. Increasing the agitation speed could reduce the diffusion layer, help disintegration process, thereby increasing the surface area, exposing more drugs to the dissolution medium and improving the rate.

During our initial dissolution method development for the drug product, USP apparatus II (paddle) with 50 rpm was evaluated and partially intact capsule was observed at the end of the 60 min. The disintegration of HPMC shell was slow and inadequate; therefore, 75 rpm was justified with supporting data that was generated at the time. However, as formulation and product knowledge continued to evolve, failure in dissolution specification occurred, further investigation on dissolution parameters became necessary. As part of the investigation, an alternative apparatus of basket (40-mesh) with 100 rpm was evaluated using the intermittent inconsistent batch with the aim to identify if the basket apparatus would provide a more robust dissolution. Table 4 shows the two sets of data demonstrating that basket method exhibited much slower dissolution and higher percent RSD at early sampling-points when compared with the paddle apparatus. This is likely due to the thicker diffusion layer generated by the basket apparatus. The basket dissolution however did catch up at 45 min sampling-point and thereafter, but it would have failed the stage 1 dissolution specification of non-torque loading (NTL) 80% at 30 min. Media deaeration is another important factor that could affect drug dissolution surface area as air bubbles could partially cover the surface of the drug particles, and that portion of the surface will not be exposed to the dissolution medium and this leads to a decrease in the dissolution rate (Sherry et al, 2010). Air bubbles can act as a barrier to dissolution if present on the dosage unit or cause particles to cling to the apparatus and vessel walls and thus introduce dissolution variations. To evaluate if

Table 5. Effect of medium deaeration on dissolution (n = 6).

Sampling point (min)	Mean % release		% RSD	
	With degas	Without degas	With degas	Without degas
10	45	24	41.9	75.3
20	80	80	11.0	19.4
30	95	89	7.8	11.2
45	95	98	4.5	2.7
60	98	97	3.3	1.9

Table 6. Summary of capsule shell investigation 40 mg granulation in 40 and 150 mg shells (n = 6).

Sampling point (min)	Mean % release		% RSD	
	40 mg Shell	150 mg Shell	40 mg Shell	150 mg Shell
10	77	60	19.1	43.6
20	95	89	2.8	7.4
30	97	92	2.4	2.9
45	98	94	2.3	3.1
60	99	94	2.4	3.5

Table 7. Summary of capsule shell investigation 150 mg granulation in 150 and 40 mg Shells (n = 6).

Sampling point (min)	Mean % release		% RSD	
	40 mg Shell	150 mg Shell	40 mg Shell	150 mg Shell
10	35	26	24.0	75.4
20	83	80	14.9	19.4
30	89	91	9.7	11.2
45	94	98	4.3	2.5
60	98	99	2.5	1.9

medium deaeration has an effect on dissolution performance of the HPMC formulations, both degassed and non-degassed media were used in the dissolution testing of the intermittent inconsistent batch. Results demonstrated that degassed medium reduced the capsule-to-capsule variations at early sampling-points and improved the dissolution rate which warranted the inclusion of the medium deaeration in the method revision Table 5. Based on the data, it is concluded that higher agitation speed and medium deaeration can improve dissolution rate and reduce dissolution variations.

HPMC shell investigation

Disintegration of capsule shell was not only affected by the hydrodynamics in dissolution vessels, but was also affected by the rate of medium penetration through the shells. Switching shells between the two formulations would indicate if the problem follows the shells, because dissolution variations were only seen in the high strength batch. Our experimental design involved redistributing the contents from the batch of capsules (40 mg) which exhibited consistent dissolution with the batch of capsules (150 mg) which provided intermittent, inconsistent results. Dissolutions of each of the original and filled capsules (n = 6) were performed as per method, and the summaries of the results are presented in Tables 6 and 7, and plotted in Figures 3 and 4. It appeared that the 40 mg granule with the 150 mg capsule shell had an average dissolution release of 88% at 20 min with 7.4% RSD for n = 6 samples. It was slower and more variable as compared to 96% release with 2.8% RSD from the original 40 mg capsules (40 mg granule in 40 mg capsule shell). The data clearly indicated that the problem followed the 150 mg shell. Nevertheless, the 150 mg granule with 40 mg capsule shell had an average dissolution release of 83% with 15.0% RSD at 20 min which was slightly faster and less variable as compared to 80% release with 19.4% RSD from the original 150 mg capsules (150 mg granule in 150 mg capsule shell). It was evident that the 150 mg shells had pronounced effect in slowing down the dissolution performance of the 40 mg formulation whereas the

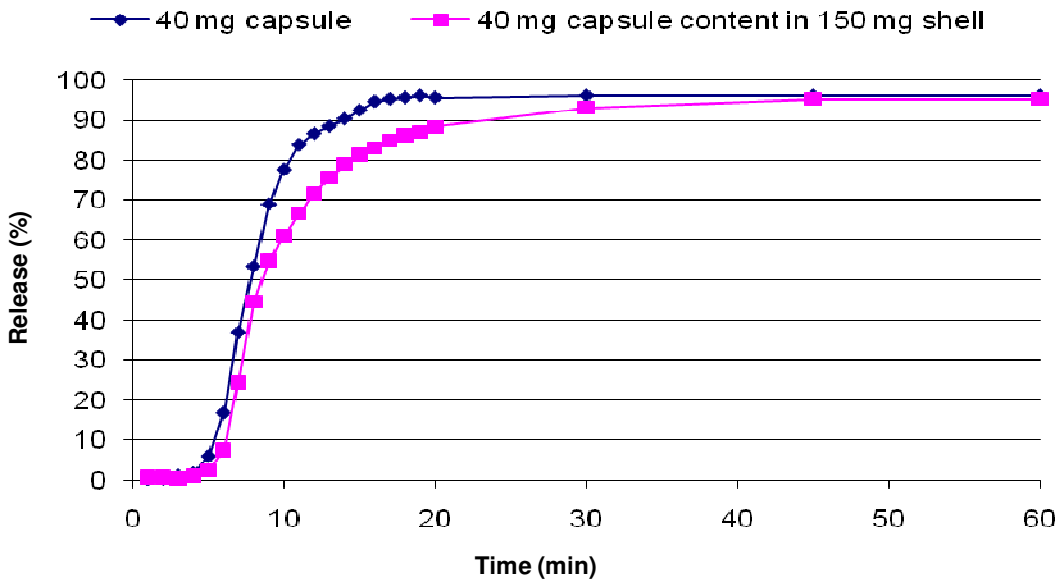

Figure 3. Dissolution profiles of 40 mg capsules (n = 6) and 40 mg granulation in 150 mg shells (n = 6).

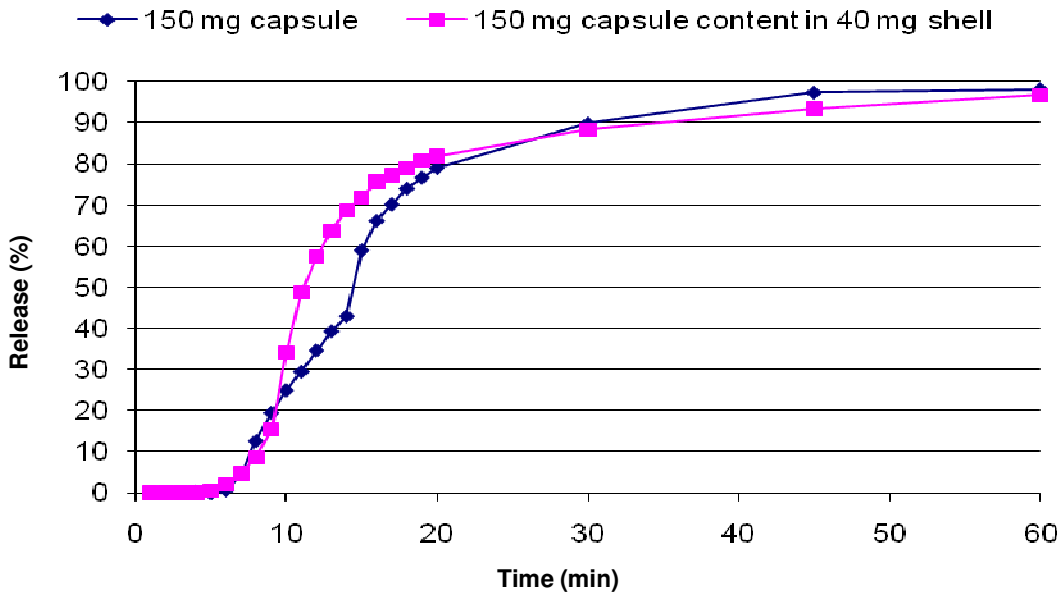

Figure 4. Dissolution profiles of 150 mg capsules (n = 6) and 150 mg granulation in 40 mg shells (n = 6).

40 mg shells only slightly improved the rate and consistency of the drug release of the 150 mg formulation. Among all the capsules that were tested, one original 150 mg capsule failed S1 dissolution specification of NLT 80% at 30 min and a couple of filled capsules with 150 mg granule in 40 mg capsule shells were just above 80% border line which indicated that the dissolution performance of the intermittent, inconsistent batch was affected by multiple factors rather than the 150 mg shells alone.

Effect of moisture content in HPMC shells on dissolution

Unlike its counterpart gelatin capsules, HPMC capsules do not undergo cross-linking under high temperature and high moisture (Digenis et al., 1994; Gold et al., 2011). The effect of moisture content in capsule shells on capsule dissolution has not been widely reported and studied in literatures; therefore, an experiment to probe the effect of shell moisture level on disintegration and dis-

Table 8. Effect of moisture content in capsule shells on dissolution.

Sampling point (min)	Mean % Release		% RSD	
	Original (4.07%)	Dried (1.46%)	Original (4.07%)	Dried (1.46%)
10	25	49	49.8	58.2
20	88	96	16.5	5.7
30	98	100	6.9	0.5
45	99	101	1.4	0.6
60	100	102	1.3	0.5

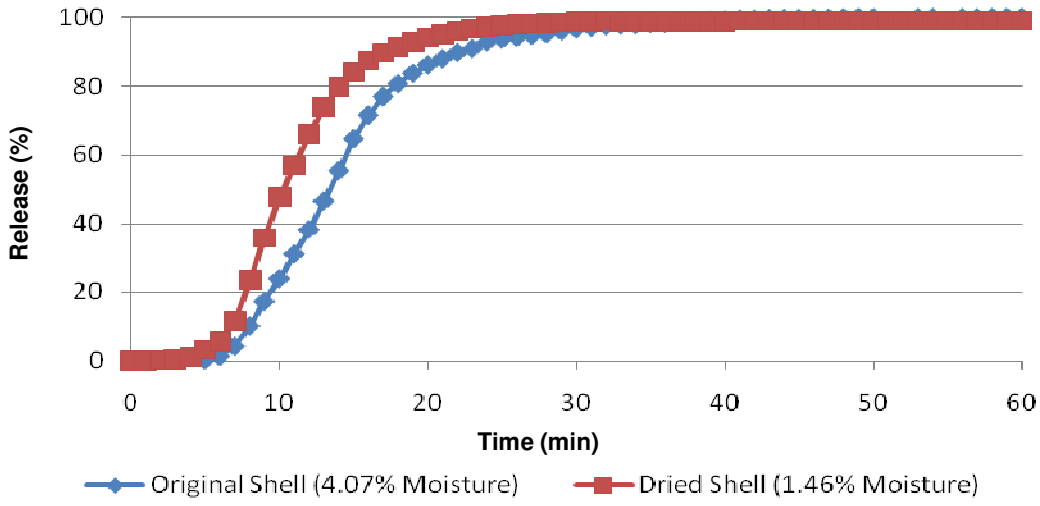

Figure 5. Effect of moisture content in HPMC capsule shells on dissolution (n = 6).

solution of the high strength formulation were conducted. The experimental details involved drying adequate amount of shells (~4.1% moisture) in a 45°C oven for 12 h. Both dried and un-dried shells were filled with HDL granules and dissolutions were performed on n = 6 capsules made with these shells. The comparison data generated from the two types of capsules demonstrating that capsules with un-dried shells exhibited a slower and variable dissolution at early sampling-points whereas a faster and consistent dissolution was obtained for capsules with dried shells Table 8 and Figure 5. Visual observation on the dissolution process that was conducted simultaneously at the time indicated that the capsules with un-dried shells did not disintegrate readily when compared with that of the capsules with dried shells.

It appears that the manufacturer suggested specification for moisture content 4 to 6%) in HPMC shell has its merit. Appropriately hydrated shell can prevent water penetration more effectively than its dried counterpart. From protecting product quality and stability perspective, it is beneficial that the capsule shells do not uptake moisture easily; however, it provides challenges for *in vitro* dissolution especially when water penetration and disintegration of capsule shells are the rate-limiting steps. In such event, perhaps formulation with more effective disintegrant could help to improve dissolution rate.

Surface dissolution of HPMC capsule shells

To help visualize the dissolution process of HPMC shells, a ActiPix SDI 300 UV area imaging system was used to enable the quantitative imaging of the surface erosion and dissolution for shells with various moisture contents. pH 6.8 sodium phosphate buffer was employed for the study. Two sets of images at 7 min time-point for a piece of dried shell (moisture undetermined, shells with 4.1% moisture were dried under 45°C for 12 h) and a piece of un-dried shell (4.1% moisture) that show the 254 nm absorbance images of areas containing shell and flowing dissolution medium Figures 6 and 7. The swell of shells from the exposure surface was significantly different between the two types of shells. The swell rate and swell size were calculated based on the surface dissolution process recorded by the SDI 300 software. The results demonstrated that the dried shell swells about four times faster than the un-dried shell (0.0405 mm/min versus 0.0093 mm/min). The dried shell had about two times the swell size as the un-dried shell at 7 min time-point. The

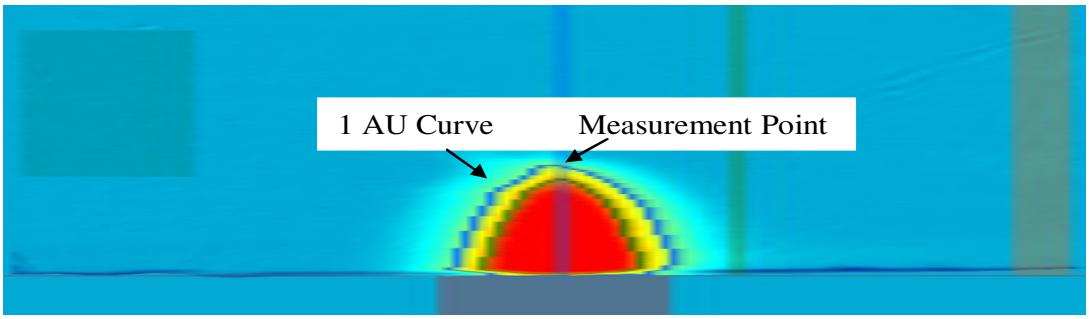

Figure 6. Surface dissolution imaging of dried shell.

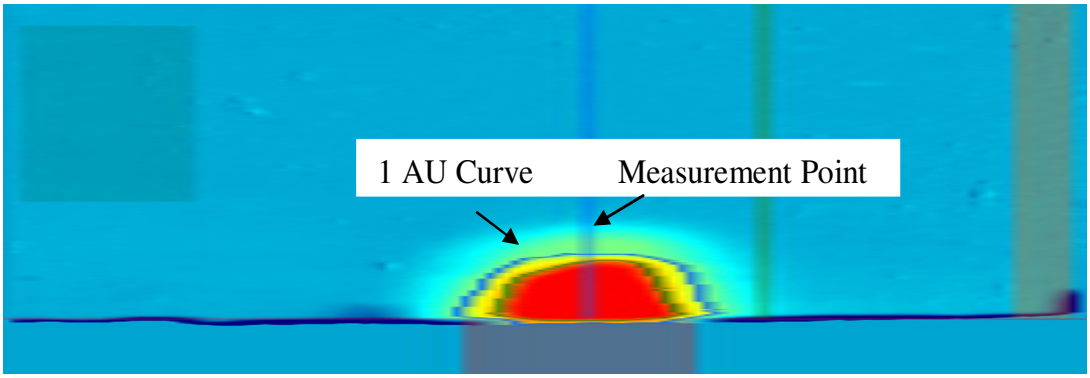

Figure 7. Surface dissolution imaging of un-dried shell.

swell height as a function of the time, indicated that medium penetration through the hydrated shell (un-dried shell) is slower when compared with the dehydrated shell (dried shell). This finding supported the hypothesis that was reported in the literature (Moawia, 2010) and our investigation in effect of moisture content in HPMC shells on dissolution on the effect of moisture content in HPMC shells on capsule dissolution.

Hydrodynamics evaluation: Effect of capsule landing positions on dissolution

The effect of capsule landing positions on the dissolution performance of the intermittent inconsistent batch was studied, because dissolution variations and robustness of the dissolution method are often affected by the insufficient hydrodynamics in dissolution vessels (Lozano et al., 1994). It had been observed in previous dissolution testing that chunks of granules with pieces of shell sometimes remained at the bottom “dead zone” of the vessels for a prolonged period of time. The effect of the “dead zone” on the HPMC capsule dissolution was unknown and worth to study. Dissolutions for capsules that landed at three positions (Figure 9) were performed with n = 2 capsules being dropped at the center, near center and off center locations prior to the start of the dissolution. The percent drug release as a function of time was generated by the UV fiber optics software at 1 min interval for a total of 60 min, with a simultaneous visual observation collected by the analyst. It was observed that the center capsules started to rupture at the shoulder of both ends and the capsule content gradually dispersed into the solution with the pile located at the “dead zone” last to disperse. In one of the two centered capsules, un-dissolved shell fragments were found above and below the capsule content at the “dead zone” area which prevented the drug from dispersing into medium for a prolonged period of time. Examination of the dissolution profile of this capsule revealed a 66% release at 30 min which would have failed the dissolution specification. A summary of the result in Table 9 illustrated the dissolution profiles of three sets of capsules landed at various locations. Capsules landed at the center had the slowest disintegration/dissolution rate at 15 min time-point when compared with capsules that landed near or off center. Based on the study results, it was concluded that the intermittent failure in S1 specification for the high strength batch could partially due to the artifact of un-dissolved shell fragment hinder the release of the capsule content when the capsules landed close or at the “dead zone”. Similar observation was reported in literature that during the dissolution of shell 1 in pH 4.5 acetate buffer, fragments of the shell may sometimes trap the powder against the bottom of the vessel, hindering fast and complete release of the drug (Sherry et al., 2010).

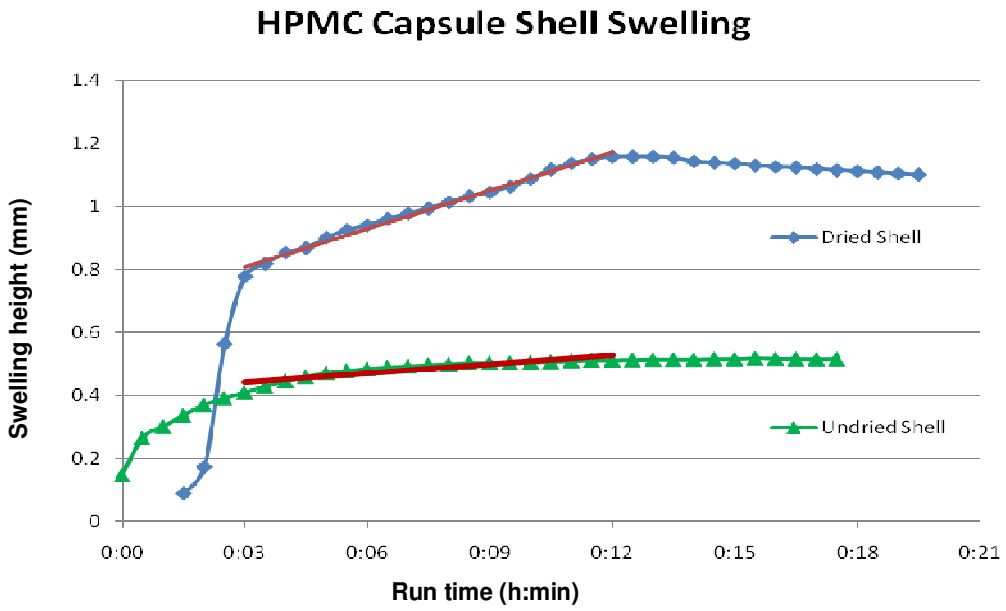

Figure 8. Swelling of HPMC capsule shell.

Table 9. Effect of capsule landing positions on dissolution.

Sampling point (min)	Release (%)					
	Center	Center	Near center	Near center	Off center	Off center
5	0	0	0	1	0	1
10	12	22	19	32	45	21
15	30	32	48	66	64	77
20	70	48	62	73	99	93
30	99	**67**	86	86	100	101
45	103	87	102	95	101	102
60	105	100	102	103	104	103

Figures in bold represent result which would fail the proposed specification of 75% (Q)+5% at stage I.

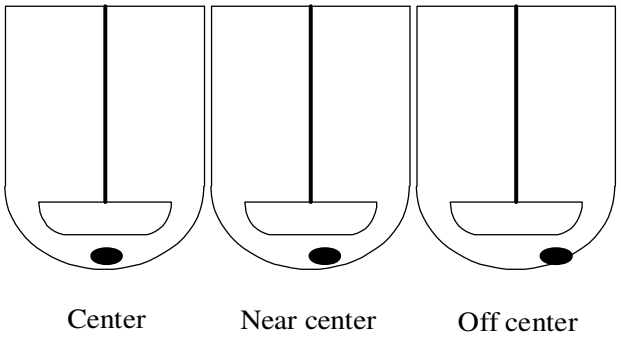

Figure 9. Capsule landing positions.

Conclusions

Here, a unique case where the same lot of HPMC shells stored in different storage conditions yielded substantially different *in vitro* dissolution release for a BCS Class III compound was presented. The root cause of the intermittent, inconsistent dissolution of the high strength batch was determined to be the higher moisture content in the HPMC shells. It appears that HPMC shells with manufacture specified moisture content would not readily uptake moisture which is a desirable element from protecting product stability and quality perspective. However, it posts challenges for the dissolution method development as shells with 4 to 6% moisture would not dissolve in dissolution media readily. To enhance the dissolution performance of the HPMC formulations, one could consider employing super-disintegrant to improve the disintegration capacity of the formulation. Another important factor that should be considered from method development perspective is to ensure adequate hydrodynamics in dissolution vessel and deaeration of dissolution medium. In our case, justification of higher

agitation speed that is beyond the compendia condition is appropriate as it would not only improve the shell disintegration thus improve the overall dissolution rate, but also reduce the effect of “dead zone” and minimize the chance of drug being trapped by shell fragments.

With the aim of fully understanding the effect of dissolution sink, apparatus, agitation, hydrodynamics, medium deaeration and effect of shell moisture content on dissolution, we are able to identify the root cause of the intermittent and inconsistent dissolution of the high strength batch and minimize the occurrences of S2 or S3 testing. With the inherent moisture content in the HPMC shells, achieving adequate hydrodynamics in dissolution vessel is vital in order to reduce intermittent dissolution failure and dissolution variations for capsule formulation with HPMC shells.

REFERENCES

Aristides D, Panos M (2006). A century of dissolution research: From Noyes and Whitney to the Biopharmaceutics Classification System. Int. J. Pharm. 321:1–11.

Cynthia KB, Hitesh PC, Beverly N (2004). Acceptable Analytical Practices for Dissolution Testing of Poorly Soluble Compounds. Pharm. Technol.12:56-65.

Digenis GA, Gold TB, Shah VP (1994). Crosslinking of Gelatin Capsules and its Relevance to their *In Vitro-In Vivo* Performance. J. Pharm. Sci. 83(7):915-921.

El-Malah Y, Nazzal S, Bottom CB (2007). Hard gelatin and hydromellose (HPMC) capsules: estimation of rupture time by real-time dissolution spectroscopy. Drug Dev. Ind. Pharm. 33:27-34.

Ewart TC, Robert AS, Dominique C, Alyson LC, Ian RW (2004). In Vitro and *in vivo* pharmacoscintigraphic evaluation of Ibuprofin Hypromellose and Gelatin Capsules. Pharma. Res. 21(5).

Gold T, Warren J, Collier D (2011). Dissolution of a Phosphate ProDrug from Hard Gelatin Capsules: A Case Study. AAPS Poster

Irene C, Brian EJ, Fridrun P (2000). The Shell dissolution of various empty hard capsules. Chem. Pharm. Bull. 48(7):951-956.

Lozano R, Joseph JM, Kline BJ (1994). Temperature, pH and agitation rate as dissolution test discriminators of zofenopril calcium tablets. J. Pharm. Biomed. Anal. 12(2):173–177.

Michael S（2011. Developing and Validating Dissolution Procedures for Improved Product Quality. Pharma Times 43:13-17.

Moawia MA (2010). HPMC Capsules: Current Status and Future Prospects. J. Pharm. Pharm. Sci. 13(3):428-442.

Nagata S (2002). Advantages to HPMC Capsules: A New Generation's capsule technology. Drug Dev. Deliv. 2(2):34-39

Robert OW III, Matthew AS, Vorapann M (2001). Method to recover a lipophilic drug from hydroxypropyl methylcellulose matrix tablets. AAPS Pharm. Sci. Tech. 2(2): 29–37.

Sherry MK, Qinghong L, Weiyi L, Yansong C (2010). Performance Qualification of a New Hypromellose Capsules. Int. J. Pharm. 386(2010):30-41.

Tuleu C, Khela MK, Evans DF, Jones BE, Nagata S, Basit AW (2007). A Scintigraphic investigation of the disintegration behavior of capsules in fasting subjects: A comparison of hypromellose capsules containing carrageenan as a gelling agent and standard gelatin capsules. Eur. J. Pharm. Sci. 30(3-4):251-5.

academicJournals

Vol. 7(22), pp. 1512-1522, 15 June, 2013
DOI 10.5897/AJPP2013.3564
ISSN 1996-0816 © 2013 Academic Journals
http://www.academicjournals.org/AJPP

African Journal of Pharmacy and Pharmacology

Full Length Research Paper

In vitro antioxidant, analgesic and cytotoxic activities of *Sepia officinalis* ink and *Coelatura aegyptiaca* extracts

Sohair R. Fahmy and Amel M. Soliman*

Department of Zoology, Faculty of Science, Cairo University, Egypt.

Accepted 29 April, 2013

The present study aims to evaluate the antitumor, antioxidant and anti-inflammatory activities of two molluscan extracts, *Sepia officinalis*, ink extract (IE) and *Coelatura aegyptiaca* extract (CE). The antioxidant activities of both extracts were evaluated using 1,1- diphenyl-2-picrylhydrazyl (DPPH) scavenging and lipid peroxidation assays. The analgesic effects were evaluated using the writhing, hot plate and formalin tests. Cytotoxicity assay was performed using sulphorhodamine B (SRB) method on hepatocellular carcinoma (HepG2) cell lines. The IE extract exhibited dose dependent radical scavenging activity. The two tested extracts showed inhibition of thiobarbituric acid–reactive substances (TBARAS) at all concentrations, with an IC50 value of 176.77 and 177.23 (µg/ml), respectively. IE and CE extracts showed analgesic action by inhibiting the acetic acid-induced writhing. IE exhibited significant anti-nociceptive actions in mice by increasing the latency period in the hot-plate test. Both extracts significantly decreased the time of paw lickings in both early and late phases. Furthermore, IE and CE showed cytotoxic activities HepG2 cell lines with IC50 value of 67 and 49.24 µg/ml, respectively. In conclusion, IE and CE extracts have antioxidant, anti-inflammatory and cytotoxic properties and can be considered as promising anticancer drugs.

Key words: Sepia ink, *Coelatura aegyptiaca*, antioxidant, anti-inflammatory, cytotoxicity.

INTRODUCTION

Nature is an attractive source of new therapeutic candidate compounds as a tremendous chemical diversity is found in millions of plants and animals species. Natural products continue to be a major source of pharmaceuticals and for the discovery of new molecular structures (Schaufelberger et al., 1991). Products from freshwater and marine sources have recently become attractive as nutraceutical and functional foods and as a source material for the development of drugs and specific health foods (Koyama et al., 2006). Emerging evidence suggests that marine natural products, especially the secondary metabolites from marine organisms, are far more likely to yield anticancer drugs than terrestrial sources (Hong et al., 2009).

In nature, animals are provided with their own protective response against their predators, likewise freshwater and marine mollusks are protected by their shells, but many of them are not fully protected by shells. Chemical defenses are used extensively by both shelled and shell-less mollusks. Caldwell (2005) has proposed that the ink of cephalopods contain compounds that are capable of disrupting predator's chemical senses, but evidences are not fully recorded.

Ink gland cells of the digestive tract in the mantle cavity degenerate and shed their contents into the ink sac, acting as a reservoir of the exhausted material. Ejection of dark ink from the sac is a defensive means that cuttlefish employed to avoid dangers and risks (Liu et al., 2011).Squid ink is a multifunctional marine bioactive-material which promotes thromboxane production, kills cancer cells, and elevates leukocyte number (Sasaki et al., 1997). Moreover, it has anti-oxidant (Liu et al., 2011), anti-radiation, anti-retrovirus and anti-bacterial properties (Zhong et al., 2009; Nithya et al., 2011; Vennila et al.,

*Corresponding author. E-mail: soliman.amel5@gmail.com. Tel: +20235676714.

2011). Egyptian freshwater mussel (Coelatura aegyptiaca) is a Molluscan bivalve that belongs to Unionoidae common in the Egypt along the River Nile from Assiut (Upper Egypt) to Damietta branches (Lower Egypt) (Moloukhia and Sleem, 2011).

Hepatocellular carcinoma (HCC) is the third most common cause of cancer mortality worldwide (Yang and Roberts, 2010). It contributes to 14.8% of all cancer mortality in Egypt, with a higher incidence in males (17.3%) than in females (11.5%) (Aleem et al., 2012). It is the second most frequent cancer type in Egyptian males after bladder cancer and the eighth most frequent in Egyptian females (Anwar et al., 2008). The primary risk factors for HCC are hepatitis B virus (HBV), hepatitis C virus (HCV), dietary aflatoxin exposure, and chronic alcohol consumption (Bosch et al., 2005).

Oxidative stress is closely related to all aspects of cancer, from carcinogenesis to the tumor-bearing state, and from treatment to prevention (Noda and Wakasugi, 2001). Epidemiologic studies have suggested that some antioxidants agent as well dietary constituents with anti-oxidant properties may be acting as naturally occurring cancer preventing agents and may explain some of the differences in cancer incidence seen in populations with varying dietary intake (Greenwald et al., 2001). Many cancer patients who are undergoing therapy take antioxidant supplements in an effort to alleviate treatment toxicity and improve long-term outcome.

It has long been recognized that infections and inflammation are related to cancer, and where there is a strong correlations between the presence of inflammation and the development of pre-cancerous lesions at various anatomic sites (Rayburn et al., 2009). During chronic inflamemation, pro-inflammatory molecules, such as cytokines, inducible nitric oxide synthase (iNOS), reactive oxygen species (ROS), and nuclear factor-kappa B (NF-kB) are upregulated (Sarkar and Fisher, 2006). Epidemiological data suggest that the incidence of breast, colorectal, and lung cancers is inversely related to the use of aspirin and non-steroidal anti-inflammatory drugs (Arun and Goss, 2004).

Taking into consideration the relation between cancer and oxidative stress on one hand and the relation between cancer and inflammation on the other hand, the present investigation aimed to evaluate the antitumor, antioxidant and anti-inflammatory activities of two molluscan extracts, the first from the ink of the marine cephalopods cuttlefish (*Sepia officinalis*) and the second from the Egyptian freshwater mussel (C. aegyptiaca).

MATERIALS AND METHODS

Preparation of cuttlefish ink extract (IE)

Fresh cuttlefish (S. officinalis) were purchased directly from a fishmonger and rapidly transferred to the laboratory where they were dissected and the ink was collected and diluted immediately with an equal volume of distilled water and mixed sufficiently. The admixture collected immediately, concentrated and lyophilized to a black residue using a lyophilizer (LABCONCO lyophilizer, shell freeze system, USA).

Preparation of crude freshwater Coelatura extract (CE)

Freshwater mussel, C. aegyptiaca were collected from the River Nile at Giza Governorate, Egypt. The crude extract was prepared as follows: 1 kg of fresh mussel was extracted in a boiler with 1 L of distilled water for 30 min 3 times. After filtration, the filtrate obtained was then concentrated and dried using a lyophilizer (LABCONCO lyophilizer, shell freeze system, USA).

Animals

Male white Swiss mice aged 9 to 12 weeks were used in all experiments. The animals were obtained from a closed random-bred colony at the animal's house, National Research Center. The used mice for any one experiment were selected from mice of similar age (±1 week) and weight (±2 g). Animals were housed in polycarbonate boxes with steel-wire tops (not more than five animals per cage) and bedded with wood shavings. Ambient temperature was controlled at 22 ±3°C with a relative humidity of 50±15% and a 12-h light/dark photoperiod. Food and water were provided ad libitum. All the animals received human care in accordance with the guidelines of the Cairo University, Faculty of Science, Zoology Department for ethical treatment of laboratory animals.

Drugs and chemicals

All drugs, chemicals and solvents were purchased from local firms (Egypt) and they were of highest purity and analytical grade.

Acute toxicity study

Swiss albino male mice weighing (18 to 26 g) were used for acute toxicity study. Acute toxicity was conducted according to OECD guidelines 420 (Fixed dose method) (Vanden et al., 1990; Whitehead and Curnow, 1992). The animals were divided into control and test groups containing six animals each. The control group received the distilled water whereas the test groups received cuttlefish ink extract (IE) and freshwater mussel extract (CE) (2000 mg/kg) intraperitoneally. After administration, the animals were observed for behavior changes and their mortality was noted after 48 h (acute) and at 14 days (chronic).

Antioxidant activity

Free radical scavenging activity

The free radical scavenging activities of each extract and ascorbic acid were analyzed by the 1,1- diphenyl-2-picrylhydrazyl (DPPH) assay (Sanchez-Moreno et al., 1998). A 1.0 ml of the test extract, at gradient final concentrations of 10 to 50 mg/ml of extract and ascorbic acid as reference standards, was mixed with 2 ml of 0.3 mM DPPH solution in methanol in 5 ml test tubes. The mixtures were incubated for 20 min in the dark at room temperature then the absorbance was taken at 517 nm. The experiment was done in triplicates. The percentage antioxidant activity was calculated as follows:

Antioxidant activity, AA (%) = 100 - [{(Abssample – Absblank) × 100}/Abscontrol].

where Abssample was the absorbance of sample solution (1.0 ml) + DPPH solution (2.0 ml, 0.3 mM), Absblank was the absorbance of methanol (2.0 ml) + sample solution (1.0 ml), Abscontrol was the absorbance of DPPH solution (0.3 mM).

Lipid peroxidation assay

The degree of lipid peroxidation was assessed by estimation of the thiobarbituric acid-reactive substances (TBARS) (Okhawa et al., 1979; Tripathi and Sharma, 1998). Briefly, different concentrations of extracts (50 to 250 µg/ml) were added to the 10% liver homogenate. Lipid peroxidation was initiated by addition of 100 µl of 15 mM FeSO4 solution to 3 ml of liver homogenate (final concentration was 0.5 mM). After 30 min, 100 µl of this reaction mixture was taken in a tube containing 1.5 ml of 0.67% TBA in 50% acetic acid. Samples were incubated at 37°C for 1 h, and then lipid peroxidation was measured using the reaction with TBA. The absorbance of the organic layer was measured at 532 nm. All reactions were carried out in duplicates. Vitamin C was used as the positive control. The percentage of inhibition of lipid peroxidation was calculated as:

Inhibition (%) = (Abscontrol – Abs test) × 100/Abscontrol.

Inhibitory concentration (IC50) values were calculated from the plotted graph of percent inhibition against the concentrations of the samples. IC50 was calculated for all the extracts and vitamin C which was used as the reference compound (positive control) with concentrations 50 to 250 µg/ml.

Determination of analgesic activity

Analgesic effects were evaluated using three different models: the writhing, and hot plate and formalin tests.

Acetic acid-induced writhing test

Acetic acid induced writhing test in mice was carried out according to the procedure earlier described by Mbagwu et al. (2007) and Nwafor et al. (2007). The animals were divided into 4 groups of 5 mice per group. Group 1 served as negative control and received 10 ml/kg of normal saline, while groups 2 and 3 were pre-treated with 200 mg/kg intraperitoneally (i.p) of cuttlefish ink extract (IE) and freshwater mussel extract (CE), respectively and group 4: received 5 mg/kg i.p of indomethacin as standard non-steroidal anti-inflammatory drug. Both extracts and indomethacin were dissolved in normal saline. After 30 min, 0.2 ml of 2% acetic acid was administered i.p. The number of writhing movements was counted for 10 min. Antinociception (analgesia) was expressed as the reduction of the number of abdominal constrictions between control animals and mice pretreated with extracts. Inhibition (%) was calculated.

Hot plate latency assay

The method of Eddy et al. (1950) was used for this study. The animals were fasted for 16 h then divided into 4 groups of 5 mice per group. Group 1 served as negative control and received 10 ml/kg of normal saline, while groups 2 and 3 were pre-treated with 200 mg/kg i.p of cuttlefish ink extract (IE) and freshwater mussel extract (CE), respectively and group 4 received 5 mg/kg of indomethacin. The animals were placed on the hot plate (maintained at 55°C). The reaction time (characterized by jumping off the animals from the hot plate) to the thermal stimuli was noted at 30 min post extract administration. The mean of the latencies of the animals on the hot plate was determined.

Formalin induced paw licking in mice

In this study animals were grouped as earlier stated in the writhing and hot plate tests. The study was performed according to the method described by Hunskaar and Hole (1997), 0.2 ml of 3% formalin was injected into the dorsal surface of the left hind paw of mice for 30 min. The test was carried out in a transparent plastic chamber (15 × 16 × 20 cm). Each animal was allowed to explore the chamber 5 min before receiving an injection of formalin. The time which the mice spent in licking the injected paws was measured as an index of pain or nociception. The tested animal was given all treatments intraperitoneally before the administration of formalin. The 1st phase (initial nociceptive response) was 5 min after formalin injection (0 to 5 min). The 2nd phase (second nociceptive response) was between 15 and 30 min, post injection.

***In vitro* assay of cytotoxicity using sulphorhodamine B (SRB) method**

The cytotoxicity assay was performed, following the method of Skehan et al. (1990), at the National Cancer Institute of Egypt on the cuttlefish ink extract (IE) and freshwater mussel extract (CE) against HepG2 (Liver cancer cell line). The cells were plated in a 96-multiwell plate (104 cells/well), for 24 h, before treatment of both extracts to allow attachment of cells to the wall of the plate. Different concentrations of both IE and CE extracts (10, 20, 30, 40 and 50 µg/ml) were added to the cell monolayer. Triplicate wells were prepared for each concentration. Monolayer cells were incubated with the tested samples for 48 h at 37°C, in an atmosphere of 5% CO2. After 48 h, the cells were fixed, washed and stained with sulphorhodamine B stain. Excess stain was washed with acetic acid and attached stain was recovered with Tris EDTA buffer. Color intensity was measured in an ELISA reader at 515 nm. The relation between surviving fraction and the IE and CE extracts concentration is plotted to get the survival curve of each tumor cell line after treatment with the extracts. Data fitting and graphics were performed by means of the Prism 3.1 computer program (Graph Pad software, USA).

Statistical analysis

Values were expressed as mean ± Standard error of mean (SEM). To evaluate differences between the studied groups, one way analysis of variance (ANOVA) with Least significant difference (LSD) post hoc test was used to compare the group means and $P<0.05$ was considered statistically significant. Statistical Package for Social Sciences (SPSS), for Windows (version 15.0, Chicago, IL, USA) was used for statistical analysis.

RESULTS

Acute toxicity

None of the 6 mice died or showed any sign of toxicity at the limit dose of 2000 mg/kg i.p for both cuttlefish ink extract (IE) and freshwater mussel extract (CE), in the first 48 h. No evidence of toxicity was noted during the period of observation. The LD_{50} in mice was therefore taken as above 2000 mg/kg i.p. The median effective

dose (ED_{50}) of IE and CE was selected based on the proposed LD_{50} obtained from the acute toxicity study. This dose was considered one tenth of the proposed LD_{50}, that is, 200 mg/kg body weight.

Antioxidant activity

The principle of antioxidant activity is the availability of electrons to neutralize any so called free radicals. Since, antioxidant mechanisms are diverse; a variety of in vitro techniques has been developed. It is better to use different assays based on different mechanisms to evaluate the antioxidant capacity. In this study, the antioxidant activity of both cuttlefish ink extract (IE) and freshwater mussel extract (CE) were evaluated using DPPH scavenging and lipid peroxidation assays.

Free radical scavenging activity

The results of DPPH scavenging activity of both extracts and ascorbic acid are shown in the Figure 1. The radical-scavenging activities were estimated by comparing the percentage of inhibition of DPPH radicals by the tested extracts and the ascorbic acid. Effect of water extract of both cuttlefish ink extract (IE) and freshwater mussel extract (CE) on DPPH free radical scavenging activity has been checked at various concentrations (10, 20, 30, 40 and 50 mg/ml) in three replications. The data were displayed with mean ± SEM of three replications. The present results showed that IE produced dose dependent inhibition of DPPH radicals ranging from (86.14 to 95.19%), while CE does not exert dose-dependent inhibition of DPPH radicals.

Anti-lipid peroxidation activity

TBA test determined the content of TBAR substances at the end of lipid peroxidation. The mean TBAR substances inhibition for the IE, CE and vitamin C were 44.38, 48.17, and 39.17%, respectively (Figure 2). In addition, the results showed that IC50 for IE, CE and vitamin C were 176.77, 177.23 and 245.45, respectively.

Analgesic activity

Acetic acid-induced writhing

Table 1 shows the effects of both cuttlefish ink extract (IE) and freshwater mussel extract (CE) on acetic acid-induced writhing in mice. The present results indicated that administration of both extracts at a dose of 200 mg/kg i.p showed significant ($P<0.05$) inhibition of writhing induced by the acetic acid as compared to the control animals. The obtained results also, showed the more potent effects of both extracts as compared to the reference drug indomethacin where the percent inhibition of writhing induced by IE and CE injections were 83.06 and 73.14%, respectively, while that of indomethacin was 38.43%.

Hot plate latency

Pretreatment with both cuttlefish ink extract (IE) and freshwater mussel extract (CE) and indomethacin (5 mg/kg, i.p) increased the response latency in the hot plate test (Figure 3). The present results showed a significant increase in the latency period ($P<0.05$) was induced only by IE extract as compared to control group.

Formalin induced paw licking in mice

In the formalin test, both IE and CE extracts (200 mg/kg, i.p) caused a significant inhibition of both phases of formalin-induced pain (Figure 4). The recorded results also showed that IE extract showed more potent effect than the standard reference drug, indomethacin (5 mg/kg, i.p).

Antiproliferative activity

Cytotoxicity of both IE and CE extracts on hepatocellular carcinoma (HepG2) cell lines was assessed using sulphorhodamine B (SRB) (Figures 5 and 6). HepG2 cells were treated with graded concentration (10, 20, 30, 40 and 50 µg/ml) of both IE and CE extracts for 24 h. Treatment of HepG2 cells with IE or CE extracts resulted in loss of cell viability. However, this inhibition was found to be steady and not affected by increment of dose. The recorded data showed that, the IC50 (concentration causing death of 50% of HepG2 cells) of both IE and CE extracts were 76 and 49.24 µg/ml, respectively (Figures 5 and 6).

DISCUSSION

Chemotherapy is currently the primary treatment modality in many tumors. However, the development of multidrug resistance (MDR) to chemotherapeutic drugs is a main obstacle for the successful treatment of malignant tumors (Tao et al., 2010). Therefore, the development of novel chemotherapeutic agents would play a key role in the treatment of refractory or relapsing cancer patients. Marine organisms are rich source for natural products. Many compounds that are derived from these organisms have generated interest both as challenging problems for

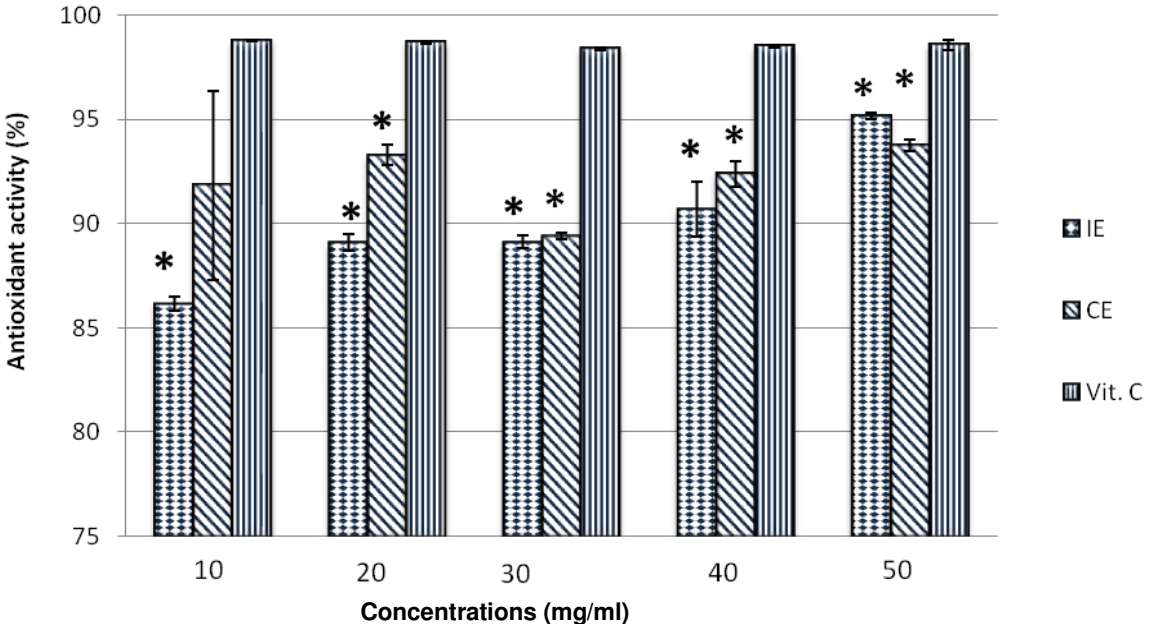

Figure 1. Antioxidant activity of both cuttlefish ink extract (IE) and freshwater clam extract (CE) and vitamin C. Each vertical column represents the mean ± SEM of change of 6 mice. Both extracts were effective compared to vitamin

Table 1. Effect of both cuttlefish ink extract (IE) and freshwater clam extract (CE) on acetic acid-induced writhing in mice. Each vertical column represents the mean ± SEM of change of 6 mice. Both extracts and indomethacin were effective compared to control.

Group	Mean number of writhings	Inhibition (%)
Control	48.40 ± 5.00	-
IE	8.20 ± 3.79*	83.06
CE	13.00 ± 1.82*	73.14
Indomethacin	29.80 ± 2.06*	38.43

*Significantly different from control group at $p<0.05$.

structure elucidation and synthesis as well as for their cytotoxicity (Schwartsmann, 2000; Schwartsmann et al., 2001). It is believed that, a rich source of anticancer drug candidates could be obtained from marine organisms or their metabolites. But, we have shown in the present study that anticancer drug candidates can be also obtained from freshwater organisms.

Given the relation between oxidative stress and cancer, it has been assumed that ingestion of antioxidants is useful in preventing carcinogenesis (Terry et al., 2000). Moreover, inhibition of inflammation using antioxidants has also been studied in relation to the risk of carcinogenesis (Kimura et al., 1998). So, if the novel cancer therapeutic drug has both antioxidant and anti-inflammatory properties at the same time, it can be a promising anticancer drug.

Cephalopod inks are chemical secretions produced by and released from the ink sac (Roseghini et al., 1996). Furthermore, freshwater bivalves occurring in Egypt represent a neglected animal group and little is known about them or their diversity; perhaps due to the fact that they have no apparent economic or medical importance (Sleem and Ali, 2008). But, recent attention has been focused upon supplements derived from freshwater foods in Egypt and their utilization as hepatoprotective agents (Fahmy et al., 2009; Fahmy and Hamdi, 2011; Soliman, 2011).

During normal metabolic processes or due to the exogenous factors and agents, reactive oxygen species (ROS) in the forms of superoxide anion radical (•O2–), hydroxyl radical (•OH), hydrogen peroxide (H2O2) may be generated. Formation of ROS can cause oxidative damage to human cells, leading to various diseases such as diabetes, cardiovascular diseases, inflammatory conditions, cancer and ageing (Joyce, 1987; Velioglu et al., 1998).

In the present study, we attempted to evaluate the antioxidant and prooxidant effects of the cuttlefish ink extract (IE) and freshwater mussel extract (CE). Antioxidant tests could be based on the evaluation of lipid peroxidation or on the measurement of free radical scavenging potency. The use of DPPH radical provides an easy, rapid and convenient method to evaluate the antioxidants and radical scavengers (Roginsky and Lissi, 2005). DPPH assay is a stable free radical widely used to evaluate the free radical-scavenging activity (RSA) of various natural products and some synthetic pure compounds. The DPPH antioxidant assay is based on

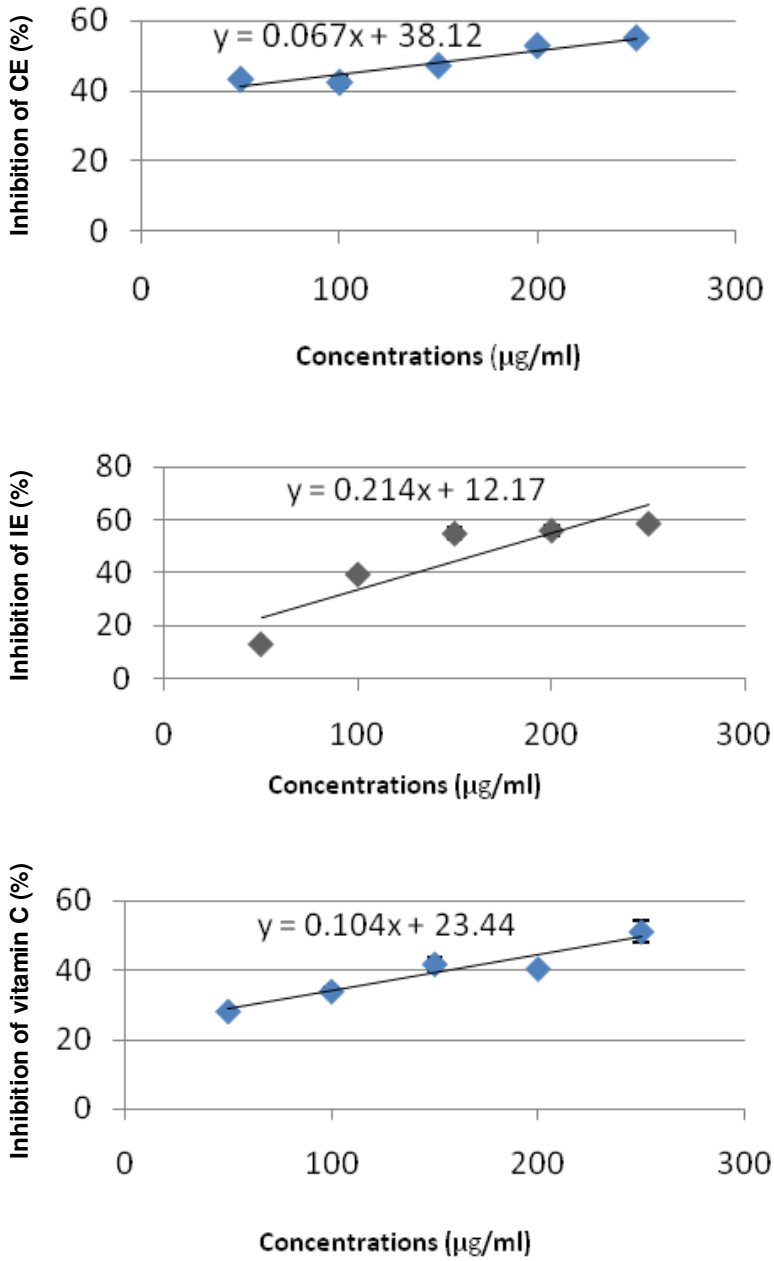

Figure 2. Effect of cuttlefish ink extract (IE), freshwater clam extract (CE) and vitamin C on TBARS in liver homogenates of male Swiss albino mice.

the ability of DPPH, a stable free radical, to be decolorized in the presence of antioxidants (Kumarasamy et al., 2007). The DPPH radical contains an odd electron, which is responsible for the absorbance at 515 to 517 nm and also for visible deep purple color. When DPPH accepts an electron donated by an antioxidant compound, the DPPH is decolorized which can be quantitatively measured from the changes in absorbance. Therefore, in this study, the selected IE and CE extracts were screened for their possible antioxidant and radical scavenging activity by DPPH technique and their IC50 values were calculated. The data recorded from this study showed that, the IE extract exhibited dose dependent radical scavenging activity. Moreover, during lipid peroxidation, low molecular weight end products, generally malondialdehyde, are formed by oxidation of polyunsaturated fatty acids that may react with two molecules of TBA to give a pinkish red chromogen (Okhawa et al., 1979). In the lipid peroxidation assay, the two tested extracts showed inhibition of peroxidation effect at all concentrations, with an IC50 value of 176.77 and 177.23 mg/ml, respectively.

Squid ink is a mixture containing melanin, protein, carbohydrate and lipid (Liu et al., 2011). Melanins are

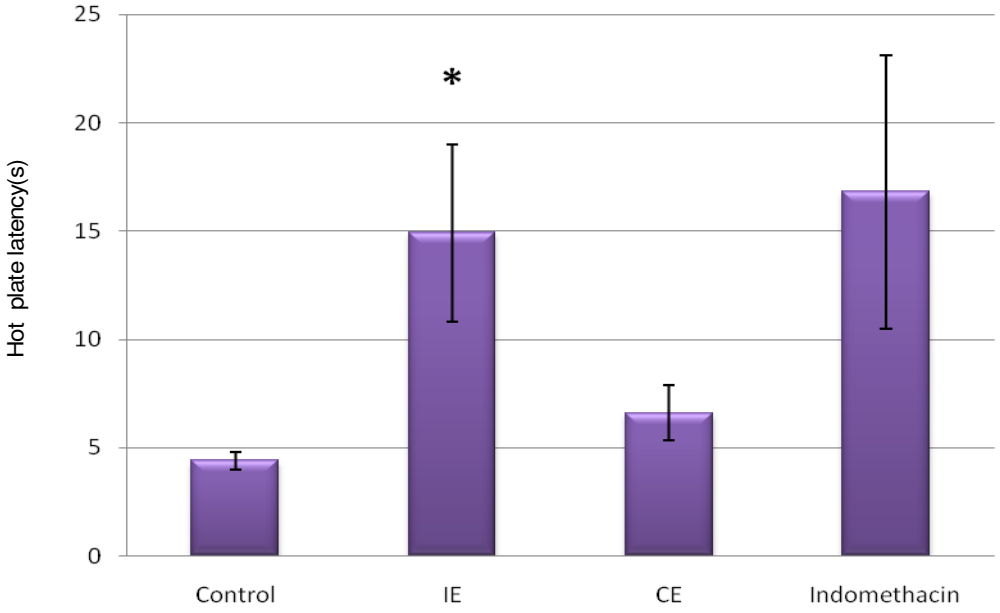

Figure 3. Effect of both cuttlefish ink extract (IE) and freshwater clam extract (CE) on hot-plate latency (sec) in mice.
Each vertical column represents the mean ± SEM of change of 6 mice. Both extracts and indomethacin were effective compared to the control.

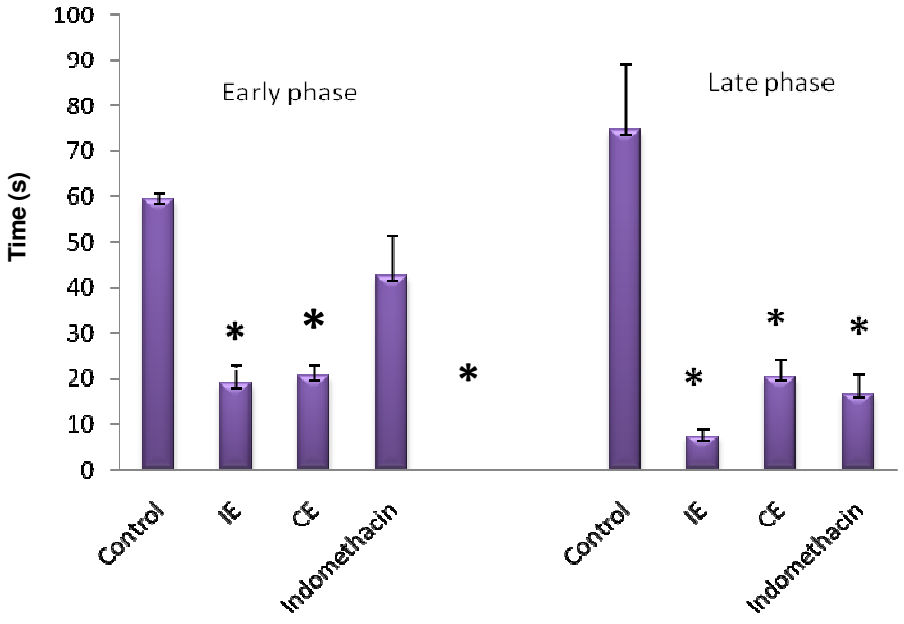

Figure 4. Effect of both cuttlefish ink extract (IE) and freshwater clam extract (CE) on formalin-induced paw licking in mice.
Each vertical column represents the mean ± SEM of change of 6 mice. Both extracts and indomethacin were effective compared to control.

efficient free radical scavengers and antioxidants (Prota, 1992). Katritzky et al. (2002) have proposed that sepia melanin is a copolymer of eumelanin constituted of approximately 20% of units of 5, 6-dihydroxyindole (DHI) and 75% of units of 5,6-dihydroxyindole-2-acid carboxylic (DHICA). Zhang et al. (2003) reported that sepia ink

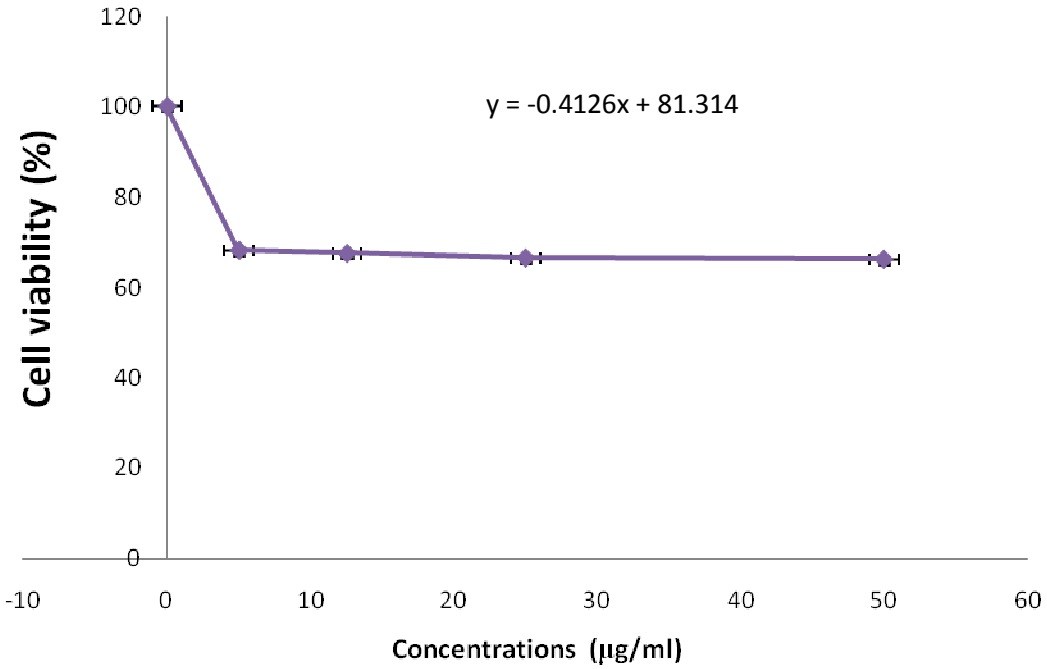

Figure 5. *In vitro* cytotoxic activity of cuttlefish ink extract (IE) on HepG2 liver hepatocellular carcinoma.

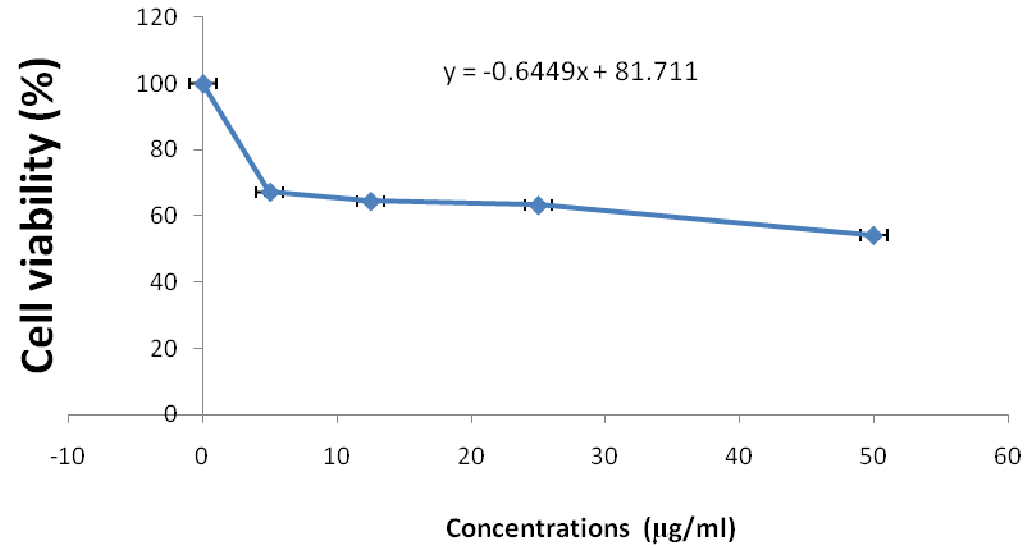

Figure 6. *In vitro* cytotoxic activity of freshwater clam extract (CE) on HepG2 liver HCC.

elevated SOD activity in the liver and kidney of mice in a dose dependent manner. Background researches showed that melanin of sepia ink, like SOD, can catalyze O2- to H2O2, and thus avoid the free radical chain reaction triggered by O2- (Chen et al., 2007). Melanin of squid ink may act as SOD due to the presence of DHI which catalyzing the disproportionation of O2•– to H2O2 and O2 (Meyskens et al., 2001). Moreover, melanins also absorb cationic metal ions such as iron and copper *in vivo* that can dramatically affect the redox state of the polymer by promoting the production of the highly reactive HO• in a Fenton type reaction (Fisher, 2003). Also, two different metabolites in the melanin, L- Dopa and dopamine effector molecules in concentrations sufficient to produce physiological effects have been identified (Lucero et al., 1994). In consonance with the study of Lucero et al. (1994) and Fiore et al. (2004) demonstrated that HPLC analysis of crude ink gland extract

in *S. officinalis* indicated the presence of L-dopa (2.18 ± 0.8 nmol/mg of protein) and dopamine (0.06 ± 0.02 nmol/mg of protein). The pro-oxidant and antioxidant actions of L-DOPA and dopamine in vitro were evaluated (Spencer et al., 1996).

Taurine is a sulfur containing amino acid which has been previously found to exhibit antioxidant properties (Das et al., 2009; Li et al., 2009). Viewed in conjunction with the report of Derby et al. (2007) and Soliman (2011), both squid ink extract and freshwater mussel extract of C. aegyptiaca, contain considerable amounts of taurine. Moreover, Soliman (2011) have shown the presence of high levels of precursor amino acids of GSH (glycine, glutamine and cysteine) in the freshwater mussel extract of *C. aegyptiaca*. It can be concluded from the aforementioned investigation that IE and CE extracts may be two potent antioxidants which is based on their chemical structures.

All the currently available analgesic drugs such as NSAIDs have more or less few adverse effects (Raquibul et al., 2009). As a result, more and more people are turning to natural products as alternative treatment of pain. Clark (2002) reported that pain continues to exert significant burdens on patients and the healthcare system. Pain represents the sum of reactions which include specialized and non-specialized tissues, as well as psychological and cognitive reactions to painful stimuli (Vaz et al., 1997). A useful way of categorizing pain for purposes of studying analgesics is to distinguish between visceral and somatic types (Pasternak, 1993). Visceral pain is perceived as a diffuse and burning sensation, while somatic is localized and sharp. As no single analgesic drug is ideal for all pains (Pirmohamed et al., 2004), additional therapies are always being sought. According to Raffa and Pergolizzi (2011), natural products might contain ingredients that offer such alternatives by acting through novel mechanisms of action or by interacting additively or synergistically through known mechanisms of action. The results of the present study revealed that, IE and CE extracts showed analgesic action in mice, by inhibiting the acetic acid-induced writhing as compared to the positive drug indomethacin. Acetic acid-induced writhing is a highly sensitive and useful test for analgesic screening. Acetic acid causes inflammatory pain by inducing capillary permeability and in part through local peritoneal receptors from peritoneal fluid concentration of prostaglandin E2 (PGE2) and prostaglandin F2α (PGF2α) (Bentley et al., 1983). So, IE and CE extracts might have some chemical constituents that are responsible to inhibit prostaglandin synthesis or to block pain sensation or might exert other specific mechanism to counteract the pain induced by acetic acid. But, this test alone can not specify the involvement of either central or peripheral activity (Chan et al., 1995). Thus, formalin test and hot-plate test are usually carried out in addition to the earlier mentioned test to distinguish between peripheral and central pain.

The hot plate test is considered to be selective for centrally acting opioid-like analgesics (Woolfe and MacDonald, 1994). Insight to hot plate test, it can be concluded that IE exhibited strong anti-nociceptive actions in mice by increasing the latency period in the hot-plate test as compared to the indomethacin, while CE did not. In these models, the increase in stress tolerance capacity of the animals as in the case of IE, indicates the possible involvement of a higher center (Vogel and Vogel, 1997). It is therefore thought that the analgesic effect of IE in the present study may involve central activity, while that of CE may involve peripheral activity.

In regard to formalin induced paw licking test in mice, the results of the present study showed that both extracts significantly decreased the number of paw lickings in both early and late phases. The formalin test in mice is a useful test for evaluating mild analgesics. The test employs an adequate painful stimulus, the animals show a spontaneous response and the test is sensitive to the commonly used analgesics. The test has two different phases, reflecting different types of pain. The first phase reflects a direct effect of formalin on nociceptors (non-inflammatory or neurogenic pain) whereas the second phase reflects inflammatory pain (Elizabetsky et al., 1995). In this study, IE and CE extracts are capable of attenuating both the neurogenic and the inflammatory phases of pain. This probably shows that the anti-nociceptive action of the extracts was mediated by both neurogenic and inflammatory mechanisms. It is well known that, centrally acting drugs such as opioids inhibit both phases equally (Shibata et al., 1989), but peripherally acting drugs such as aspirin and indomethacin only inhibit the late phase. Therefore, IE and CE extracts in the present study indicated to exert their action centrally not peripherally.

HCC represents the fifth most common malignancy and regarded as the main cause of mortality in patients with chronic liver diseases. HCC is a tumor characterized by high local invasiveness and high metastatic efficiency. Because of the high demand for anti-cancer drugs, attention has recently been focused on investigation and screening of pharmaceutical anticancer compounds in the natural products. The results of this study revealed that IE and CE showed potent and cytotoxic activities against HepG2 cell lines with IC50 67 and 49.24 µg/ml, respectively.

Results of the present study showed the antinociceptive and the antioxidant effects of both IE and CE extracts. It is well known that there are links between the inflammatory and nociceptive, oxidative and cancer processes and the ability to inhibit any of the processes will definitely lead to the inhibition of the others (Zakaria et al., 2011). Takaya et al. (1994) confirmed the antitumor activity of a peptidoglycan fraction from the squid (Illex argentinus) ink against Meth A fibrosarcoma in mice. Our results are in conformity with the results obtained by them.

Lu et al. (1994), working with cuttlefish ink in mice found increased humoural immunity in ink treated mice. The antitumor fraction of the I. argentinus ink was separated by Phenyl Sepharose CL-4B chromatography into three fractions: illexin peptidoglycan, tyrosinase, and the complex of them (Naraoka et al., 2000). The third fraction containing the illexin peptidoglycan and tyrosinase showed the highest activity against Meth A tumour in BALB/c mice, suggesting the role of both components in antitumour activity of squid ink. The melanin free ink of the cuttlefish, *S. officinalis* is shown to have toxic effect on a variety of cell lines and the active factor was identified as tyrosinase (Russo et al., 2003).

Chemotherapeutic drugs can induce cell death through two ways: necrosis and apoptosis. Apoptosis is an energy-dependent form of programmed cell death that differs from necrosis (Koh et al., 2005). Necrosis is an acute form of cell death and causes cell lysis that is typically followed by an inflammatory response, which then can produce side effects. Therefore, new types of antitumor drugs should induce apoptosis, not necrosis, in tumor cells. Russo et al. (2003) showed that, purified sepia tyrosinase was found to induce a significant increase in caspase 3 activity in PC 12 cells, leading eventually to an irreversible apoptotic process.

Conclusions

The HCC remains a malignant disease leading to death. Significant progress must be made in the management of the disease. Because of its complexity, a multidisciplinary approach must be implemented to support the different aspects in HCC. It can be concluded from the results of this study that, IE might exert its antitumor effect through apoptotic effect rather than necrotic effect. Further study will be needed to deduce the pathway by which CE exert its antitumor effect. A better understanding of the molecular and histological changes may be responsible for the occurrence of the disease and should allow the development of new diagnostics and effective treatments for HCC.

REFERENCES

Aleem E, Elshayeb A, Elhabachi N, Mansour AR, Gowily A, Hela A (2012). Serum IGFBP 3 is a more effective predictor than IGF 1 and IGF-2 for the development of hepatocellular carcinoma in patients with chronic HCV infection. Oncol. Lett. 3(3):704-712.

Anwar WA, Khaled HM, Amra HA, El-Nezami H, Loffredo CA (2008). Changing pattern of hepatocellular carcinoma (HCC) and its risk factors in Egypt: possibilities for prevention. Mutat. Res. 659:176-184.

Arun B, Goss P (2004). The role of COX-2 inhibition in breast cancer treatment and prevention. Semin. Oncol. 31:22-29.

Bentley GA, Newton SH, Starr J (1983). Studies on the antinociceptive action of agonist drugs and their interaction with opoid mechanisms. Br. J. Pharmacol. 79(1):125–134.

Bosch FX, Ribes J, Cleries R, Diaz M (2005). Epidemiology of hepatocellular carcinoma. Clin. Liver Dis. 9(2):191–211.

Caldwell RL (2005). An observation of inking behavior protecting adult Octopus bocki from predation by Green Turtle (*Chelonia mydas*) hatchlings. Pac. Sci. 59(1):69-72.

Chan TE, Tsai HY, Tian-Shang W (1995). Antiinflammatory and analgesic activities from the root of *Angelica pubescens*. Planta Med. 61:2-8.

Chen SG, Xue CH, Xue Y, Li ZJ, X. Gao X, Ma Q (2007). Studies on the free radical scavenging activities of melanin from squid ink. Chin. J. Mar. Drugs 26(1):24-27.

Clark JD (2002). Chronic pain prevalence and analgesic prescribing in a general medical population. J. Pain Sym. Manag. 23:131–137.

Das J, Ghosh J, Manna P, Sinha M, Sil PC (2009). Taurine protects rat testes against NaAsO2-induced oxidative stress and apoptosis via mitochondrial dependent and independent pathways. Toxicol. Lett. 187(3):201–210.

Derby CD, Kicklighter CE, Johnson PM, Zhang X (2007). Chemical composition of inks of diverse marine mollusks suggests convergent chemical defenses. J Chem. Ecol. 33(5):1105-1113.

Eddy NB, Touchberry CF, Lieberman IE (1950). Synthetic analgesics, a methadone isomers and derivatives. J. Pharmacol. Exp. Ther. 98(2):121-137.

Elizabetsky E, Marschner J, Souza DO (1995). Effects of linalool on glutamatergic system in the rat cerebral cortex. Neurochem. Res. 20:461-465.

Fahmy SR, Hamdi SAH (2011). Curative effect of the Egyptian marine *Erugosquilla massavensis* extract on carbon tetrachloride-induced oxidative stress in rat liver and erythrocytes. Eur. Rev. Med. Pharmacol. Sci. 15(3):303-312.

Fahmy SR, Hamdi SAH, Abdel-Salam AS (2009). Curative effect of dietary freshwater and marine crustacean extracts on carbon tetrachloride-induced nephrotoxicity. Austr. J. Basic Appl. Sci. 3(3):2118-2129.

Fiore G, Poli A, Di Cosmo A, d'Ischia M, Palumbo A (2004). Dopamine in the ink defense system of *Sepia officinalis*: biosynthesis, vesicular compartmentation in mature ink gland cells, nitric oxide (NO)/cGMP-induced depletion and fate in secreted ink. Biochem. J. 378:785-791.

Fisher CJ (2003). Melanin: The Pigmented Truth. Free Radicals Biol. Med. pp.1-10.

Greenwald P, Clifford CK, Milner JA (2001). Diet and cancer prevention. Eur. J. Cancer 37(8):948-965.

Hong K, Gao AH, Xie QY, Gao H, Zhuang L, Lin HP,Yu HP, Li J,Yao XS, Goodfellow M, Ruan JS (2009). Actinomycetes for marine drug discovery isolated from mangrove soils and plants in China. Mar. Drugs 7(1): 24–44.

Hunskaar S, Hole K (1997). The formalin test in mice; Dissociation between inflammatory and non-inflammatory pain. Pain 30:103-114.

Joyce DA (1987). Oxygen radicals in disease. Adv. Drug React. Bull. 127:476-479.

Katritzky AR, Akhmedov NG, Denisenko SN, Denisko OV (2002). 1H NMR spectroscopic characterization of solutions of sepia melanin, sepia melanin free acid and human hair melanin. Pigment Cell Res. 15(2):93-97.

Kimura I, Kumamoto T, Matsuda A, Kataoka M, Kokuba (1998). Effects of BX 661 A, a new therapeutic agent for ulcerative colitis, on reactive oxygen species in comparison with salazosulfapyridine and its metabolite sulfapyridine. Arzneimittelforschung 48(10):1007–1011.

Koh DW, Dawson TM, Dawson VL (2005). Mediation of cell death by poly (ADP-ribose) polymerase-1. Pharmacol. Res. 52:5-14.

Koyama T, Chounan R, Uemura D, Yamaguchi K, Yazawa K (2006). Hepatoprotective effect of a hot-water extract from the edible thorny oyster *Spondylus varius* on carbon tetrachloride -induced liver injury in mice. Biosci. Biotechnol. Biochem. 70(3):729-731.

Kumarasamy Y, Byres M, Cox PJ, Jaspars M, Nahar L, Sarker SD (2007). Screening seeds of some Scottish plants for free-radical scavenging activity. Phytother. Res. 21(7):615-621.

Li CY, Deng YL, Sun BH (2009). Taurine protected kidney from oxidative injury through mitochondrial-linked pathway in a rat model of nephrolithiasis. Urol. Res. 37(4):211-220.

Liu H, Luo P, Chen S, Shang J (2011). Effects of Squid Ink on Growth Performance, Antioxidant Functions and Immunity in Growing Broiler Chickens. Asian-Australian J. Anim. Sci. 24(12):1752–1756.

Lu C, Xie G, Hong M, Zhong J (1994). Effects of cuttle fish ink on immunologic function in mice. Chin. J. Mar. Drugs 13(4): 23-25.
Lucero MT, Farrington H, Gilly WF (1994). Qualification of L-Dopa and dopamine in squid ink: implications for chemoreception. Biol. Bull. 187:55-63.
Mbagwu HO, Anene RA, Adeyemi OO (2007). Analgesic, antipyretic and antiinflammatory properties of *Mezoneuron benthamianum* Baill Caesalpiniaceae. Niger. Q. J. Hos. Med. 17(1):35 – 41.
Meyskens FL, Farmer P, Fruehauf JP (2001). Redox regulation in human melanocytes and melanoma. Pigment Cell Res. 14:148-154.
Moloukhia H, Sleem S (2011). Bioaccumulation, fate and toxicity of two heavy metals common in industrial wastes in two aquatic Molluscs. J. Am. Sci. 7(8):459-464.
Naraoka T, Chung HS, Uchisawa H, Sasaki J, Matsue H (2000). Tyrosinase activity in antitumour compounds of squid ink. Food Sci. Technol. Res. 6(3):171-175.
Nithya M, Ambikapathy V, Panneerselvam A (2011). Effect of pharaoh's cuttlefish ink against bacterial pathogens. Asian J. Plant Sci. Res. 1(4):49-55.
Noda N, Wakasugi H (2001). Cancer and Oxidative Stress. J. Japan Med. Assoc. 44(12):535–539.
Nwafor PA, Jacks TW, Ekanem AU (2007). Analgesic and anti-inflammatory effects of methanolic extract of *Pausinystalia mecroceras* stem bark in rodents. Int. J. Pharmacol. 3(1):86-90.
Okhawa H, Ohishi W, Yagi K (1979). Assay formulation lipid peroxides in animal tissues by thiobarbituric acid reaction. Anal. Biochem. 95:51-353.
Pasternak GW (1993). Pharmacological mechanisms of opioid analgesics. Clin. Neuropharmacol.16:1-18.
Pirmohamed M, James S, Meakin S, Green C, Scott AK, Walley TJ, Farrar K, Park BK, Breckenridge AM (2004). Adverse drug reactions as cause of admission to hospital: prospective analysis of 18 820 patients. Br. Med. J. 329: 15–19.
Prota G (1992). Melanins and Melanogenesis. Academic Press, New York.
Raffa RB, Pergolizzi JV Jr (2011). Deciphering the mechanism(s) of action of natural products: analgesic peroxide oil as example. J. Clin. Pharm. Ther. 36(3):283-98.
Raquibul HSM, Jamila M, Majumder MM, Akter R, Hossain MM, Ehsanul HMM, Ashraful AM, Jahangir R, Sohel RM, Arif M, Rahman S (2009). Analgesic and antioxidant activity of the hydromethanolic extract of *Mikania scandens* (l.) Willd leaves. Am. J. Pharmacol. Toxicol. 4(1):1-7.
Rayburn ER, Ezell SJ, Zhang R (2009). Anti-Inflammatory Agents for Cancer Therapy. Mol. Cell Pharmacol. 1(1):29-43.
Roginsky V, Lissi EA (2005). Review of methods to determine chain-breaking antioxidant activity in food. Food Chem. 92:235-254.
Roseghini M, Severini C, Erspamer GF, Erspamer V (1996). Choline esters and biogenic amines in the hypobranchial gland of 55 molluscan species of the neogastropod Muricoidea superfamily. Toxicon 34(1):33-55.
Russo GL, Nisco ED, Fiore G, Di Donato P, d' Ischia M, Palumbo A (2003). Toxicity of melanin free ink of *Sepia officinalis* to transformed cell lines: identification of the active factor as tyrosinase. Biochem. Biophys. Res. Comm. 308(2):293-299.
Sanchez-Moreno C, Larrauri JA, Saura-Calixto F (1998). A procedure to measure the antiradical efficiency of polyphenol. J. Sci. Food Agric. 76(2):270-276.
Sarkar D, Fisher PB (2006). Molecular mechanisms of aging-associated inflammation. Cancer Lett. 236:13-23.
Sasaki J, Ishita K, Takaya Y, Uchiswa H, Matsue H (1997). Antitumor activity of squid ink. J. Nutr. Sci. Vitaminol. 43(4):455-461.
Schaufelberger DE, Koleck MP, Beutler JA, Vatakis AM, Alvarado AB, Andrews P, Marzo LV, Muschik GM, Roach J, Ross JT (1991). The Large-Scale Isolation of Bryostatin 1 from Bugulaneritina following Current Good Manufacturing Practices. J. Nat. Prod. 54:1265-1270.
Schwartsmann G (2000). Marine organisms and other novel natural sources of new anticancer drugs. Ann. Oncol. 11:235-243.
Schwartsmann G, Rocha AB, Berlinck R, Jimeno J (2001). Marine organisms as a source of new anticancer agents. Lancet Oncol. 2(4):221-225.
Shibata S, Cassone VM, Moore RY (1989). Effects of melatonin on neural activity in the rat suprachiasmatic nucleus *in vitro*. Neurosci. Lett. 97:140-144.
Skehan P, Storeng R, Scudiero D, Monks A, McMahon JM, Vistica D, Warren JT, Bokesch H, Kenney S, Boyd MR (1990). New Colorimetric cytotoxicity assay for anticancer-drug Screening. J. Nat. Cancer Inst. 82(13):1107-1112.
Sleem SH, Ali TG (2008). Application of RADP-PCR in taxonomy of certain freshwater Bivalves of Genus *Coelatura*. Glob. J. Mol. Sci. 3(1):27-31.
Soliman AM (2011). The extract of Coelatura aegyptiaca, a freshwater mussel, ameliorates hepatic oxidative stress induced by monosodium glutamate in rats. Afr. J. Pharm. Pharmacol. 5(3):398-408.
Spencer JP, Jenner A, Butler J, Aruoma OI, Dexter DT, Jenner P (1996). Evaluation of the pro-oxidant and antioxidant actions of L-DOPA and dopamine *in vitro*: implications for Parkinson's disease. Free Radical Res. 24(2):95-105.
Takaya Y, Uchisawa H, Matsue H, Narumi F, Sasaki J, Iahada KL (1994). An investigation of the antitumour peptidoglycan fraction from the squid ink. Biol. Pharm. Bull. 17(6):846-851.
Tao L, Zhang J, Liang Y, Chen L, Zheng L, Wang F, Mi Y, She Z, To KKW, Lin Y, Fu L (2010). Anticancer effect and structure-activity analysis of marine products isolated from metabolites of mangrove fungi in the South China Sea. Mar. Drugs 8(4):1094-1105.
Terry P, Lagergren J, Ye W, Nyrén O, Wolk A (2000). Antioxidants and cancers of the esophagus and gastric cardia. Int. J. Cancer 87(5):750–754.
Tripathi YB, Sharma M (1998). Comparison of the antioxidant action of the alcoholic extract of *Rubia cordifolia* with Rubiadin. Indian J. Biochem. Biophys. 35(5):313-316.
Vanden HMJ, Clark DG, Fielder RJ, Koundakjian PP, Oliver GJA, Pelling D, Tomlinson NJ, Walker A (1990). The international validation of a fixed-dose procedure as an alternative to the classical LD_{50} test. Food Chem. Toxicol. 28:469-482.
Vaz ZR, Mata LV, Calixto JB (1997). Analgesic effect of herbal medicine Catuma in thermal and chemical models of nociception in mice," Phytother. Res. 11:101-106.
Velioglu YS, Mazza G, Gao L, Oomah BD (1998). Antioxidant activity and total phenolics in selected fruits, vegetables, and grain products. J. Agric. Food Chem. 46(10):4113–4117.
Vennila R, Rajesh kRK, Kanchana S, Arumugam M, Balasubramanian T (2011). Investigation of antimicrobial and plasma coagulation property of some molluscan ink extracts: Gastropods and cephalopods. Afr. J. Biochem. Res. 5(1):14-21.
Vogel HG, Vogel WH (1997). Drug Discovery and Evaluation; Pharmacological Assays." Springer Verlag, Germany. Chapter H, pp. 368-370.
Whitehead A, Curnow RN (1992). Statistical evaluation of the fixed-dose procedure. Food Chem. Toxicol. 30:313-324.
Woolfe G, MacDonald AD (1994).The evaluation of the analgesic action of pethidine hydrochloride. J. Pharmacol. Exp. Ther. 80:300-307.
Yang JD, Roberts LR (2010). Epidemiology and management of hepatocellular carcinoma. Infect. Dis. Clin. North Am. 24(4):899–919.
Zakaria ZA, Mohamed AM, Mohd JNS, Rofiee MS, Somchit MN, Zuraini A, Arifah AK, Sulaiman MR (2011). In vitro cytotoxic and antioxidant properties of the aqueous, chloroform and methanol extracts of *Dicranopteris linearis* leaves. Afr. J. Biotechnol. 10(2):273-282.
Zhang YJ, Xu XY, Wang BQ (2003). The influence of compound sepia capsules on SOD activity in mice. Chin. New Med. 2(1): 23-27.
Zhong JP, Wang G, Shang JH, Pan JQ, Li K, Huang Y, Liu HZ (2009). Protective effects of squid ink extract towards hemopoietic injuries induced by cyclophosphamide. Mar. Drugs 7(1):9-18.

academicJournals

Vol. 7(22), pp. 1523-1530, 15 June, 2013
DOI 10.5897/AJPP2013.3566
ISSN 1996-0816 © 2013 Academic Journals
http://www.academicjournals.org/AJPP

African Journal of Pharmacy and Pharmacology

Full Length Research Paper

Synthesis and neuropharmacological evaluation of some new isoxazoline derivatives as antidepressant and anti-anxiety agents

Jagdish Kumar[1], Gita Chawla[1]*, Himanshu Gupta[2], Mymoona Akhtar[1], Om prakash Tanwar[3] and Malay Bhowmik[4]

[1]Department of Pharmaceutical Chemistry, Faculty of Pharmacy, Hamdard University, New Delhi-110062, India.
[2]Faculty of Pharmacy, Hamdard University, New Delhi, India.
[3]Drug Design and Medicinal Chemistry Laboratory, Hamdard University, New Delhi-110062, India.
[4]Neuro behavioral Pharmacology Lab., Hamdard University, New Delhi-110062, India.

Accepted 18 April, 2013

A series of 3-(furan-2-yl)-5-(substituted phenyl)-4,5-dihydro-1,2-oxazole derivatives (2a to j) were synthesized by Claisen Schmidt condensation of 2-acetyl furan with different types of aromatic aldehyde, as chalcones and their subsequent cyclization to 4,5-dihydro-1,2-oxazole with hydroxylamine hydrochloride. The chemical structures of the synthesized compounds were confirmed by IR, ^{1}H NMR, ^{13}C-NMR and mass spectrometric data. This study further involves evaluation of synthesized compounds for antidepressant and antianxiety activities using force swimming test (FST) and elevated plus maze method, respectively. Most of the tested compounds were found to be moderate to significant activities at the dose level of 10 mg/kg, compared to reference drugs imipramine and diazepam, respectively. Compound 4-[3-(furan-2-yl)-4,5-dihydro-1,2-oxazol-5-yl]phenol (2e) emerged as the most potent antidepressant agent acting through monoamine oxidase (MAO) inhibition without any significant neurotoxicity. The molecular docking study were also carried out on the falcipain-2 receptor (PDB id: 2Z5X) for all the compounds and compound 2e was found to occupy in the receptor cavity and forms hydrogen bond and hydrophobic interactions with active residues.

Key words: Isoxazoline, Claisen Schmidt condensation, antidepressant, antianxiety.

INTRODUCTION

Anxiety is a common central nervous system (CNS) disorder due to various stress factors (physiological, psychological and sociological) resulting in disturbance of daily life. Nowadays with increasing competition, anxiety has become one of the wide spread psychiatric disorder affecting around 1/8th of the total population globally consequently turned into an important area of research in psychopharmacology (Crowley and Lucki, 2005; Koksal and Bilge, 2007). Moreover, depression is also increasingly becoming ubiquitous and serious mental disease by impacting on all aspects of a person's life. The etiology of depression (Henn et al., 2004; Gartside and Cowen, 2006; Deecher et al., 2006; Sanchez, 2006) is suggested to be the dysfunction of monoamine neurotransmitters in CNS, such as serotonin (5-hydroxytryptamine, or 5-HT), dopamine (DA) and norepinephrine (NE), but the specific etiology of major depression is still far from clear (Sanchez, 2006; Huang et al., 2006; Andersen et al., 2008).

*Corresponding author. E-mail: drgitachawla@gmail.com; gchawla@jamiahamdard.ac.in. Tel.: +91-9910090780, +91-11-26059688-Ext. 5610

The predominant monoamine theory (Owen and Whitton, 2006) combines depression with lowered concentrations of monoamine neurotransmitters at brain synapses. Treatment of depression thus may be achieved by restoring the monoamine levels to normal. Tricyclics (TCA), monoamine oxidase (MAO) inhibitors, selective serotonin reuptake inhibitors (SSRI), serotonine norepinephrine reuptake inhibitors (SNRI), norepinephrine dopamine reuptake inhibitors (NDRI), norepinephrine reuptake inhibitors (NRI), serotonin modulators and norepinephrine serotonin modulators are the major antidepressant drug classes used for the treatment of depressive disorders (Henn et al., 2004; Gartside and Cowen, 2006).

Nitrogen and oxygen containing five member heterocyclic compounds, have gained considerable attention due to the wide spectrum of pharmacological activi-ties. Among these, isoxazoline represents one of the most diverse bioactive moiety exhibiting a wide range of biological properties such as antidepressant, antianxiety (Gil et al., 2009; David et al., 1994; Edwin and Lilianna, 2004; Andres et al., 2007; Ignacio and Gil, 2007, 2004, 2008; Mary et al., 2011; Winters et al., 1985; Cesura et al., 1992; Amrein et al., 1999), anti-stress (Maurya et al., 2011; Andersen et al., 2008), anticonvulsant (Balalaie et al., 2000), antiviral (Lee et al., 2009), anti-inflammatory (Dannahardt et al., 2000), anti-inflammatory and analgesic activities (Jayashankar et al., 2009). Several isoxazoline derivatives have also been patented as therapeutic agents having antidepressant and anxiolytic activities. Recent studies have shown that isoxazoles are good inhibitors of brain enzymes like MAO. Moreover, isocarboxazid an isoxazole derivative is an irreversible and nonselective monoamine oxidase inhibitor (MAOI) used as antidepressant and anxiolytic (Fagervall and Ross, 1986). Similarly furan nucleus finds a wide variety of bioactive applications like cytotoxicity, anti-inflammatory (Chen et al., 2006), anti-tuberculosis (Tangallapally et al., 2006), anti-tumor (Sun et al., 2010), antidepressant, anticonvulsant (Zuhal et al., 2007), and MAO inhibitors (Kelekci et al., 2009; Jayaprakash et al., 2008; Karuppasamy et al., 2010).

Therefore, in this study, the target compounds were designed keeping the isoxazole bioactive moiety with the aim that the aforementioned molecules would have promising antidepressant and antianxiety properties.

MATERIALS AND METHODS

All the chemicals used were laboratory grade and procured from E. Merck (Germany) and S.D. Fine Chemicals (India). Melting points were determined by the open tube capillary method and are uncorrected.

The thin layer chromatography (TLC) plates (silica gel G) were used to confirm the purity of commercial reagents used, compounds synthesized and to monitor the reactions as well. Two different solvent systems: toluene:ethyl acetate:formic acid (5:4:1) and benzene:acetone (9:1) were used to run the TLC and spots were located under iodine vapors/UV light. IR spectra were obtained on a Perkin-Elmer 1720 FT-IR spectrometer (KBr Pellets). ^{1}H-NMR spectra were recorded on a Bruker AC 400 MHz, spectrometer using TMS as internal standard in DMSO-d_6.

Chemistry

General procedure for the preparation of 1-(furan-2-yl)-3-(substituted phenyl)prop-2-en-1-one (1a to j)

A mixture of 2-acetyl furan (0.01 mol) and appropriate aromatic aldehydes (0.01 mol) in absolute methanol (30 ml) were stirred at room temperature in the presence of base (aqueous solution of potassium hydroxide 40%; 15 ml) till completion of the reaction. The reaction mixture was kept overnight at room temperature and then poured into crushed ice followed by neutralization with HCl. The solid separated was filtered, dried and crystallized from ethanol. The purity of the chalcones was checked by TLC.

General procedure for the preparation of 3-(furan-2-yl)-5-(substituted phenyl)-4,5-dihydro-1,2-oxazole (2a to j)

To a solution of compounds 1a to j (0.01 mol) in absolute ethanol (50 ml), it was added dry pyridine (1 ml) and hydroxylamine hydrochloride (0.01 mol), and the contents was refluxed for 8 to 10 h and was left overnight. The solvent was evaporated and the residue was poured into cold water; the solid mass that separated out was filtered, washed with water dried and crystallized from methanol.

3-(Furan-2-yl)-5-phenyl-4,5-dihydro-1,2-oxazole (2a)

Yield 58%; m.p. 112°C. FTIR (KBr pellet) cm^{-1}: 1656 (C=N), 1352 (C–O–N), 1052 (C-O-C). ^{1}H NMR (DMSO-d_6) δ (ppm): 7.07–8.10 (7H, m, ArH), 6.18 (m, 1H, (furan CH); 5.78 (1H, m, $CH_{isoxazoline}$), 3.62 (1H, dd, J = 11.5, 5.6 Hz, $CH_{isoxazoline}$), 3.59 (1H, dd, J = 9.3, 7.5 Hz, $CH_{isoxazoline}$); ^{13}CNMR (DMSO-d_6) δ (ppm): 150.0, 145.4, 140.0, 139.4, 127.7, 126.9, 126.2, 125.3, 116.0, 115.2, 79.2, 42.9. MS: m/z 213 (M+). Elemental analysis: Calculated for $C_{13}H_{11}NO_2$: C, 73.23; H, 5.20; N, 6.57; found: C, 73.34; H, 5.28; N, 6.62%.

5-(4-Chlorophenyl)-3-(furan-2-yl)-4,5-dihydro-1,2-oxazole (2b)

Yield 65%; m.p. 142°C. FTIR (KBr pellet) cm^{-1}: 1661 (C=N), 1356 (C–O–N), 1058 (C-O-C). ^{1}H NMR (DMSO-d_6) δ (ppm): 7.10–7.34 (6H, m, ArH), 6.08 (m, 1H, (furan C-CH); 5.81 (1H, m, $CH_{isoxazoline}$), 3.61 (1H, dd, J = 11.2, 5.4 Hz, $CH_{isoxazoline}$), 3.60 (1H, dd, J = 9.2, 7.7 Hz, $CH_{isoxazoline}$); ^{13}CNMR (DMSO-d_6) δ (ppm): 150.0, 145.4, 139.4, 134.6, 129.9, 129.2, 124.0, 116.0, 115.2, 79.2, 42.9. MS: m/z 247 (M^+) and 249 (M+2). Elemental analysis: Calculated for $C_{13}H_{10}ClNO_2$: C, 63.04; H, 4.07; N, 5.66; found: C, 63.18; H, 4.12; N, 5.72%.

5-(4-Bromophenyl)-3-(furan-2-yl)-4,5-dihydro-1,2-oxazole (2c)

Yield 64%; m.p. 118°C. FTIR (KBr pellet) cm^{-1}: 1667 (C=N), 1354 (C–O–N), 1066 (C-O-C). ^{1}H NMR (DMSO-d_6) δ (ppm): 7.08–7.24 (6H, m, ArH), 6.15 (m, 1H, (furan C-CH); 5.67 (1H, m, $CH_{isoxazoline}$), 3.65 (1H, dd, J = 11.7, 5.6 Hz, $CH_{isoxazoline}$), 3.58 (1H, dd, J = 9.7, 7.9 Hz, $CH_{isoxazoline}$); ^{13}CNMR (DMSO-d_6) δ (ppm): 150.0, 145.4, 139.4, 132.4, 128.7, 124.7, 122.2, 116.0, 115.2, 79.2, 42.9. MS: m/z 292 (M^+) and 294 (M+2). Elemental analysis: Calculated for $C_{13}H_{10}BrNO_2$: C, 53.45; H, 3.45; N, 4.79; found: C,

53.57; H, 3.54; N, 4.86%.

5-(4-Fluorophenyl)-3-(furan-2-yl)-4,5-dihydro-1,2-oxazole (2d)

Yield 58%; m.p. 112 ºC. FTIR (KBr pellet) cm^{-1}: 1661 (C=N), 1357 (C–O–N), 1057 (C-O-C). ^{1}H NMR (DMSO-d_6) δ (ppm): 7.11–7.28 (6H, m, ArH), 6.17 (m, 1H, (furan C-CH); 5.73 (1H, m, $CH_{isoxazoline}$), 3.65 (1H, dd, *J* = 11.7, 5.7 Hz, $CH_{isoxazoline}$), 3.61 (1H, dd, *J* = 9.4, 7.7 Hz, $CH_{isoxazoline}$); ^{13}CNMR (DMSO-d_6) δ (ppm): 159.4, 150.0, 145.4, 139.0. 127.7, 122.2, 116.0, 115.6, 115.2, 79.2, 42.9. MS: m/z 231 (M+). Elemental analysis: Calculated for $C_{13}H_{10}FNO_2$: C, 67.53; H, 4.36; N, 6.06; found: C, 67.62; H, 4.45; N, 6.14%.

4-[3-(Furan-2-yl)-4,5-dihydro-1,2-oxazol-5-yl]phenol (2e)

Yield 64%; m.p. 126°C. FTIR (KBr pellet) cm^{-1}: 1651 (C=N), 1357 (C–O–N), 1049 (C-O-C). ^{1}H NMR (DMSO-d_6) δ (ppm): 6.75–7.26 (6H, m, ArH), 6.13 (s, 1H, Ar-OH), 6.12 (m, 1H, (furan C-CH); 5.80 (1H, m, $CH_{isoxazoline}$), 3.59 (1H, dd, *J* = 11.3, 5.7 Hz, $CH_{isoxazoline}$), 3.58 (1H, dd, *J* = 9.6, 7.6 Hz, $CH_{isoxazoline}$); ^{13}CNMR (DMSO-d_6) δ (ppm): 157.8, 150.0, 145.4, 139.4, 129.8, 118.9, 118.2, 116.0, 115.2, 79.0, 42.9. MS: m/z 229 (M+). Elemental analysis: Calculated for $C_{13}H_{11}NO_3$: C, 68.11; H, 4.84; N, 6.11; found: C, 68.22; H, 4.92; N, 6.18%.

3-(Furan-2-yl)-5-(4-methylphenyl)-4,5-dihydro-1,2-oxazole (2f)

Yield 54%; m.p. 138°C. FTIR (KBr pellet) cm^{-1}: 1656 (C=N), 1352 (C–O–N), 1052 (C-O-C). ^{1}H NMR (DMSO-d_6) δ (ppm): 2.13 (s, 3H, Ar-CH_3), 7.10–7.24 (6H, m, ArH), 6.20 (m, 1H, (furan C-CH); 5.81 (1H, m, $CH_{isoxazoline}$), 3.65 (1H, dd, *J* = 11.6, 5.8 Hz, $CH_{isoxazoline}$), 3.57 (1H, dd, *J* = 9.5, 7.8 Hz, $CH_{isoxazoline}$); ^{13}CNMR (DMSO-d_6) δ (ppm): 151.6, 149.2, 140.2, 138.8, 131.0, 129.5, 124.1, 114.5, 110.8, 79.2, 42.8, 20.6. MS: m/z 227 (M+). Elemental analysis: Calculated for $C_{14}H_{13}NO_2$: C, 79.99; H, 5.77; N, 6.16; found: C, 80.03; H, 6.23; N, 6.23%.

5-(4-Methoxyphenyl)-3-(furan-2-yl)-4,5-dihydro-1,2-oxazole (2g)

Yield 58%; m.p. 134-136°C. FTIR (KBr pellet) cm^{-1}: 1651 (C=N), 1357 (C–O–N), 1054 (C-O-C). ^{1}H NMR (DMSO-d_6) δ (ppm): 3.43 (s, 3H, Ar-OCH_3), 6.87–7.29 (6H, m, ArH), 6.10 (m, 1H, (furan C-CH); 5.78 (1H, m, $CH_{isoxazoline}$), 3.61 (1H, dd, *J* = 11.3, 5.7 Hz, CH), 3.59 (1H, dd, *J* = 9.1, 7.6 Hz, $CH_{isoxazoline}$); ^{13}CNMR (DMSO-d_6) δ (ppm): 151.7, 145.4, 139.4, 138.8, 131.0, 124.1, 129.5, 116.0, 115.2, 79.2, 46.8, 42.6. MS: m/z 243 (M+). Elemental analysis: Calculated for $C_{14}H_{13}NO_3$: C, 69.12; H, 5.39; N, 5.76; found: C, 69.23; H, 5.42; N, 5.84%.

4-[3-(Furan-2-yl)-4,5-dihydro-1,2-oxazol-5-yl]aniline (2h)

Yield 56%; m.p. 106°C. FTIR (KBr pellet) cm^{-1}: 1658 (C=N), 1357 (C–O–N), 1055 (C-O-C). ^{1}H NMR (DMSO-d_6) δ (ppm): 3.36 (s, 2H, Ar-NH_2), 6.50–7.07 (6H, m, ArH), 6.08 (m, 1H, (furan C-CH); 5.79 (1H, m, $CH_{isoxazoline}$), 3.63 (1H, dd, *J* = 11.6, 5.7 Hz, $CH_{isoxazoline}$), 3.60 (1H, dd, *J* = 9.5, 7.6 Hz, $CH_{isoxazoline}$); ^{13}CNMR (DMSO-d_6) δ (ppm): 150.6, 145.4, 145.3, 139.4, 127.2, 120.0, 116.4, 116.0, 115.2, 79.2, 42.9. MS: m/z 228 (M+). Elemental analysis: Calculated for $C_{13}H_{12}N_2O_2$: C, 68.41; H, 5.30; N, 12.27; found: C, 68.52; H, 5.41; N, 12.34%.

N,N-Dimethyl-4-[3-(furan-2-yl)-4,5-dihydro-1,2-oxazol-5-yl]aniline (2i)

Yield 62%; m.p.140°C. FTIR (KBr pellet) cm^{-1}: 1652 (C=N), 1357 (C–O–N), 1053 (C-O-C). ^{1}H NMR (DMSO-d_6) δ (ppm): 2.84 (s, 6H, Ar-N-$(CH_3)_2$), 6.44–7.08 (6H, m, ArH), 6.12 (m, 1H, (furan C-CH); 5.80 (1H, m, $CH_{isoxazoline}$), 3.65 (1H, dd, *J* = 11.7, 5.7 Hz, $CH_{isoxazoline}$), 3.60 (1H, dd, *J* = 9.4, 7.6 Hz, $CH_{isoxazoline}$); ^{13}CNMR (DMSO-d_6) δ (ppm): 151.3, 148.3, 145.4, 139.4, 128.8, 118.6, 116.0, 115.2, 113.4, 79.2, 42.9, 40.3. MS: m/z 256 (M+). Elemental analysis: Calculated for $C_{15}H_{16}N_2O_2$: C, 70.29; H, 6.29; N, 10.93; found: C, 70.33; H, 6.36; N, 10.98%.

5-(3,4-Dimethoxyphenyl)-3-(furan-2-yl)-4,5-dihydro-1,2-oxazole (2j)

Yield 58%; m.p. 125°C. FTIR (KBr pellet) cm^{-1}: 1656 (C=N), 1352 (C–O–N), 1052 (C-O-C). ^{1}H NMR (DMSO-d_6) δ (ppm): 3.85 (s, 6H, Ar-$(OCH_3)_2$), 6.44–7.07 (5H, m, ArH), 6.11 (m, 1H, (furan C-CH); 5.80 (1H, m, $CH_{isoxazoline}$), 3.65 (1H, dd, *J* = 11.6, 5.8 Hz, $CH_{isoxazoline}$), 3.57 (1H, dd, *J* = 9.4, 7.6 Hz, $CH_{isoxazoline}$); ^{13}CNMR (DMSO-d_6) δ (ppm): 150.0, 149.8, 148.2, 145.4, 139.4, 130.5, 121.3, 116.0, 115.2, 113.5, 110.2, 80.3, 56.0, 42.8. MS: m/z 273 (M+). Elemental analysis: Calculated for $C_{15}H_{15}NO_4$: C, 65.92; H, 5.53; N, 5.13; found: C, 65.98; H, 5.62; N, 5.23%.

Pharmacological screening

Antidepressant activity (Forced swim test in mice)

Behavioral despair or forced swim test (FST) was proposed as a model to test antidepressant activity by Porsolt et al. (1977). It was suggested that mice or rats when forced to swim in restricted space from where they cannot escape are induced to a characteristic behavior of immobility. This behavior reflects a state of despair which can be reduced by several agents which are therapeutically effective in human depression. The behavioral despair test is employed to assess the antidepressant activity of synthesized derivatives. Albino mice of 20 to 25 g in a group of six each were used and on the first day of the experiment (pretest session), mice were individually placed in a cylindrical recipient (Plexiglass cylinder) of dimensions (diameter, 10 cm; height, 25 cm) containing 10 cm of water 25°C. The animals were left to swim for 6 min before being removed, dried and returned to their cages. The procedure was repeated 24 h later, in 5 min swim session (test session). The synthesized compounds (10 mg kg^{-1}), and imipramine, as a reference antidepressant drug (10 mg kg^{-1}) were suspended in a 1% aqueous solution of Tween 80. The drugs were injected intraperitoneally (ip) in a standard volume of 0.5 ml/20 g body weight, 1 h prior to the test. Control animals received 1% aqueous solution of Tween 80. Then, the mice were dropped individually into the Plexiglass cylinder and left in the water for 6 min. After the first 2 min of the initial vigorous struggling, the animals were immobile. A immobility time is the time spent by mice floating in water without struggling, making only those moment necessary to keep the head above the water. The total duration of immobility was recorded during the last 4 min of the 6 min test session.

MAO inhibition

The synthesized compounds 2b, 2d, 2e, and 2f tested to determine their activity toward MAO rat brain mitochondria were isolated according to (Basford et al., 1967; Johnston et al., 1968). The inhibitory effects of compounds on MAO were determined using a

fluorimetric method as described by Matsumoto et al. (1985), Weissbach et al. (1960) and Knoll et al. (1972). The mitochondrial fractions were incubated at 38°C for 30 min with the substrate. The incubation mixture containing 0.1 ml phosphate buffer (0.25 M, pH 7.4), mitochondrial suspension (6 mg/ml), the substrate (0.1 mM) and test compounds at five different concentrations ranging from 0.5 nM to 0.1 M (0, 0.5 nM, 5 nM, 5 mM, 5 mM and 100 mM) were dissolved in propylene glycol. The mixture was incubated at 37°C for 60 min and inhibition was quenched by adding perchloric acid. The samples were centrifuged at 10,000 g for 5 min and the supernatant was completed to 2.7 ml using 1 N NaOH and measured with a Spectrofluorimeter (RF-5301PC Shimadzu). The values were from 3 independent samples that were measured in duplicate. The average value of the duplicate measurements was used for the statistical analysis. Protein concentration was determined according to a previously reported method. The MAO results are expressed as percent inhibition (Table 2).

Docking studies

Docking studies were performed using Glide module of the Schrodinger-9 software on the falcipain-2 receptor (PDB id: 2Z5X). Receptor preparation was done using protein preparation wizard using defaults options and the final root-mean-square deviation (RMSD) was used as <30 Å. The structures were sketched in maestro graphical user interface and were energy minimized/cleaned up by Lig prep module of same software using OPLS_2005 force field and proper protonation states were assigned with the ionizer subprogram at pH 7.2 ± 0.2 (Lig Prep 2009). A grid of 20 Å was set for the docking calculations. Glide XP module was used for final docking studies (Glide, 2009).

Antianxiety activity

Elevated plus maze apparatus for mice (Moser, 1989; Rabbani et al., 2004; Pellow et al., 1985; Kulkarni, 2002; Sienkiewicz et al., 2003) consisted of two open (16 × 5 cm^2) and two closed arms (16 × 5 × 12 cm^3) facing each other with an open roof. The entire maze is elevated of a height of 25 cm. Concentration of each compounds (10 mg/kg) were used in the form of suspensions in 1% tween 80. All solutions were prepared freshly on test days and given intraperitoneally (ip) in a volume of 2 ml/kg body weight of mice. The experimental animals were treated with Diazepam (2 mg/kg, n = 6), or the compounds (10 mg/kg) 60 min before evaluation in the maze. The control group was given saline with 1% tween 80. Test begun with the mice placed singly in the center of plus-maze facing one open arm. The number of entries and the time spent in closed and open arms was recorded for 5 min. Entry into an arm was defined as the animal placing all four paws onto the arm. Total exploratory activity (number of entries, time spent in open and closed arms) were also registered. After each test, the maze was carefully cleaned up with a wet tissue paper (10% ethanol solution). Groups of six male albino mice (20 to 24 g) were conditioned to laboratory environment (12 h light and 12 h dark), with free access to water and food. Data obtained in the test were compared against the control group by using the ANOVA method and followed by a post Dunnett test. The results of elevated plus maze (EPM)have been summarized in Table 3.

Neurotoxicity (NT)

Assessment of motor coordination in Rota-Rod test was used to evaluate NT. With the aim of investigating test compounds induced any changes in motor coordination of the animals, Rota-Rod test was performed. The animal was placed on a 1 inch diameter knurled wooden rod rotating at 6 rpm. Normal mice remain on a rod rotating at this speed indefinitely. Neurologic toxicity was defined as the failure of the animal to remain on the rod for 1 min.

Statistical analyses

The obtained experimental data were analyzed by one way analysis of variance (ANOVA) followed by Dunnet's test and were used to evaluate the results, using InStat Graph Pad (version 3.06, Graph Pad Software Inc., San Diego, CA, USA). The results are expressed as mean + Standard error of mean (SEM); n represents the number of animals. Differences between data sets were considered as significant when p value was less than 0.05.

RESULTS AND DISCUSSION

Chemistry

As shown in Figure 1, the intermediate chalcones 1a to j was synthesized by Claisen-Schmidt condensation of 2-acetyl furan and the appropriate substituted aromatic aldehydes. Cyclization of 1a to j with hydroxylamine hydrochloride in the presence of dry pyridine afforded 2a to j. The structures of the new compounds 2a to j were confirmed by elemental analyses and spectral data. The physical constants of isoxazoline derivatives (2a-j) are shown in (Table 1). The IR spectrum of compound 2a showed absorption peak at 1352 cm^{-1} due to C-O and 1656 cm^{-1} for C=N stretching vibrations. The structure was further conformed by its ^1H NMR spectrum, which showed two double doublet at δ 3.62 and 3.59 for CH_2 protons of isoxazoline ring. The CH proton at C-5 of isoxazoline was obtained as a multiplet at δ 5.78. Thus, disappearance of signals of the olefinic protons and appearance of CH_2 and CH proton signals in the spectrum confirmed the formation of isoxazoline ring. The mass spectrum of the compound 2a showed molecular ion peak M^+ at m/z 213 corresponding to molecular formula $C_{13}H_{11}NO_2$.

Pharmacological activity

All the synthesized compounds were tested *in vivo* in order to evaluate their antidepressant and antianxiety activity. The pharmacological data of all the compounds is reported in Table 3. These compounds when screened for their antidepressant activity by forced swimming test at 10 mg kg^{-1} i.p., exhibited substantive antidepressant activity. All the substitutions were made at the phenyl ring to evaluate their structural activity relationship. The results of antidepressant activity showed that compounds having electron releasing groups at the para position of phenyl ring like 2g (p-OCH_3), 2h (p-NH_2), 2i (p-N,N-$(CH_3)_2$) and 2j (m,p-$(OCH_3)_2$) moderately decreased the immobility time (from -1.96 to -3.15%). However, para substituted derivatives having electron withdrawing groups significantly decreased the immobility time with respect to control. For example, compounds 2b (p-Cl, -

Table 1. Physicochemical parameters of the synthesized compounds (2a-j).

Compound	R	Molecular formula	Molecular weight	Yield (%)	Melting Point (°C)
2a	H	$C_{13}H_{11}NO_2$	213.23	58	112
2b	4-Cl	$C_{13}H_{10}ClNO_2$	247.67	65	142
2c	4-Br	$C_{13}H_{10}BrNO_2$	292.12	57	98
2d	4-F	$C_{13}H_{10}FNO_2$	231.22	60	115
2e	4-OH	$C_{13}H_{11}NO_3$	229.23	64	126
2f	4-CH_3	$C_{14}H_{13}NO_2$	227.25	54	138
2g	4-OCH_3	$C_{14}H_{13}NO_3$	243.25	58	134-136
2h	4-NH_2	$C_{13}H_{12}N_2O_2$	228.24	56	106
2i	4-$N(CH_3)_2$	$C_{16}H_{18}N_2O_2$	270.32	62	140
2j	3,4-$(OCH_3)_2$	$C_{15}H_{15}NO_4$	273.28	58	125

Table 2. Antidepressant activity, neurotoxicity of the newly synthesized compounds and *in vitro* MAO inhibition activity on rat brain mitochondria by kynuramine fluorimetric assay.

Compound	Antidepressant activity (FST)		MAO Inhibition	Neurotoxicity
	Immobility time (s) (mean ± SEM)	Change from control (%)	Monoamine oxidase inhibition[a] (%)	Coordination time in s (mean ± SEM)
2a	162.83±0.60**	-1.64	Nt	Nt
2b	155.66±0.33**	-5.95	35.50±0.42	58.00±0.57
2c	158.50±0.42**	-4.23	Nt	46.16±0.47
2d	154.33±0.42**	-6.75	39.50±0.76	59.83±0.60
2e	153.16±0.30**	-7.46	47.33±0.49	62.00±0.57
2f	161.83±0.60**	-2.22	22.33±0.42	47.16±0.60
2g	163.33±0.33*	-1.31	Nt	49.66±0.66
2h	162.83±0.47**	-1.61	Nt	44.50±0.92
2i	163.16±0.54*	-1.41	Nt	Nt
2j	163.83±0.47^{ns}	-1.01	Nt	Nt
Imipramine	149.00±0.57**	-9.97	Nt	Nt
Control	165.50±0.42	0.0	Nt	Nt
Tranylcypro mine[b]	Nt	Nt	84.50±0.76	Nt

[a]Each value is the mean from three separate experiments with SE of mean. All compounds were used at a final concentration of 5×10^{-4} M. [b]Concentration of tranylcypromine used 5.0×10^{-6} M. Values represent the mean ± SEM (n = 6). *Significantly compared to control (Dunnet's test; $p < 0.05$). ** Significantly compared to control (Dunnet's test; $p < 0.01$). ns = denotes not Significantly compared to control and Nt = denotes not tested

Table 3. Anti anxiety activity of the newly synthesized compounds (Elevated plus maze test in mice).

Compound	Preference to open arm (%)	Open arm	
		No. of entries (mean ± SEM)	Average time spent (mean ± SEM)
2a	10.96	3.16±0.30	32.00±0.57**
2b	12.36	3.33±0.42	35.83±0.60**
2c	13.62	3.00±0.25	38.83±0.60**
2d	15.58	5.16±0.47	45.50±0.42**
2e	15.86	5.50±0.42	46.00±0.57**
2f	15.22	4.50±0.42	43.83±0.60**
2g	15.40	4.16±0.47	44.50±0.76**
2h	10.43	3.33±0.42	29.00±0.57**
2i	14.69	4.66±0.33	42.00±0.57**
2j	9.93	2.16±0.30	28.00±0.57**
Control	5.88	2.00±0.25	16.16±0.47
Diazepam (2 mg kg^{-1}, ip)	18.10	4.66±0.42	52.50±0.42**

Values represent the mean ± SEM (n = 6). *Significantly compared to control (Dunnet's test; $p < 0.01$).

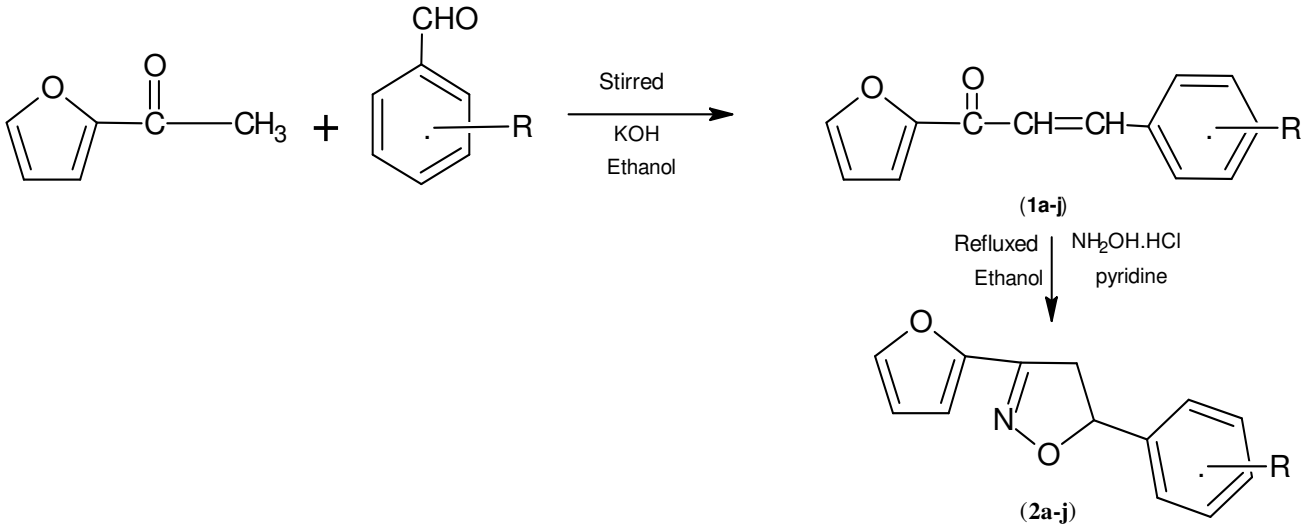

Figure 1. (furan-2-yl)-5-(substituted phenyl)-4,5-dihydro-1,2-oxazole derivatives (**2a** to **j**).

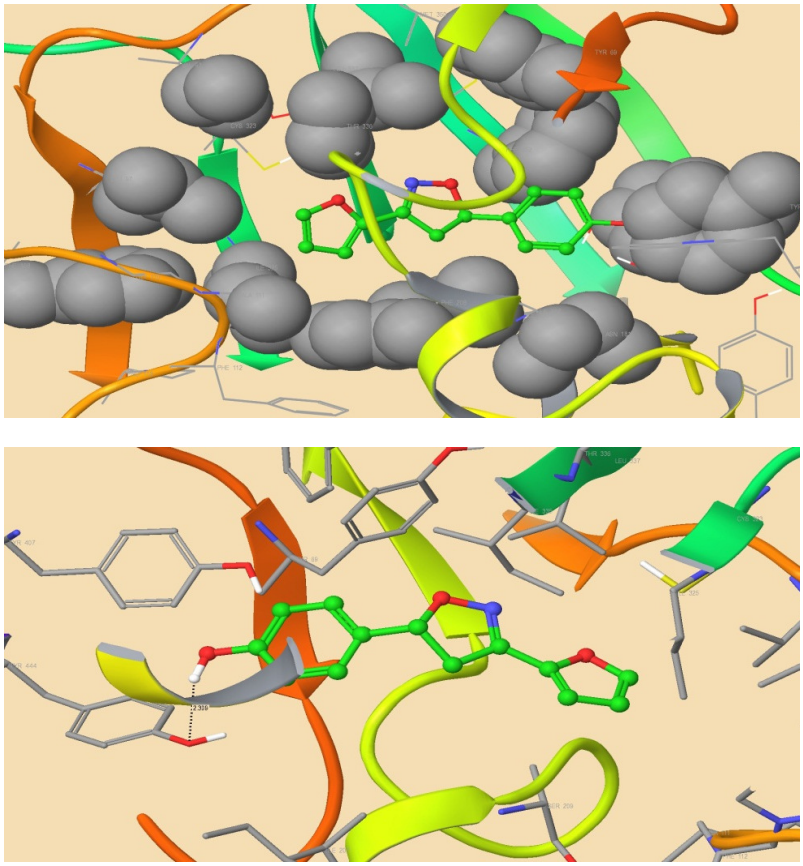

Figure 2. H-Bond docking pose of compound 2e on the falcipain-2 receptor (PDB id: 2Z5X).

7.71%), 2c (p-Br, -5.92%), 2d (p-F, -9.00%) and 2e (p-OH, -10.58), were the most active antidepressant agents. Some of the compounds like 2a and p-CH_3 (2f) substituted derivatives also showed good antidepressant activity. The preliminary structure:activity relationship (SAR) for this particular isoxazoline series suggest that substitution of electron withdrawing group at the para position of phenyl ring results in increase in antidepressant

activity while substitution with electron releasing group led to compounds having low antidepres-sant activity. Based on the promising antidepressant activities of the isoxazoline derivatives, some selected compounds were also evaluated for their MAO inhibitory effects by kynuramine fluorimetric assay method. Results of MAO inhibition study in Table 2 revealed that test compounds 2b, d, e and f produce weak to moderate MAO inhibition ranging between(22.33 and 47.33% at a final concentration of 5×10^{-4} M and maximum inhibition of 47.33% was obtained from compound 2e as compared to standard tranylcypromine 84.50%. Thus, indicating that the antidepressant activity of isoxazoline derivatives could be due to MAO inhibitory activity. These compounds were also evaluated for their motor coordination test by rotarod method to assess their neurotoxicity. The results of rotarod test indicated that none of the compound was neurotoxic at highest dose of 10 mg/kg (ip) as compared to standard drug imipramine. The compound 2e showed very good binding and prominent interactions on the falcipain-2 receptor (PDB id: 2Z5X). The compound 2e is well occupied in the receptor cavity and forms hydrogen bond and hydrophobic interactions (Figure 2).

The anxiolytic activity of the synthesized compounds was evaluated *in vivo* in mice by elevated plus maze test. The tested compounds showed anxiolytic activity ranging from 9.93 to 15.86% preference to open arm, whereas diazepam showed 18.10% preference to open arm (Table 3). Among 10 compounds (2a to j), six compounds (2c, d, e, f, g and i) showed better antianxiety activity when compared with standard diazepam. It was found that compound 2e possess both antidepressant and anti-anxiety activities. This compound could be further investigated as a new possible candidate in the treatment of anxiolytics and antidepressants.

Conclusion

A series of 3-(furan-2-yl)-5-(substituted phenyl)-4,5-dihydro-1,2-oxazole derivatives (2a to j) were synthesized as antidepressant and antianxiety agents. Out of these, 4-[3-(furan-2-yl)-4,5-dihydro-1,2-oxazol-5-yl]phenol (2e) emerged as the most potent antidepressant agent acting through MAO inhibition without any significant neurotoxicity. The observed MAO inhibitory action could also be responsible for its promising antianxiety effects.

ACKNOWLEDGEMENTS

The authors are grateful to Vice Chancellor, Jamia Hamdard for providing necessary facility and CDRI Lucknow for providing mass spectral data. One of the authors Mr. Jagdish Kumar Arun thank the University Grants Commission (UGC), New Delhi, for providing him RGN-SRF.

REFERENCES

Amrein R, Martin JR, Cameron AM (1999). Moclobemide in patients with dementia and depression. Adv. Neurol. 80:509-519.

Andersen SL, Teicher MH (2008). Stress, sensitive periods and maturational events in adolescent depression. Trends Neurosci. 4:183-191.

Andres JI, Alcazar J, Alonso JM, Alvarez RM, Bakker MH, Biesmans I, Cid JM, Lucas AID, Drinkenburg W, Fernández J, Font LM, Iturrino L, Langlois X, Lenaerts I, Martínez S, Megens AA, Pastor J, Pullan S, Steckler T (2007). Tricyclic isoxazolines: Identification of R226161 as a potential new antidepressant that combines potent serotonin reuptake inhibition and α_2-adrenoceptor antagonism. Bioorg. Med. Chem. 15:3649-3660.

Balalaie S, Sharifi A, Ahangarian B (2000). Solid phase synthesis of isoxazole and pyrazole derivatives under microwave irradiation. Indian J. Heterocycl. Chem. 10:149-150.

Basford RE (1967). Preparation and properties of brain mitrochondria. Methods Enzymol. 10:96-101.

Cesura AM, Pletscher A (1992). The new generation of monoamine oxidase inhibitors. Prog. Drug Res. 38:171-297.

Chen YL, Zhao YL, Lu CM, Tzenga CC, Wang JP (2006). Synthesis, cytotoxicity, and anti-inflammatory evaluation of 2-(furan-2-yl)-4-(phenoxy)quinoline derivatives. Part 4 Bioorg. Med. Chem. 14:4373-4378.

Crowley JJ, Lucki I (2005). Opportunities to discover genes regulating depression and antidepressant response from rodent behavioral genetics. Curr. Pharm. Des. 11:157-169.

Dannahardt G, Kiefer W, Kramer G, Maehrlein S, Nowe U, Fiebich B (2000). The Pyrrole Moiety as a Template for COX-1/COX-2 Inhibitors. Eur. J. Med. Chem. 35:499-510.

David SG, James TW, Michael WD, Jorge DB, Michael JB, James PS, George M C, Mark WH, Stephen PA, Michael W (1994). Novel Isoxazoles which Interact with Brain Cholinergic Channel Receptors Have Intrinsic Cognitive Enhancing and Anxiolytic Activities. J. Med. Chem. 37:1055-1059.

Deecher DC, Beyer CE, Johnston G, Bray J, Shah S, Abou-Gharbia M, Andree TH (2006). Desvenlafaxine succinate: A new serotonin and norepinephrine reuptake inhibitor. J. Pharmacol. Exp. Ther. 318(2):657-665.

Edwin W, Lilianna B (2004). Synthesis and pharmacological assessment of derivatives of isoxazolo[4,5-d]pyrimidine. Bioorg. Med. Chem. 12:265-272.

Fagervall I, Ross SB (1986). Inhibition of monoamine oxidase in monoaminergic neurones in the rat brain by irreversible inhibitors. Biochem. pharmacol. 35:1381-1387.

Gartside S, Cowen P (2006). Pharmacology of drugs used in the treatment of mood disorders. Psychiatry 5:162-166.

Gil JIA, Fernandez GEJ, Alcazar VMJ (Janssen Pharmaceutica NV, Belgium), (2002). PCT Int. Appl. W00266, 484: Chem. Abstr. 134:201298z.

Glide (2009) version 5.5, Schrödinger, LLC, New York, NY.

Henn FA, Vollmayr B, Sartorius A (2004). Mechanisms of depression: the role of neurogenesis. Drug Discovery Today: Disease Mechanisms 1:407-411.

Huang JQ, Li LY, Dong WX, Weng ZJ, Jin H, Ni XL, Zhang SJ, Huang CF, Gu FH (2006). Synthesis and antidepressant activities of aryl alkanol piperazine derivatives. Chin. J. Med. Chem. 16: 270-276.

Ignacio J, Gil A (2007). Substituted amino isoxazoline derivatives and their use as antidepressants. United State Pat. US 7,265,103 B2

Ignacio J, Gil A (2004). Isoxazoline derivatives as antidepressants. United State Pat. US 0122037 A1

Ignacio J, Gil A (2008). Isoxazoline indole derivatives with an improved antipsychotic and anxiolytic activity. United State Pat. US 0113988 A1.

Jayaprakash V, Sinha BN, Ucar G, Ercan A (2008). Pyrazoline-based mycobactin analogues as MAO-inhibitors, Bioorg. Med. Chem. Let. 18:6362-6368.

Jayashankar B, Lokanath Rai KM, Baskaran N, Sathish HS (2009). Synthesis and pharmacological evaluation of 1,3,4-oxadiazole bearing bis(heterocycle) derivatives as anti-inflammatory and analgesic agents. Eur. J. Med. Chem. 44:3898-3902.

Johnston JP (1968). Some observations upon a new inhibitor of monoamine oxidase in brain tissue. Biochem. Pharmacol. 7:1285-1297.

Karuppasamy M, Mahapatra M, Yabanoglu S, Ucar G, Sinha BN, Basu A, Mishra N, Sharon A, Kulandaivelu U, Jayaprakash V (2010). Development of selective and reversible pyrazoline based MAO-A inhibitors: Synthesis, biological evaluation and docking studies. Bioorg. Med. Chem. 18:1875-1881.

Kelekci NG, Ozgun SO, Ercan A, Yelekci K, Sibel SZ, Ucar G, Bilgin AA (2009). Synthesis and molecular modeling of some novel hexahydroindazole derivatives as potent monoamine oxidase inhibitors. Bioorg. Med. Chem. 17:6761-6772.

Knoll J, Magyar K (1972). Puzzling pharmacological effects of monoamine oxidase [MAO] inhibitors. Adv. Biochem. Psychopharmacol. 5:393-408.

Koksal M, Bilge SS (2007). Synthesis and Antidepressant-Like Profile of Novel 1-Aryl-3-[(4- benzyl)piperidine-1-yl]propane Derivatives. Arch. Pharm. Chem. Life Sci. 340:299-303.

Kulkarni SK (2002). Animals Behavioral Models for Testing Anti-Anxiety Agents. In: Hand book of Experimental Pharmacology, 3rd ed., Delhi, Vallabh Prakashan, 27-37.

Lee YS, Park SM, Kim BH (2009). Synthesis of 5-isoxazol-5-yl-2'-deoxyuridines exhibiting antiviral activity against HSV and several RNA viruses. Bioorg. Med. Chem. Lett. 19:1126-1128.

Lig Prep (2009). version 2.3, Schrodinger, LLC, New York, NY.

Mary, Sheeja TL, Mathew A, Varkey J (2011). Design synthesis and pharmacological evalution of isoxazole analogues derived from natural piperine. Asian J. Pharm. Health Sci. 2:256-260.

Matsumoto T, Suzuki O, Furuta T, Asai M, Kurokawa Y, Rimura Y, Katsumata Y, Takahashi I (1985). A sensitive fluorometric assay for serum monoamine oxidase with kynuramine as substrate. Clin. Biochem. 18:126-129.

Maurya R, Ahmad A, Gupta P, Chand K, Kumar M, Jayendra, Rawat P, Rasheed N, Palit G (2011). Synthesis of novel isoxazolines via 1, 3-dipolar cycloaddition and evaluation of anti stress activity. Med. Chem. Res. 20:139-145.

Moser PC (1989). An evaluation of the elevated plus-maze test using the novel anxiolytic Buspiron. Psychopharmacology (Berl) 99:48-53.

Owen JCE, Whitton PS (2006). Chronic treatment with antidepressant drugs reversibly alters NMDA mediated regulation of extracellular 5-HT in rat frontal cortex. Brain Res. Bull. 70:62-67.

Pellow S, Chopin P, File SE, Briley M (1985). Validation of open: closed arm entries in an elevated plus-maze as a measure of anxiety in the rats. J. Neurosci. 14:149-167.

Porsolt RD, Bertin A, Jalfre M (1977). Behavioral despair in mice: A primary screening test for antidepressants. Arch. Int. Pharmacodyn. Ther. 229:327-336.

Rabbani M, Sajjadi SE, Vaseghi G, Jafarian A (2004). Anxiolytic effects of Echium amoenum on the elevated plus maze model of anxiety in mice. Fitoterapia 75:475-464.

Sanchez C (2006). Allosteric modulation of monoamine transporters - new drug targets in depression Drug Discovery Today: Ther. Strategies 4:483-488.

Sienkiewicz-Jarosz H, Szyndler J, Członkowska AI, Siemiatkowski M, Maciejak P, Wisłowska A, Zienowicz M, Lehner M, Turzyńska D, Bidziński A, Płaźnik A (2003). Rat behavior in two models of anxiety and brain [3H] muscimol binding: pharmacological, correlation, and multifactor analysis. Behav. Brain Res. 145:17-22.

Sun HL, Wanga TT, Lv ZL, Feng JL, Geng DP, Li YM, Li K, (2010). Synthesis, chiral resolution, and determination of novel furan lignin derivatives with potent anti-tumor activity. Bioorg. Med. Chem. Lett. 20:1961-1964.

Tangallapally RP, Lee REB, Lenaerts AJM, Leea RE (2006). Synthesis of new and potent analogues of anti-tuberculosis agent 5-nitro-furan-2-carboxylic acid 4-(4-benzyl-piperazin-1-yl)- benzylamide with improved bioavailability. Bioorg. Med. Chem. Lett. 16:2584-2589.

Weissbach H, Smith TE, Daly JW, Witkop B, Udenfriend S (1960). A Rapid Spectrophotometric Assay of Monoamine Oxidase Based on the Rate of Disappearance of Kynuramine J. Biol. Chem. 235:1160-1163.

Winters G, Milan, Sala A, Monza (1985). Antiinflammatory and anxiolytic isoxazol-[5,4-B]pyridines. United State Patent, patent no. 4530927.

Zuhal O, Kandilci HB, Gumusxel B, Unsal C, Bilgin AA (2007). Synthesis and studies on antidepressant and anticonvulsant activities of some 3-(2-furyl)-pyrazoline derivatives. Eur. J. Med. Chem. 42:373-379.

UPCOMING CONFERENCES

1st Annual Pharmacology and Pharmaceutical Sciences Conference (PHARMA2013).Conference Dates: 18th – 19th November 2013

International Conference on Pharmacy and Pharmacology, Bangkok, Thailand, 24 Dec 2013

Conferences and Advert

November 2013
1st Annual Pharmacology and Pharmaceutical Sciences Conference (PHARMA 2013).

December 2013
ICPP 2013 : International Conference on Pharmacy and Pharmacology
Bangkok, Thailand December 24-25, 2013

December 2013
46th Annual Conference of Pharmacological Society of India

African Journal of Pharmacy and Pharmacology

Related Journals Published by Academic Journals

- *Journal of Medicinal Plant Research*
- *Journal of Dentistry and Oral Hygiene*
- *Journal of Parasitology and Vector Biology*
- *Journal of Pharmacognosy and Phytotherapy*
- *Journal of Veterinary Medicine and Animal Health*

academicJournals